Polymeric Materials for Detection of Chemical Warfare Agents

by

Bhoomi Het Mavani

A thesis

presented to the University of Waterloo

in fulfilment of the

thesis requirement for the degree of

Master of Applied Science

in

Chemical Engineering

Waterloo, Ontario, Canada, 2021

Author's Declaration

I hereby declare that I am the sole author of this thesis. This is a true copy of the thesis, including any required final revisions, as accepted by my examiners.

I understand that my thesis may be made electronically available to the public.

Acknowledgements

I am extremely grateful to my supervisor Professor Alexander Penlidis for giving me an opportunity to pursue my MASc thesis under his supervision. This thesis would not have been possible without his relentless encouragement, guidance, and support. He not only molded me to become a better researcher but also a good and confident individual. I owe him a great debt of gratitude.

I would like to give special thanks to my colleague Dr. Alison J Scott for training me in the lab and helping me to get on board during my initial steps (and all that under Covid)! I am grateful to my friends Rohan Shorey for lending his ear every now and then, and for interesting lunch break and corridor discussions; and Jaynik Vyas for encouraging me to embark on this journey.

I am thankful to the Chemical Engineering department of University of Waterloo for being instrumental in making this thesis possible. I am grateful for collaborations with Prof. Eihab Abdel-Rahman (and his research group), Prof. Raafat Mansour (and his research group) and Dr. Nina Heinig (SEM lab). I am also grateful to Prof. Tizazu Mekonnen for the use of the Optical Microscope and Dylan Jubinville for helping me with it.

I owe my deepest gratitude to my greatest support system and life partner- my husband Het Mavani. Throughout my studies, Het made available his support in several ways, helped me with my presentations and kept me sane. Finally, I would like to extend my deepest thanks to my parents (Sunil and Chhaya Barai), grandparents (Anupam and Anjana Barai and Mansukh and Indu Kakkad), and brother (Milap Barai) for their support during my studies.

Abstract

Chemical Warfare Agents (CWAs) are toxic synthetic chemicals that can have incapacitating or lethal effects. The 1997 Chemical Weapons Convention (1997 CWC) restricted production, stockpiling and use of CWAs, including their precursors/munitions, and classified them under specific categories. However, it is difficult to completely eliminate and prohibit production of CWAs, as many related chemicals find applications in manufacturing industries. Therefore, it is important to rapidly detect and identify CWAs present in our surroundings.

Phosgene is a relatively simple molecule, easy to synthesize and more accessible among all commonly known CWAs. Therefore, it is of interest to devise gas sensing polymeric materials for its detection. However, due to the highly toxic nature and restricted use of phosgene or other CWAs, "simulants" or "surrogate" molecules (similar physical and chemical properties but less toxic than CWAs) are used in research and development of sensors for detection of CWAs. Formaldehyde being chemically and physically 'similar' to phosgene was selected as a surrogate gas while evaluating sensing materials.

Polyaniline (PANI) and poly (2,5-dimethyl aniline) (doped and undoped with metal oxides) were tested for their ability to detect formaldehyde. PANI was doped with different loadings of In_2O_3 and P25DMA was doped with 20 wt.% of TiO_2 and 10% NiO. Sensing materials were tested for their sensitivity and selectivity towards formaldehyde. Sensing materials were finally tested for their stability to evaluate effects of environmental factors on their sensing performance. Sensing materials were also characterized using techniques such as scanning electron microscope (SEM), energy dispersive x-rays (EDX), and X-ray diffraction (XRD), in order to explain and obtain extra corroboration of sorption trends.

PANI doped with 1.25% In_2O_3 and P25DMA with 10% NiO were found to be most suitable for sensing formaldehyde with respect to sensitivity (low detection limit). With respect to selectivity, PANI doped with 5% In_2O_3 was most selective towards formaldehyde over benzene, whereas PANI with 10% In_2O_3 was most selective towards formaldehyde over acetaldehyde. Pristine PANI was equally selective towards formaldehyde and acetaldehyde. PANI and P25DMA sensing materials were found to be very stable with respect to other environmental factors (temperature and ageing).

The final selection of an appropriate sensing material becomes an interesting trade-off between sensitivity and selectivity, if the objective is the identification of an 'optimal' sensing material. An optimal sensing material can be specific to the application and its targets. On considering all the results and observations, it was concluded that PANI with 5% In_2O_3 was optimal in that trade off sense.

Table of Contents

List of Figures

List of Tables

Chapter 1: Motivation, Objectives and Outline

1.1 Motivation and Objectives

Chemical warfare agents (CWAs) are synthetic toxic organic analytes that can have incapacitating or lethal effects on humans. The four main agent classes for CWAs are nerve, blister, choking and blood agents. Among all CWAs, phosgene (known also as chlorinated gas or carbonyl dichloride) is extensively used in manufacturing industries, which makes it comparatively more accessible. It is very important to be able to identify and monitor the concentration of CWAs (like phosgene) in our surroundings. Therefore, the central idea is to design a sensing material that can detect the gas of interest and be incorporated in a wearable micro gas sensor.

Phosgene being highly toxic, it is difficult to handle in academic settings. Formaldehyde and phosgene have many physical and chemical similarities, while formaldehyde is comparatively less toxic. Hence, formaldehyde was employed as a surrogate gas for this research.

Polymeric sensing materials should be sensitive and selective towards formaldehyde gas. Potential sensing materials must also be stable towards such factors as environmental degradation and ageing.

It is also important that the sensing material is within sensor constraints. A MEMS (microelectromechanical systems) sensor is selected for this application. A MEMS sensor is a miniature sensor in size and can only accommodate a minimal amount of sensing material. For the sensor to be of low cost and miniature in size, it should also be a low energy device. Therefore, sensing materials should be able to detect formaldehyde at room temperature. For the sensor to be reusable, the sensing material requires to be able to regenerate rather readily by desorbing the sorbed analyte.

1.2 Outline

Chapter 2 contains an introduction to chemical warfare agents (CWAs) and a review of the techniques used for sensing CWAs. It also has a discussion on simulants/surrogates used for detection of CWAs and justifies the choice of employing formaldehyde as surrogate gas for this study. Important sensing characteristics for sensing materials are discussed next. Having established formaldehyde as the target analyte, sensing materials that have been used in the literature for sensing formaldehyde are scrutinized. The chapter ends with a short discussion of deposition of sensing materials on a sensor.

Chapter 3 contains the experimental procedures and descriptions of instruments used in this study. Synthesis steps for preparing polymeric materials are described in detail, followed by a description

of the gas sorption test set-up and other pieces of equipment used for characterizing sensing materials. The chapter ends with a brief description of the deposition set-up utilized for depositing sensing materials on the MEMS sensor (the MEMS sensor has been designed and manufactured by our collaborating groups in Systems Design Engineering and Electrical/Computer Engineering).

Results and discussion are divided and presented in four different chapters: Sensitivity Studies (Chapter 4), Selectivity Studies (Chapter 5), Stability Studies (Chapter 6) and Characterization Studies (Chapter 7).

The fourth chapter consists of experimental results from the gas sorption tests conducted to evaluate the sensitivity of the polymeric sensing materials for three gas analytes- formaldehyde, benzene, and acetaldehyde. Sorption trends are observed upon varying the backbone of the sensing material with and without metal oxide doping.

Chapter 5 contains selectivity results collected and analyzed while studying the affinity of polymeric sensing materials towards formaldehyde in the presence of interferent gases such as benzene and acetaldehyde. Based on the sensitivity studies in Chapter 4, a relative comparison between sensitivity and selectivity trends is also discussed, where applicable.

The sixth chapter reports results from stability studies conducted to ensure the repeatability and stability of polymeric sensing materials. Several comparisons are presented covering the effects of temperature, ageing, amount of sensing material and source of sensing material.

The sorption results are complemented in Chapter 7 discussing surface characteristics of the polymeric materials that also corroborate the trends observed in earlier chapters (Chapter 4 and 5). The chapter ends with a quick note on possible sensing mechanisms for detecting formaldehyde.

Chapter 8 contains concluding remarks and recommendations for future work. Both short-term and long-term recommendations are explicitly listed in this chapter. Chapter 8 is followed by the list of references cited throughout this thesis.

In addition, twelve technical appendices are presented at the end of the thesis (A to L). The appendices provide information complementary to thesis chapters. This information ranges from physico-chemical characteristics/solubility properties all the way to data tables and data/error analysis using statistical methodology. The final appendix (Appendix M) contains copyright permissions for reproducing (from the open literature) several figures in Chapters 2 and 7.

Chapter 2: Literature Background

2.1 Chemical Warfare Agents (CWAs)

A substance can be categorized as a Chemical Warfare Agent (CWA) based on its characteristics of high toxicity, imperceptibility to sensing, rapidity of action, and persistency, as listed in the Chemical Weapons Convention (CWC) [1]. The Organisation of Prohibition of Chemical Weapons (OPCW) also classifies precursors, munitions and devices used or designed with an intention to cause death or harm using the toxicity of these chemicals as 'Chemical Weapons' [2].

German military forces were the first to use modern chemical weapons to cause mass casualty on April 22, 1915, in Belgium, during World War I (WW I) [3]. CWAs are highly toxic synthetic chemicals that have lethal or incapacitating effects on humans [4] [5]. Sarin and Soman gases, for example, are highly toxic nerve agents, which can cause death within one minute of ingestion of 0.1 mg per kg of body weight [6]. CWAs can also be classified based on their persistence. A choking agent like phosgene is a non-persistent agent due to its higher volatility, while the oily blister agent, sulphur mustard, is a persistent gas with low volatility.

Many CWAs and their precursors are used as intermediates in several chemical manufacturing industries. For example, phosgene is widely used in plastics, pesticides and dye manufacturing [7]. Therefore, it is important to be able to detect and monitor the concentration of CWAs.

CWAs can be classified based on historical development, chemical structure and properties, reaction mechanism and physicochemical effects in humans [8]. The most common classification of chemical warfare agents based on their target organs in the human body is given in Table 1 and includes Nerve, Blister, Choking and Blood Agents [5].

Table 1 also has a list of common CWA simulants; a simulant, as the word signifies, may be used instead of the agent itself for research and development purposes; simulants (or surrogates) mimic or simulate the CWA behaviour based on a chemical similarity that leads to similar properties without the high toxicity levels. (More details on CWA simulants are given in Section 2.3).

Table 1: Classification of chemical warfare agents (CWAs)

Agent Class	Common Agents	Target Organs in Humans	CWA simulants
Nerve Agents	G Agents (Tabun (GA), Sarin (GB), Soman (GD)); V Agents (VM, VG, VE, VR and VX)	Nervous system	Dimethyl methyl phosphonate (DMMP) Diethyl chlorophosphate (DCP) Diisopropyl fluoro phosphonate (DFP)
Blister Agents	Mustard Gas (H) Lewisite (L)	Skin	2-chloroethyl ethyl sulfide 1,5-dichloropentane
Choking Agents	Phosgene (CG)	Respiratory tract	Triphosgene, Dichloromethane
Blood Agents	Hydrogen Cyanide (AC)	Circulatory system	Methyl cyanide (acetonitrile)

2.1.1 Nerve Agents

Nerve agents are phosphoric acid esters and belong to the organophosphorus (OP) family of compounds [9]. They are known as AChE (acetylcholinesterase) inhibitors and are chemically similar to some agricultural insecticides [8]. The function of AChE is to hydrolyze the neurotransmitter acetylcholine (ACh) enzyme that is released at different locations in the human nervous system. The phosphorous moiety in the OP compounds binds to an active centre of AChE and irreversibly inhibits its hydrolyzing action leading to confusion, convulsion, and paralysis [5]. Therefore, these chemical weapons acquired their name of 'nerve agents' [5]. The nerve agents are classified as G-series and V-series. Many studies suggest that V-agents are more stable and lethal compared to G-agents, with a relative potency as VX>GD≈GF>GB>GA [10]. The most common G-agents are Tabun (GA), Sarin (GB), and Soman (GD), and V-agents are VM, VG, VE, VR and VX [11]. The V-series of nerve agents is ten times more toxic than Sarin gas.

Nerve agents have similar physical and chemical properties as some pesticides and insecticides used in the agricultural industry [9]. The similarities between nerve agents and agricultural chemicals date back to the early 1930s. Many literature sources suggest that G-type (German-type) nerve agent, Tabun (GA), was first developed by a German chemist during an effort to develop organophosphorus-based insecticides in 1936 [5] [12]. Eventually, Sarin (GB) and Soman (GD) were prepared by the same research group in 1938 and 1944, respectively [12]. Furthermore, V-agents (venom or venomous-type) were developed by Great Britain in 1950, in a similar situation. Nerve agents exist in a liquid state in pure form but can be delivered in vapour or aerosol (mostly). On the release of a nerve agent, the reaction starts with the cleavage of the P-X bond.

2.1.2 Blister Agents

Blister agents are the class of CWAs commonly known to cause severe damage to the skin on exposure, but they are also capable of causing injuries in the eyes and respiratory tract [5] [13].

Commonly known blister agents are Mustard gas (H), Lewisite (L) and phosgene oxime (CX). Mustard gas can further be classified as sulphur-containing mustard (HD, also know as Levenstein mustard; chemically as bis (2-chloroethyl) sulfide)), and nitrogen-containing mustard (HN) [13] [14]. Nitrogen mustard mainly consists of HN1 [bis (2-chloroethyl) ethylamine], HN2 (2,20-dichloro-N-methyl diethylamine), and HN3 [tris (2-chloroethyl) amine hydrochloride] [14].

Mustard gas was first discovered and synthesized in the 1800s. More specifically, sulphur mustard was used to cause mass casualties during World War I. Agent H acquired its name due to its typical garlic or mustard smell. Although nitrogen mustard gas and Lewisite are less stable and difficult to store or transport, they are still used due to their interesting non-flammable characteristics and other applications in medicine, respectively [5].

2.1.3 Choking Agents

Choking agents, as the name suggests, are synthetic toxic chemicals that can cause severe damage to lungs and other parts in the human respiratory tract (and choke one to death on exposure in extreme cases). The most commonly known choking agent is phosgene gas (CG), a carbonyl dichloride compound.

Phosgene gas was used in the first known attack using a chemical weapon in 1915. It is widely used in the manufacturing industries of pesticides, dyes, and plastics. It is a primary precursor for synthesizing methylene diphenyl isocyanate and toluene diisocyanate [15]. Phosgene is commonly produced in industries by catalytic chlorination of carbon monoxide.

Phosgene is highly volatile with a boiling point of 8.2°C. It is a colourless gas that resembles the smell of freshly cut hay.

2.1.4 Blood Agents

Blood agents are known for their rapid action on exposure and leading to painful death in a few minutes [13]. There are two commonly known blood agents: hydrogen cyanide (AC) and cyanogen chloride (CK).

Blood agents are highly volatile poisonous chemicals at room temperature and are readily absorbed in the bloodstream. They bind to the oxygen in the blood leading to suffocation and death in a few minutes on exposure.

Hydrogen cyanide is an important raw material for several compounds in different industries (polymers and mining of precious metals). It is a colourless gas and smells like bitter almonds. It is unstable, lighter than air and disperses in air quickly.

2.2 Techniques for Detection of CWAs

CWAs are toxic chemicals and cannot be employed for academic lab-scale experiments to design a sensor for their sensing for evident reasons. Hence, other "chemically similar" molecules, commonly known as 'simulant' or 'surrogate' molecules, are utilized instead to design a sensor (see Section 2.3 for a detailed discussion on simulants for CWAs).

Several attempts have been made to detect and monitor CWAs using different remote sensing or point sensing techniques [13]. In remote sensing techniques, the samples are collected from the site, and identification and detection of the CWA take place at a particular distance from the actual site or a remote laboratory. For point sensing techniques, on the other hand, the identification and evaluation of the CWA take place on-site using handheld devices. Remote sensing of the CWAs can be performed using techniques such as gas chromatography (GC), Infrared spectrometry, and Raman spectrometry. Commonly known point sensing techniques consist of colorimetry, ion mobility spectrometry, flame photometry, Surface Acoustic Wave (SAW) sensors, chemiresistors, and MEMS sensors. Some point sensing techniques use stand-alone sensors but are often combined with remote sensing techniques to confirm findings further.

Both current remote and point sensing techniques have their advantages and disadvantages. Remote sensing techniques are accurate, but the employed sensors are bulky, expensive, require a trained person to test and understand the results, and are relatively time-consuming. Remote sensing techniques are quite advantageous over point sensing techniques in case of evaluation and investigation after the event. Point sensing techniques offer quick detection with handheld and portable devices, and are comparatively cheaper and simple to operate than remote sensing devices. But point sensing techniques may not be accurate and have higher chances of false results,

shorter life of the device, less information, and, more importantly, most of the techniques are not capable of detecting different CWAs with one sensing device.

Although point sensing devices have their own drawbacks, their advantages may outweigh the drawbacks in case of CWA detection. Hence, there is a high demand for point sensing devices for quick identification and real-time monitoring of CWAs in our surroundings. The principles of most of the existing sensing techniques for CWA identification/monitoring are briefly discussed in the next sub-sections.

2.2.1 Chemical Principles

Colorimetric Indicator
A colorimetric indicator is a paper-based technique that indicates the presence of a particular compound via a colour change. The indicator paper is coated with a reagent that changes colour due to a chemical reaction on exposure to the target compound. Jo et al. prepared a colorimetric indicator, with poly(quinoxaline) conjugated polymer dots based on poly(vinyl alcohol) (PVA)−silica nanofibers to detect diethyl chlorophosphate (DCP) [16]. DCP is a nerve agent simulant. They reported selective detection of ethanolic DCP in the case of hybrid nanostructure solution and film. But colorimetric indicators depend on the chemical reaction between the reagent and the simulant for the colour change. Therefore, presence of the ethanol in the solution might bias the chemical reaction conditions. Several colorimetric indicators currently exist which might be selective to a particular CWA simulant but have other, more severe, drawbacks such as operating temperature and low sensitivity.

Ion Mobility Spectrometer (IMS)
Ion mobility spectrometry is based on the identification of ionized gas-phase molecules with their characteristic drift velocity. The gas-phase molecules are ionized, driven and separated by applying an electric field in the presence of inert gas at atmospheric pressure and are identified based on their drift velocity. Zimmermann et al. presented a miniaturized ion mobility sensor for the detection of nerve agents and blister agents [17] to low concentrations. They reported that blister agents like nitrogen mustard, sulphur mustard and Lewisite are undetectable in low concentrations under humid conditions [17]. IMS is relatively quick but poses disadvantages like complex sensor design, high cost, low signal-to-noise ratio, low selectivity, and inability to detect gas molecules in the presence of humidity.

Flame Photometry
When gas molecules are exposed to a flame in a flame photometer, they absorb energy, jump to a higher energy level and emit light of a specific intensity when they return to the ground state. This sensing technique has good sensitivity for molecules containing phosphorous and sulphur and

7

hence, it is commonly used for the detection of nerve agents. Flame Photometry only indicates if the molecules contain sulphur or phosphorous but it is not capable of identifying the particular CWA molecule [18] (it has selectivity issues).

Fluorescence sensor

A fluorescence sensor is a solution-based sensing technique. It can be an on-off type sensor [19] or a ratiometric sensor [20]. Fluorescence sensors are based on fluorophores that are capable of changing their fluorescence characteristics like intensity and wavelength on chemically interacting with a CWA. Fluorescence sensors are commonly used for the detection of CWAs (like nerve agents and blister agents) containing sulphur and phosphorous. Khan et al. reported a fluorescence sensor to detect nerve agent simulant, diethyl chlorophosphate (DCP), using iminocoumarin-benzothiazole. The reaction mechanism for this sensor is based on a standard nucleophilic attack at the phosphorus atom of the DCP by the solution probe. They reported that the solution probe, originally green in colour, changed to light gold in 30 minutes of encountering the DCP molecules [19]. Fluorescence sensors are expensive, involve more complex chemistry, have a longer response time and are not portable.

In summary, currently available commercial detectors for detection of CWAs based on electrochemical principles are rather expensive, not portable, and exhibit rather long response time. If portable, they are of single-use only.

2.2.2 Sensors

A sensor is a device that is capable of transforming information about the interaction between analyte and sensor into a measurable signal. A typical sensor consists of a sensing material (for interaction and detection of the analyte) and a transducer (for identifying the change and converting it into a measurable signal), as shown in Figure 1 (based on a concept of a figure in reference [21]). The sensing layer in a chemical sensor can be an organic sensing material (like conducting polymeric materials) or an inorganic sensing material (like metal oxides). Sensors can be based on measuring different properties of the sensing material such as a change in mass, resistance or conductivity, and frequency.
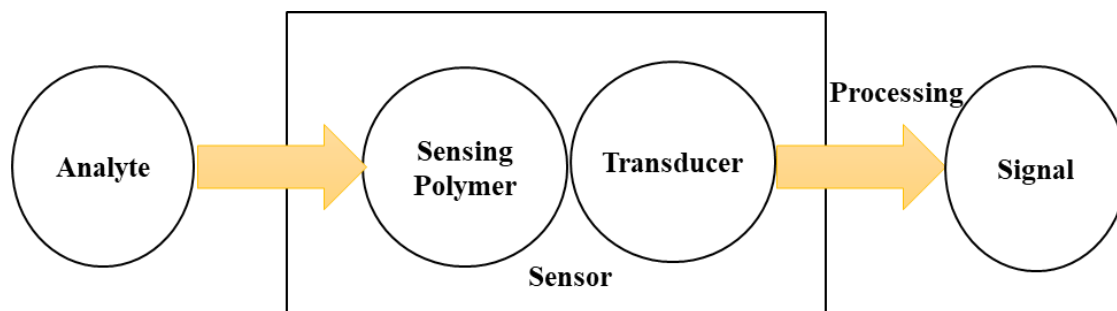
Figure 1: Schematic diagram of a chemical sensor with a polymeric sensing material

Surface Acoustic Wave (SAW) Sensors

Surface Acoustic Wave (SAW) sensors are based on a piezoelectric substrate. The sensing material is placed between transducers and the acoustic wave is allowed to pass through the sensing material. The mass of sensing material changes upon coming in contact and interacting with the gas analyte leading to a change in the wave frequency. The mass changes in the sensing material are due to the absorption of the analyte molecules upon it. Matatagui et al. [22] presented an array of polymeric material-based SAW sensors for the detection of four CWA simulants, as shown in Table 2.

Table 2: CWA and their simulants considered to design a SAW sensor array [22]

CWA	Simulant
Sarin	Dimethyl methyl phosphonate (DMMP)
Nitrogen mustard	Dipropylene glycol monomethyl ether (DPGME)
Distilled Mustard	Dimethylacetamide (DMA) 1,2-Dichloroethane (DCE) 1,5-Dichloropentane (DCP)
Phosgene	Dichloromethane (DCM)

Poly (cyanopropyl methyl siloxane) (PCPMS) was able to detect DMMP (Sarin gas simulant) down to 0.05 ppm while it was not able to detect DCE and DCM at low concentrations [22].

Microelectromechanical Sensors (MEMS)

A MEMS sensor is a microcantilever-based sensor as shown in Figure 2. The microcantilever is coated with a film of sensing material (probe molecule) that comes in contact with the target molecule. The change in mass of the sensing material (as a result of the interaction with the analyte) changes the resonant frequency of the cantilever. This mechanical action of the cantilever is converted into an electrical signal, which indicates detection of the analyte.
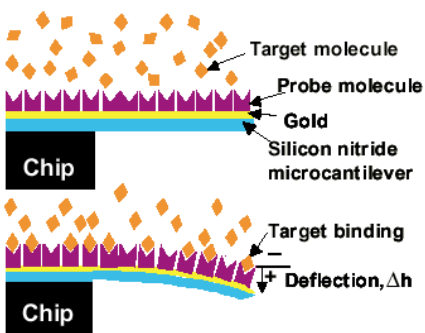
Figure 2: Microcantilever of a MEMS sensor [23] (by permission)

Meier et al. reported a MEMS microsensor based on a 4-element sensor array consisting of two metal oxides (SnO_2 and TiO_2) for sensing nerve agents [24]. The MEMS sensor was able to detect nerve agents down to a few ppb but could not discriminate between different agents. The sensor was operated at an elevated temperature range (325 C to 475 C). The signal started drifting after 14 hours of operation. Metal oxide sensing materials may have high sensitivity but lack selectivity and stability due to the elevated temperature operation. MEMS sensors can also be based on polymeric sensing material to overcome drawbacks posed by metal oxide sensing materials (see Section 2.7).

Chemiresistive Sensors

Chemiresistve sensors are very simple and easy to fabricate. Such a sensor consists of a resistive sensing material attached to one or more electrodes with a source of electrical current. The resistivity (or conductivity) of the sensing material changes on interaction with the analyte. The measured change in resistivity indicates the presence of the analyte in the surroundings. The sensing material in the case of a chemiresistor is generally a film or membrane of a conducting polymeric material. Vrij et al. investigated a polyaniline-amine composite-based chemiresistive sensor for room temperature sensing of phosgene [25]. They reported that incorporating amines (like ethylenediamine and phenylenediamine) and metanilic acid, phosgene can be detected down to 0.01 ppm concentrations. The amine additive tends to react with phosgene to produce HCL that further dopes polyaniline and changes its resistivity. They also indicated that these sensors are suited for one time use only.

2.3 Surrogates/Simulants for CWAs

As described in Section 2.1, CWAs are highly toxic synthetic chemicals and can cause severe injuries with even small quantities. As mentioned earlier, production, stockpiling and use of these chemical warfare agents, including their munitions and precursors, are restricted. Since the stakes are very high, it is important to understand, evaluate and analyze their behaviour for quick detection. Therefore, stimulant/surrogate gases are used to design sensors and sensing materials for research-related academic laboratory activities.

A good CWA stimulant should mimic the CWA's physical and chemical properties but would possess comparatively much lower toxicity than the agent itself [10]. Lavoie et al. described an ideal CWA simulant as one that only has bioavailability of its agent but not the bioactivity [26]. Bioavailability manifests to the physicochemical properties of the molecules like diffusion, sorption, or solubility, while bioactivity emphasizes the extent of the interaction. It is important for the simulant to not only have similar physicochemical properties as the agent but also have relatively low toxicity, similar intended use (for example, sorption isotherm for evaluation of simulant by sorption experiments) [10], low cost, and be easy to handle in academic research laboratory settings.

There are several stimulants for CWAs, but none can mimic the agent exactly due to their different potential environmental pathways (i.e., sorption, hydrolysis, volatilization and other biological processes) [10].

Many potential simulants (as cited in Section 2.1) have been used to mimic and investigate the behaviour of different CWAs so far in the literature. Many of these surrogate gases are still toxic, just less so than the actual CWAs. So, even for research with simulants or surrogate gases, special installations are needed, which are not only expensive but also can pose serious safety concerns.

This thesis is concerned with the detection of phosgene due to the ease of its availability and synthesis. The two commonly used simulants in the literature for evaluating sensing materials for phosgene are triphosgene [27] and dichloromethane (DCM) [22]. See Figure 3 for the typical chemical structures.
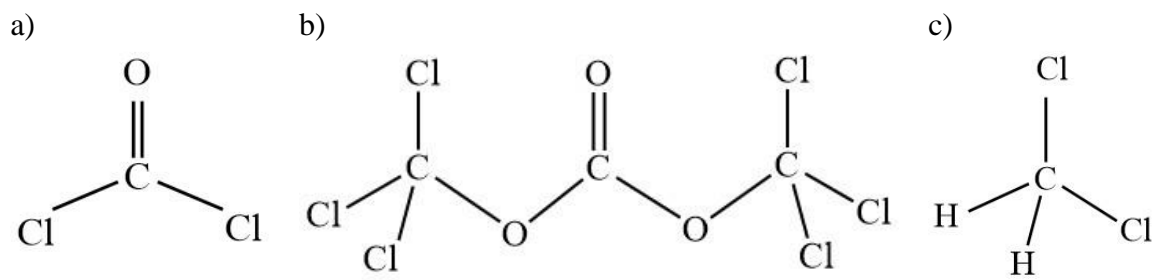
Figure 3: Chemical structures of a) phosgene, b) triphosgene, c) dichloromethane (DCM)

Triphosgene is a solid, non-volatile compound, that is used as a precursor to synthesize phosgene [28]. It is commonly used in organic synthesis and can be catalytically decomposed into phosgene using a tertiary amine [29]. There are several limitations and safety concerns to employ triphosgene as a simulant. Firstly, triphosgene is a bulkier molecule in size compared to phosgene, so it might not be a good representative of the size of phosgene molecule and bias the results while evaluating sensing materials for their sorption capabilities based on the free volume available for the analyte. Secondly, with more than one carbon-oxygen functional groups in triphosgene, chemical properties like polarity and hydrogen bonding capabilities are different compared to phosgene itself. Thirdly, triphosgene has similar toxicity levels as that of phosgene itself.

Dichloromethane (DCM) is a volatile liquid at room temperature. Although dichloromethane has a similar chemical formula as that of phosgene, the absence of the carbonyl functional group changes its chemical properties such as polarity, dipole movement, hydrogen bonding capability and shape. (Phosgene has a trigonal planar geometry while chloromethane has trigonal pyramidal). Dichloromethane is a Lewis acid while phosgene is a Lewis base.

As a preliminary research and development target, significantly fewer toxic compounds should be used. For instance, instead of phosgene, one might employ a molecule which contains a carbonyl group, like aldehydes. In particular, formaldehyde and acetaldehyde can be used as they are chemically and physically similar to phosgene. Therefore, after taking into account chemical and physical similarities, and toxicity of the potential surrogates used in the literature, formaldehyde (F) was selected as a potential surrogate for evaluating materials for phosgene detection. A comprehensive justification for selecting formaldehyde as a surrogate gas is presented in Section 2.4.

2.4 Formaldehyde as a Surrogate Gas

Gases such as formaldehyde and acetaldehyde can be used, since they not only pose similar chemical properties as those of phosgene (they contain a carbonyl group and are similar in size) but are significantly less toxic compared to phosgene (see Figure 4). Hence, formaldehyde was selected as the main surrogate gas due to its similar shape, size, and orientation. Acetaldehyde can then be employed as a potential interferent.
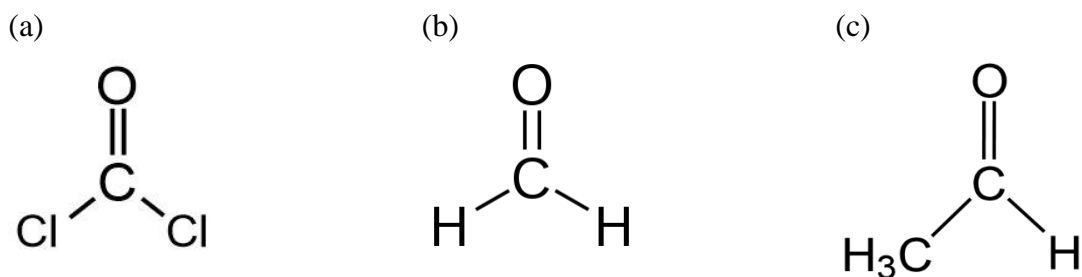
Figure 4: Similarity of chemical structures of a) phosgene, b) formaldehyde, and c) acetaldehyde

Gas analytes, or volatile organic compounds (VOCs), interact with polymeric sensing materials through various sensing mechanisms. The dominant sensing mechanisms vary from one analyte to the next and are strongly influenced by the functional groups (i.e., the overall functionality of the molecule in question). Three characteristics of aldehydes that can be employed for their sensing using polymeric materials are polarity, hydrogen bonding, and Lewis base behaviour.

The oxygen atom in each molecule (Figure 4) draws electron density towards itself; this results in a dipole with a negative charge on the oxygen (this means that aldehydes are polar). The higher the dipole moment, the more polar the molecule. Formaldehyde and acetaldehyde are both polar, so the sensing materials selected should take advantage of that characteristic. The oxygen atom on phosgene is also negatively charged, but the chlorine atoms counteract the charge distribution somewhat. Therefore, the dipole moment for phosgene is lower (D = 1.17) compared to formaldehyde (D = 2.33) and acetaldehyde (D = 2.70), but the molecule still has polar characteristics that can be exploited for sensing.

Two polar molecules are attracted to one another through electrostatic forces. The more polar the molecules, the stronger the attraction. A special case of this is called hydrogen bonding. This occurs when a highly electronegative atom (like nitrogen, oxygen or fluorine), is bound to hydrogen. This large electronegativity difference results in the nitrogen, oxygen, or fluorine atom pulling most of the electron density away from the hydrogen atom and thus, a large dipole is created. This results in electrostatic forces strong enough to create a weak (physical) bond between the hydrogen of one molecule and the nitrogen, oxygen, or fluorine of another molecule. Polyaniline (PANI), for example, contains amine (NH) groups, which promote hydrogen bonding with compatible analytes [30].

Finally, there are two lone pairs of electrons on the oxygen; these cause the molecule to act as a Lewis base. Lewis bases behave as nucleophiles; this means that they will seek out electron-deficient atoms to donate a lone pair of electrons. This electron donation is not a "complete" transfer, as the electron density is shared between the two molecules. Therefore, a weak physical bond is formed. As such, sensing materials that behave as Lewis acids are ideal. A Lewis acid is characterized as an electron-deficient atom, such as a positively charged hydrogen or carbon atom [30]. Lavoie et al. suggested that CWAs and their mimics possessing similar hydrophobicity and polarity might interact and sorb similarly on the sensing material [26].

Ariyageadsakul et al. conducted DFT (Density Functional Theory) studies to evaluate polyaniline ES (emeraldine salt) as a gas sensing material to detect carbonyl compounds such as formaldehyde, phosgene, and acetone. The interaction binding energies of PANI ES (polyaniline emeraldine salt) to formaldehyde, −8.13 (−7.65) kcal/mol, and to phosgene −4.83 (−3.91) kcal/mol, were comparatively weaker than towards acetone 12.28 (−11.23) kcal/mol [31]. The charge analysis suggested a lower charge transfer between PANI ES and phosgene compared to PANI ES and formaldehyde. This lower binding energy and charge transfer in the case of phosgene can be accounted for by the presence of two highly electronegative chlorine atoms on the carbonyl group.

Therefore, a sensing material capable of reasonably detecting formaldehyde by exploiting its sensing properties might also demonstrate a good signal when exposed to phosgene. A list of potential sensing materials for several CWAs and other gas analytes can be found in Appendix A.

Many sensors and sensing materials have been evaluated in the literature for the detection of formaldehyde as it is a very common volatile organic compound (VOC) capable of polluting indoor air. A detailed literature review on sensing materials for formaldehyde is presented in Section 2.7.

2.5 3S Concept: Sensitivity, Selectivity and Stability

Any sensing material can be characterized based on important sensing characteristics such as sensitivity, selectivity, stability, operating temperature, and response and recovery times. The performance of sensing materials is influenced by their microstructure, surface morphology, porosity, interaction energy, catalytic activity, and chemical reactivity [31] [32].

2.5.1 Sensitivity

The sensitivity of a sensor refers to the detection of the lowest concentration of the analyte in question. A sensor is considered sensitive when it can produce a greater change in signal on a small change in the concentration of the analyte. The sensor or the sensing material may display a different degree of sensitivity for different ranges of concentration of the analyte.

For a sensing material, sensitivity is its ability to detect and sorb the lowest concentration of the target analyte. It can be calculated as the amount of the target analyte sorbed divided by the total concentration of the target analyte upon exposure (Equation 2.1):

$$Sensitivity = \frac{Target\ analyte\ sorbed}{Total\ analyte\ concentration} \qquad\qquad 2.1$$

The higher the concentration of the target analyte sorbed, the better the sensitivity of the sensing material. The sensing material can be considered sensitive if it displays a sensitivity greater than 0.45. Of course, all these literature estimates are rough guidelines and their validity depends on the specific case.

For a sensor, sensitivity is the minimum detectable signal, which is also known as limit of detection (LOD). LOD for a sensor is defined as three times the level of background or baseline noise.

2.5.2 Selectivity

Selectivity is a measure of how much the sensing material prefers the target analyte over possible other interferent gas(es), when exposed to a mixture of gases. It can be quantified as the ratio of the concentration of the target analyte sorbed to the concentration of the interferent gas sorbed (Equation 2.2).

$$Selectivity = \frac{Target\ analyte\ sorbed}{Interferent\ gas\ sorbed} \qquad\qquad 2.2$$

It is important to conduct selectivity studies since the target analyte (usually) exists with several other interferent gases that may interfere with the analyte signal and give misleading information. For instance, in case of sensing formaldehyde, it is practical to study the interaction of the sensing material in the presence of gases with the same functional groups such as acetaldehyde, or molecules with similar size such as methanol, and possibly molecules with other functional groups such as ethanol, acetone and benzene, as they might exhibit a similar sensing mechanism.

A common characteristic in the literature is that almost 95% of the published papers investigate sensitivity only, and hardly ever selectivity or stability.

2.5.3 Stability

Stability is related to several aspects, including the mechanical integrity of the sensing material, reusability of the sensing material, and effectiveness of the sensing material with ageing. Stability studies are important, since an ideal sensor should be able to resist adverse environmental conditions and still detect the target analyte.

2.5.4 Other Sensor Characteristics

Other important sensing characteristics are response and recovery times, and operational temperature. Operational temperature can also be classified as a sensor stability factor, depending on the final sensor application. In this thesis, we deal with room temperature sensors. Response and recovery times may be more important for the final sensor package (sensor 'functionalization' and manufacturing).

Response and Recovery times- Response time is the time required to achieve 90% of the maximum signal, whereas recovery time is the time required to return to 10% of the baseline signal. The response and recovery times are also important properties of the sensor as quick detection is one of the basic requirements while designing a sensor for toxic gas analytes.

Operating temperature- The operating temperature is the temperature at which the sensor operates. The operating temperature plays an important role in gas sensors as it can alter the sensing properties of the sensor. Sensors based on metal oxide sensing materials are generally operated at elevated temperatures (say, above 150-200 ℃, and more typically in the 350-450 C range), and therefore require a heating source within the sensor. On the other hand, most of the sensors based on polymeric materials are capable of sensing gases at room temperature.

2.6 Sensors for Detection of Formaldehyde

Formaldehyde has been extensively used in the manufacturing of plastics and resins. It is a common indoor and outdoor toxic organic pollutant. Therefore, several techniques have been explored for developing a reliable sensor for formaldehyde detection. Different techniques for sensing formaldehyde in air can be classified as shown in Figure 5.
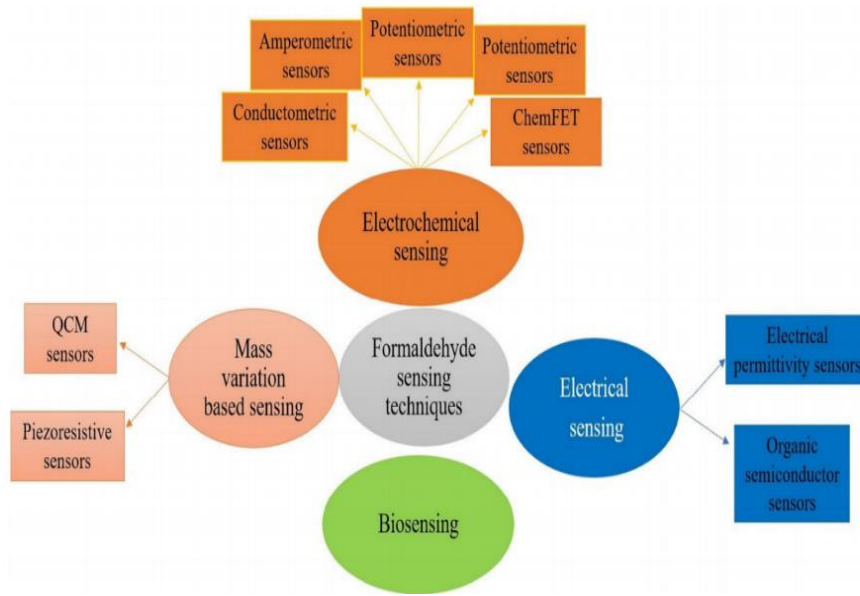
Figure 5: Classification of formaldehyde sensing techniques [33] (by permission)

A comprehensive review of sensors for sensing formaldehyde has recently been presented by Kukkar et al. [33]. The two most common types of sensing materials on which the majority of sensors are based are a) inorganic and b) organic sensing materials. Inorganic sensing materials are metal oxide sensors (MOS) like NiO, In_2O_3, TiO_2, ZnO, WO_3, MoO_3 etc. These metal oxides display enhanced sensitivity and low LOD, operated at high temperatures (typically 300 C- 400 C). Therefore, they require an integrated heating source in the sensor, which ultimately increases the size, complexity and energy requirement of the sensor. Moreover, the high operating temperatures may consequently lead to more than typical sensor 'wear and tear' (baseline drift and stability issues). On the other hand, organic material-based sensors consist of (often conducting) polymeric materials (as sensing materials), like polyaniline (PANI), polypyrrole (PPy), poly (3,4-ethylene-dioxythiophene) (PEDOT), polyethyleneimine (PEI), polydimethylsiloxane (PDMS), etc. Organic conducting polymeric sensing materials are acceptably stable and capable of sensing volatile organic compounds (VOCs) at room temperature. Polymeric materials like PANI are very versatile and can be further customized and modified by the addition of dopants to modify the PANI morphology or modify the synthesis procedure to improve sensing properties [32].

This thesis is focused on formaldehyde sensing using polymeric nanomaterials (e.g., PANI and/or modified PANI via addition of metal oxides as dopants).

2.7 Organic Sensing Materials and Doping

Most of research work on formaldehyde gas sensors considered the conductivity/resistivity properties of polyaniline (PANI) and/or polypyrrole (PPy), both well known conductive polymers.

This is also evident from the summary of sensors (based on relatively recent literature) cited in Table 3.

Polyaniline (PANI) is the most well known conducting polymer synthesized using aniline monomer. It can exist in three different forms based on its oxidation states (as shown in Figure 6). The oxidation state of PANI can be identified using UV-Vis [34]. The basic structure of PANI contains n reduced benzenoid diamine units and m oxidized quinoid diamine repeating units.
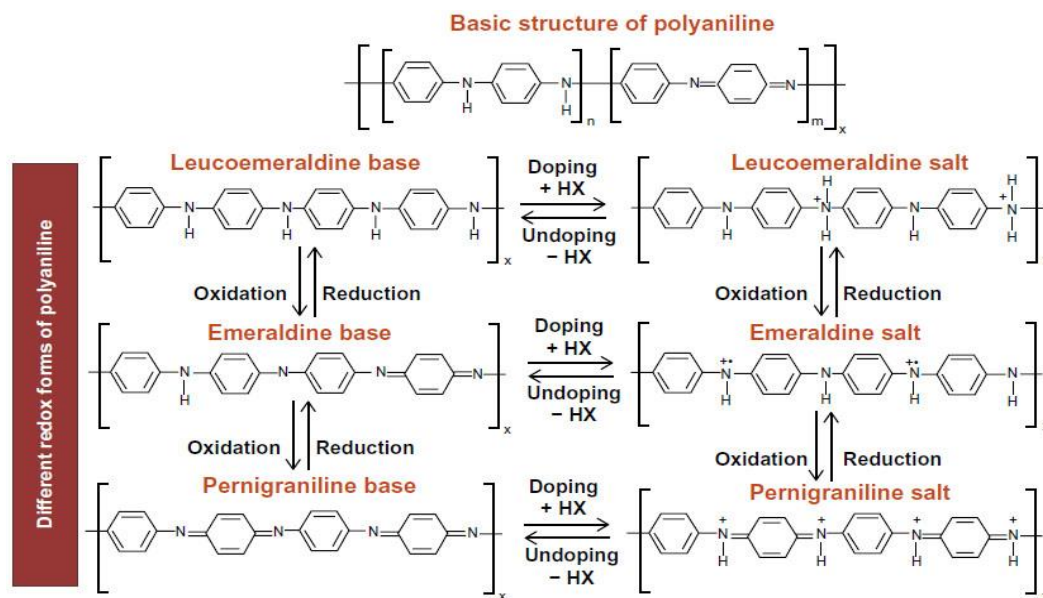
Figure 6: Different forms of PANI [35] (by permission, open access)

The m:n ratio changes the form of PANI and is responsible for different possible molecular structures. The three basic and most common forms of PANI are Leucoemeraldine, Emeraldine and Pernigraniline, with m:n ratios of 0:1, 1:1, and 1:0, respectively [36]. The amine groups in the PANI structure can be protonated in the presence of H^+ ions or HX dopants, which generates 'defects' to increase the conductivity of polyaniline. The protonated form of PANI is known as 'salt', whereas the unprotonated form is known as 'base' [37]. The protonated emeraldine has an average conductivity of 10^{-2} S/m, whereas the average conductivity of the corresponding emeraldine base is 1.4 x 10^{-10} S/m [38] [39].

The sensing characteristics of these polymeric materials can be enhanced by incorporating dopants (acids or amines) to increase their conductivity [40] [41], or metal oxide nanoparticles to modify their structure/surface morphology [42]. The result is the preparation of organic/inorganic hybrid structures for increased charge transport [43], or molecularly imprinted polymers on nanotubes, all purportedly enhancing sensitivity [44].

Table 3 summarizes some common conducting polymeric materials examined in the literature for the detection of formaldehyde, including recent efforts to use PANI- or PPy-based polymeric

materials (with and without metal oxides). Most (if not all) of these efforts tried to exploit the conductivity/resistivity properties of the polymeric material in order to detect the gas.

The sensitivity of the sensing material in chemiresistive sensors is typically measured as a difference in electrical resistances: one during exposure to analyte gas (in some carrier gas, usually nitrogen or air) and one during exposure to carrier gas only (see Equation 2.3):

$$Sensitivity \ (S\%) = \frac{Rg - Ra}{Ra} \times 100 = \frac{\Delta R}{Ra} \times 100 \qquad 2.3$$

Rg and Ra are the electrical resistances exhibited by the sensing material in an analyte gas and in a carrier gas, respectively. It must be noted that S% is reported using equation 2.3 for all cases of Table 3, except for Case #7 and Case #10. For Case #7, the corresponding reference is not clear as to how the sensitivity was calculated. For Case #10, sensitivity was measured as the difference in concentration of formaldehyde in the absence and presence of the sensing material in the testing chamber [42].

Table 3: Summary of sensing materials for formaldehyde (F)

Case #	Sensing Material	Dopant	Sensor Type	Temperature	Sensitivity (S %)	Ref.
1	Polypyrrole, (PPy) $_x$MoO$_3$ hybrid films		Chemiresistor	Room Temperature	6% on exposure to 1000 ppm F 2% on exposure to 1000 ppm of acetaldehyde (Ac)	[45]
2	(PANI) $_x$MoO$_3$ hybrid films		Chemiresistor	Room temperature	8% on exposure to 50 ppm F 3.8% on exposure to 50 ppm Ac	[46]
3	Poly (o-anisidine), (PoANIS)$_x$ MoO$_3$ hybrid films		Chemiresistor	100 C	2.4% when exposed to 10 ppm F 4.4% when exposed to 10 ppm Ac	[47]

4	Poly (2,5-dimethylaniline) $(PDMA)_xMoO_3$ hybrid films		Chemiresistor	100 C	3.9% when exposed to 10 ppm F 4.7% when exposed to 10 ppm Ac	[48]
5	Poly (N-methyl aniline) $(PNMA)_xMoO_3$ hybrid films		Chemiresistor	~80 C	2.6% when exposed to 9.1 ppm of F 2.8% when exposed to 9.6 ppm of Ac	[49]
6	Polystyrene/Polyaniline (PS/PANI), (core/shell)		Chemiresistor sensor with interdigitated electrodes (IDEs)	Room Temperature	18.7% on exposure to 10 ppm F	[50]
7	Polyaniline (PANI)	HNO_3	Chemiresistor	Room temperature	78.57% on exposure to 2 ppm F (this reference does not explain how the sensitivity was calculated; hence, estimate is unreliable)	[40]
8	PPy molecularly imprinted on a TiO_2 nanotube array		Chemiresistor	Room temperature	13% on exposure to 1 ppm F	[44]
9	PANI	LYS (lysine hydrochloride)	Chemiresistor	Room temperature	21% on exposure to 100 ppm F (fitted value using Langmuir-like adsorption law)	[41]
10	PANI	TiO_2	Concerntration-based	Room Temperature	~0.45 ppm when exposed to 0.6 ppm of F (but estimate seems unreliable)	[42]

Wang et al. [46] prepared a PANI (organic "guest") intercalated MoO_3 (inorganic "host") hybrid thin-film sensor for sensing VOCs. The hybrid material $(PANI)_xMoO_3$ was stacked alternately with charged molybdenum trioxide layers and PANI layers, as shown in Figure 7. The layers were held together due to the electrostatic interaction between PANI and MoO_3. The authors observed an increase in resistance signal response by 8% on exposure to F 50 ppm ($R_g/R_a= 1.08$) and 3.8 % on exposure to 50 ppm Ac ($R_g/R_a= 1.038$) [46]. In addition, a very weak response was observed in the case of other gases such as chloroform, acetone, and ethanol, while absolutely no response was observed in the case of aromatic gases such as toluene and xylene.
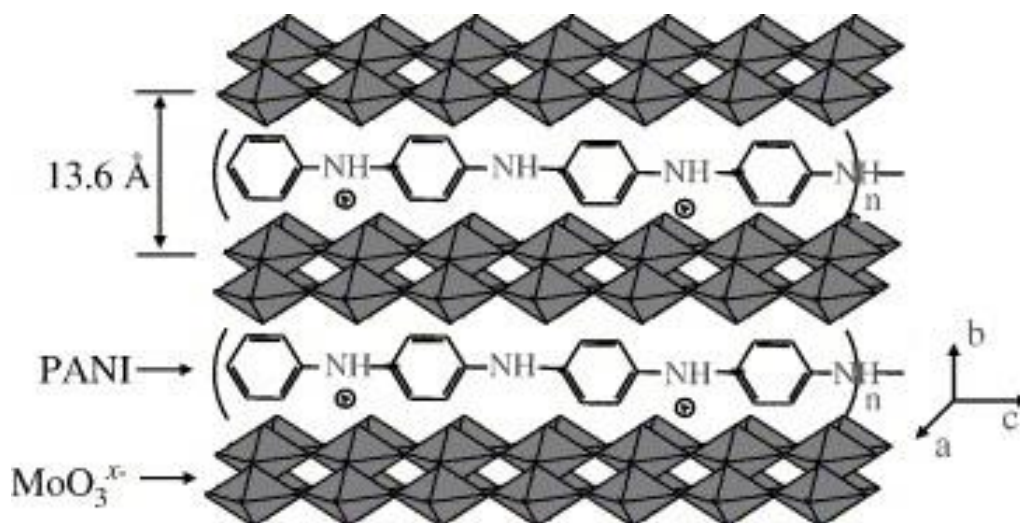
Figure 7: Schematic of PANI and MoO3 intercalated layered structure [46] (by permission)

Wang et al. [46] speculated that the possible sensing mechanism for the higher sensitivity of $(PANI)_xMoO_3$ for polar gases like aldehydes could be due to the hydrogen bonding between MoO_3 and H-C=O of the aldehydic gases. This also indicates that while designing a sensing material based on the interaction of a material and the functional group of the analyte, other gases with the same functional group might act as an interferent and consequently pose a selectivity issue.

A similar organic/inorganic hybrid material with a different polymeric backbone was prepared by Matsubara et al. [45]. They prepared a $(PPy)_xMoO_3$ layered hybrid sensing material for sensing VOCs. They reported that on exposure to methanol gas an increase in resistance was observed even though MoO_3 is an n-type semiconductor and resistance would decrease on exposure to analytes [45]. This phenomenon was speculated to be due to the physical effect and partial charge transfer caused by the insertion of the methanol in the interlayers of PPy and MoO_3. Further, on exposing $(PPy)_xMoO_3$ to 1000 ppm of various VOCs, a higher response was observed for formaldehyde (sensitivity S=6%), followed by acetaldehyde and chloroform (both with S=2%), whereas other polar gases displayed a very weak signal [45]. It should be noted that no signal was observed in the case of toluene and xylene. They also established that the selectivity of the organic/inorganic hybrids could be controlled by modifying the organic guest.

21

On comparing the sensitivity results from Wang et al. [46] for (PANI)$_x$MoO$_3$ and Matsubara e al. [45] for (PPy)$_x$MoO$_3$, it is interesting to note that (PANI)$_x$MoO$_3$ seemed to be more sensitive towards formaldehyde than (PPy)$_x$MoO$_3$. Moreover, it must be noted the (PANI)$_x$MoO$_3$ was more selective to formaldehyde as it exhibited a lower response to acetaldehyde and no response to other VOCs. On the other hand, (PPy)$_x$MoO$_3$ displayed a comparatively lower response to formaldehyde and exhibited a response when exposed to other VOCs (see Figure 8 for a visual comparison). This indicates that PANI seems to be a better sensing material than PPy. Therefore, it would be worth exploring other PANI derivatives for sensing formaldehyde.

a)

b)
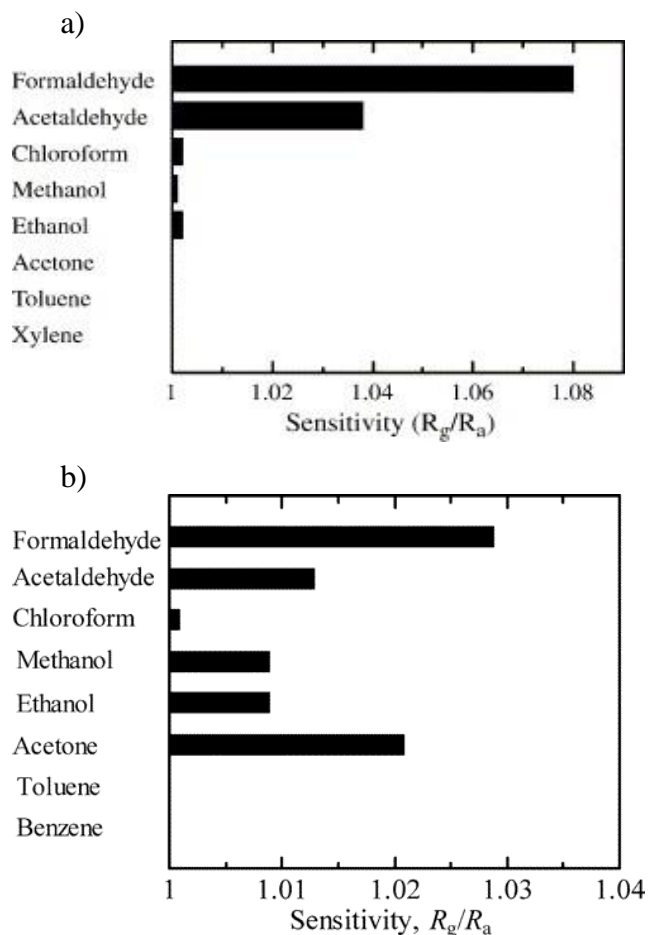
Figure 8: Sensitivity magnitude plot for (PANI)$_x$MoO$_3$ on exposure to various VOCs at 50 ppm [46] (by permission); b) Sensitivity plot for (PPy)$_x$MoO$_3$ on exposure to various VOCs at 1000 ppm [45] (by permission)

Itoh et al. [49] reported sensing of formaldehyde by an organic/inorganic hybrid material, (PNMA)$_x$MoO$_3$, based on a polyaniline derivative, poly (N-methyl aniline) (organic "guest") and MoO$_3$ (inorganic "host"). They observed an increase in resistance of the hybrid nanomaterial on exposure to aldehydic gases. Unlike (PPy)$_x$MoO$_3$ and (PANI)$_x$MoO$_3$ discussed earlier, a very

similar response was observed for both formaldehyde (S=2.6%) and acetaldehyde (S=2.8%) in the case of (PNMA)$_x$MoO$_3$ [49]. They suggested that an increase in the response of (PNMA)$_x$MoO$_3$ compared to that in the case of (PANI) $_x$MoO$_3$ can be attributed to the presence of an extra methyl group on the benzene ring. PNMA seems to have more "cave-like" gaps that are more readily able to accommodate acetaldehyde compared to PANI [49]. They also proposed a probable structural arrangement of (PANI) $_x$MoO$_3$ and (PNMA)$_x$MoO$_3$, as shown in Figure 9.
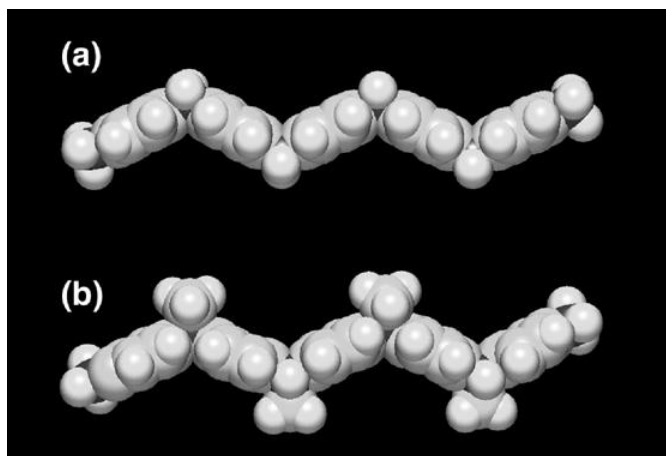
Figure 9: Proposed structural arrangement for a) (PANI) $_x$MoO$_3$ and b) (PNMA)$_x$MoO$_3$ [49] (by permission)

Another study was conducted by the same group [48] by fabricating a polyaniline derivative (poly (2,5-dimethylaniline) (PDMA)) based on intercalated nanohybrid materials and evaluated its sensitivity for VOCs. Itoh et al [48] prepared a (PDMA)$_x$MoO$_3$ layered hybrid structure and evaluated it for its sensitivity to VOCs such as formaldehyde, acetaldehyde, chloroform, methanol, ethanol, acetone, benzene, toluene, and xylene. On exposing (PDMA)$_x$MoO$_3$ to 10 ppm concentration of these VOCs (at 100 C), they observed a very high response towards aldehydic gases such as formaldehyde (S=3.9%) and acetaldehyde (S=4.7%), a weak response to chloroform and very little to no response in the case of the other VOCs. It is interesting to note that (PDMA)$_x$MoO$_3$ exhibited a larger response to acetaldehyde than formaldehyde [48]. This seems different from the typical (PANI)$_x$MoO$_3$ and (PNMA)$_x$MoO$_3$ response which displayed a higher response for formaldehyde than acetaldehyde. Although (PDMA)$_x$MoO$_3$ exhibited a higher response to formaldehyde compared to (PANI)$_x$MoO$_3$ and (PNMA)$_x$MoO$_3$, it might pose a selectivity issue as it is more sensitive to acetaldehyde than formaldehyde.

A similar trend (higher affinity to acetaldehyde than formaldehyde) was also observed when Itoh et al. [47] evaluated another PANI derivative-based hybrid material, poly(o-anisidine) ((PoANIS)$_x$MoO$_3$). A distinct change in resistance of the (PoANIS)$_x$MoO$_3$ hybrid thin film to aldehydes and alcohol gas was observed while no response towards other gases like chloroform, acetone, and aromatics gases. Moreover, they also indicated that a significant response was observed in particular for aldehydic gas; with a stronger response to acetaldehyde (4.4%)

compared to formaldehyde (2.4%). This suggested that the sensing affinity of (organic)$_x$MoO$_3$ hybrid structures towards different gases is affected by the presence of a particular functional group and the capability of VOCs to penetrate in the interlayers of these hybrid structures. The VOCs penetrate into the interlayer of the hybrid structures by a diffusion process. Hence, the higher sensitivity of the hybrid structures (PDMA)$_x$MoO$_3$ and (PoANIS)$_x$MoO$_3$ for acetaldehyde than formaldehyde, whereas other hybrid structures like (PNMA)$_x$MoO$_3$ may be equally sensitive to both aldehydic gases.

(PANI)$_x$MoO$_3$ and (PPy)$_x$MoO$_3$ show higher sensitivity towards formaldehyde than acetaldehyde probably due to favourable solubility parameters. A solubility parameter for polymers is defined as:

$$\delta = \frac{\rho}{M} \times \sum Fi \qquad\qquad 2.4$$

where δ, ρ, M and Fi stand for solubility parameter, density, molecular weight and molar attraction group constant, respectively. Table 4 cites several typical values for solubility parameters.

Table 4: Solubility parameters for some polymers and acetaldehyde

Organic Guest Backbone	Solubility Parameter (MPa)$^{1/2}$	Reference
Polypyrrole (PPy)	13.4	[48]
Polyaniline (PANI)	19.1	[47]
Poly(o-anisidine) (PoANIS)	20.5	[47]
Poly(N-methylaniline)	-	
Poly(2,5-dimethylaniline) (PDMA or P25DMA)	21.0	[48]
Acetaldehyde	21.1	[48]

From the solubility parameter values listed in Table 4, it is clear that polymers with solubility parameter values close to acetaldehyde may exhibit a strong response to acetaldehyde. This shows that the solubility parameter values are another indicator for pairing polymers with analytes.

There are two interesting trends to note from the discussion on sensing capabilities of PPy, PANI and PANI derivatives (hybrid structures) earlier. Firstly, PANI seems to be more sensitive and selective towards aldehydic gases compared to PPy. Secondly, on modifying PANI by substituting a hydrogen of the benzene ring by a methyl group, its sensitivity towards formaldehyde is observed to be decreasing on increasing the number of methyl groups. It should also be noted that not only does the sensitivity towards formaldehyde decrease but sensitivity towards acetaldehyde increases with an increase in the number of the methyl groups on benzene. This synergistic sensitivity trend can be a result of larger "cavities" and spaces created as a consequence of steric hindrance caused

by the presence of the methyl group(s) on the benzene ring in the PANI backbone. The larger the number of the methyl groups on the benzene ring, the greater the steric hindrance. Now that "cavities" and available interstitial spaces are comparatively larger in PANI derivatives, they can accept slightly bigger aldehydic gas molecules (than formaldehyde), like acetaldehyde, more readily. The sensitivity trend also aligns with the solubility parameter values listed in Table 4. PDMA (21.0 $(MPa)^{1/2}$) has a solubility parameter value closer to that of acetaldehyde (21.1 $(MPa)^{1/2}$) compared to that of PANI (19.1 $(MPa)^{1/2}$).

Hence, from the above discussion, it is clear that PANI and P25DMA are potentially good polymeric sensing materials for sensing aldehydic gases. In particular, PANI seems to be a better sensing material for formaldehyde and P25DMA for acetaldehyde.

Now that it has been established that PANI and PANI derivatives are potential polymeric sensing materials, the literature was specifically explored for PANI-based sensing of formaldehyde.

Srinives et al. [41] prepared a PANI-based thin-film sensor for sensing formaldehyde. They reported that the pristine PANI response on exposure to 100 ppm of formaldehyde was as low as 3%. Therefore, the PANI was functionalized with lysine hydrochloride (LYS) to improve the response and reported a 21% response signal on exposure to 100 ppm of formaldehyde [41]. It must be noted that the response signal values are fitted values using a Langmuir-like adsorption law. They proposed a sensing scheme of PANI functionalized with LYS for sensing formaldehyde as a nucleophilic addition reaction. The reaction between amines of PANI with LYS and formaldehyde led to the formation of Schiff base and water. As a result, the water formed during this reaction protonated the PANI and consequently decreased the resistance. Generally, water decreases the resistance of PANI and Schiff base increases the resistance, but they report dominance of the effect of water in this case [41], although evidence is not provided to support the claim. An enhanced response was observed for PANI with LYS as LYS accelerated the reaction between formaldehyde and the amine groups, due to the presence of extra amine functional groups compared to pristine PANI.

Zhu et al. [42] designed a PANI doped with TiO_2 and compared its performance with existing commercial activated carbon. They observed a 0.45 ppm sorption of F in 0.5 g of PANI/TiO_2 sensing material on exposure to about 0.6 ppm of trace formaldehyde gas. The sorption capacity was about 0.67 mg of formaldehyde/g of PANI/TiO_2, and 0.5 mg of formaldehyde/g of activated carbon via the Langmuir model [42]. This indicates that PANI/TiO_2 is a potentially good sensing material for formaldehyde.

Tang et al. [44] prepared a PPy-based formaldehyde sensor using Molecularly Imprinted Polymers (MIP) on a TiO_2-nanotube array (NTA) to overcome typical shortcomings of MIPs (low surface to volume ratio) and increase sensitivity. They observed a 13% increase in conductance response on exposing PPy-based MIP to formaldehyde of 1ppm concentration [44]. The MIP sensing layer consisted of a mixture of pyrrole-3-carboxylic acid and pyrrole. They suggested that the sensitive sensing of formaldehyde by PPy-based MIP layer is due to an increase in surface to volume ratio by synthesizing it on TiO_2-NTA, and that the selective sensing is due to its 'fishnet'-like morphology [44].

2.8 Deposition of Sensing materials

In general, physical deposition techniques are simple and flexible, as they can use previously synthesized polymeric materials. Given the micro-scale of the sensor, the solid (or powder) polymer cannot easily be placed directly on the "sense" plate. Therefore, most physical deposition techniques rely on creating a liquid mixture (a solution, dispersion or suspension) of the polymeric material in some solvent; the liquid aids in transporting a very small amount of the polymeric material to the target location. The polymer is then well dispersed, and the solvent evaporates to leave the polymer on the sense plate.

One of the major challenges with the physical deposition of PANI (and its derivatives) is the poor solubility of polyaniline in most standard solvents. Therefore, before exploring physical deposition techniques, solubility considerations were taken into account.

Several potential solvents for PANI are listed in Table 5, based on information from the literature. Solvents have been categorized as "good", "moderate" and "poor", given the findings of previous research (some of these findings are very qualitative and without much evidence, hence not so reliable). "Good" solvents have reportedly dissolved PANI completely to give a homogenous solution. In contrast, "moderate" solvents did not dissolve the polymer completely; rather, they formed a dispersion or micro-suspension. Finally, "poor" solvents leave several undissolved particles in solution, many of which are visible to the naked eye (i.e., the polymer forms aggregates; some aggregates precipitate, some "float"). Given the similar properties of PANI and P25DMA, we assume tentatively that the observations for PANI will also apply to P25DMA.

Table 5: Evaluation of solvents for PANI

Category of Solvent	Solvent	Remarks	Solubility (g PANI/100ml solvent, unless otherwise stated)	Reference
Good	NMP	Solubility of PANI in NMP decreased with an increasing particle size of PANI		[51]
		NMP is the best solvent for producing high-quality free-standing films of emeraldine base	1g/25ml of NMP	[52]
		Modified PANI for improved solubility	<9	[53]

Good	DMF	--	0.24	[52]
		Modified PANI is soluble in polar solvents like DMF, NMP and DMSO	<9	[53]
Good	DMSO	--	0.32	[52]
		Modified PANI is soluble in polar solvents like DMF, NMP and DMSO	<9	[53]
Good	DMPU	DMPU is a better solvent for PANI than NMP, thermodynamically speaking	--	[54]
Moderate	Chloroform	--	<3	[53]
		PANI-DBSA is completely soluble in chloroform	--	[55]
Moderate	MEK	Non-polar solvent	<6	[53]
Moderate	Acetic acid solution (aq)	Slightly soluble in 80% acetic acid (aq)	0.32	[56] [52]
Moderate	Formic acid solution (aq)	Slightly soluble in 60% and 88% formic acid (aq)	0.8 g in 60% solution of formic acid 1.8 g in 88% solution of formic acid	[52] [56]
Moderate	Methanol	Methanol shows higher solubility than water, propanol, and ethanol for PANI-EB	--	[57]
Poor	Butyl Acetate	Non-polar solvent	<3	[53]
Poor	Xylene	Non-polar solvent	<2	[53]
Poor	Ethanol	--	--	[57] [58]
Poor	Acetone	--	--	[58]
Poor	Benzene	PANI has poor solubility in non-polar solvents	--	[58]

Acronyms- (aq) = aqueous, DBSA = dodecyl benzenesulfonic acid, DMF = dimethylformamide, DMPU = dimethyl propylene-urea, DMSO = dimethyl sulfoxide, EB = emeraldine base, MEK = methyl ethyl ketone, NMP = N-Methyl-2-pyrrolidone, PANI = polyaniline

2.8.1 Solubility Parameters

Solubility parameters are helpful indicators of solubility. When a solvent's solubility parameter is close to the solute's solubility parameter, the solute is more likely to be soluble in the specific solvent.

The Hildebrand solubility parameter (δ) is related to the Hansen parameters as follows:

$$\delta = (\delta_d^2 + \delta_p^2 + \delta_h^2)^{1/2} \qquad\qquad 2.5$$

where δ_d, δ_p, δ_h are the Hansen parameters representing contributions from dispersion interactions (d), polar interactions (p), and hydrogen bonding interactions (h), respectively [59].

Several estimates of the Hildebrand parameter have been reported for PANI. For example, the empirical value of the Hildebrand solubility parameter was reported as $\delta=22.2$ MPa$^{1/2}$ when characterized by the solvent interaction parameters δ_d, δ_p, δ_h [60]. In contrast, the same group reported a solubility parameter estimate for PANI based on heat of vaporization of $\delta=23.8$ MPa$^{1/2}$ [59]. Even more Hildebrand solubility parameters for different forms (oxidation states) of PANI have been estimated using semi-empirical techniques: PANI-EB (Emeraldine base) = 24.2 MPa$^{1/2}$, and PANI-LE (Leuco-emeraldine base) = 22.7 MPa$^{1/2}$ [60]. With these Hildebrand solubility parameters in mind, one can explore potential solvents that might be suitable for PANI dissolution (and subsequent deposition). Some Hildebrand solubility parameters for common solvents are provided in Table 6 for reference; the information was obtained from [61] and [59].

Table 6: Hildebrand solubility parameter estimates for solvents (and PANI)

Solvent	δ (MPa$^{1/2}$)
Xylene	18.2
Butylamine	18.6
Benzene	18.7
Chloroform	18.7
Piperidine	19.3
Methyl ethyl ketone	19.3
Propylamine	19.7
Acetone	19.7

Dimethyl hydrazine	19.8
Picoline	20.9
Pyridine	21.7
Tetramethyl urea	21.7
Quinoline	22
Morpholine	22.1
Aniline	22.6
Dimethylacetamide	22.7
m-Cresol	22.7
Hexamethyl-phosphor amide	23.2
Benzyl alcohol	23.5
NMP	23.7
DMF	24.1
Ethylene Diamine	25.3
DMSO	26.4
2-Pyrrolidine	28.4
Methanol	29.7
Pyrrolidine	-
Benzylamine	-
Butyl acetate	-

Acronyms- DMF = dimethylformamide, DMSO = dimethyl sulfoxide, NMP = N-Methyl-2-pyrrolidone

Given the solubility parameter range reported for PANI, the solvents highlighted in green might be suitable. However, we can also use the Hansen method to determine appropriate solvents; this is described in Section 2.8.2. One, of course, should note that, whether Hiderbrand or Hansen, these are parameter values, often estimated only approximately or based on unreliable data. Hence, there is a wide range of values reported, so one should exercise caution.

2.8.2 Hansen Method

According to the Hansen solubility parameter model, the polymer is characterized as having a "solubility sphere" in 3D-space defined by δ_d, δ_p, δ_h. The centre of the solubility sphere is $(2\delta'_d, \delta'_p, \delta'_h)$ and the radius of the sphere is R. The radius of the sphere calculated for PANI was R=6 by sampling the Hansen space with a series of solvents. The interaction distance (r) for a given solvent was defined as:

$$r = [4(\delta_d - \delta'_d)^2 + (\delta_p - \delta'_p)^2 + (\delta_h - \delta'_h)^2]^{1/2} \qquad 2.6$$

The polymer could be soluble in a given solvent if the value of r < R. Therefore, solvents with values of r < 6 could be suitable for PANI [59]. The r values for several solvents are shown in Table 7; these data were again obtained from [61] [59]. Once more, the solvents in "green" seem to have more affinity with PANI, and there is overlap with the "green" area of Table 6.

Table 7: Interaction distance for solvents

Solvent	r (MPa$^{1/2}$)
Tetramethyl urea	1.4
Hexamethyl-phosphor amide	2
Pyridine	3.2
Dimethylacetamide	3.2
Morpholine	4
Picoline	4
NMP	4.1
Propylamine	4.1
Butylamine	4.9
Dimethyl hydrazine	5
Quinoline	5.1
Piperidine	5.2
DMF	5.3
Aniline	5.3

m-Cresol	5.5
Benzyl alcohol	5.5
Ethylenediamine	6.8
DMSO	8.2
2-Pyrrolidine	9.8
Pyrrolidine	-
Benzylamine	-

Acronyms- DMF = dimethylformamide, DMSO = dimethyl sulfoxide, NMP = N-Methyl-2-pyrrolidone

To summarize, four solvents were identified as "good" in Table 5; these have reportedly allowed for the complete dissolution of PANI and the preparation of homogeneous solutions. Given the solubility parameters described herein, both N-methyl pyrrolidone (NMP) and dimethylformamide (DMF) are strong candidates. Dimethyl propylene-urea (DMPU) may also be a possibility, but dimethyl sulfoxide (DMSO) solubility parameters do not seem compatible with polyaniline.

Chapter 3: Experimental

3.1 Synthesis of Sensing Materials

After carefully considering the literature background, undoped and doped polyaniline (PANI) and PANI derivatives such as poly(2,5-dimethylaniline) (P25DMA) were selected, synthesized, and characterized for sorption capabilities and morphology. A detailed list of polymeric materials is presented later in Table 8 (Section 3.2.2).

For the synthesis of PANI and P25DMA, aniline and 2,5-dimethylaniline monomers, and ammonium persulfate (APS) initiator were purchased from Sigma-Aldrich (Oakville, Ontario, Canada). Metal oxide (MO) nanoparticles (used for doping) of indium (III) oxide (In_2O_3) (nanopowder), <100 nm particle size), 99.9% trace metals basis), nickel (II) oxide (NiO) (particle size <50 nm, concentration of 99.8%), and titanium (IV) oxide (TiO_2) (particle size 21 nm, concentration of 99.5%) were also purchased from Sigma-Aldrich. Deionized (DI) water was used as the reaction medium, and for washing and rinsing, and ethanol (ACS grade) was used as received for additional washing and rinsing of the synthesized polymers.

3.1.1 Synthesis of PANI (Undoped)

PANI synthesized in the lab is referred to as PANI (L) in this thesis. PANI was prepared using aniline monomer, APS, and DI water in the same proportions as the recipe in Stewart et al. [62]. The starting formulation involved 1.02 g (1 ml) of aniline and 50 ml of deionized water, which were mixed in a 100 ml round bottom flask using a sonicator for 30 min. The flask containing the reaction mixture was cooled for 30 min at -1 °C in a cooling bath. Later, 2.5 g of APS was dissolved in 12 ml of DI water and added to the reaction mixture, and the reaction was initiated. The reaction mixture was left to polymerize at -1 °C for 6 hours. The flask was given a swirl every 15 min for the first hour and subsequently every 30 min for the remaining 5 hours. After completion of the 6 hours, the polymer solution was filtered using Whatman #5 filter paper and washed with DI water first and then with ethanol at least three times. The polymer powder was then left to dry in the fumehood for 24hrs or more. The polymer powder was then scraped, collected and stored in a vial in a cool dry place.

3.1.2 Synthesis of P25DMA (Undoped)

For P25DMA, 0.4g of 2,5-dimethylaniline and 20 ml of deionized water were mixed in a 100 ml round bottom flask. The rest of the synthesis procedure followed the same steps as for PANI synthesis in Section 3.1.1.

3.1.3 Synthesis of Doped Materials

In this case, the appropriate dopant was added up to 20% by weight.

For instance, in case of PANI doped with 5% In_2O_3, the starting solution involved 5% indium oxide (by weight with respect to monomer), 95% aniline (by weight), and 50 ml of deionized water (all added in a 100 ml round bottom flask). The rest of the synthesis procedure followed the same steps as for PANI synthesis in Section 3.1.1.

In another example, in P25DMA with 20% TiO_2, the starting solution involved 20% titanium dioxide (by weight with respect to monomer), 80% 2,5 dimethylaniline (by weight), and 20 ml of deionized water (again in a 100 ml round bottom flask). The rest of the synthesis procedure followed the same steps as for undoped P25DMA synthesis in Section 3.1.2.

3.1.4 Other Materials Employed

Polyaniline was also purchased from Sigma-Aldrich, and is referred to as PANI (S). PANI (S) had a molecular weight (Mw) of 100,000 and was used as received, mainly for comparison purposes.

Poly(methyl methacrylate) or PMMA and poly(acrylic acid) or PAAc were purchased and used as received. PMMA samples with two different molecular weights (Mw = 1,000,000 and Mw = 500,000) were synthesised in the lab (by another operator, as described in reference [63]). Another PMMA sample (Mw ~15,000) was purchased from Sigma-Aldrich.

The purchased PAAc samples had three different molecular weights: Mn = 130,000 (number-average molecular weight) and Mv = 450,000 (viscosity-average molecular weight), both from Sigma-Aldrich. The third sample had a Mw = 1,000,000 (weight-average molecular weight), from Polysciences, Inc (Warrington, PA, USA).

3.2 Gas Sorption Experiments

3.2.1 Gas Test Set-up

Analyte-containing gases used for sensing material evaluation were purchased from Praxair (Mississauga, Ontario, Canada). Gases containing 10 parts-per-million (ppm) of formaldehyde (F), 10 ppm of benzene, 5 ppm of formaldehyde, and 5 ppm of acetaldehyde were of standard grade, in nitrogen. Pure nitrogen (also from Praxair, 5.0 grade) was used to purge samples before being tested.

The test set-up for sorption studies has been described previously in reference [64]. Each polymeric sensing material is exposed to a gas (containing known concentrations of one or more analytes), and the amount of analyte that sorbs onto the sensing material is measured. If the sensing material being evaluated is sensitive to the target analyte, higher quantities of the analyte are sorbed. All sorption measurements are taken at room temperature (~23-24°C) (unless otherwise stated) and approximately 15 psi.

The set-up uses a difference in gas concentration (before and after exposure to the sensing material) to establish how much of the target analyte has been sorbed. Before exposure, a "blank" run can be analyzed by a highly accurate Varian 450 gas chromatograph (GC) (with a specialized photon discharge helium ionization detector (PDHID)) to determine the gas concentration for the case of no sorption. After exposure to the sensing material, the gas stream flows into the GC, which can distinguish between similar analytes and record concentrations down to the parts-per-billion (ppb) level. A schematic of the sorption test set-up is shown in Figure 10, and photos of the lab set-up are shown in Figure 11.
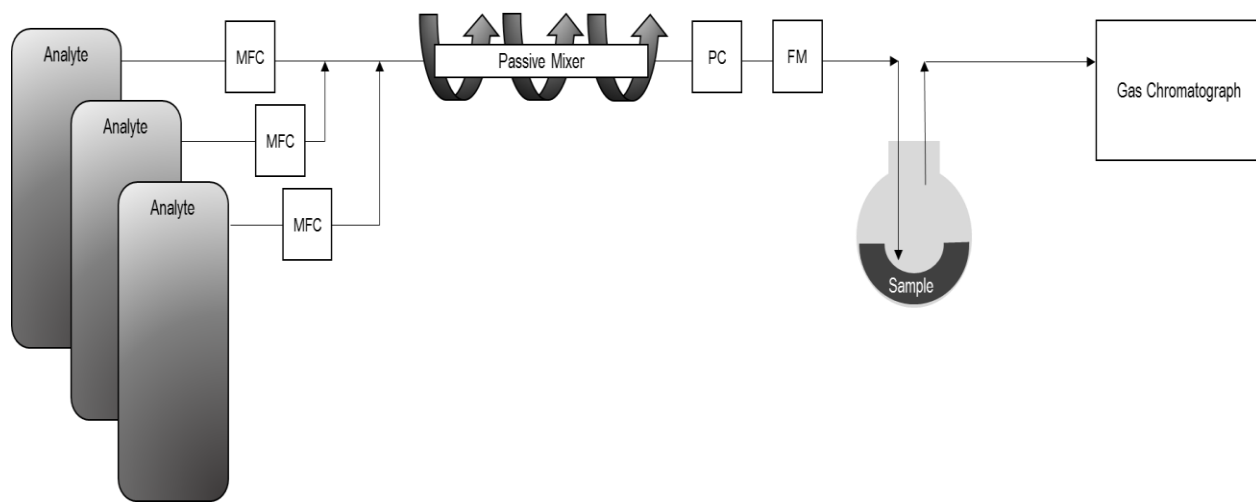
Figure 10: Schematic representation of gas test set-up

a)

b)
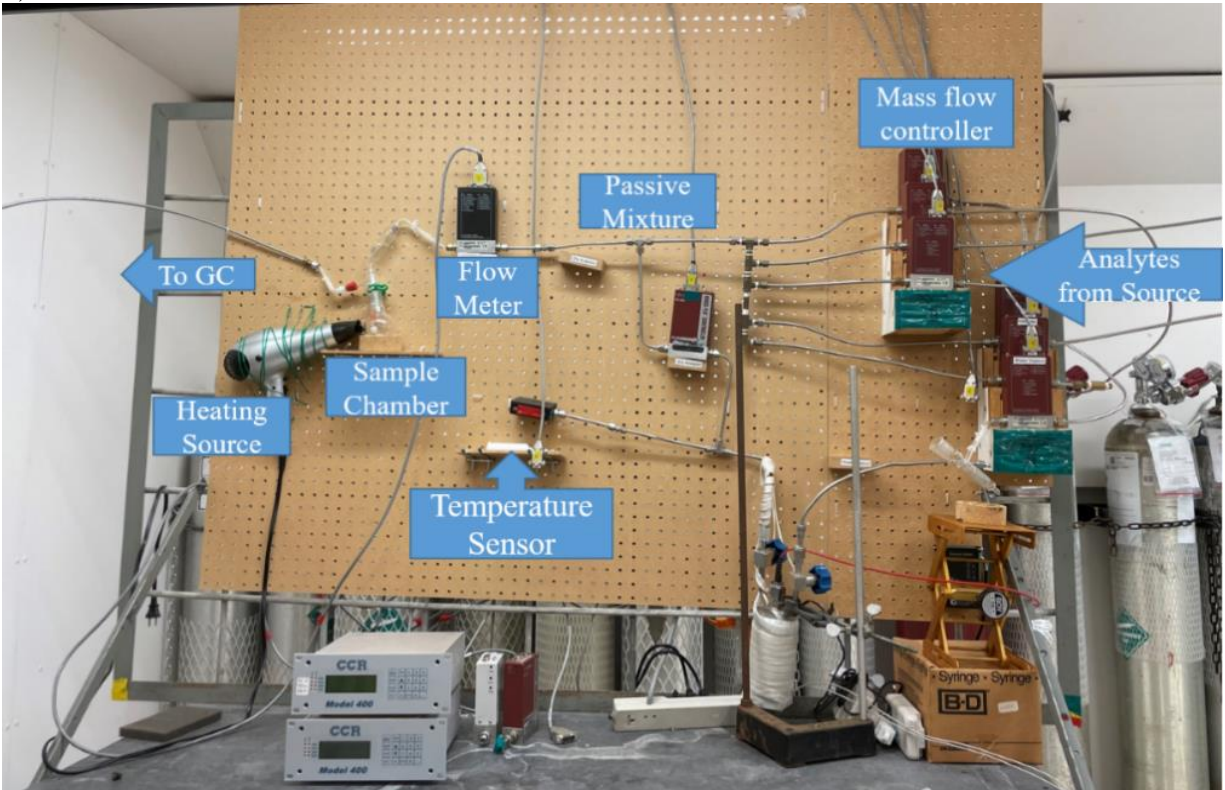
c)

Figure 11: Photos of set-up for evaluation of sensing materials a) cylinders of gas analytes; b) sample gas flow set-up; c) gas chromatograph

For instance, the specific procedure for measuring PANI's ability to sorb formaldehyde from a 10 ppm formaldehyde source is outlined below:

1. 10 ppm formaldehyde in nitrogen balance is introduced to the system at a rate of 200 sccm for 1 hour, to ensure that the entire test system contains 10 ppm formaldehyde.

2. A blank (empty) flask is present in place of the sample flask (recall Figure 10), to let all of the formaldehyde coming from the tank go directly into the gas chromatograph.

3a. The GC measures the gas concentration under these conditions, to obtain a baseline for the day. This would be close to 10 ppm but may change slightly from day to day (due to random fluctuations). The gas concentration is measured every 12 minutes until two consecutive readings are stable. This typically takes between one and two hours and indicates that the system has reached steady-state.

3b. While establishing the baseline for the day, the flask containing the PANI sample is purged under pure nitrogen flow at 200 sccm.

4. Once the baseline is established (or "blank" value) for the day, the blank flask is replaced with the flask containing the PANI sample. Now, the flowing formaldehyde gas is exposed to the sensing material. If it is an appropriate sensing material for formaldehyde, some of the formaldehyde gas will be sorbed (adsorbed or absorbed) by the sensing material and the rest will be en route to GC. Since some of the formaldehyde is sorbed by the PANI, the GC will record a lower formaldehyde concentration. Again, the formaldehyde concentration is recorded every 12 minutes until two (or, sometimes, more) consecutive stable measurements are obtained.

5. Finally, the concentration of formaldehyde sorbed by the PANI sample can be calculated by:

$$\text{ppm sorbed by polymer}$$
$$= \text{ppm measured before exposure to polymer} - \text{ppm measured after exposure to polymer}$$

The same process is repeated for all sensing materials and all gas analytes. In the case of a mixture of gases, for instance, formaldehyde/benzene (5/5ppm) is obtained from 10 ppm of formaldehyde in nitrogen balance and 10 ppm benzene in nitrogen balance source (cylinder) by setting the gas flowrates at about 100 sccm for each analyte.

A detailed list of the sensing materials tested for sorption when exposed to different analytes is presented in Section 3.2.2

3.2.2 Gas Analytes Tested

Sensing materials were tested for important sensing characteristics such as sensitivity, selectivity, and stability. All sorption tests used 0.1g of PANI and/or doped PANI (with a metal oxide) or other sensing materials (e.g., modified PANI, PAAc or PMMA, etc.), unless otherwise stated. A mass of 0.1g of polymer was weighed and deposited in a 100 ml round bottom flask with about 5 ml of ethanol. In the case of the PMMA, acetone was used instead of ethanol for deposition. The flask was further swirled for a minute and the flask was left open for the ethanol to evaporate in the fumehood.

For all gas sorption studies, potential polymeric sensing materials were evaluated based on the amount of the gas sorbed by 0.1 g of polymer. For sensitivity, the sensing materials were exposed to a single gas source such as formaldehyde (F) 10 ppm, benzene (B) 10 ppm, and 5 ppm acetaldehyde (Ac). For selectivity of F over other gases, sensing materials were exposed to a mixture of two gases such as F/B (5/5 ppm each), and F/Ac (2.5/2.5 ppm each). For stability studies (effect of temperature), the sensing materials were exposed to F 10 ppm (source) and the temperature was varied by heating the flask containing the sensing material from ~25°C to ~60°C. For stability studies (effect of ageing), the sensing materials prepared at different times in the last decade were exposed to F 10 ppm gas source. The effects of pressure and humidity are of lesser

importance in this thesis, since the effect of pressure is equivalent to a concentration effect (which has been studied in detail), whereas the effect of humidity is implicitly taken into account, as the experimental set-up is not hermetically closed.

Over almost 15 months of experimentation, the average lab temperature was between 20 and 25 C. Humidity levels were between 40% and 60%. We did our best to collect data under similar environmental conditions (for instance, if we knew in advance that the forecast for a specific week in the summer called for humidity levels higher than typical lab levels, say, above 60%, we would postpone the trials to the following week). Please note that the ventilation system in the E6 building is often unreliable. That caused delays in experimentation, if the data points collected were unreliable due to unexpected temperature and humidity fluctuations.

Table 8 lists all the sorption trials performed for analyzing polymeric sensing materials for their capability to sorb formaldehyde or other gas analytes. Please note that each trial may require about one week (sometimes up to ten days) from synthesis to sorption testing to final property characterization/data analysis.

Table 8: List of gas sorption tests

Case no.	Sensing material	Source	Purpose of test
1	PANI or PANI (L)	F (10 ppm)	Sensitivity of F
2	P25DMA	F (10 ppm)	Sensitivity of F
3	PANI with 5% In_2O_3	F (10 ppm)	Sensitivity of F
4	PANI with 10% In_2O_3	F (10 ppm)	Sensitivity of F
5	PANI with 2.5% In_2O_3	F (10 ppm)	Sensitivity of F
6	PANI with 1.25% In_2O_3	F (10 ppm)	Sensitivity of F
7	P25DMA	F (10 ppm)	Sensitivity of F
8	P25DMA with 20% TiO_2	F (10 ppm)	Sensitivity of F
9	P25DMA with 10% NiO	F (10 ppm)	Sensitivity of F
10	PANI	B (10 ppm)	Sensitivity of B
11	P25DMA	B (10 ppm)	Sensitivity of B
12	PANI with 5% In_2O_3	B (10 ppm)	Sensitivity of B
13	PANI with 10% In_2O_3	B (10 ppm)	Sensitivity of B
14	P25DMA with 20% TiO_2	B (10 ppm)	Sensitivity of B
15	PANI	Ac (5 ppm)	Sensitivity of Ac

16	P25DMA	Ac (5 ppm)	Sensitivity of Ac
17	PANI with 5% In_2O_3	Ac (5 ppm)	Sensitivity of Ac
18	PANI with 10% In_2O_3	Ac (5 ppm)	Sensitivity of Ac
19	PANI with 2.5% In_2O_3	Ac (5 ppm)	Sensitivity of Ac
20	PANI with 1.25% In_2O_3	Ac (5 ppm)	Sensitivity of Ac
21	P25DMA	Ac (5 ppm)	Sensitivity of Ac
22	P25DMA with 20% TiO_2	Ac (5 ppm)	Sensitivity of Ac
23	P25DMA with 10% NiO	Ac (5 ppm)	Sensitivity of Ac
24	PANI	F/B (5/5 ppm)	Selectivity of F over B
25	P25DMA	F/B (5/5 ppm)	Selectivity of F over B
26	PANI with 5% In_2O_3	F/B (5/5 ppm)	Selectivity of F over B
27	PANI with 10% In_2O_3	F/B (5/5 ppm)	Selectivity of F over B
28	PANI with 2.5% In_2O_3	F/B (5/5 ppm)	Selectivity of F over B
29	PANI with 1.25% In_2O_3	F/B (5/5 ppm)	Selectivity of F over B
30	P25DMA	F/B (5/5 ppm)	Selectivity of F over B
31	P25DMA with 20% TiO_2	F/B (5/5 ppm)	Selectivity of F over B
32	PANI	F/Ac (2.5 ppm)	Selectivity of F over Ac
33	P25DMA	F/Ac (2.5 ppm)	Selectivity of F over Ac
34	PANI with 5% In_2O_3	F/Ac (2.5 ppm)	Selectivity of F over Ac
35	PANI with 10% In_2O_3	F/Ac (2.5 ppm)	Selectivity of F over Ac
36	PANI with 2.5% In_2O_3	F/Ac (2.5 ppm)	Selectivity of F over Ac
37	PANI with 1.25% In_2O_3	F/Ac (2.5 ppm)	Selectivity of F over Ac
38	P25DMA	F/Ac (2.5 ppm)	Selectivity of F over Ac
39	P25DMA with 20% TiO_2	F/Ac (2.5 ppm)	Selectivity of F over Ac
40	P25DMA with 10% NiO	F/Ac (2.5 ppm)	Selectivity of F over Ac
41	PAAc 450K	B (10 ppm)	Sensitivity of B
42	PAAc 130K	B (10 ppm)	Sensitivity of B
43	PAAc 1M	B (10 ppm)	Sensitivity of B
44	PMMA 1M	B (10 ppm)	Sensitivity of B

45	PMMA 15K	B (10 ppm)	Sensitivity of B
46	PMMA 0.5M	B (10 ppm)	Sensitivity of B
47	PAAc 450K	F (10 ppm)	Sensitivity of F
48	PAAc 1M	F (10 ppm)	Sensitivity of F
49	PMMA 1M	F (10 ppm)	Sensitivity of F
50	PANI with 5% In_2O_3 with temperature (T) variation	F (10 ppm)	Sensitivity of F
51	0.3g of PANI (L)	F (10 ppm)	Sensitivity of F
52	0.5g of PANI (L)	F (10 ppm)	Sensitivity of F
53	0.1g of PANI (S)	F (10 ppm)	Sensitivity of F
54	0.5g pf PANI (S)	F (10 ppm)	Sensitivity of F

Note: PANI or PANI (L) refers to PANI synthesized in the lab, whereas PANI (S) refers to commercially available PANI from Sigma.

3.3 Characterization of Sensing Materials

3.3.1 Energy Dispersive X-Rays (EDX) and Scanning Electron Microscopy (SEM)

SEM analyses were performed selectively for the representative samples in Table 9, whereas EDX analysis was even more selective.

SEM stubs were prepared by sticking roughly 1 cm^2 pieces of carbon tape on each stub. The polymer sample was suspended in a small volume of ethanol, pipetted, and deposited on the carbon tape, labelled, and left for ethanol to evaporate at room temperature. All the less conductive or non-conductive polymers (like doped and undoped P25DMA) were gold coated. The gold coating helps to increase the conductivity of the sample. As a result, the sample scatters the beam when an electron beam is focused to obtain an image of the surface of the sample.

The same stubs were used for EDX as well. For SEM/EDX analyses, a Zeiss Ultra Plus FESEM machine (WATLAB facilities) was used to capture the images at different magnifications (see Figure 12 for the test set-up). The instrument was equipped with 3 different detectors, SE2, BSD and In-lens. In-lens seemed to be appropriate for most of the sample images. A 10 kV of accelerating voltage was applied while capturing the surface morphology of the samples.

Table 9: Sample Characterization using SEM, EDX and XRD

Sample name	Techniques to characterize the sample		
PANI (polyaniline)	SEM	XRD	
PANI doped with 0.625 wt.% In_2O_3	SEM		
PANI doped with 1.25 wt.% In_2O_3	SEM		
PANI doped with 2.5 wt.% In_2O_3	SEM	XRD	EDX
PANI doped with 5 wt.% In_2O_3	SEM		
PANI doped with 10 wt.% In_2O_3	SEM	XRD	EDX
P25DMA (poly(2,5 dimethylaniline))	SEM		
P25DMA doped with 20% TiO_2	SEM	XRD	EDX
P25DMA doped with 10% NiO	SEM		
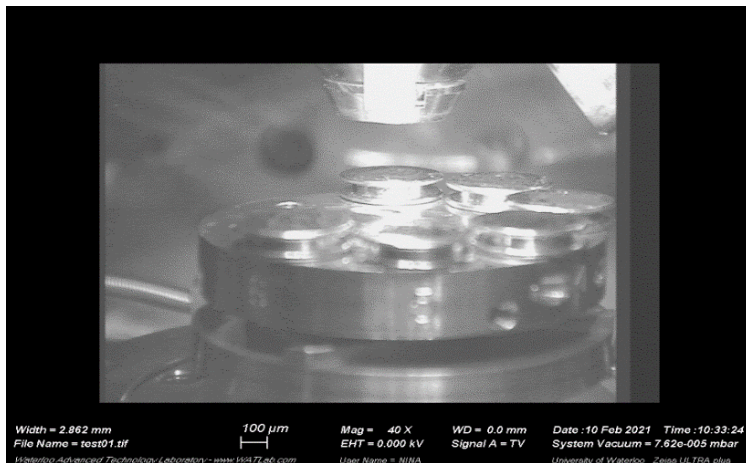
Figure 12: SEM/EDX test set-up

The SEM uses a focused electron beam to scan the surface and create an image. The electron beam interacts with the surface by scattering the beam to attain information of the surface morphology (and composition). There are light and dark regions in a typical SEM image. The contrast is due to the difference in scattering capabilities of the higher and lower atomic number of the elements present in that area. For example, regions with carbon will appear to be comparatively darker than the ones containing a metal oxide (see Chapter 7 for more details)

3.3.2 X-Ray Diffraction (XRD)

XRD was performed for selective samples (see Table 9). XRD glass slides were prepared by sticking a double-sided sticky tape of 1 cm^2 on the glass slide. The polymer suspended in ethanol was deposited on the sticky tape and the ethanol was left to evaporate. The samples for XRD were prepared by Dr. Nina Heinig of the WATLAB facility. A PANalytical Material Powder Diffractometer (MPD)-Pro was used to study and analyze the crystallinity of the polymeric samples. The source was a Cu tube at 45 kV and 35 mA (K-alpha1 = 1.540598 Å; K-Alpha2 = 1.544426 Å; K-Beta = 1.39225 Å), and scans were performed at 25°C over the range of 2θ = 5° to 90°.

XRD is a technique used to characterize the amorphous or crystalline nature of the polymer. It is based on the interaction of the 'constructive' monochromatic X-rays and the polymer sample. The X-rays are generated from the cathode ray tube, concentrated and directed towards the sample. The interaction of the X-rays and sample is 'constructive' when it satisfies Braggs law nλ=2dsinθ. These diffracted rays are then processed and analyzed. The samples are scanned over a range of 2θ to cover all possible diffractions of the crystal lattice.

3.4 Deposition of Sensing Materials on MEMS Sensor

After considering different physical deposition methods (as discussed in Section 2.8), most of the physical deposition methods can be performed using a polymeric "solution". A polymeric solution is a mixture of polymeric material suspended or dispersed in some appropriate solvent. The polymeric "solution" is then applied on the sensor using a semi-automated deposition set-up described further in Section 3.4.2.

Note: This does not belong directly to the objectives of this thesis. Deposition on the actual sensor is the main objective of the researchers in the department of Systems Design Engineering. The thesis author has closely collaborated and interacted with these researchers, by providing assistance with respect to suggesting promising polymeric materials to be subsequently evaluated with respect to their viability in deposition.

3.4.1 Solubility testing

One of the major challenges with physical deposition of PANI (and its derivatives) is the rather poor solubility of polyaniline in most standard solvents. Therefore, before exploring physical deposition techniques, solubility considerations were taken into account.

Once the two most promising solvents were selected (NMP and DMF) as per Section 2.8, the solubility of polyaniline was investigated experimentally. Furthermore, solutions were also

prepared using other solvents such as dimethyl sulfoxide (DMSO), tetrahydrofuran (THF), ethylene glycol (EG) and water. PANI was available from two sources: commercial polyaniline (purchased from Sigma) and polyaniline synthesized in the lab (see Section 3.1), designated as PANI (S) and PANI (L), respectively. The solubility testing was performed by preparing 10 ml of PANI "solutions" in 20 ml vials.

In a 20 ml vial, different wt.% of PANI was mixed with 10 ml of respective solvent (NMP, DMF, DMSO, and THF). The solutions were mixed by shaking them for about a minute and were left to stand for a day. Further details about solubility testing are provided in Appendix B. The solutions were subsequently transferred to a petri dish to investigate film casting (see Appendix C for more details on film casting). In order to accommodate the sensor fabrication steps, PANI (L) and PANI (S) were additionally treated with the EKC 265 etchant, as described in Appendix D (eventually deposited in a 100 ml round bottom flask using the same steps described earlier in Section 3.2.2 and tested for sorption of formaldehyde). The EKC 265 is a strong solvent (surface cleaning agent, actually) commonly employed for electronic circuit surface cleaning (Electrical Engineering).

3.4.2 Deposition Set-up

The deposition of a polymeric sensing material on the MEMS sensor was performed using a semi-automated deposition set-up as shown in Figure 13. The system consists of two main systems: a commercial microplotter, SonoPlot Microplotter Desktop [65], and a nano stage.
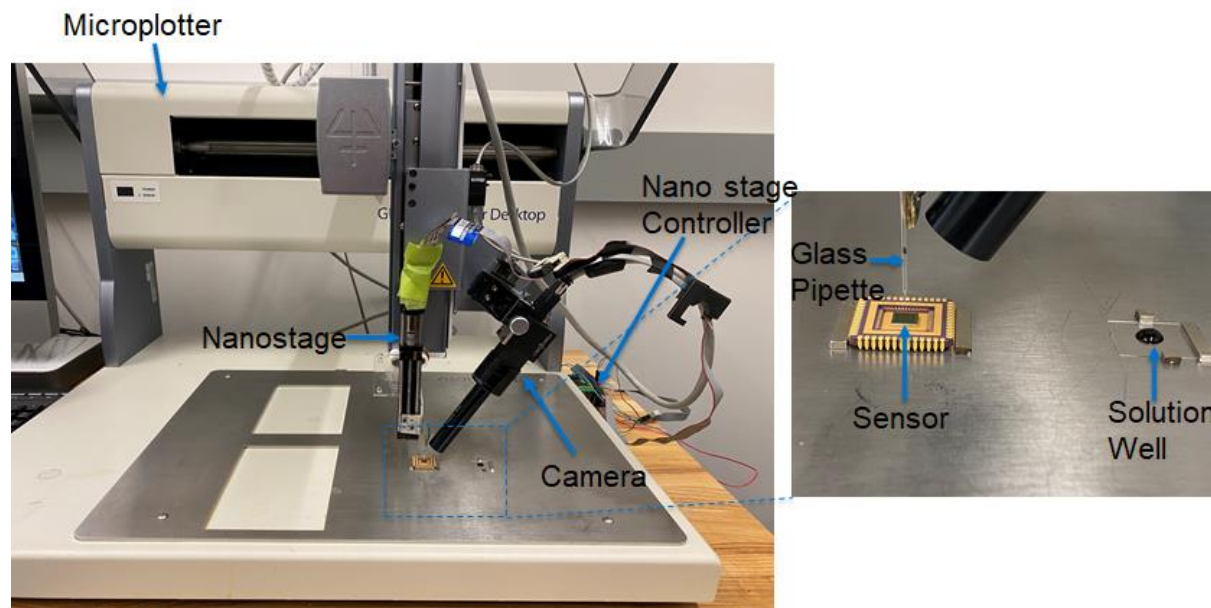
Figure 13: Experimental set-up of the semi-automated deposition process.

A Microplotter instrument is capable of applying picoliters of fluid to a surface to create features as small as 30 micrometres (microns) wide due to its use of a novel form of fluid ejection based on ultrasonic pumping.

To dispense fluid on a sensor, the dispenser head was loaded with the polymer solution and made to contact the surface of the sensor. The micropipette/microneedle (dispenser) is attached to the piezoelectric element as shown in Figure 14. When current is supplied to this element, it vibrates and pumping action occurs in the pipette, and fluid is dispensed on the microplotter instrument. This electronically controlled pumping action makes it possible to put very small amounts of fluid on a surface (e.g., MEMS sensor device) and quite precisely.

When the dispenser is brought close enough to the surface, a droplet will be touched off. The ultrasonics are then deactivated and the dispenser is retracted from the surface. SonoGuide is the main control interface for the Microplotter Desktop instrument. Movement of the positioning system, calibration of substrates, and operation of the dispensers are all controlled through this software.
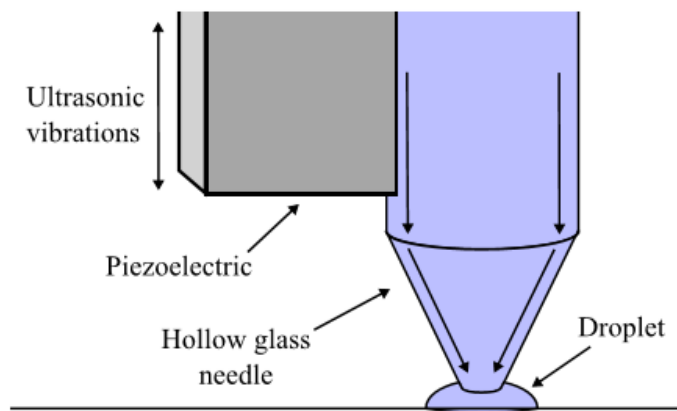
Figure 14: Fluid deposition

Specifications

Feature size: 30 µm - 200 µm
Feature types: Droplets
Deposition volume: ≥ 1.8 pL
Deposition variability: As low as 10% (or less)
Viscosity: ≤ 450 cP

Chapter 4: Results and Discussion – Sensitivity Studies

4.1 Formaldehyde (F) Gas Sensitivity Studies

Undoped PANI and P25DMA were initially evaluated for their sensitivity towards formaldehyde by exposing them to F 10 ppm source using the gas test set-up described in Section 3.2.1. From the sorption plot presented in Figure 15, it seems that PANI sorbs an average of 1.32 ppm of F, while P25DMA seems to sorb 1.16 ppm of F from F 10 ppm source.
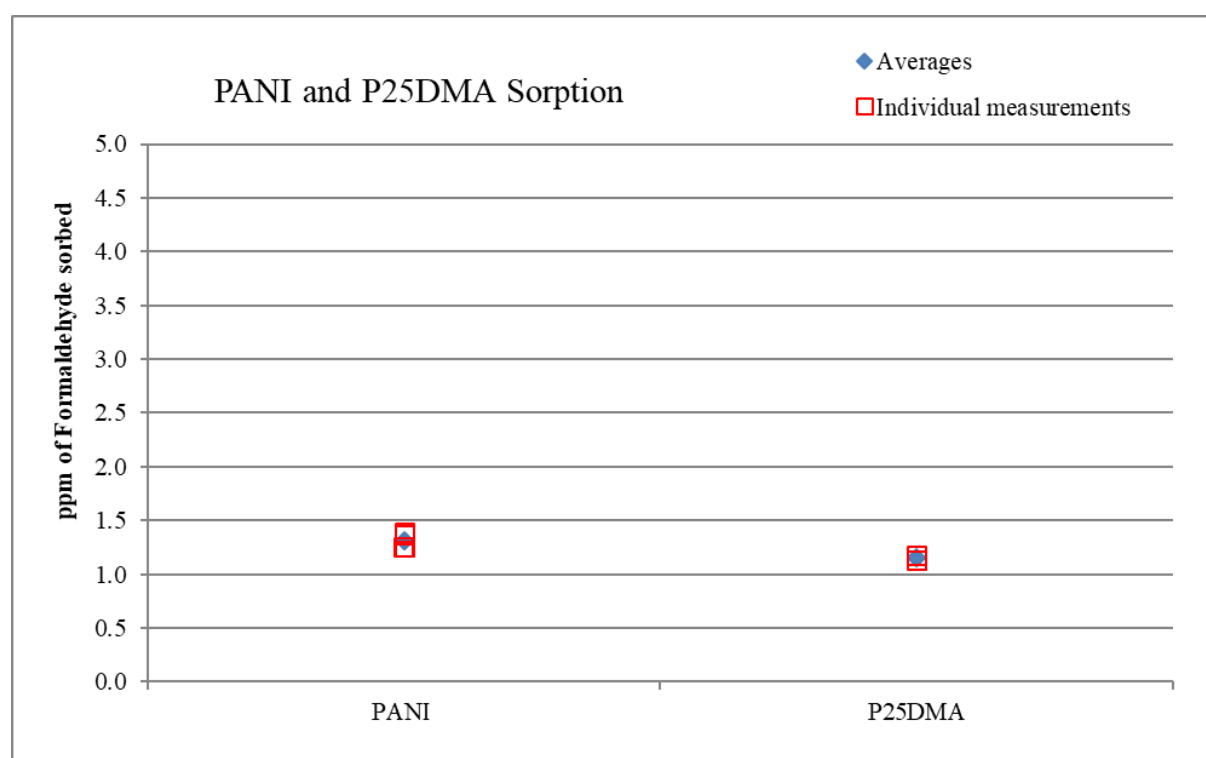
Figure 15: Formaldehyde sorption (in ppm) for PANI and P25DMA; (Source: F 10 ppm)

The results presented in Figure 15 suggest that PANI seems to sorb slightly more formaldehyde than P25DMA on exposure to F 10 ppm source, suggesting that PANI is marginally superior. The PANI and P25DMA sorption of F results presented in Figure 15 are also in agreement with the sorption trends observed by Wang et al. [46] and Itoh et al. [48]. Wang et al. [46] observed an 8% response on exposure to 50 ppm F source in the case of $(PANI)_xMoO_3$ and Itoh et al. [48] observed 3.9% on exposure to 10 ppm F source in the case of $(P25DMA)_xMoO_3$.

The (slightly) lower sorption of F with P25DMA compared to PANI can be attributed to the presence of two methyl groups in P25DMA. The methyl groups in P25DMA seem to cause more

steric hindrance and also lower packing efficiency compared to PANI [62]. This suggests that the backbone and surface morphology of the polymeric material seem to influence its sensing characteristics.

It is common knowledge that on increasing the surface to volume ratio of a sensing material the overall sorption increases. Therefore, to enhance sensitivity of PANI (or P25DMA) towards formaldehyde, one might keep the same backbone but add a dopant in order to modify the surface morphology and increase the surface to volume ratio of the polymeric sensing material.

Metal oxides are known to possess higher surface areas and are used as catalysts for several chemical reactions. Therefore, a metal oxide dopant was incorporated in the PANI and P25DMA to investigate whether one could enhance sorption of formaldehyde.

What determined the selection of our dopants?

PANI was doped with In_2O_3. From the literature, In_2O_3

- is an n-type semiconductor with bandgap of 3.55-3.75eV [66].
- exhibits a relatively large surface area compared to other metal oxides due to its hollow cubic structure [67]
- is sensitive and selective to oxidizing gases [66]

P25DMA was doped with TiO_2 and NiO because:

- both TiO_2 and NiO are semiconductors with high surface area [42] [68]
- the metal oxides create 'kinks' on coordinating with the PANI backbone, which results in more 'cavities' and enhances sorption of gas analytes in PANI [30]

4.1.1 PANI and doped PANI with MO

Doped PANI with 5% In_2O_3 was evaluated for its sorption of F by exposing it to a 10 ppm F source and compared with the existing PANI sorption of F data. As shown in Figure 16, on incorporating PANI with 5% In_2O_3, the sensitivity towards F increases. PANI with 5% In_2O_3 seems to sorb an average of 1.63 ppm of F on exposure to a 10 ppm F source. The increase in sorption of F on doping PANI with indium oxide can be attributed to the hollow porous nature of the indium metal oxide [67]. (Later, Chapter 7 will look at additional corroborations of sorption performance of different sensing materials). Therefore, the In_2O_3 dopant seemed to have (at first glance) a positive effect on increasing the sensitivity of PANI towards F, hence it seemed to be a promising dopant.
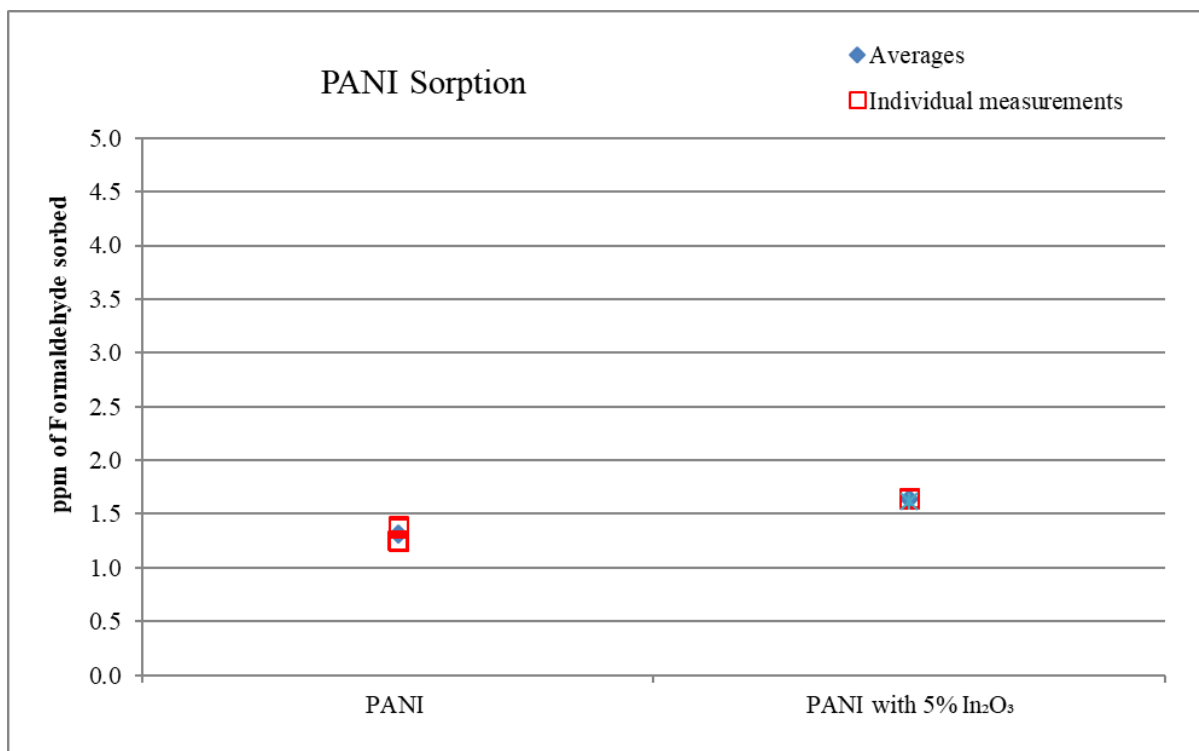
Figure 16: Formaldehyde sorption (in ppm) for PANI and PANI with 5% In_2O_3; (Source: F 10 ppm)

Next, PANI samples doped with different weight % levels of In_2O_3 (above and below 5%) were prepared and assessed for sorption. Summary results are shown in Table 10 and Figure 17/Figure 18. Figure 18 shows basically the same information as Figure 17 but in % sorption (as most of papers in the literature report % sorption but without necessarily specifying the source).

The interesting observation in Figure 17/Figure 18 is the identification of an optimum dopant concentration. To the author's knowledge, this is a first in the literature.

Figure 17/Figure 18 show that on decreasing weight percent of In_2O_3 dopant in PANI, the sensitivity of PANI towards F seems to increase. This seemed counterintuitive at first glance, at least based on previous sensor literature statements (that eventually were deemed unreliable and uncorroborated). Hence, a whole series of PANI materials doped with different wt. % of In_2O_3 was synthesized and tested for its sensitivity towards F. On exposing PANI with 1.25% of In_2O_3, sorption of F was enhanced even further. PANI with 1.25% In_2O_3 sorbed an average of 2.49 ppm of F when exposed to 10 ppm F source, as shown in Table 10 and Figure 17/Figure 18. The improvement in sensitivity can be attributed to the change in morphology of PANI on decreasing the amount of the In_2O_3 dopant (discussed in detail in Chapter 7).

Table 10: Average sorption values (in ppm of F) for PANI and doped PANI with different wt.% In_2O_3

Sensing Material	Average sorption values
PANI	1.315 ± 0.037749 ppm of F
PANI with 1.25% In_2O_3	2.49 ± 0.015 ppm of F
PANI with 2.5% In_2O_3	1.99 ± 0.005 ppm of F
PANI with 5% In_2O_3	1.6425 ± 0.00707 ppm of F
PANI with 10% In_2O_3	1.08 ± 0.01 ppm of F

Note: $\pm$ values above indicate the estimate of one standard error (se) for the average sorption value (see Appendix E for steps to estimate standard error)

Sensing Material	95% Confidence Interval
PANI	1.315 ± 0.120118 ppm of F
PANI with 1.25% In_2O_3	2.49 ± 0.19 ppm of F
PANI with 2.5% In_2O_3	1.99 ± 0.06353 ppm of F
PANI with 5% In_2O_3	1.6425 ± 0.0225 ppm of F
PANI with 10% In_2O_3	1.08 ± 0.12706 ppm of F

The validity of our statements regarding our sorption results was also verified using statistical tools. Raw data trends and statistical analysis for selected samples are presented in Appendix F and Appendix G, respectively.
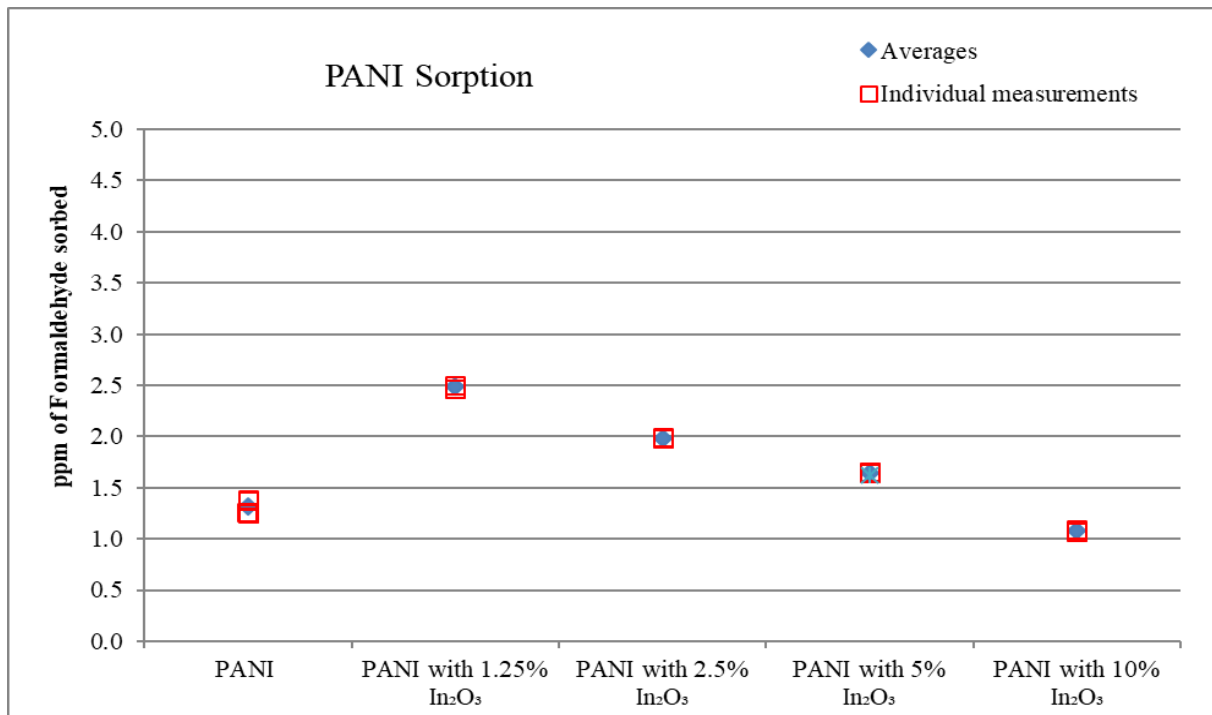
Figure 17: Formaldehyde sorption (in ppm) for PANI and doped PANI with different wt.% In_2O_3 dopant; (Source: F 10 ppm)

48
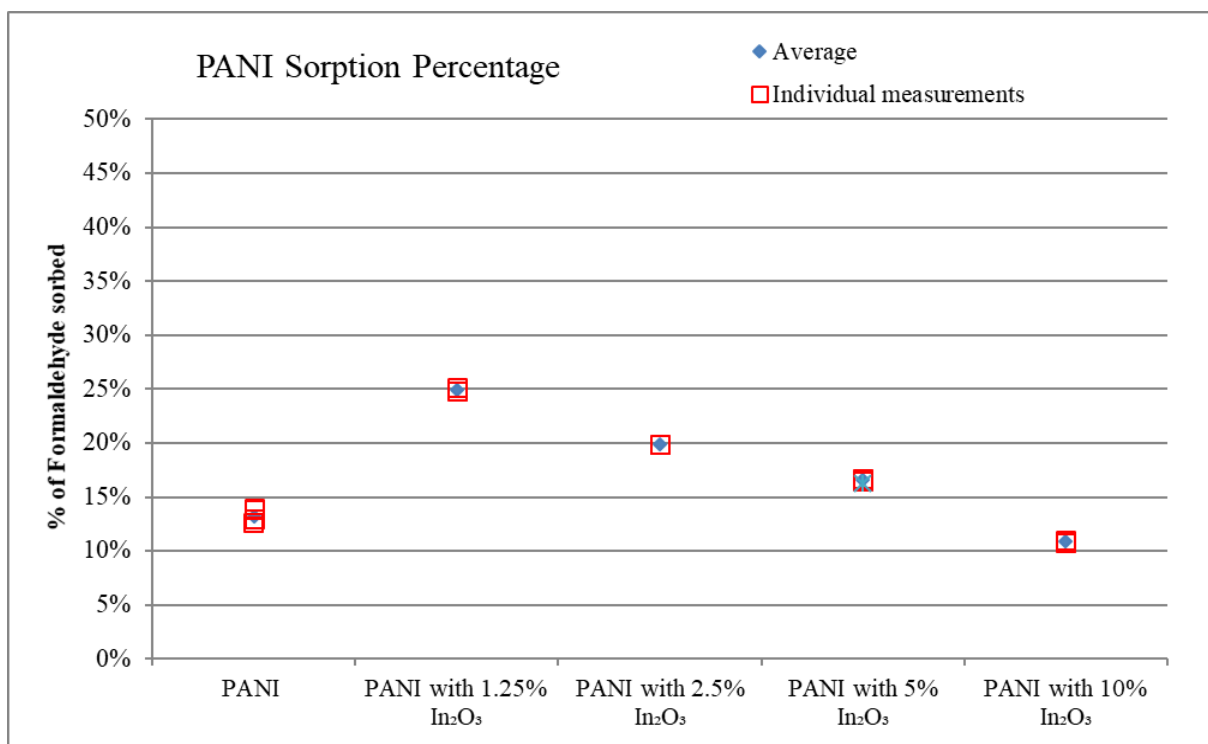
Figure 18: Formaldehyde sorption (in %) for PANI and doped PANI with different wt.% In_2O_3 dopant; (Source: F 10 ppm)

4.1.2 P25DMA and doped P25DMA with MO

As observed in Figure 15, the sorption of F onto P25DMA was found to be slightly lower than the sorption of F onto pure PANI. Stewart et al. [69] had observed that doping P25DMA with more TiO_2 enhanced the sorption of most of the toxic gas analytes [69]. In particular, P25DMA doped with 20% TiO_2 sorbed the highest amount of gas analytes compared to other undoped and doped P25DMA with TiO_2 [69]. Hence, in an attempt to improve the formaldehyde sorption performance of P25DMA, P25DMA was doped with 20% TiO_2.
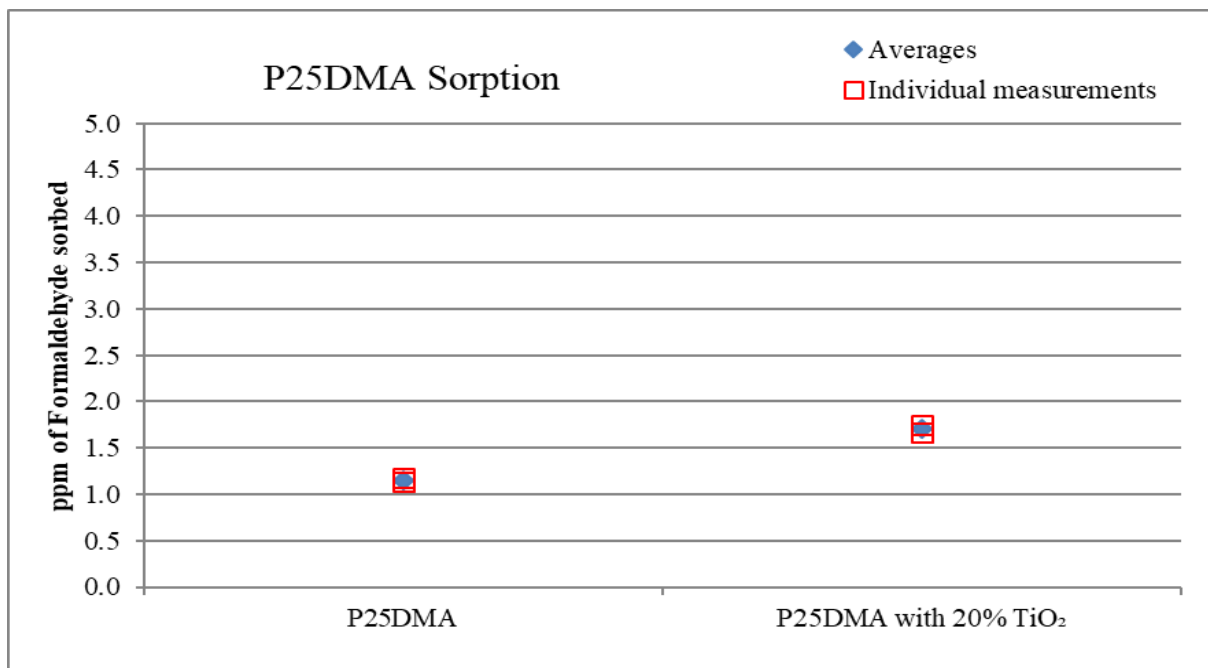
Figure 19: Formaldehyde sorption (in ppm) for P25DMA and P25DMA with 20% TiO_2; (Source: F 10 ppm)

As shown in Figure 19, P25DMA doped with 20% TiO_2 seemed to perform better than undoped P25DMA for sorption of F. On doping P25DMA with TiO_2, it was observed that its sorption of F increased by about 0.55 ppm compared to P25DMA. This indicated that the dopant had quite an effect on the F sensitivity of P25DMA. The enhancement in the P25DMA sorption of F on doping with TiO_2 was also due to a change in morphology of the polymer on the addition of dopant (discussed further in Section 7.2). The introduction of 'kinks' due to the TiO_2 addition seems to increase the available interstitial space of P25DMA with 20% TiO_2 compared to pristine P25DMA.

As discussed earlier (Section 2.7), NiO seems to be a potential metal oxide for formaldehyde sensing. Therefore, it was deemed worth testing doped P25DMA with NiO for formaldehyde (at 10 ppm).

As shown in Table 11 and Figure 20/Figure 21, P25DMA with 10% NiO seems to sorb F more than twice as much as undoped P25DMA; and roughly 1 ppm more than P25DMA with 20% TiO_2 when exposed to F 10 ppm source.

P25DMA doped with 10% NiO seems to be a good contender for sorption of F due to its high sensitivity. The better sensitivity of P25DMA can be attributed to the ability of NiO to form 'kinks' (like TiO_2 earlier) and a "boat-like" structure formed with the polymer backbone, which is discussed in more detail in Section 7.4.

Table 11: Average sorption values (in ppm of F) for P25DMA and doped P25DMA with metal oxide.

Sensing Material	Average sorption values
P25DMA	1.16 ± 0.025 ppm of F
P25DMA with 20% TiO_2	1.71 ± 0.04 ppm of F
P25DMA with 10% NiO	2.95 ± 0.03 ppm of F

Note: $\pm$ values above indicate the estimate of one standard error (se) for the average sorption value

Sensing Material	95% Confidence Interval
P25DMA	1.16 ± 0.31765 ppm of F
P25DMA with 20% TiO_2	1.71 ± 0.50824 ppm of F
P25DMA with 10% NiO	2.95 ± 0.31765 ppm of F
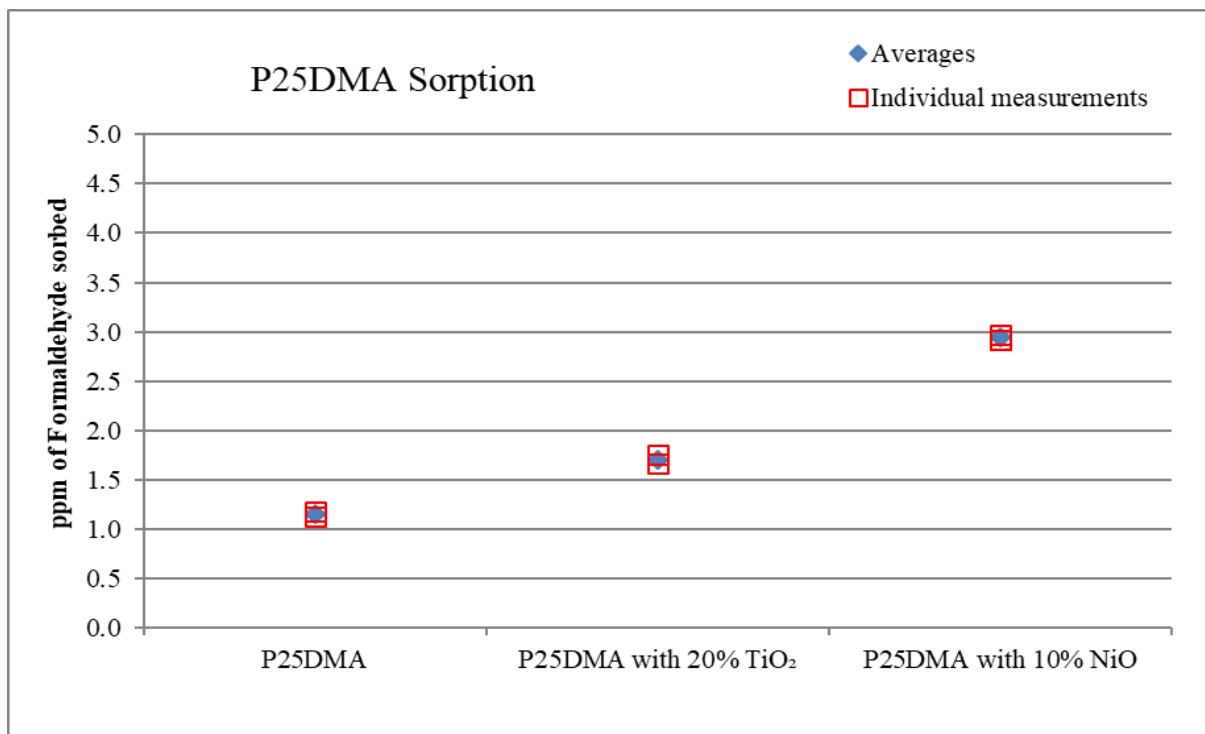
Figure 20: Formaldehyde sorption (in ppm) P25DMA and doped P25DMA with metal oxide; (Source: F 10 ppm)
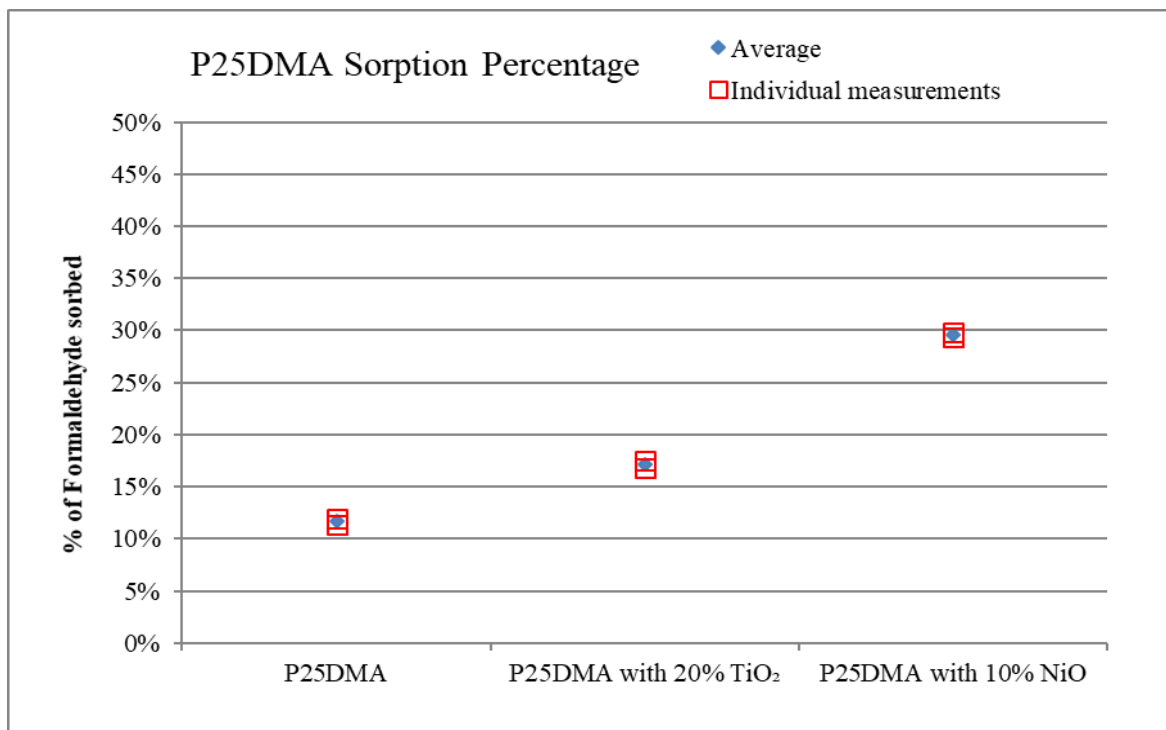
Figure 21: Formaldehyde sorption (in %) of P25DMA and doped P25DMA with metal oxide; (Source: F 10 ppm)

4.1.3 PAAc and PMMA

PAAc (poly(acrylic acid)) was established [63] to not sorb benzene (B) from a source of 10 ppm B. Similarly, PMMA (poly(methyl methacrylate)) was established to not sorb any acetone (Ac) from a 5 ppm Ac source in ref. [70]. To identify a zero sorption material (very useful in order to accommodate sensor requirements for establishing a zero (no sorption) baseline), PAAc and PMMA were tested for their sorption of F from a 10 ppm F source. If the materials were to exhibit zero sorption from a 10 ppm source, then they would also exhibit zero sorption from a 5 ppm or 1 ppm gas source.

Hence, in parallel to PANI and P25DMA, PAAc and PMMA samples (with different molecular weights) were tested for sorption of F by exposing them to an F 10 ppm source. From Table 12, it is evident that PAAc and PMMA do not sorb any F from the employed 10 ppm F source. Figure 22 and Figure 23 show that regardless of the molecular weight level of these polymeric materials, neither of them seems to sorb any F. The sorption data for representative PAAc and PMMA sorption trials were statistically analysed and confirmed for their zero sorption values (see Appendix H for statistical analysis). The zero sorption for PMMA and PAAc can be attributed to the 'flat' plate-like surface morphology of the corresponding polymeric substrates (as discussed further in Section 7.2).

Table 12: Average sorption values for PAAc and PMMA with different molecular weights.

Sensing Material	Average sorption values
PAAc 450K	0.03 ± 0.015 ppm of F
PAAc 1M	0.07 ± 0.01 ppm of F
PMMA 1M	0.09 ± 0.01 ppm of F

Note: $\pm$ values above indicate the estimate of one standard error (se) for the average sorption value

Sensing Material	95% Confidence Interval
PAAc 450K	0.03 ± 0.19 ppm of F
PAAc 1M	0.07 ± 0.127 ppm of F
PMMA 1M	0.09 ± 0.127 ppm of F
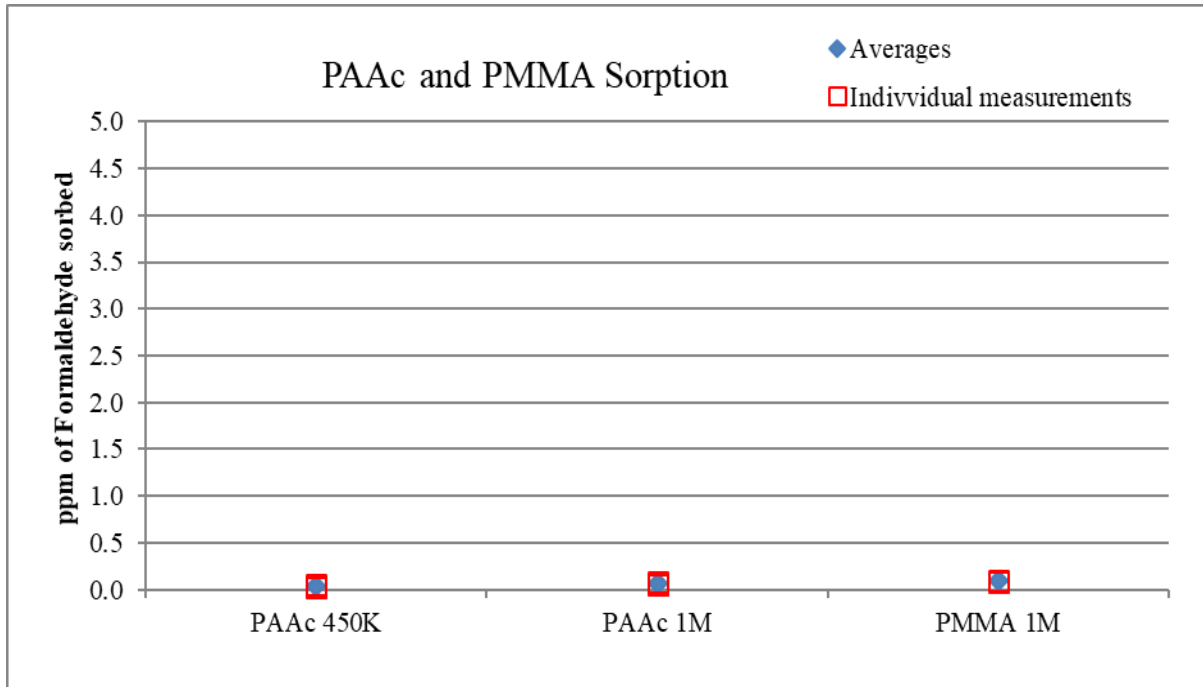
Figure 22: Formaldehyde sorption (in ppm) for PAAc and PMMA with different molecular weights (Source: F 10 ppm)
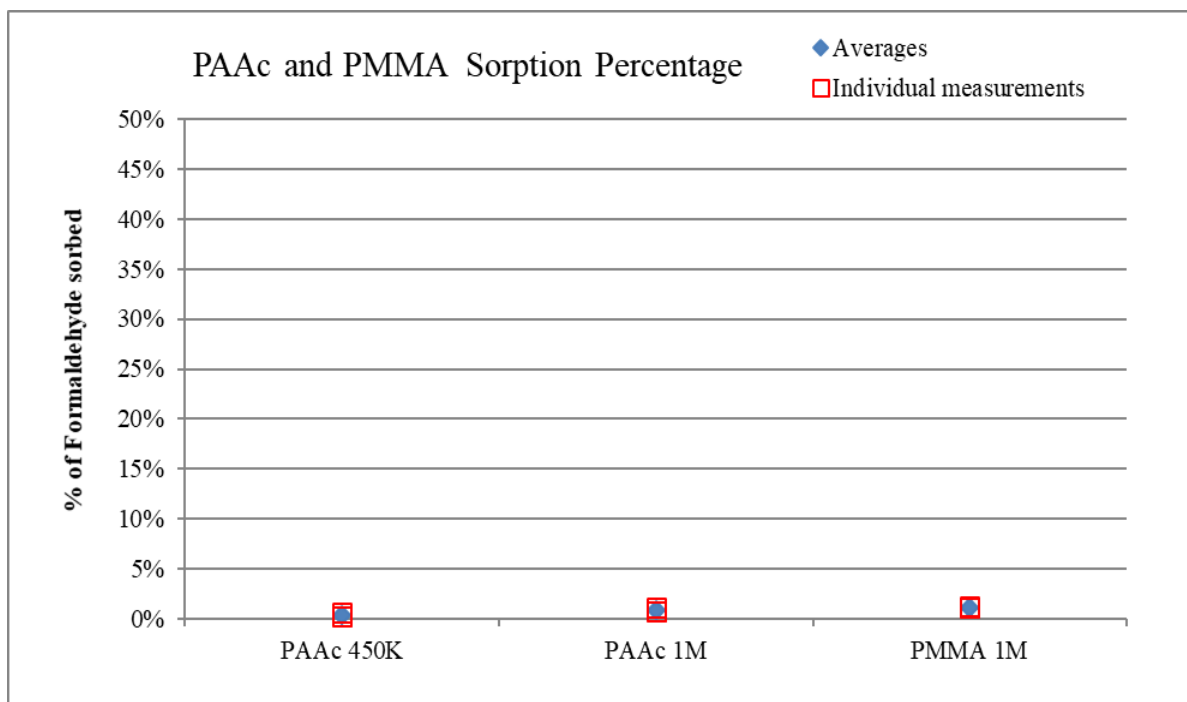
Figure 23: Formaldehyde sorption (in %) for PAAc and PMMA with different molecular weights; (Source: F 10 ppm)

4.2 Benzene (B) Gas Sensitivity Studies

Benzene was considered as a typical interferent gas, representative of aromatic hydrocarbons that are usually present in small amounts in many environments, accompanying other gaseous chemicals. It is the least complex aromatic hydrocarbon and is a good representative of interferent gases for the application. The potentially good sensing materials for formaldehyde should ideally sorb maximum of formaldehyde on exposure to F source and sorb less to zero ppm of interferent gas (benzene gas) on exposure to B source.

4.2.1 PANI and doped PANI with MO

Selected PANI polymers were tested for sorption of B to compare and contrast their benzene sensitivity trends (with the aim to pursue selectivity of F over B trends, discussed in Chapter 5). PANI with 5% In_2O_3 seems to sorb the least B compared to PANI and PANI with 10% In_2O_3 when exposed to 10 ppm B source, as shown in Table 13 and Figure 24/Figure 25. This indicates that doped PANI with In_2O_3 sorption trends for F sorption from F 10 ppm source and B sorption from B 10 ppm source are in reverse directions. PANI with 5% In_2O_3 sorbs more F than PANI with 10% In_2O_3 (as discussed in Section 4.1.1). PANI with 5% In_2O_3 seems to sorb less B than PANI with

54

10% In_2O_3. This indicates that PANI with 5% In_2O_3 is a potentially good sensing material and might have better selectivity towards formaldehyde over benzene. The selectivity trends for F are discussed in Chapter 5.

Table 13: Average sorption values for PANI and doped PANI with different wt.% of In_2O_3

Sensing Material	Average sorption values
PANI	0.97 ± 0.015 ppm of B
PANI with 5% In_2O_3	0.76 ± 0.025 ppm of B
PANI with 10% In_2O_3	1.5 ± 0.03 ppm of B

Note: $\pm$ values above indicate the estimate of one standard error (se) for the average sorption value

Sensing Material	95% Confidence Interval
PANI	0.97 ± 0.19 ppm of B
PANI with 5% In_2O_3	0.76 ± 0.31765 ppm of B
PANI with 10% In_2O_3	1.5 ± 0.38118 ppm of B
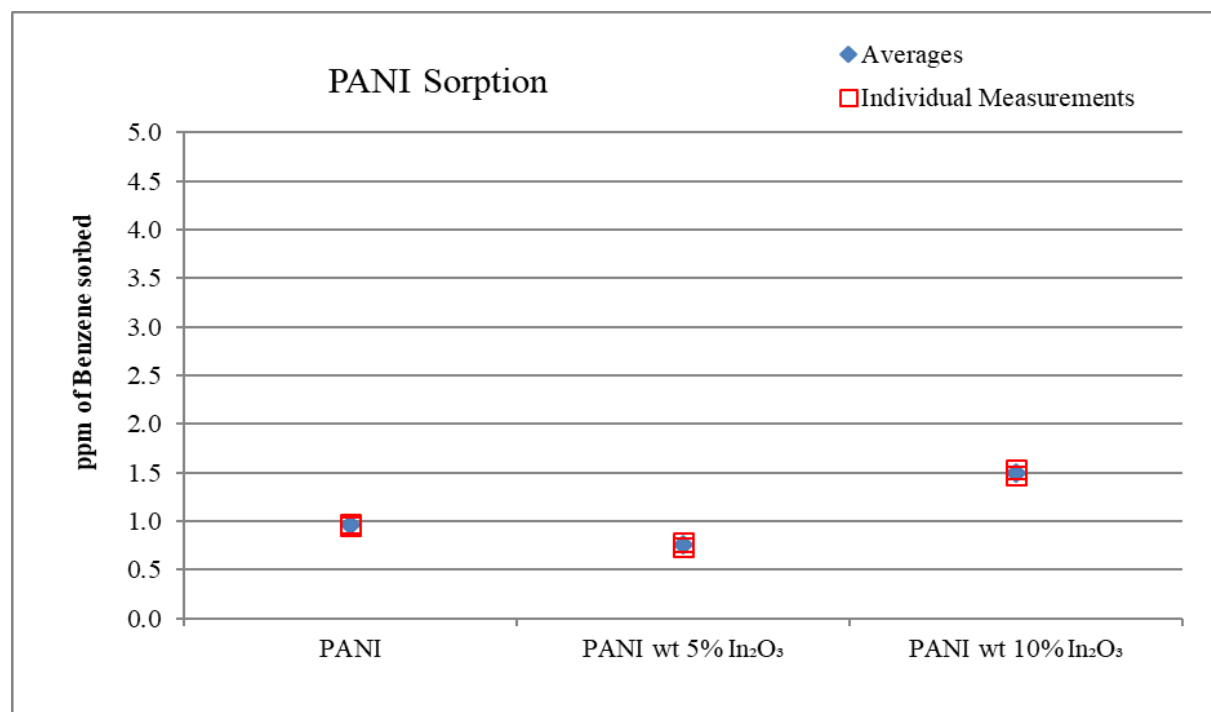
Figure 24: Benzene sorption (in ppm) for PANI and doped PANI with different wt.% of In_2O_3; (Source: B 10 ppm)
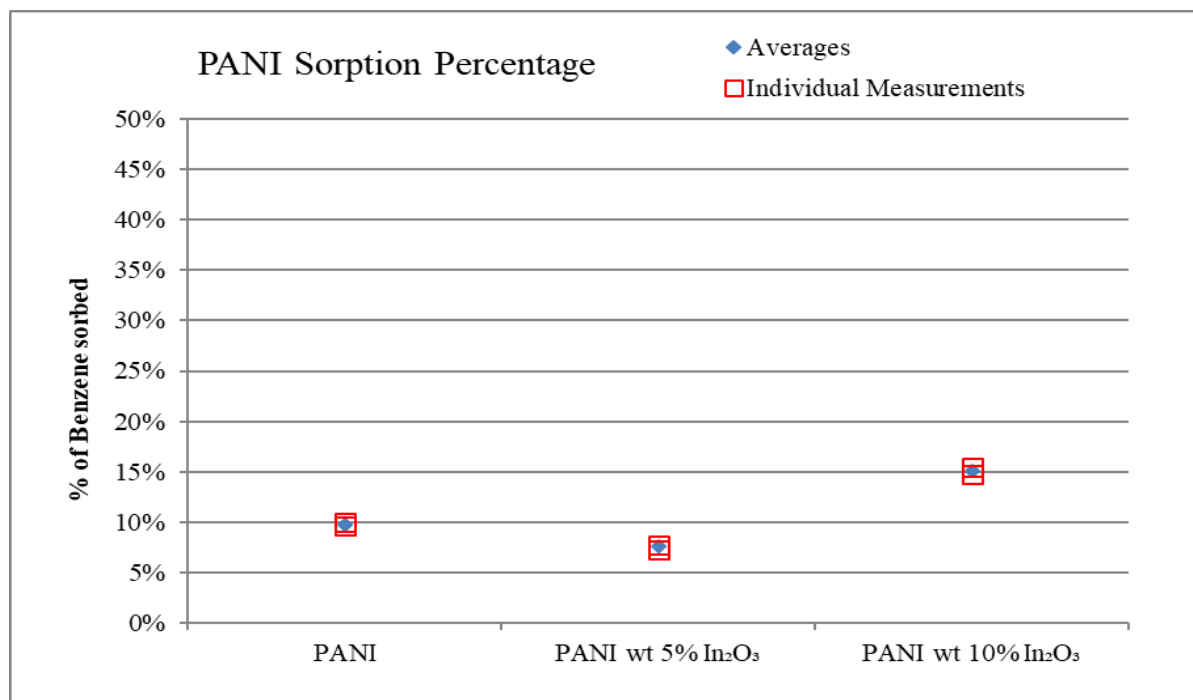
Figure 25: Benzene sorption (in %) for PANI and doped PANI with different wt.% of In_2O_3; (Source: B 10 ppm)

4.2.2 P25DMA and doped P25DMA with MO

Selected P25DMA and doped P25DMA samples were tested for their sorption of B by exposing them to a 10 ppm B source. As shown in

Table 14 and Figure 26/Figure 27, P25DMA seems to sorb more B from a 10 ppm B source compared to doped P25DMA with 20% TiO_2. This again suggests that doped P25DMA follows similar trends as doped PANI for sorption of B. The materials that sorb F comparatively better than others are poor at sensing B, which suggests that doped P25DMA with 20% TiO_2 might possess a better selectivity towards F over B. Selectivity trends for P25DMA and doped P25DMA with 20% TiO_2 are discussed in Section 5.1.2. The poor sensitivity of P25DMA with 20% TiO_2 towards B compared to pristine P25DMA can be indicative of smaller 'cavities' and increase in packing efficiency of P25DMA due to addition of TiO_2 dopant. Smaller 'cavities' in P25DMA with 20% TiO_2 seem to not readily accommodate larger (bulkier) molecules like benzene.

Table 14: Average sorption values for P25DMA and P25DMA with 20% TiO_2

Sensing Material	Average sorption values
P25DMA	1.88 ± 0.055 ppm of B
P25DMA with 20% TiO_2	0.82 ± 0.04 ppm of B

Note: $\pm$ values above indicate the estimate of one standard error (se) for the average sorption value

Sensing Material	95% Confidence Interval
P25DMA	1.88 ± 0.6988 ppm of B
P25DMA with 20% TiO_2	0.82 ± 0.5 ppm of B
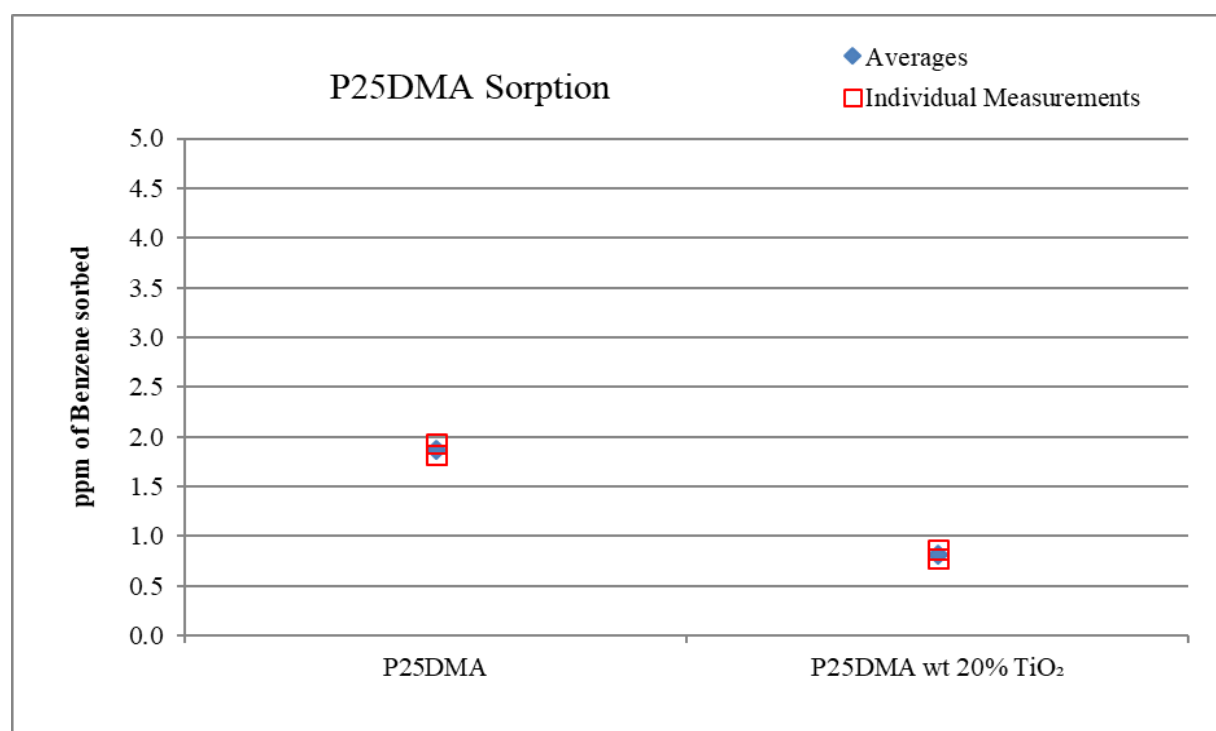
Figure 26: Benzene sorption (in ppm) for P25DMA and P25DMA with 20% TiO_2; (Source: B 10 ppm)
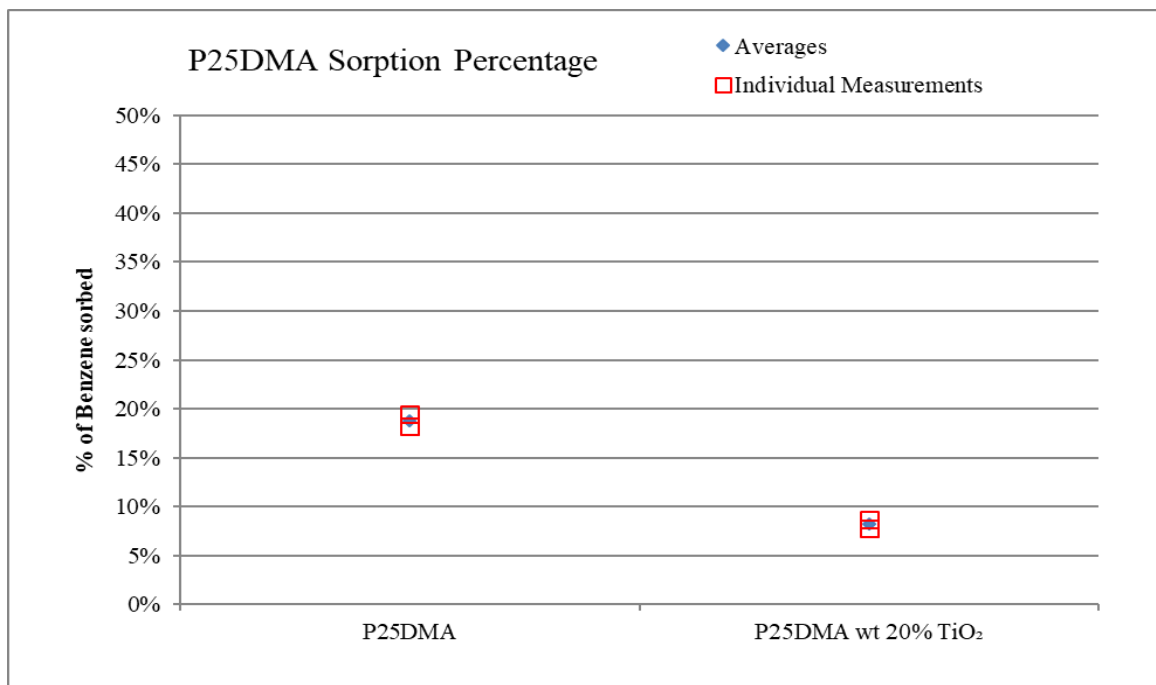
Figure 27: Benzene sorption (in %) for P25DMA and P25DMA with 20% TiO_2; (Source: B 10 ppm)

4.2.3 PAAc and PMMA

PAAc and PMMA were tested for their sorption of B from a 10 ppm B source, based on a similar logic as discussed earlier for F (Section 4.1.3). Again, if the materials were to exhibit zero sorption from a 10 ppm source, then they would also exhibit zero sorption from a 5 ppm or 1 ppm gas source. From Table 15 it is evident that PAAc and PMMA do not sorb any B from the employed 10 ppm B source. Figure 28/Figure 29 show that regardless of the molecular weight level of these polymeric materials, neither of them seem to sorb any B. The sorption results of PAAc and PMMA are similar to the sorption levels observed when they were exposed to F 10 ppm source.

Table 15: Average sorption values for PAAc and PMMA with different molecular weights

Sensing Material	Average sorption values
PAAc 130K	0.03 ± 0.01 ppm of B
PAAc 450K	0.03 ± 0.015 ppm of B
PAAc 1M	0.06 ± 0.015 ppm of B
PMMA 15K	0.06 ± 0.015 ppm of B
PMMA 0.5M	0.05 ± 0.005 ppm of B
PMMA 1M	0.06 ± 0.005 ppm of B

Note: ± values above indicate the estimate of one standard error (se) for the average sorption value

Sensing Material	95% Confidence Interval
PAAc 130K	0.03 ± 0.127 ppm of B
PAAc 450K	0.03 ± 0.19 ppm of B
PAAc 1M	0.06 ± 0.19 ppm of B
PMMA 15K	0.06 ± 0.19 ppm of B
PMMA 0.5M	0.5M- 0.05 ± 0.063 ppm of B
PMMA 1M	0.06 ± 0.063 ppm of B

Figure 28: Benzene sorption (in ppm) for PAAc and PMMA with different molecular weights; (Source: B 10 ppm)
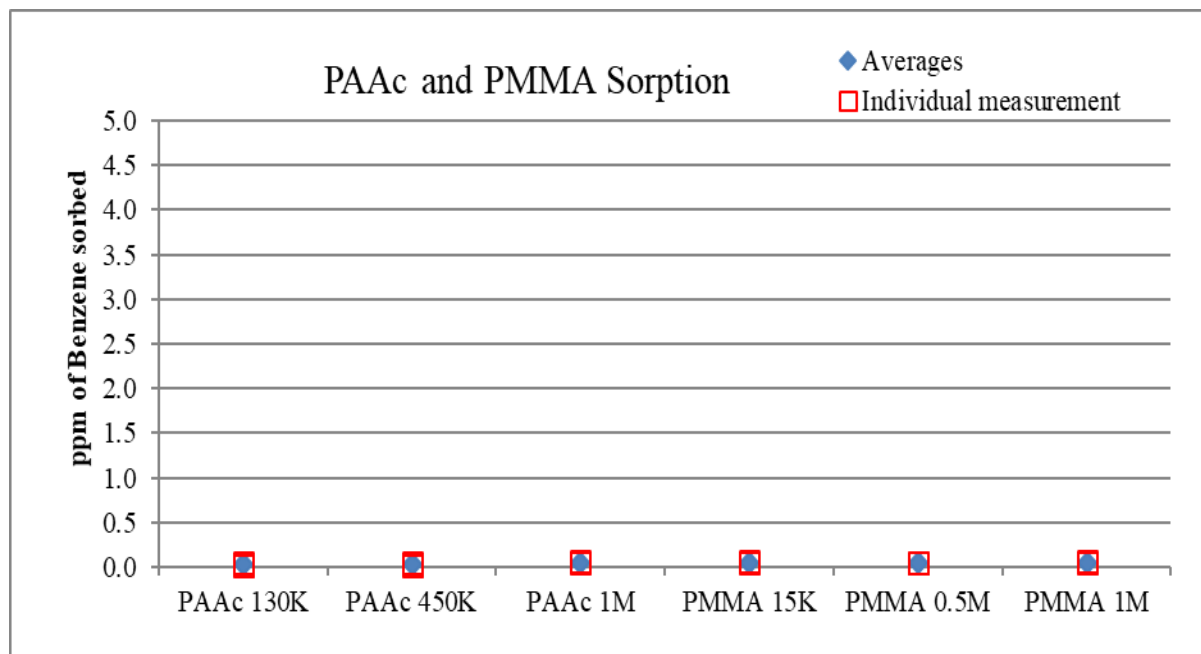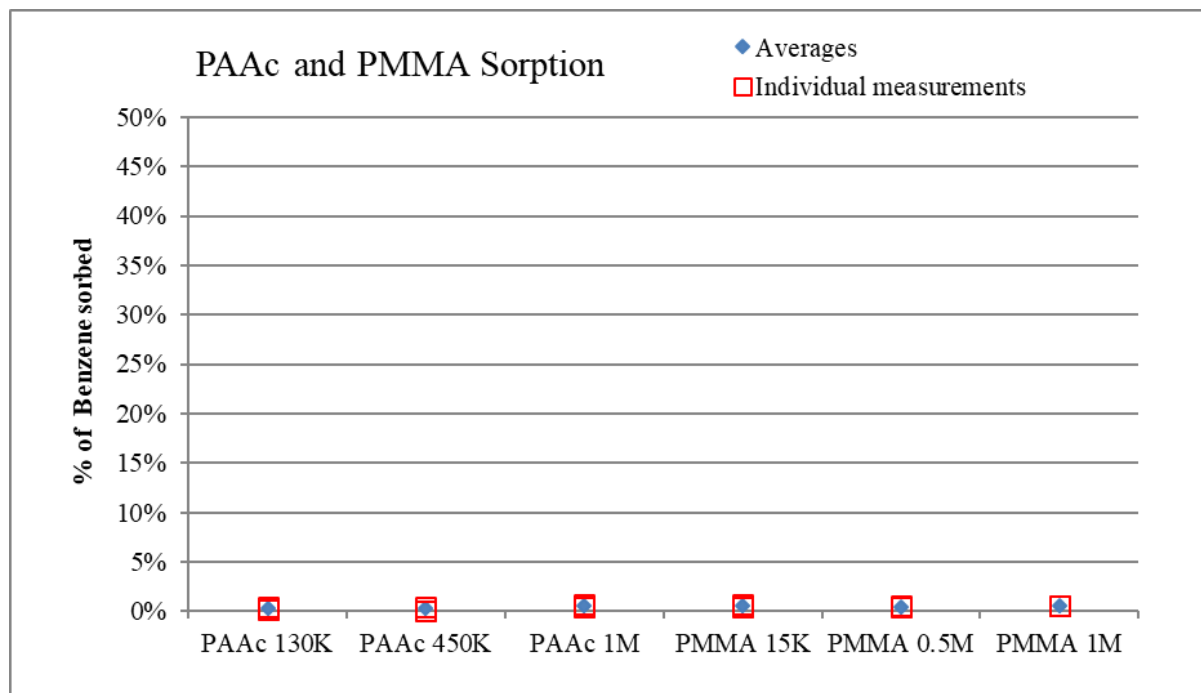
Figure 29: Benzene sorption (in %) for PAAc and PMMA with different molecular weights; (Source: B 10 ppm)

4.3 Acetaldehyde (Ac) Gas Sensitivity Studies

4.3.1 PANI and doped PANI with MO

As described earlier, formaldehyde and acetaldehyde are chemically very similar (recall Section 2.4). Due to their similarity in structure, polarity and dipole movement, acetaldehyde can pose selectivity issues and interfere with the formaldehyde signal. Evaluating the sorption of formaldehyde and acetaldehyde simultaneously provides information about how these sensing materials would behave when exposed to a "worst case scenario" interferent. To build on prior work (discussed in Section 4.1 and Section 4.2), the materials evaluated herein were some of the most promising materials that were identified during the analysis of material responses to gas mixtures containing formaldehyde and benzene (10 ppm source). Specifically, PANI (without and with In_2O_3) and P25DMA (without and with TiO_2 dopant) were exposed to pure acetaldehyde (5 ppm Ac in nitrogen), and afterwards to a gas mixture containing formaldehyde and acetaldehyde for selectivity studies (discussed later in Chapter 5).

On exposing PANI samples to acetaldehyde, it was observed that PANI sorption of Ac seems to improve on doping PANI with In_2O_3 similar to the formaldehyde sorption trend for undoped and doped PANI with In_2O_3. But PANI with 1.25% In_2O_3 seems to sorb more Ac than PANI with higher wt.% (2.5% and 5%) of In_2O_3 (even if slightly) but lower than PANI with 10% In_2O_3 (even

if slightly); see Table 16 for average sorption values. It seems that PANI with 10% In_2O_3 sorbs more than the rest of the materials (see Figure 30/Figure 31 for sorption trends). The sorption trends of Ac for PANI doped with In_2O_3 seem to not follow the exact pattern as sorption trends of F for PANI doped with In_2O_3.

It is interesting to note that PANI doped with different wt.% of In_2O_3 (except for PANI with 10% In_2O_3) not only seems to be quite promising for sorption of F from an F 10 ppm source (as discussed in Section 4.1.1) but also for sorption of Ac from an Ac 5 ppm source. This suggests that PANI with different wt.% of In_2O_3 (except for PANI with 10% In_2O_3) might not be very selective towards formaldehyde since it seems to exhibit good affinity towards both (formaldehyde and acetaldehyde) aldehydic gases.

Only PANI with 10% In_2O_3 seems to exhibit a higher response to Ac than to F (see Figure 18 and Figure 31). Therefore, one might say that PANI with 10% In_2O_3 seems to have more affinity towards Ac than F. This also suggests that PANI with 10% In_2O_3 might be more selective towards Ac than formaldehyde (selectivity results for F and Ac are presented in Chapter 5)

Table 16: Average sorption values (in ppm of Ac) for PANI and doped PANI with different wt. % of In_2O_3

Sensing Material	Average sorption values
PANI	0.59 ± 0.0149304 ppm of Ac
PANI with 1.25% In_2O_3	1.22 ± 0.015 ppm of Ac
PANI with 2.5% In_2O_3	1.10 ± 0.1067942 ppm of Ac
PANI with 5% In_2O_3	1.10 ± 0.01414 ppm of Ac
PANI with 10% In_2O_3	1.44 ± 0.0232289 ppm of Ac

Note: ± values above indicate the estimate of one standard error (se) for the average sorption value

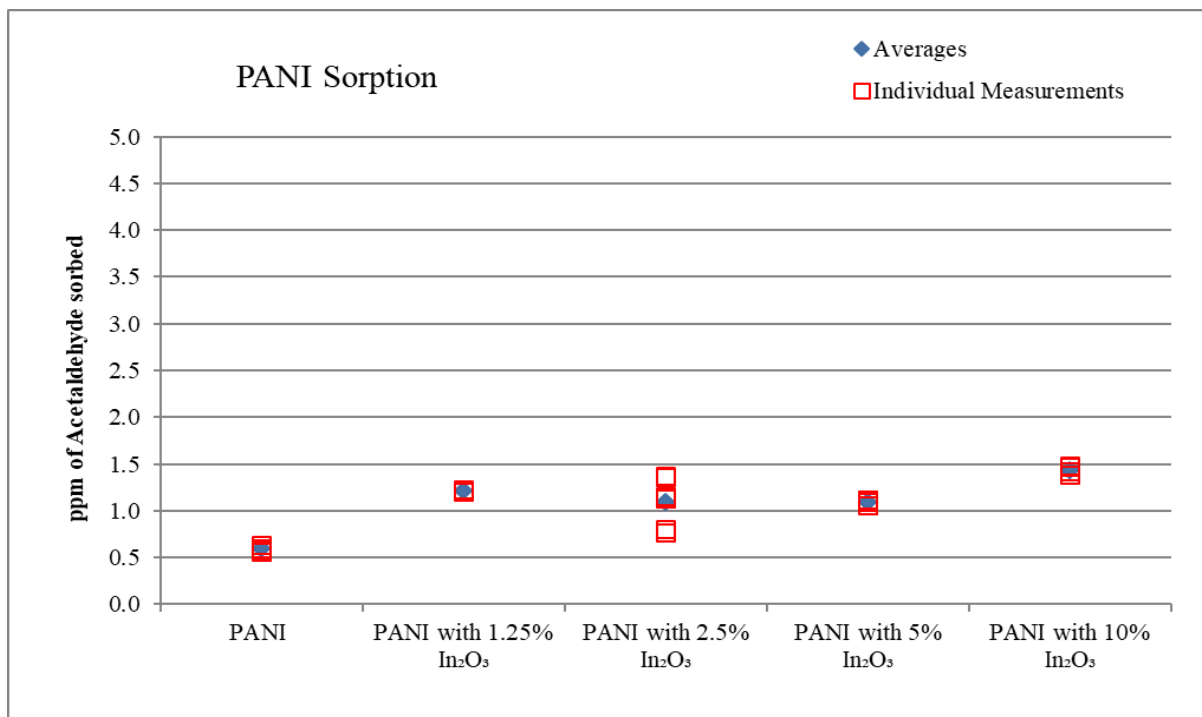| Sensing Material	95% Confidence Interval
PANI	0.59 ± 0.0475 ppm of Ac
PANI with 1.25% In_2O_3	1.22 ± 0.19059 ppm of Ac
PANI with 2.5% In_2O_3	1.10 ± 0.2745679 ppm of Ac
PANI with 5% In_2O_3	1.10 ± 0.045 ppm of Ac
PANI with 10% In_2O_3	1.44 ± 0.0739 ppm of Ac

Figure 30: Acetaldehyde sorption (in ppm) for PANI and doped PANI with different wt. % of In_2O_3; (Source: Ac 5 ppm)
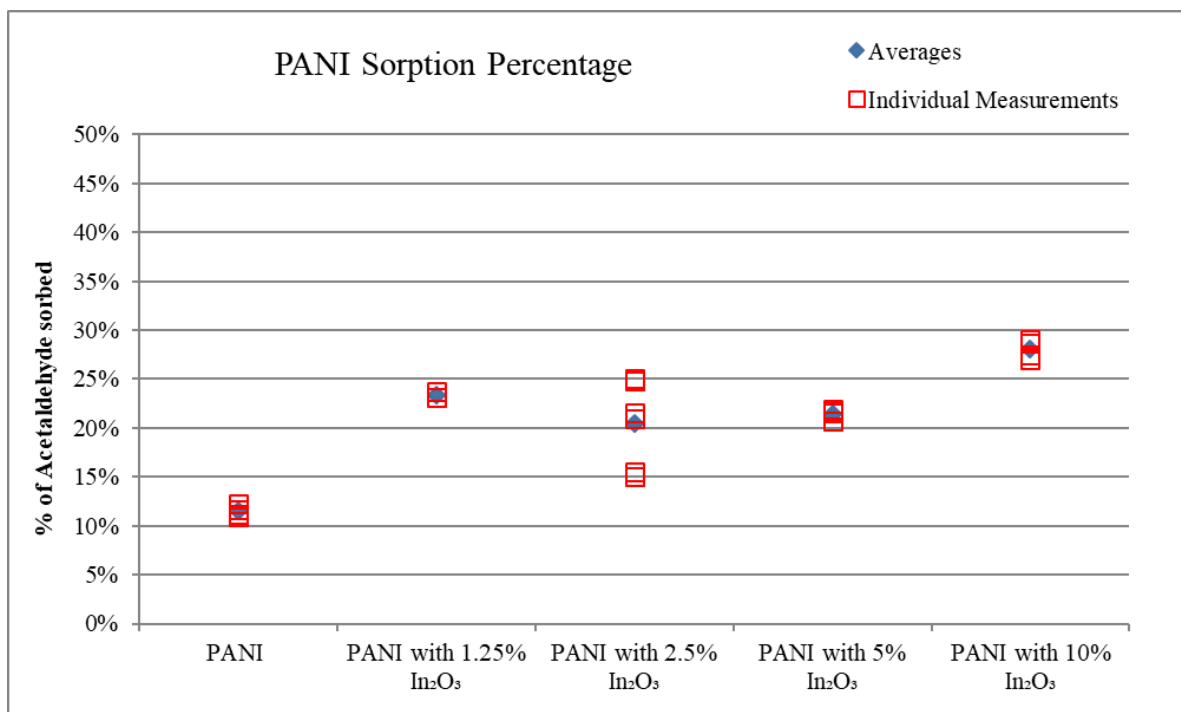

Figure 31: Acetaldehyde sorption (in %) for PANI and doped PANI with different wt. % of In_2O_3; (Source: Ac 5 ppm)

4.3.2 P25DMA and doped P25DMA with MO

P25DMA doped with 20% TiO_2 and P25DMA with 10% NiO displayed good sorption of F when exposed to a 10 ppm F source (as discussed in Section 4.1.2). It is also suspected that P25DMA might have a higher affinity towards acetaldehyde than formaldehyde as deduced from the comparison presented in Section 2.7 based on the solubility parameters (recall Table 4). Therefore, P25DMA and doped P25DMA were worth exploring further for their sorption capabilities of Ac.

On exposing P25DMA and doped P25DMA with MO (TiO_2 and NiO) to 5 ppm Ac source, it seems that P25DMA with 10% NiO is more sensitive to Ac compared to P25DMA and P25DMA with 20% TiO_2, even if slightly (see Table 17 and Figure 32/Figure 33 for typical sorption values and trends).

On comparing Figure 21 and Figure 33, it is evident that P25DMA with 10% NiO sorbs almost equivalent amounts of F (~30%) (see Figure 21), when exposed to F 10 ppm source, and Ac (a bit less than 30%) (Figure 33), when exposed to Ac 5 ppm source. P25DMA and P25DMA with 20% TiO_2 seem to have slightly more affinity towards acetaldehyde than formaldehyde. The higher affinity of P25DMA towards Ac compared to F can be attributed to the considerably close solubility parameters of P25DMA (21.1 $(MPa)^{1/2}$) and acetaldehyde (21.0 $(MPa)^{1/2}$) [48]. It is suspected that P25DMA with 10% NiO might have a reasonable selectivity towards F over Ac, while P25DMA and P25DMA with 20% TiO_2 might be equally or more selective to F over Ac, when exposed to F and Ac gas mixture sources.

Table 17: Average sorption values (in ppm of Ac) for P25DMA and doped P25DMA

Sensing Material	Average sorption values
P25DMA	1.07 ± 0.1184 ppm of Ac
P25DMA with 20% TiO_2	1.22 ± 0.042303 ppm of Ac
P25DMA with 10% NiO	1.44 ± 0.02 ppm of Ac

Note: $\pm$ values above indicate the estimate of one standard error (se) for the average sorption value

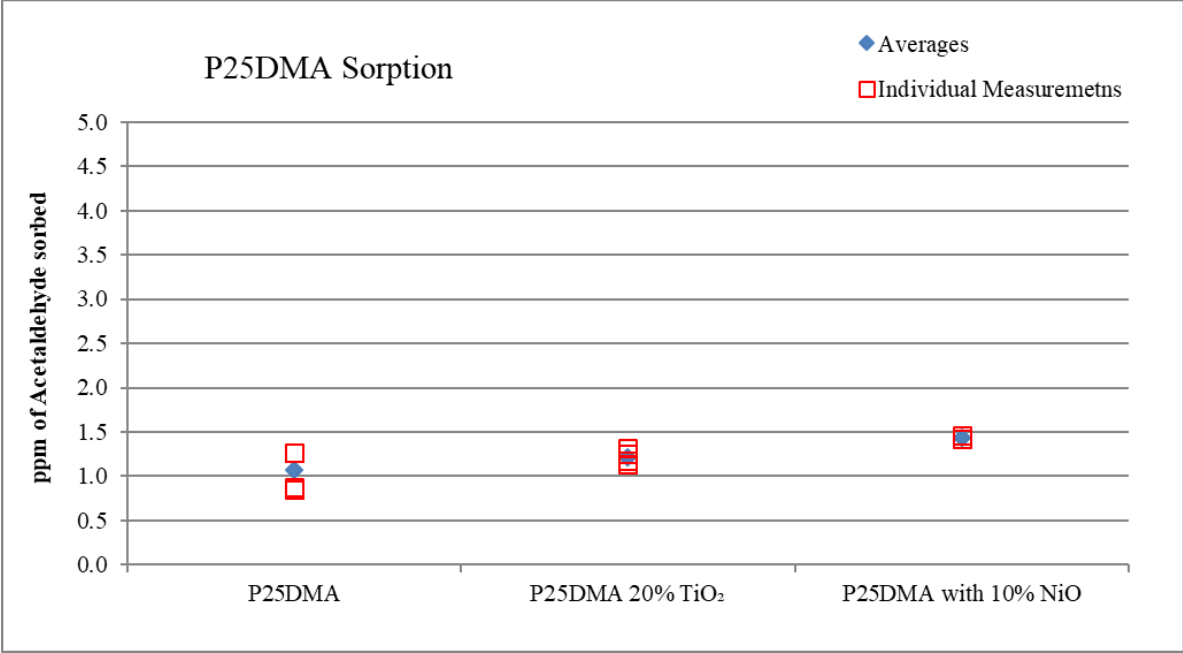| Sensing Material	95% Confidence Interval
P25DMA	1.07 ± 0.3768353 ppm of Ac
P25DMA with 20% TiO_2	1.22 ± 0.13461 ppm of Ac
P25DMA with 10% NiO	1.44 ± 0.25412 ppm of Ac

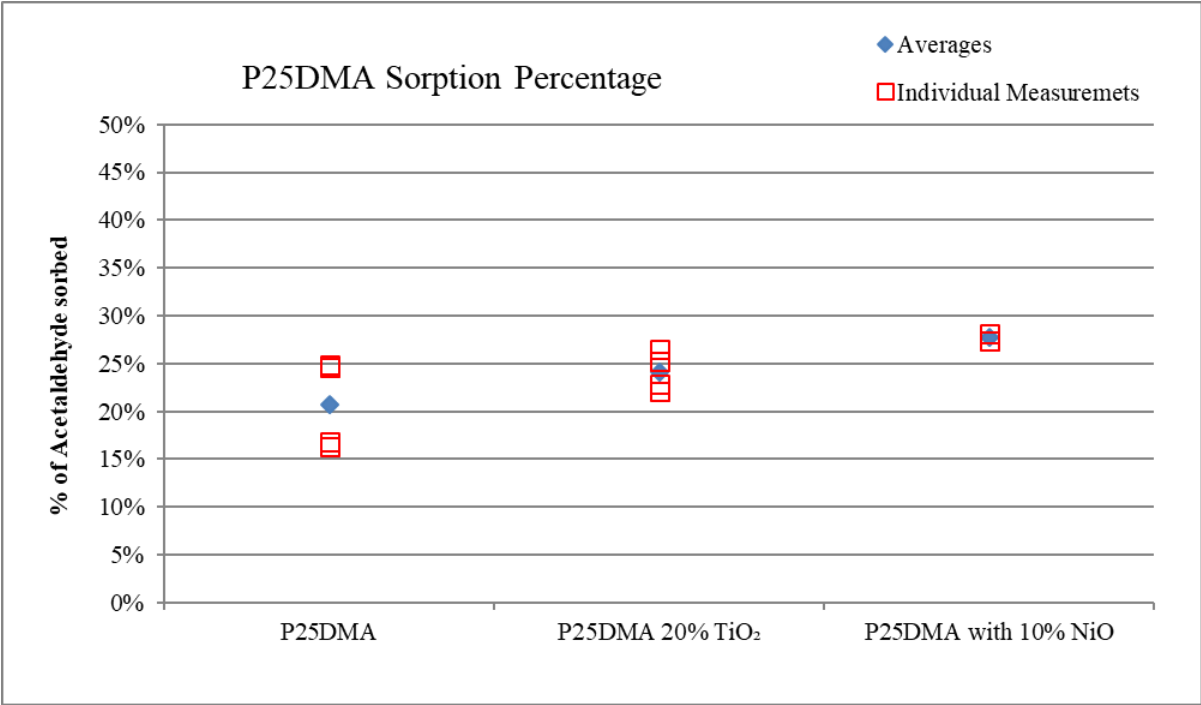Figure 32: Acetaldehyde sorption (in ppm) for P25DMA and doped P25DMA; (Source: Ac 5 ppm)

Figure 33: Acetaldehyde sorption (in %) for P25DMA and doped P25DMA; (Source: Ac 5 ppm)

Chapter 5: Results and Discussion – Selectivity Studies

5.1 Formaldehyde over Benzene (F/B) Selectivity Studies

Selectivity studies can be conducted in two ways. Firstly, by exposing sensing materials to an individual single gas source and comparing their sorption value for different analytes. Secondly, by exposing the sensing material to two or more gas mixtures (of equal concentrations) and then comparing the sorption values. The latter is a more realistic approach as it gives an actual perspective on how a sensing material would interact with the analyte in the presence of other interferent gases. The approach does take into account possible synergistic and/or antagonistic interactions between analytes and substrates. It is more tedious experimentally but certainly more complete. As such, it is sorely missing in the body of sensor literature (with only a few exceptions).

Therefore, using the latter approach the potential sensing materials were tested for their selectivity/affinity towards F in the presence of interferent gases like B and/or Ac. A sample of raw data for "blanks" with F/B (5/5 ppm each) gas mixture source is presented in Appendix I. One can readily realize the good reproducibility of our trials.

Like in the earlier sensitivity studies of Chapter 4, selectivity studies started with evaluation of selectivity of F over B for undoped PANI and P25DMA. As shown in Figure 34, P25DMA (~ 0.82 ppm of F) seems to sorb marginally more F compared to PANI (~0.62 ppm of F) in the presence of B from a F/B (5/5 ppm) gas mixture source. This, at first glance, is a trend opposite to earlier trends in Section 4.1 on sensitivity.
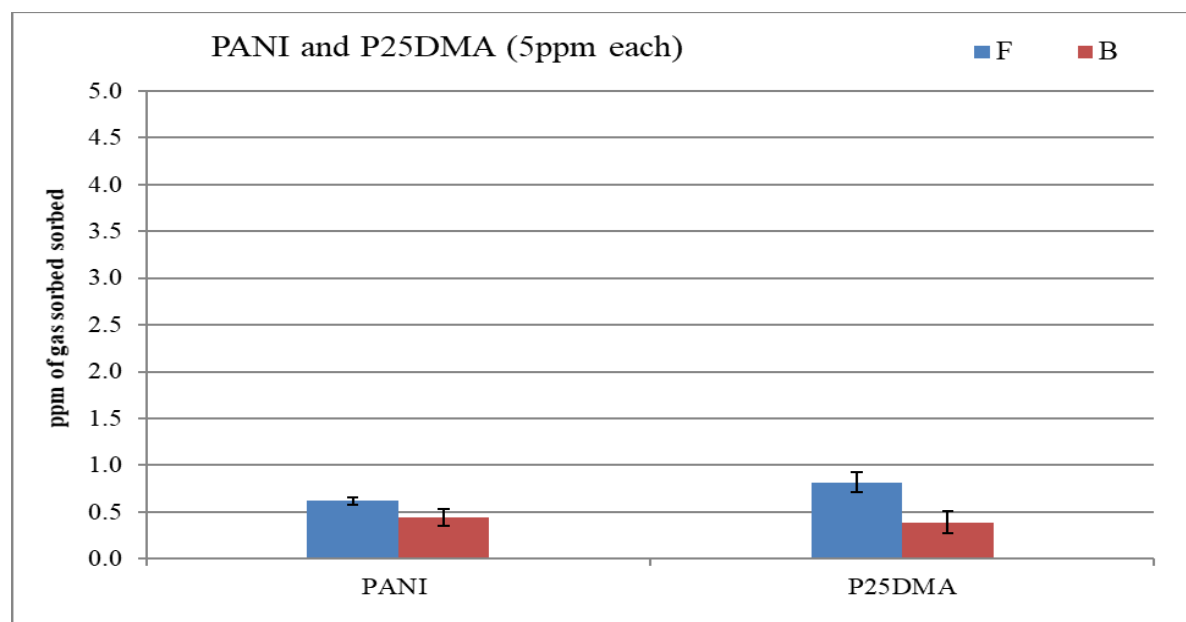

Figure 34: F & B sorption (in ppm) for PANI and P25DMA; (Source: F/B, 5/5 ppm)

Figure 34 shows that PANI seems to sorb less F in the presence of B compared to P25DMA; and that P25DMA seems to have a higher selectivity compared to PANI (that is, it sorbs a higher amount of F than B from a source of F/B (5 ppm each)). While the average selectivity (F/B) of PANI is 1.45, the average selectivity of P25DMA is 2.20. This difference is not huge but is observable. The difference in trends (a result of gas molecule interactions with the available "sorption sites" from the sensing material) has been observed before in the literature [71].

Again, to investigate ways to enhance sorption of F and improve the selectivity towards F over B, the previously prepared doped PANI and P25DMA were evaluated for their selectivity of F over B. The F over B selectivity results for PANI and P25DMA were also confirmed using statistical tools and this is also presented in Appendix I.

5.1.1 PANI and doped PANI with MO

The selectivity of pure PANI was compared to PANI doped with In_2O_3 at 5% and 10% loadings. As shown in Table 18 and Figure 35/Figure 36, the trends observed for the sorption of F (from the F/B gas mixture) are comparable to the trends observed when F 10 ppm was the only gas source (as shown in Figure 17/Figure 18). That is, the sorption of formaldehyde increases when PANI is doped with 5% In_2O_3, but the sorption does not increase further on doping PANI with 10% In_2O_3. Not only the amount of F sorbed but also the selectivity ratio of F over B is higher for PANI with 5% In_2O_3 (3.91) than PANI with 10% In_2O_3 (0.92) (see Table 19 for average selectivity values).

Also from the sensitivity trends discussed in Chapter 4, a synergistic effect was observed. On decreasing the In_2O_3 loading in PANI from 10% to 1.25%, the sorption of F from F 10 ppm source seemed to be significantly increased. So far, selectivity trends seem to align with sensitivity trends (PANI 5% In_2O_3 seems to show better selectivity of F over B than PANI with 10% In_2O_3). Hence, it was worth evaluating selectivity of F over B for PANI doped with lower than 5% of In_2O_3.

PANI with 2.5% In_2O_3 and PANI with 1.25% In_2O_3 were evaluated for their selectivity of F over B by exposing them to F/B (5/5 ppm each) gas mixture source. From Figure 17/Figure 18 and Figure 24/Figure 25, it seems that although PANI doped with 1.25% In_2O_3 seems to sorb more F when exposed to F 10 ppm source, it does not seem to exhibit enhanced sorption of F over B from F/B (5/5 ppm each) source. PANI with 1.25% In_2O_3 seems to sorb the least B but it does not sorb more F compared to PANI and doped PANI with different wt.% of In_2O_3. Therefore, improvement in sorption of F with a decrease in wt.% of In_2O_3 in PANI from 5% to 1.25% does not stand true for sorption of F from an F/B gas mixture (see Table 18 and Table 19, and Figure 35/Figure 36 for average sorption and selectivity values). It must also be noted that on decreasing the In_2O_3 loading in PANI from 5 wt. % to 1.25 wt. % the selectivity ratio of F over B also decreases. The increase in selectivity ratio with a decrease in In_2O_3 loading in PANI as observed on decreasing In_2O_3 from 10 wt.% to 5 wt.% in PANI does not stand true for decreasing In_2O_3 from 5 wt.% to 1.25 wt.% in PANI.

Table 18: Average sorption values for PANI and doped PANI with different wt.% of In_2O_3

	PANI		PANI with 1.25% In_2O_3		PANI with 2.5% In_2O_3		PANI with 5% In_2O_3		PANI with 10% In_2O_3	
	Average sorption values (in ppm)									
	F	B	F	B	F	B	F	B	F	B
5 ppm F and 5 ppm B	0.62 ± 0.01498	0.44 ± 0.038	0.86 ± 0.025	0.36 ± 0.01	1.35 ± 0.0165	0.60 ± 0.095	1.67 ± 0.026	0.55 ± 0.1489	0.61 ± 0.058	0.67 ± 0.0751

Note: ± values indicate the estimate of one standard error (se)

	PANI		PANI with 1.25% In_2O_3		PANI with 2.5% In_2O_3		PANI with 5% In_2O_3		PANI with 10% In_2O_3	
	95% Confidence Interval									
	F	B	F	B	F	B	F	B	F	B
5 ppm F and 5 ppm B	0.62 ± 0.038	0.44 ± 0.099	0.86 ± 0.317	0.36 ± 0.127	1.35 ± 0.05	0.60 ± 0.2977	1.67 ± 0.08	0.55 ± 0.46578	0.61 ± 0.185	0.67 ± 0.239

Table 19: Average selectivity values for PANI and doped PANI with different wt. % of In_2O_3

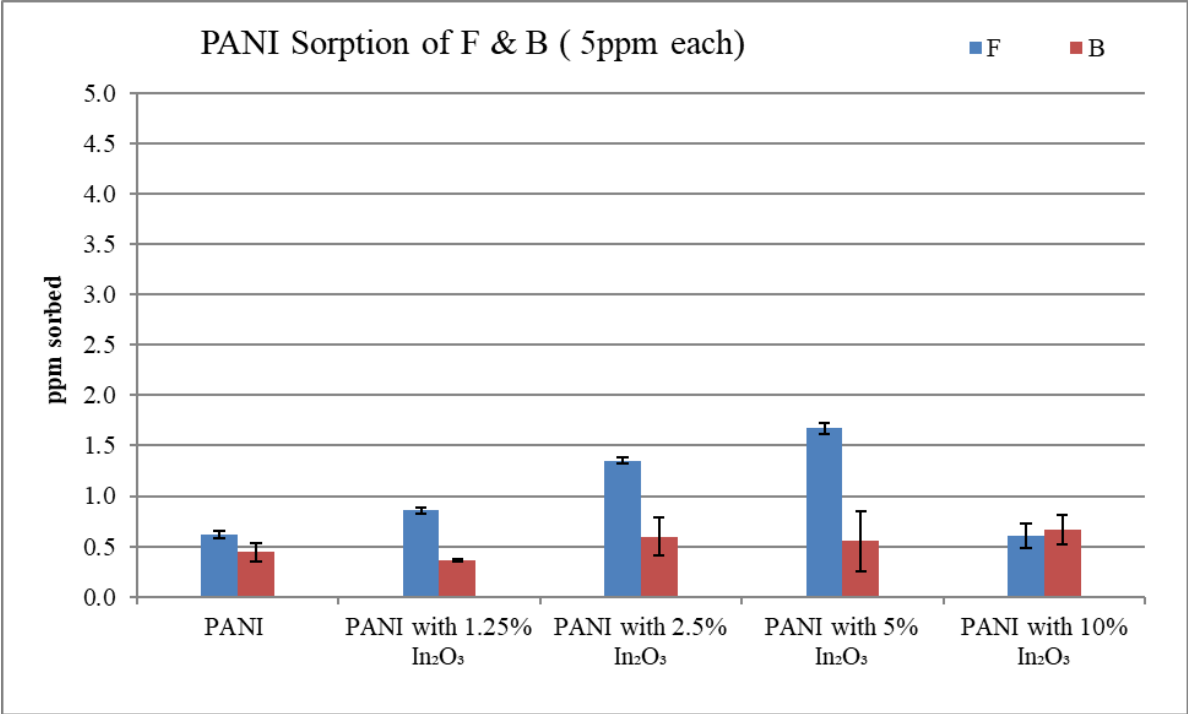| Sensing Material	Average selectivity values of F over B
PANI	1.46
PANI with 1.25% In_2O_3	2.37
PANI with 2.5% In_2O_3	2.46
PANI with 5% In_2O_3	3.91
PANI with 10% In_2O_3	0.92

Figure 35: F & B sorption (in ppm) for PANI and doped PANI with different wt. % of In_2O_3; (Source: F/B, 5/5 ppm)
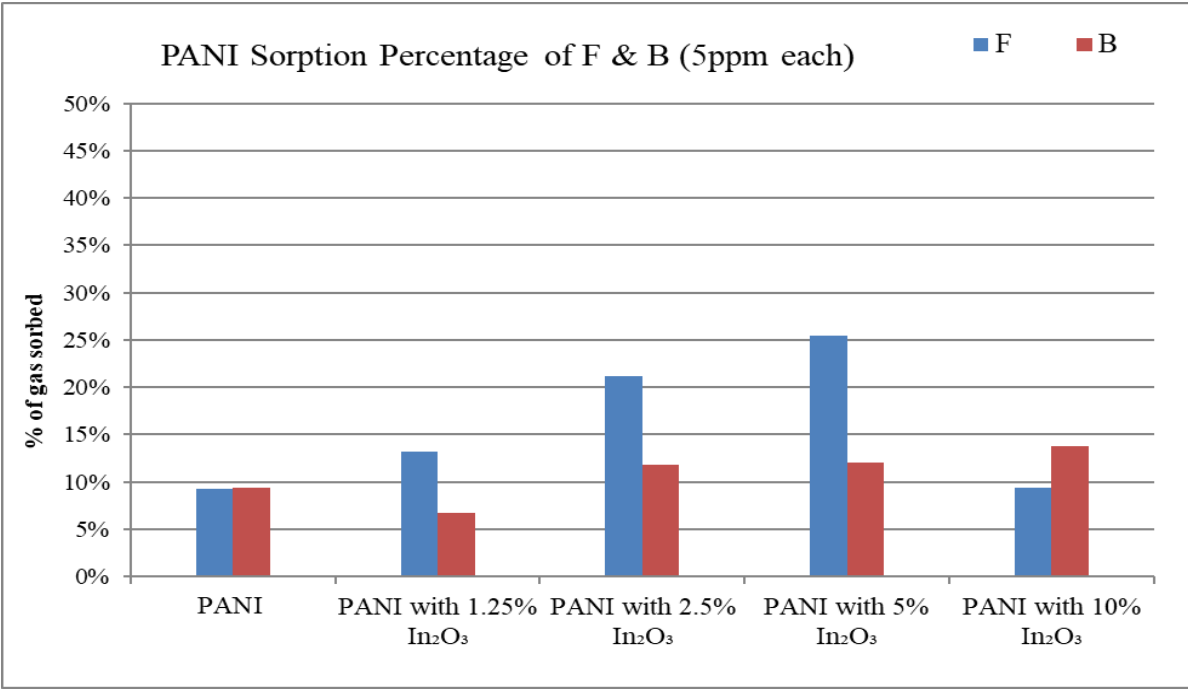

Figure 36: F & B sorption (in %); for PANI and doped PANI with different wt. % of In_2O_3; (Source: F/B, 5/5 ppm)

After evaluating PANI with 2.5% In_2O_3 and PANI with 1.25% In_2O_3 for their selectivity of F over B, the selectivity trends for PANI and doped PANI with different loadings of In_2O_3 are now clear. On decreasing or increasing In_2O_3 dopant further than 5 wt. % in PANI, the selectivity towards F over B seems to be decreasing.

Furthermore, the selectivity trends seem to be opposite to the sensitivity trends for PANI with different loadings of In_2O_3 in the 1.25% to 5% range. Sensitivity trends (towards F when exposed to F 10 ppm source) seem to increase on decreasing the wt.% of In_2O_3 in PANI from 5% to 1.25%, while selectivity trends seem to increase on increasing the wt.% of In_2O_3 in PANI from 5% to 1.25%. Overall, it is evident from Figure 17/Figure 18 and Figure 24/Figure 25 (Chapter 4) that PANI with 5% In_2O_3 has good sensitivity, highest selectivity (among other PANI samples doped with In_2O_3 materials), and is therefore a potential candidate (a good compromise overall) for sensing formaldehyde in a concentration range of about 5 to 10 ppm. The statistical analysis presented in Appendix I is also in agreement with the selectivity trends for PANI with different wt.% of In_2O_3.

The reverse sensitivity and selectivity trends for PANI doped with In_2O_3 can be explained further with the changing surface morphology of PANI with varying wt. % of In_2O_3 dopant (discussed in Chapter 7).

5.1.2 P25DMA and doped P25DMA with MO

P25DMA, when exposed to F 10 ppm, seems to sorb less F compared to the modified P25DMA with a metal oxide such as TiO_2 and NiO (as discussed in Section 4.1.2). P25DMA, when exposed to B 10 ppm source, seems to sorb more B compared to the modified P25DMA with a metal oxide such as TiO_2 (as discussed in Section 4.2.2). Hence, it is speculated that P25DMA on its own might have a lower selectivity towards F over B and doped P25DMA with TiO_2 might have a better selectivity of F over B. But these are just speculations deduced from the sensitivity studies conducted and discussed earlier in Chapter 4. Therefore, to check the hypothesis, P25DMA and doped P25DMA were exposed to a gas mixture of F/B (5/5 ppm each) source.

When P25DMA and P25DMA doped with 20% TiO_2 were exposed to formaldehyde and benzene simultaneously (5 ppm each), P25DMA with 20% TiO_2 seemed to sorb less F than pure P25DMA (see Table 20, Figure 37 and Figure 38).

The selectivity of F over B seems to be the same for both doped (with TiO_2) and undoped P25DMA: P25DMA had an average selectivity (F/B) of 2.20, while P25DMA with 20% TiO_2 had an average selectivity of 2.23. Therefore, the experimental results do not indicate that doping P25DMA with 20% TiO_2 has any major impact on selectivity of F over B.

Table 20: Average sorption values for P25DMA and doped P25DMA

	P25DMA		P25DMA with 20% TiO$_2$	
	Average sorption values (in ppm)			
	F	B	F	B
5 ppm F and 5 ppm B	0.82 ± 0.053444	0.39 ± 0.059354	0.66 ± 0.036142	0.32 ± 0.058

Note: $\pm$ values indicate the estimate of one standard error (se)

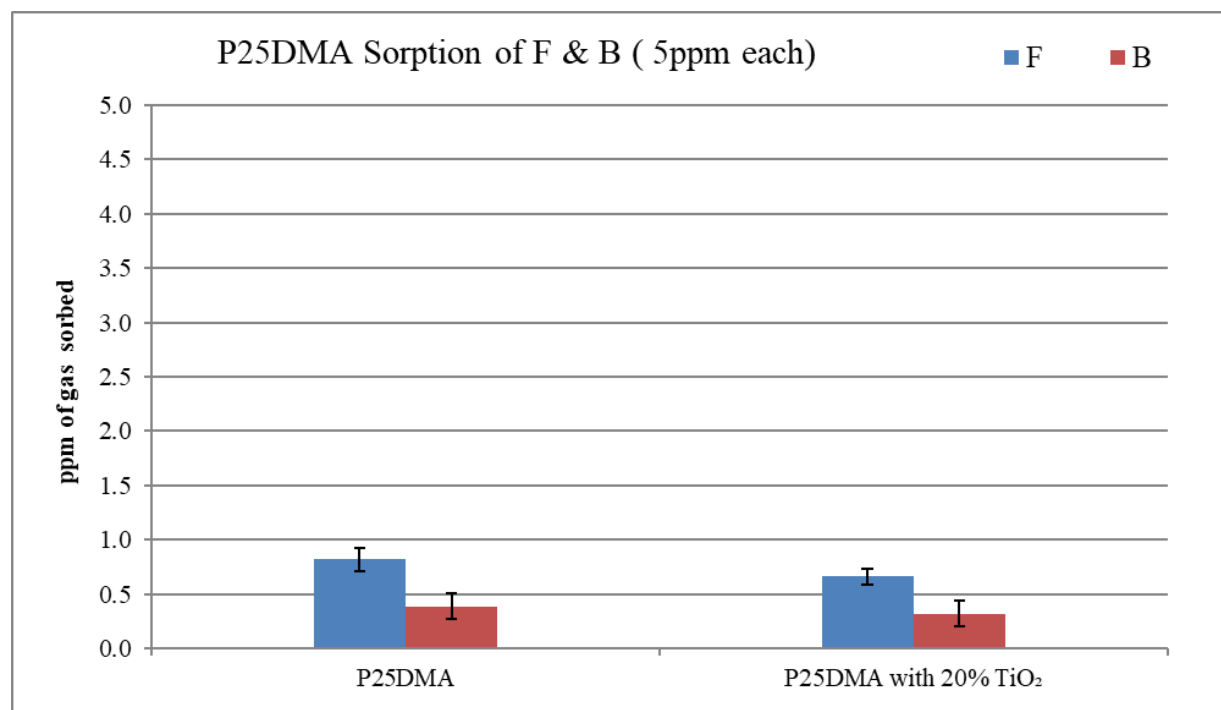|	P25DMA		P25DMA with 20% TiO$_2$	
	95% Confidence Interval (in ppm)			
	F	B	F	B
5 ppm F and 5 ppm B	0.82 ± 0.17	0.39 ± 0.188865	0.66 ± 0.115	0.32 ± 0.1846291

Figure 37: F & B sorption (in ppm) for P25DMA and doped P25DMA; (source: F/B, 5/5 ppm)
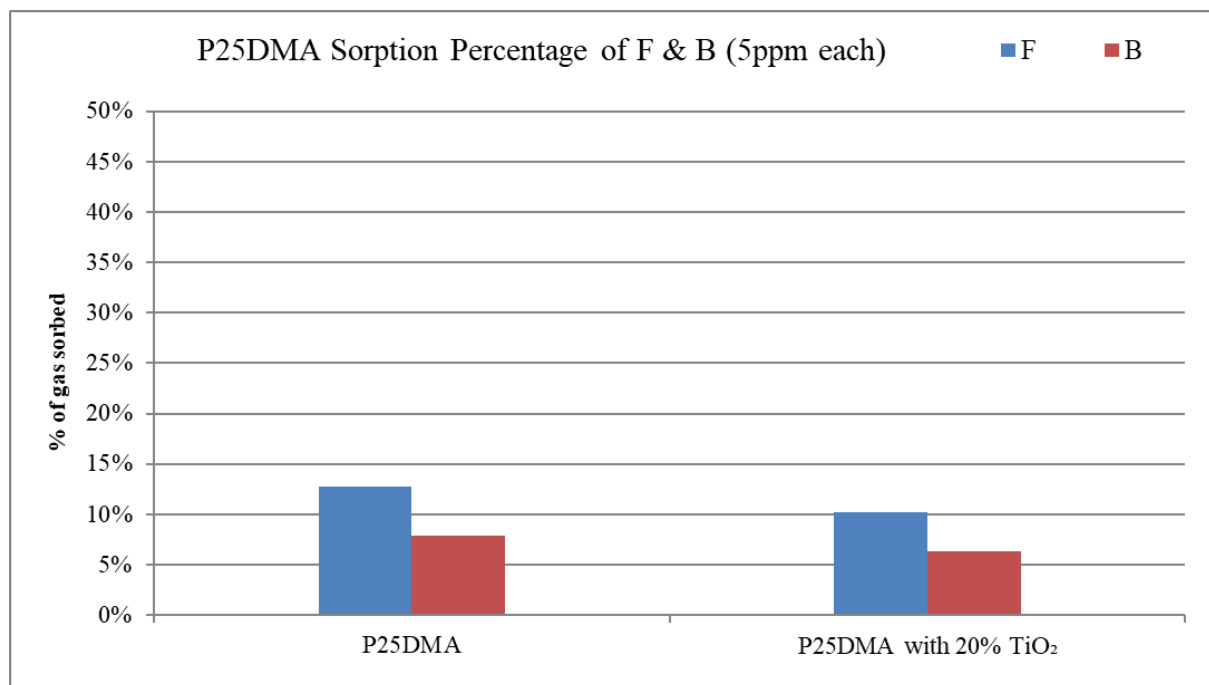
Figure 38: F & B sorption (in %) for P25DMA and doped P25DMA; (source: F/B, 5/5 ppm)

5.2 Formaldehyde over Acetaldehyde (F/Ac) Selectivity Studies

It has been mentioned several times in this thesis that acetaldehyde might pose a selectivity issue while sensing formaldehyde due to their chemical and structural similarities. Therefore, it is important to evaluate the interaction between sensing materials and formaldehyde in the presence of acetaldehyde as an interferent gas. Therefore, all the sensing materials tested so far for their sensitivity to F were evaluated for their selectivity to F over Ac by exposing them to a source of F/Ac, 2.5/2.5 ppm each (see Appendix J for raw data trends and statistical analysis of blank trials for the F/Ac gas mixture).

5.2.1 PANI and doped PANI with MO

PANI and doped PANI with different wt.% of In_2O_3 were exposed to a gas mixture of F/Ac (2.5/2.5 ppm each). On comparing sorption values for PANI and doped PANI with different wt.% of In_2O_3 in Table 21, PANI seems to have sorbed more F and more Ac (from a mixture of F/Ac (2.5/2.5 ppm)) compared to PANI doped with any amount of In_2O_3. This again shows the reverse order when compared to the results obtained when PANI and doped PANI with different wt.% of In_2O_3 were exposed to single gas (Ac 5 ppm) (Section 4.3.1, Figure 30/Figure 31, indicated that

71

acetaldehyde sorption was higher for In_2O_3 doped PANI than for pure PANI). It was also observed that when materials were exposed to a gas mixture containing F and Ac, the sorption of F and sorption of Ac both decreased with an increase in In_2O_3 dopant concentration (over the range of 2.5% to 10% by weight).

PANI with 10% metal oxide seems to have a slightly better selectivity of F over Ac than all other doped and undoped PANI materials tested for sorption (see Table 21 for average sorption values and Table 22 for selectivity values). Although PANI with 10% In_2O_3 seems to be more selective, selectivity values for F/Ac fall within a similar range. It must also be noted from Table 22 and Figure 39/Figure 40 that PANI with better selectivity of F over Ac seems to exhibit lower sensitivity for F and Ac together among all the tested doped and undoped PANI materials.

Table 21: Average sorption values for PANI and doped PANI with different wt. % of In_2O_3

	PANI		PANI with 1.25% In_2O_3		PANI with 2.5% In_2O_3		PANI with 5% In_2O_3		PANI with 10% In_2O_3	
	Average sorption values (in ppm)									
	F	Ac	F	Ac	F	Ac	F	Ac	F	Ac
2.5 ppm F and 2.5 ppm Ac	0.96 ± 0.0958	0.95 ± 0.0267	0.52 ± 0.01	0.38 ± 0.01	0.61 ± 0.050	0.50 ± 0.00629	0.56 ± 0.022	0.49 ± 0	0.34 ± 0.058	0.22 ± 0.0025

Note: ± values indicate the estimate of one standard error (se)

	PANI		PANI with 1.25% In_2O_3		PANI with 2.5% In_2O_3		PANI with 5% In_2O_3		PANI with 10% In_2O_3	
	95% Confidence Interval									
	F	Ac	F	Ac	F	Ac	F	Ac	F	Ac
2.5 ppm F and 2.5 ppm Ac	0.96 ± 0.3	0.95 ± 0.085	0.52 ± 0.127	0.38 ± 0.127	0.61 ± 0.1608	0.50 ± 0.02	0.56 ± 0.07	0.49 ± 0.0	0.34 ± 0.1857	0.22 ± 0.0079

Table 22: Average selectivity values for PANI and doped PANI with different wt. % of In_2O_3

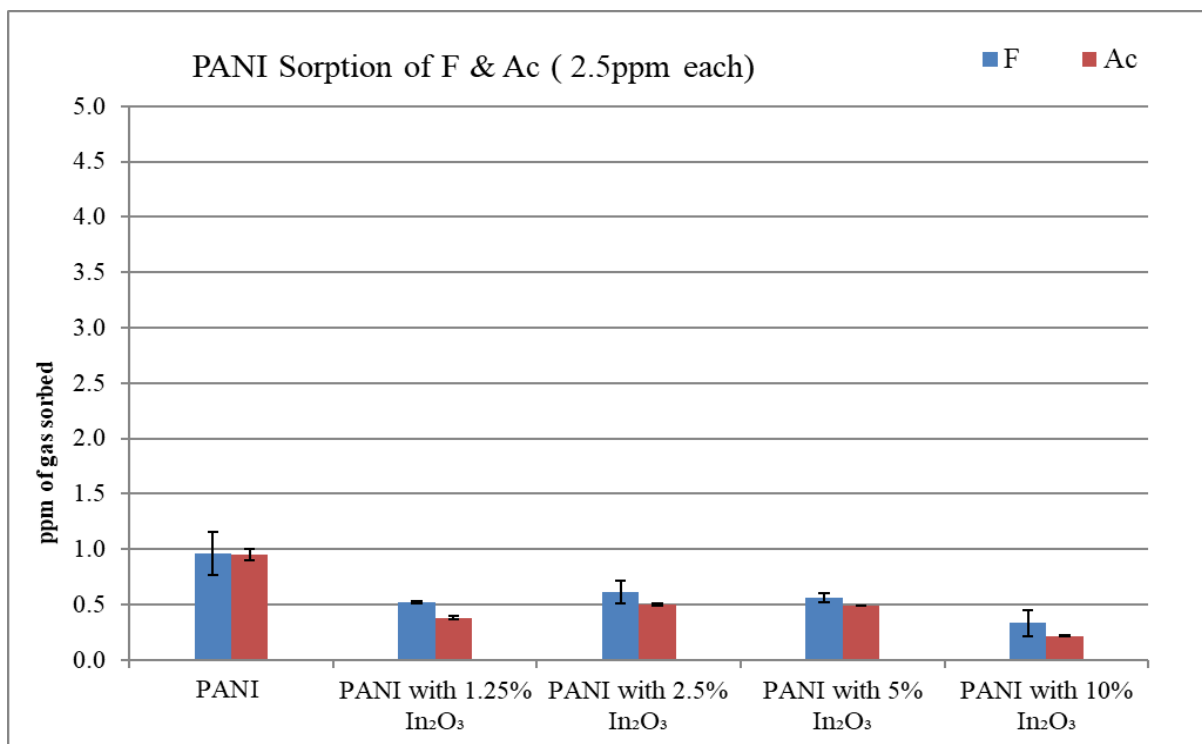| Sensing Materials	Average selectivity values of F over Ac
PANI	1.00
PANI with 1.25 In_2O_3	1.37
PANI with 2.5% In_2O_3	1.22
PANI with 5% In_2O_3	1.18
PANI with 10% In_2O_3	1.55

Figure 39: F & Ac sorption (in ppm) for PANI and doped PANI with different wt. % of In_2O_3; (Source: F/Ac, 2.5/2.5 ppm)
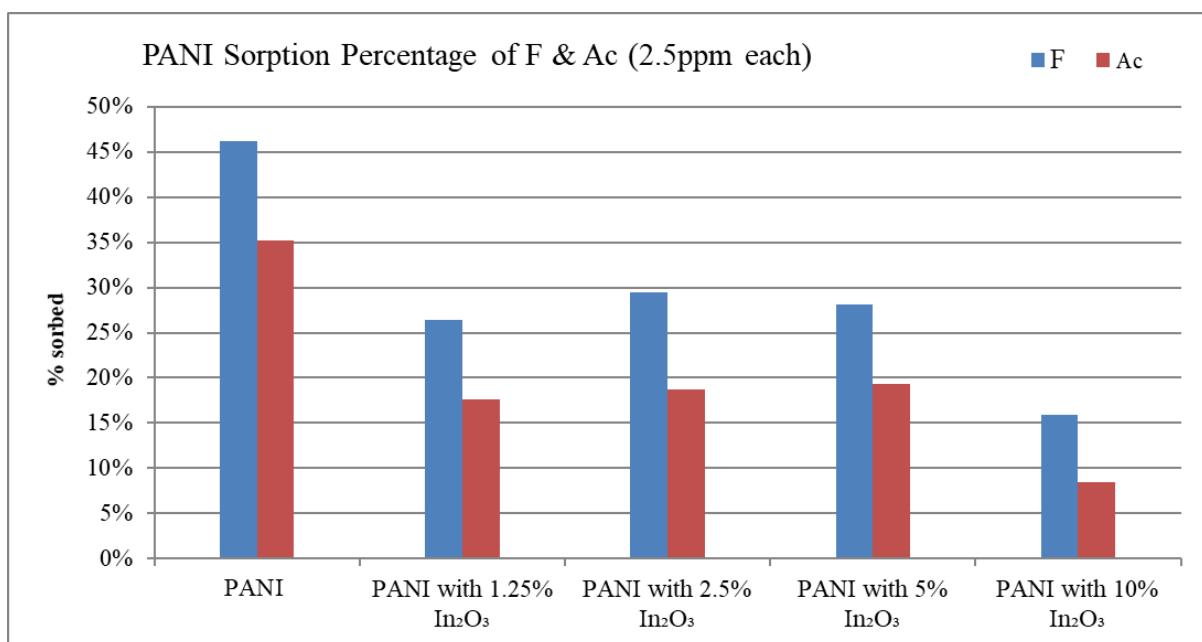

Figure 40: F & Ac sorption (in %) for PANI and doped PANI with different wt. % of In_2O_3; (Source: F/Ac, 2.5/2.5 ppm)

Overall, given the chemical similarity between formaldehyde and acetaldehyde, selectively sorbing formaldehyde from a F/Ac mixture (especially at quite a low ppm-level concentration) is noteworthy.

5.2.2 P25DMA and doped P25DMA with MO

Based on the sensitivity results of F and Ac for P25DMA doped with 10% NiO, one might say that P25DMA with 10% NiO is equally sensitive (~30%) towards F and Ac. P25DMA and P25DMA with 20% TiO_2 sorb more Ac (from a 5 ppm Ac source) (20% and 25% Ac, respectively) than F (from a 10 ppm F source) (10% and ~16%, respectively). Therefore, one might speculate that P25DMA and doped P25DMA with 20% TiO_2 might have higher affinity towards acetaldehyde compared to formaldehyde. Hence, P25DMA, P25DMA with 20% TiO_2, and P25DMA with 10% NiO were exposed to a mixture of F/Ac (2.5/2.5 ppm each) to evaluate their selectivity of F over Ac.

As shown in Table 23, P25DMA with 10% NiO seems to sorb F and Ac almost as much as P25DMA on its own, while P25DMA with 20% TiO_2 sorbed relatively lower and equal amounts of F and Ac. The average selectivity for P25DMA with 10% NiO was found to be 1.32, while selectivity for P25DMA was 1.09 and for P25DMA with 20% TiO_2 was 0.98. Therefore, P25DMA with 10% NiO seems to have better selectivity for F over Ac (even if slightly), compared to P25DMA and P25DMA with 20% TiO_2. Doping P25DMA with metal oxide does not seem to have any significant effect on its selectivity of F over Ac. Given the chemical similarity of these two gas analytes, this was as expected. Figure 41/Figure 42 show the overall picture with P25DMA (F/Ac) trials.

Table 23: Average sorption values (in ppm of Ac) for P25DMA and doped P25DMA

	P25DMA		P25DMA with 20% TiO$_2$		P25DMA with 10% NiO	
	Average sorption values (in ppm)					
	F	Ac	F	Ac	F	Ac
2.5 ppm F and 2.5 ppm Ac	0.71 ± 0.1342	0.64 ± 0.149	0.51 ± 0.0234	0.52 ± 0.0025	0.72 ± 0	0.55 ± 0.005

Note: ± values indicate the estimate of one standard error (se)

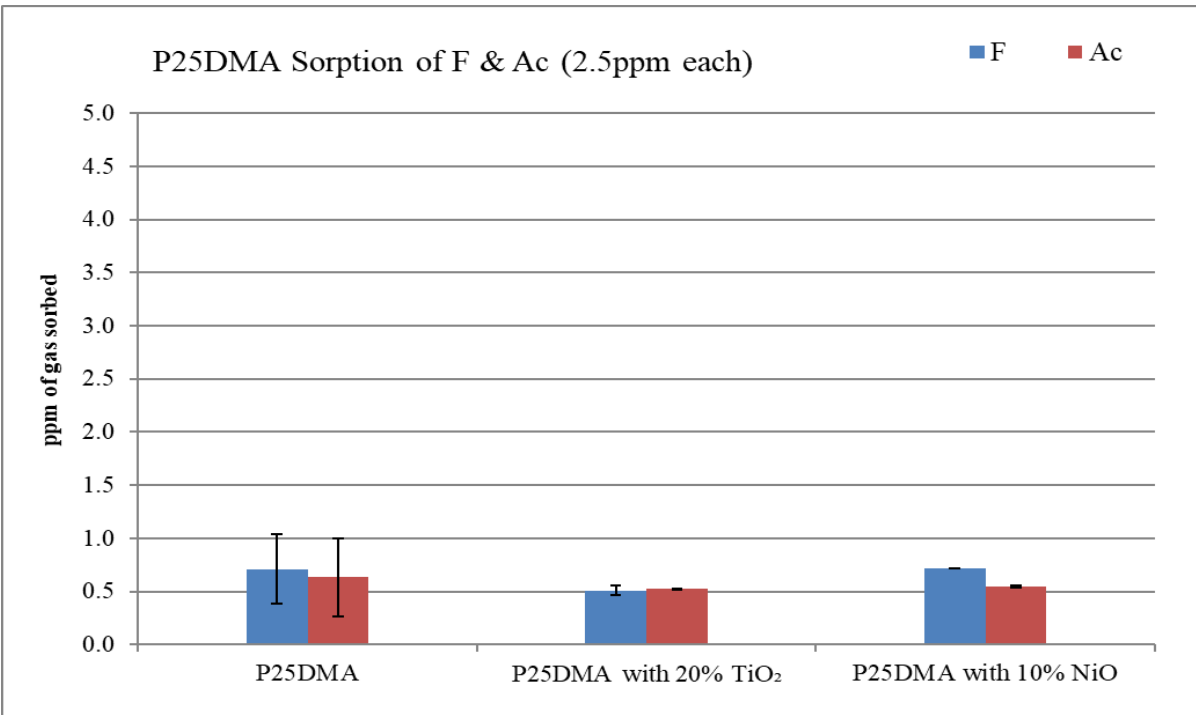|	P25DMA		P25DMA with 20% TiO$_2$		P25DMA with 10% NiO	
	95% Confidence Interval (in ppm)					
	F	Ac	F	Ac	F	Ac
2.5 ppm F and 2.5 ppm Ac	0.71 ± 0.345154	0.64 ± 0.382285	0.51 ± 0.0746	0.52 ± 0.007955	0.72 ± 0	0.55 ± 0.0635

Figure 41: F & Ac sorption (in ppm) for P25DMA and doped P25DMA; (Source: F/Ac, 2.5/2.5 ppm)
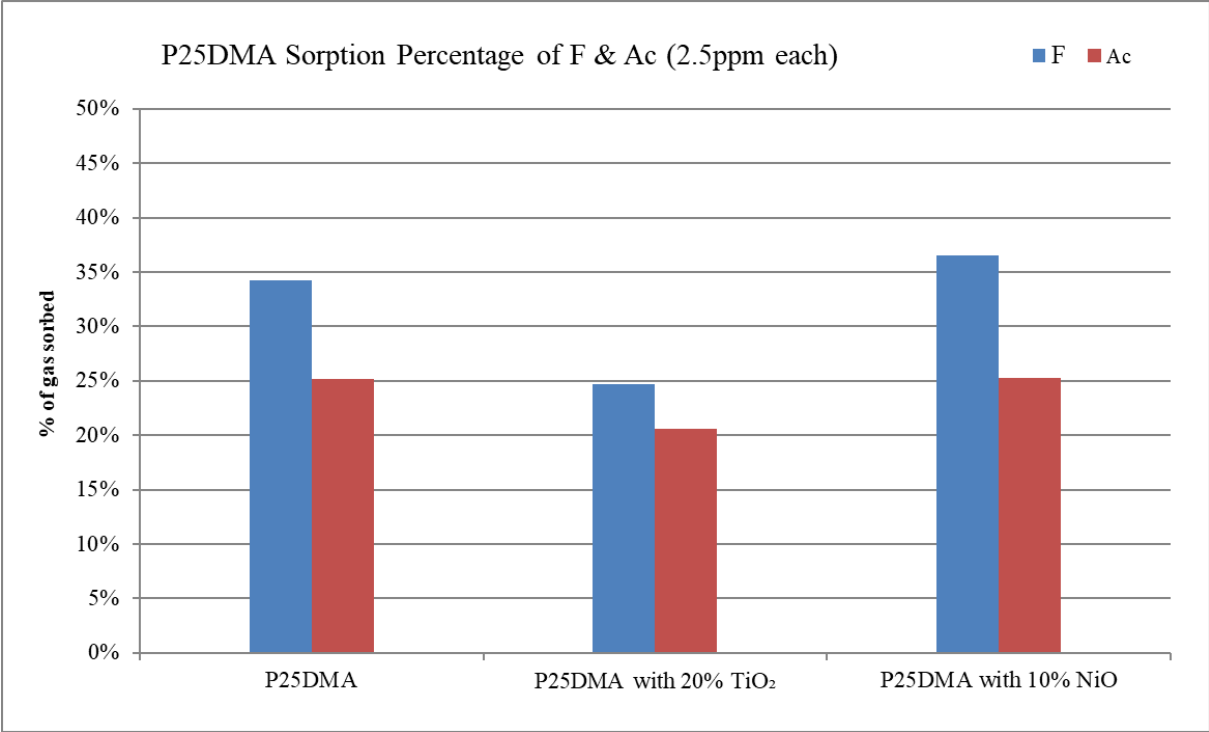

Figure 42: F & Ac sorption (in %) for P25DMA and doped P25DMA; (Source: F/Ac, 2.5/2.5 ppm)

The selectivity results provide extra corroboration for the sensitivity results (discussed earlier in Chapter 4) that P25DMA and doped P25DMA seem to be equally sensitive to both F and Ac. The lower selectivity of P25DMA and doped P25DMA towards F over Ac seems be due to the synergistic effect of the chemical similarity of F and Ac. Both F and Ac have the same functional group and similar dipole moment. One would have expected a slightly larger steric hindrance due the presence of the two methyl groups on P25DMA and a slightly larger size for the Ac molecule, however the differences do not seem significant enough to cause large differences in selectivity. Benzene is a much bulkier molecule, so both P25DMA and doped P25DMA seem to have comparatively better selectivity of F over B (as discussed in Section 5.1.2).

Chapter 6: Results and Discussion – Stability Studies

Sensitivity and selectivity are the two main characteristics that one requires for proper evaluation of gas sensing materials for any target gas analyte. Sensitivity is the only characteristic usually evaluated in the literature (although most of the literature papers report a percentage of change in resistance, without translating it necessarily to ppm of analyte sorbed). Selectivity and stability characteristics are hardly ever discussed. Stability of sensing materials is a third characteristic, with a 'looser' definition, involving the effects of environmental factors on sensing materials. A sensitive and selective but not stable sensing material might restrict the applications of the related sensor, and/or give unreliable results. The most important factors for stability studies are the effects of temperature and ageing.

6.1 Effect of Temperature on Sorption of Sensing Materials

To evaluate the sorption of selected polymeric material with varying temperature, PANI samples were exposed to F 10 ppm (source) and the temperature was varied by heating the flask containing the sensing material using a regular hair dryer (and monitoring by a temperature sensor) from ~25°C to ~60°C (as shown in Chapter 3, Figure 11b). PANI with 5% In_2O_3 was selected to study the effect of varying temperature since it seemed to be a potential polymeric material for sensing formaldehyde (as per the sensitivity and selectivity results discussed earlier in Chapter 4 and Chapter 5). The effects of pressure and humidity are of lesser importance herein, since the effect of pressure is equivalent to a concentration effect, which has been well studied, whereas the effect of humidity is implicitly taken into account, as the flasks always allow for some leakage.

From the sorption values for PANI with 5% In_2O_3 presented in Table 24, the ability of PANI with 5% In_2O_3 to sorb seems to increase with an increase in temperature compared to the case of PANI with 5% In_2O_3 at (constant) room temperature. Heating and cooling temperature profiles for non-isothermal PANI with 5% In_2O_3 sorption of F are presented in Appendix K. Both heating and cooling temperature profiles display good reproducibility.

Table 24: Average sorption values for PANI with 5% In_2O_3

Sensing Material	Average Sorption Values
PANI with 5% In_2O_3	1.64 ± 0.007 ppm of F
PANI with 5% In_2O_3 with variable T	4.18 ± 0.1298 ppm of F

Note: $\pm$ values indicate the estimate of one standard error (se)

Sensing Material	95% Confidence Interval
PANI with 5% In_2O_3	1.64 ± 0.0225 ppm of F
PANI with 5% In_2O_3 with variable T	4.18 ± 0.4129 ppm of F

PANI with 5% In_2O_3 was observed to sorb about 2.5 times more F when exposed to F 10 ppm source at higher temperature compared to room temperature (as shown in Figure 43/Figure 44). The increase in sorption can be attributed to the relaxation of the PANI chains on increasing temperature. The relaxation of PANI chains allowed F to access and interact with more active sites of the sensing material.

The good sorption of F on PANI with 5% In_2O_3 at levels above room temperature also indicate that PANI with 5% In_2O_3 is stable and does not lose its ability to detect F at higher temperatures.
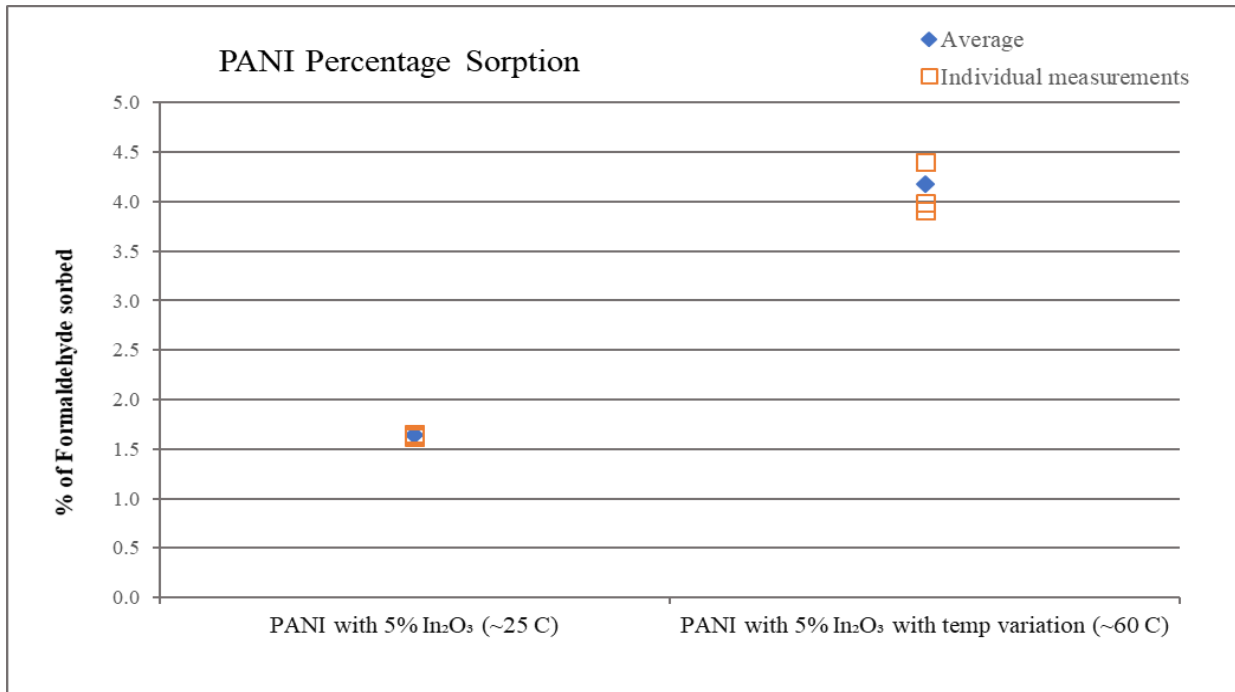

Figure 43 : Formaldehyde sorption (in ppm) for PANI with 5% In_2O_3 with constant and varying temperature conditions; (Source: F 10 ppm)
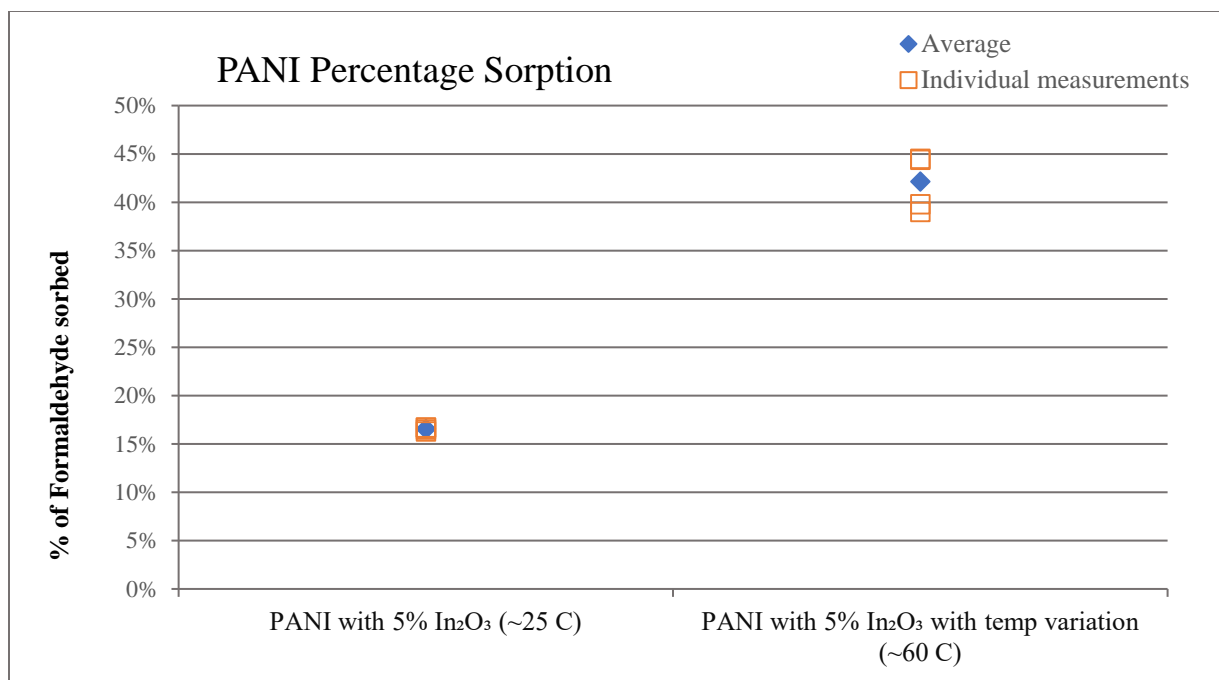
Figure 44: Formaldehyde sorption (in %) for PANI with 5% In_2O_3 with constant and varying temperature conditions; (Source: F 10 ppm)

6.2 Effect of Aging on Sorption of Sensing Materials

Ageing effects are more important and indicative of the stability of the sensing materials. To demonstrate the effect of ageing, a summary plot is shown Figure 45, showing results with PANI, tested over about a decade. The materials were prepared using the same synthesis procedures and recipe components, and by different operators. Testing was also performed by different operators over many years in the lab. Figure 45 displays the results from this rather comprehensive ageing study conducted by exposing the PANI samples to F 10 ppm source.
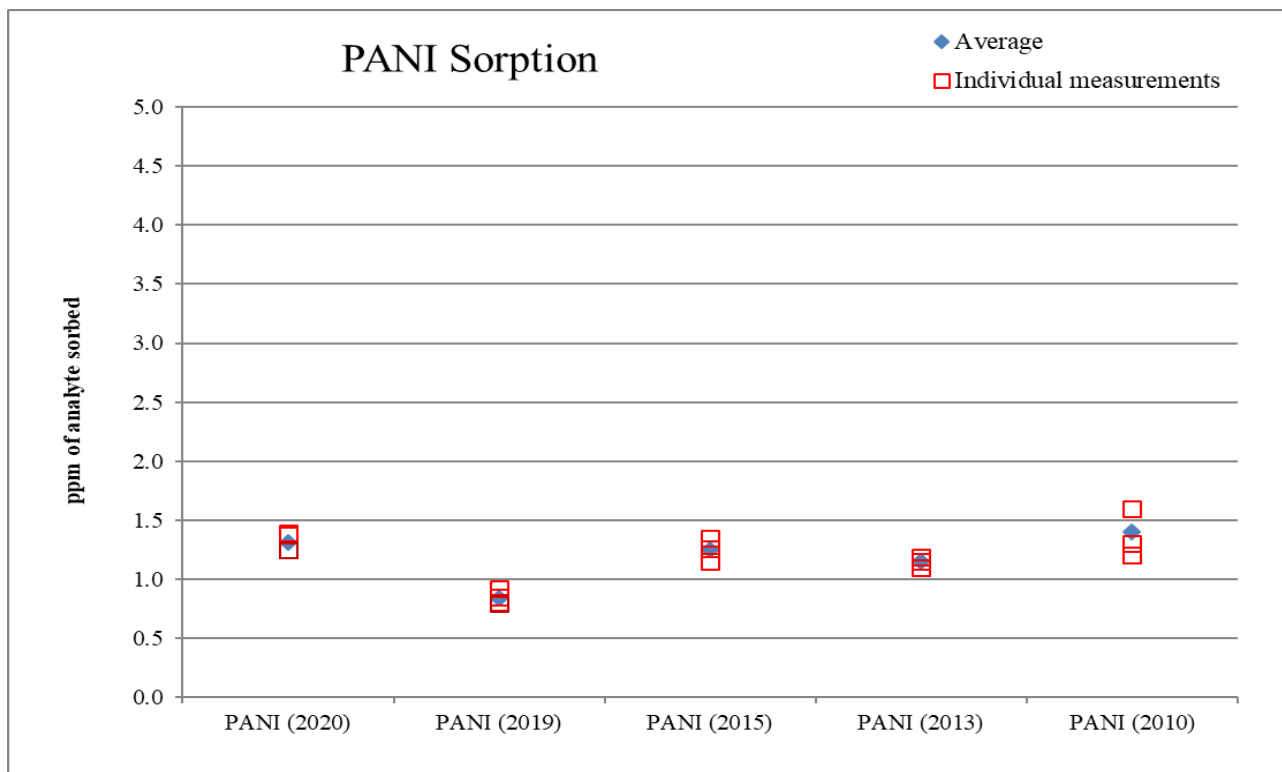
Figure 45: Formaldehyde sorption (in ppm) sorption of PANI (source: 10 ppm F)

It must be noted from Figure 45 that all five PANI samples seem to sorb an average of ~1.4 ppm of F from F 10 ppm and ageing has almost no effect on PANI sorption of F.

6.3 Effect of Polymer Source

To evaluate the performance (sensitivity) of sensing materials from different sources, two, polyaniline samples (as described in Section 3.1) were employed. Different masses of PANI synthesized in the lab (L) and received from Sigma (S) were tested for sorption. F at 10 ppm was used as the source of gas for the sorption tests.

The results presented in Table 25 and Figure 46/Figure 47 indicate that the lab-synthesized PANI (L) and the PANI purchased from Sigma (S) sorb formaldehyde at similar levels. In parallel, investigating the impact of mass on sorption revealed that the sorption of formaldehyde onto PANI seemed to increase as the mass of PANI increased, as expected.

Table 25: Average values of sorption (in ppm) of PANI (L) and PANI (S) for formaldehyde (F)

Polymer Mass	Average sorption values of PANI (L)	Average sorption values of PANI (S)
0.1 g	1.315 ± 0.03775 ppm of F	1.44 ± 0.02056 ppm of F
0.3 g	1.53 ± 0.0298 ppm of F	--
0.5 g	1.80 ± 0.0165 ppm of F	2.10 ± 0.034 ppm of F

Note: ± values indicate the estimate of one standard error (se) for the average sorption value.

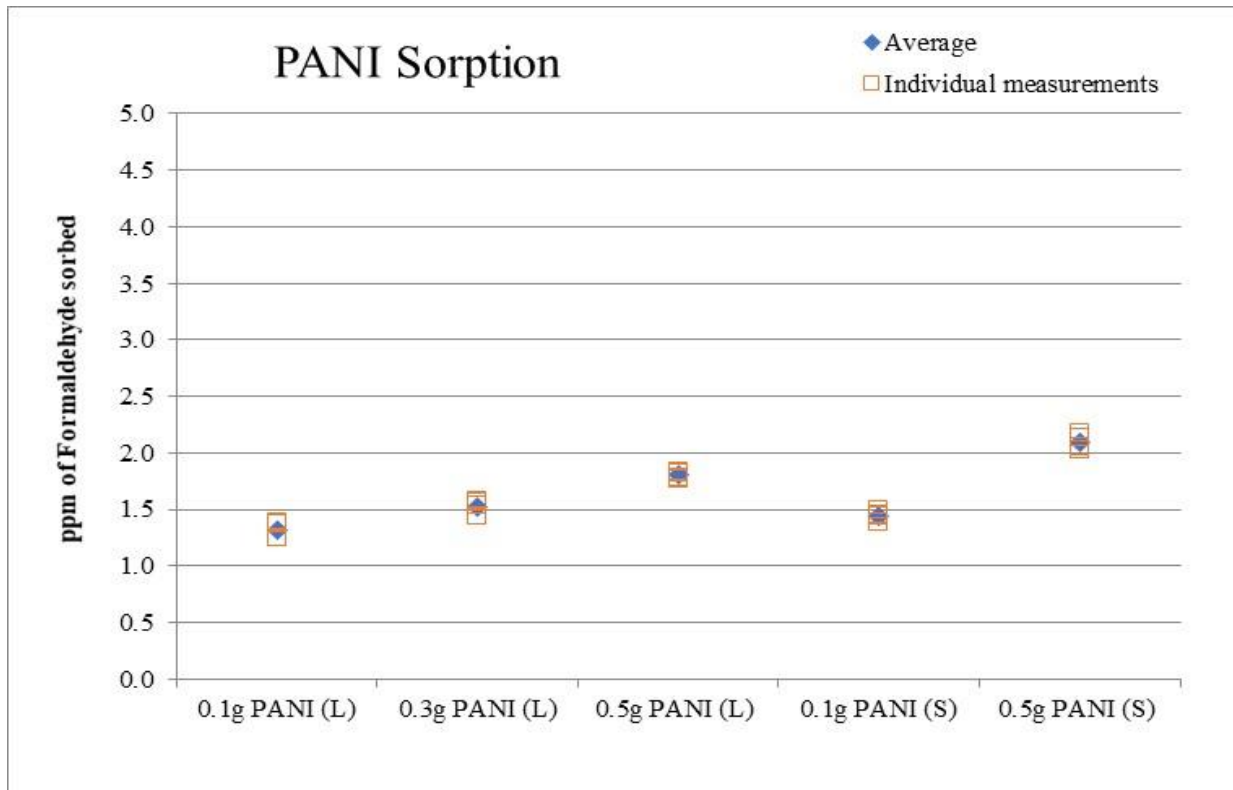| Polymer Mass	95% Confidence Interval for PANI (L)	95% Confidence Interval for PANI (S)
0.1 g	1.315 ± 0.120118 ppm of F	1.44 ± 0.0.0654 ppm of F
0.3 g	1.53 ± 0.0949 ppm of F	
0.5 g	1.80 ± 0.052567 ppm of F	2.10 ± 0.1082 ppm of F

Figure 46: Formaldehyde sorption (in ppm) for PANI (L) and PANI (S); (Source: F 10 ppm)
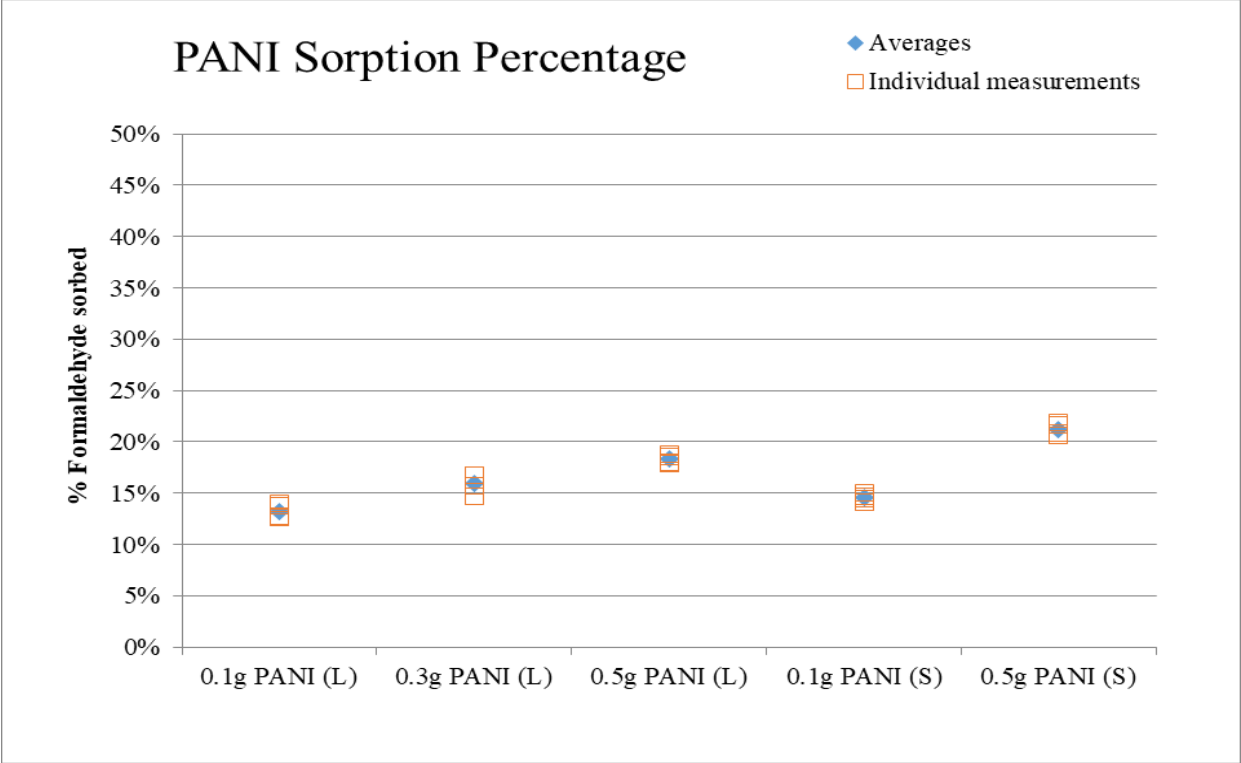
Figure 47: Formaldehyde sorption (in %) for PANI (L) and PANI (S); (Source: F 10 ppm)

Chapter 7: Results and Discussion – Characterization Studies

7.1 Dopant Incorporation

Doped PANI and P25DMA with metal oxide were established as good sensing materials (performing better than their undoped counterparts) for formaldehyde (Chapter 4 and Chapter 5). It was postulated that a reasonable amount of sorption could be related to the incorporation of the metal oxide in PANI and P25DMA.

The metal oxide incorporation was studied using data obtained from EDX (Energy Dispersive X-Rays). Data obtained for selected doped PANI and doped P25DMA from EDX are shown in Table 26. Firstly, the metal oxide incorporation results make sense, except for the upper bound of the recipe with 2.5% indium oxide. One cannot incorporate more metal oxide than was originally present in the synthesis recipe. Secondly, one never expects perfect incorporation and detection by EDX. Usually, even under more or less ideal conditions, the detected metal oxide weight % will be lower than what has been used in the recipe (error sources are in both dispersions of metal oxide (during synthesis) and detection during EDX (one has to live with a finite number of images and hence investigated areas of the sample). Thirdly, a higher relative error is expected at lower weight % of metal oxide in the recipe (due to the above reasons). Hence, the incorporation results (and confirmations by EDX) of Table 26 look reasonable.

More specifically, the % of metal oxide incorporation was measured over the area of a full image for roughly 96 seconds to get a good representation of the whole sample. For PANI with 2.5% In_2O_3, the incorporation estimate for the full imaged area was fairly close to what was available during synthesis, however, the localized spot estimation ranged roughly from 4.44% to 47.89% of In_2O_3 (see Figure 48 for a representative example of two 'spots' scanned). This suggests that In_2O_3 seems to disperse in the polymer as clusters/aggregates of indium oxide nanoparticles in and around the polymer chains. This is evident from the white coloured clusters (indium oxide) present between the black coloured polymer (carbon) in Figure 48, which can also be seen more clearly in Figure 50d, Figure 51d and Figure 52c at a higher magnification. Consequently, metal oxide incorporation could also have a significant effect on surface morphology and therefore, sorption capabilities of the polymeric nanocomposites. Figure 49 is a reminder of trends for sensitivity for different sensing materials, doped and undoped, for formaldehyde (F) sorption from a 10 ppm source of F (discussed earlier in Chapter 4). The formation of clusters of In_2O_3 nanoparticles in the polymer matrix seems to be enhancing the sorption of the target gas (F) analyte, as evident from Figure 49.

Table 26: Measured metal oxide incorporation in different polymeric materials

Polymeric Nanocomposite (synthesis conditions)	Weight percent of the metal oxide incorporation (average and % error bounds)
PANI with 2.5% In_2O_3	1.93% (1.1194%, 2.74%)
PANI with 5% In_2O_3	2.94% (1.97%, 3.9%)
PANI with 10% In_2O_3	7.36% (6.31%, 8.41%)
P25DMA with 20% TiO_2	14.42% (12.42%, 16.42%)

Note: In Table 26, average incorporation levels from EDX are cited, followed by % error bounds (in parentheses) on the wt. % of the metal oxide incorporation; error bounds were obtained from several EDX measurements on different spots of the same sample.
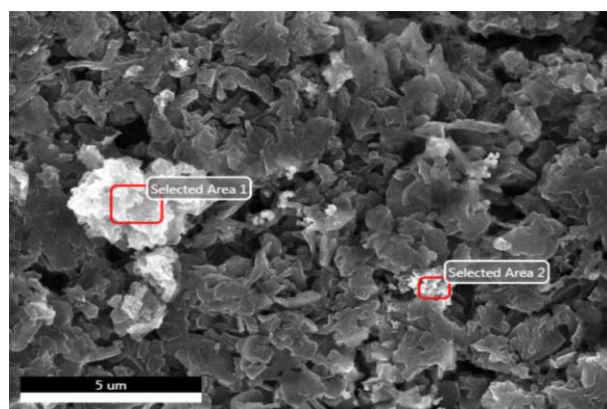

Figure 48: PANI with 2.5% In_2O_3 'spots' selected for localized EDX scans (5000X magnification)
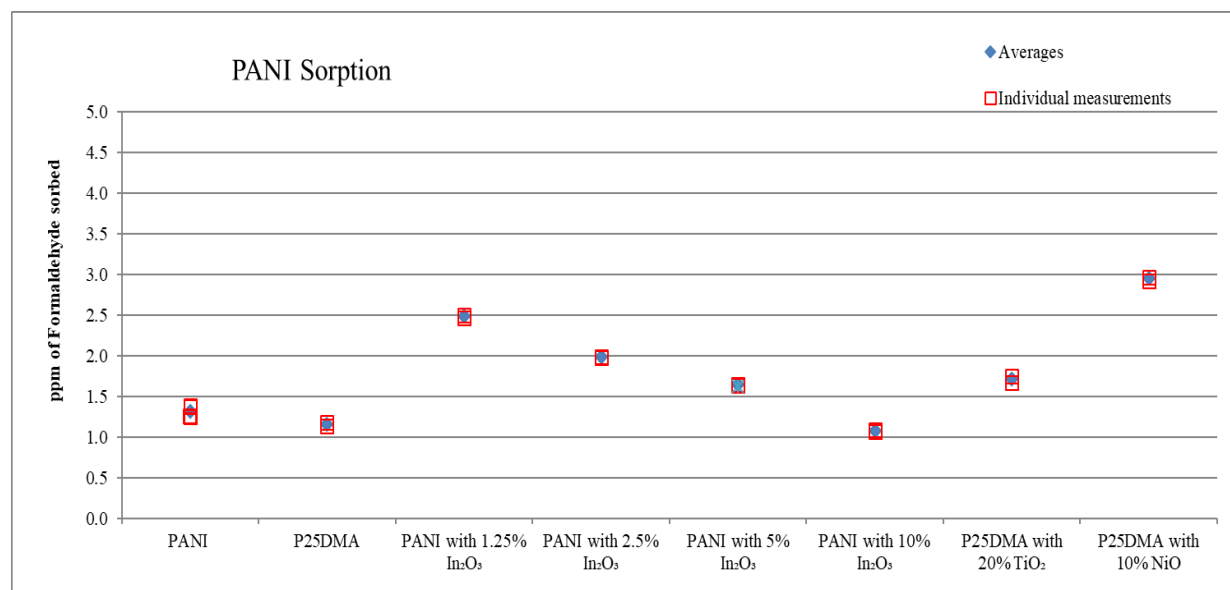

Figure 49: Formaldehyde sorption for doped and undoped PANI and P25DMA (in ppm) (Source: 10 ppm F)

7.2 Surface Morphology

PANI- The surface morphology of the polymeric materials was studied using SEM images shown in Figure 50 to 52. Figure 51 represents the same samples as in Figure 50, but with higher magnification (1000X in Figure 50 vs 5000X in Figure 51). In Figure 50a, PANI exhibits a 'grainy particulate' morphology (typical of long polymeric chains that are entangled and form a fibrous structure), offering sufficient interstitial space/area among the 'grains', almost like a porous catalyst particle or a polymer particle produced by suspension polymerization. This 'porous' grainy/fibrous surface seems to behave as if having 'pores and cavities', which can trap the gas analyte molecules as they pass over the polymer sample. The fibrous structure of PANI with several 'cavities' tends to increase the surface area of the polymer that promotes more interactions between the polymer molecules and the gas analyte, hence more sorption and higher sensitivity of the polymeric materials for the gas analyte (relative to a 'flat solid' surface). The 'cavities' (interstitial space) bear a resemblance to the hollow catalyst spherical particle that forms a porous/fibrous structure as it fractures accommodating an exothermic polymerization (or an exothermic catalytic reaction).

In principle, metal oxide dopants can be added to improve the selectivity/sensitivity of a sensing material [72], [73]. The dopant can affect the sensitivity/selectivity by incorporating (dispersing) in different ways inside the polymer structure, thus increasing the surface area, enhancing the folding of the polymer chains, and improving mechanical and physical integrity. On the other hand, homogeneous incorporation may fail completely; in such a case, the presence of the metal oxide may destroy an otherwise good (for sensitivity/selectivity) structure of the polymer. Therefore, it is important to select an appropriate metal oxide dopant by considering factors such as target analyte, polymer to be doped, polymer synthesis procedure, doping process, and the physical/chemical properties of the dopant.
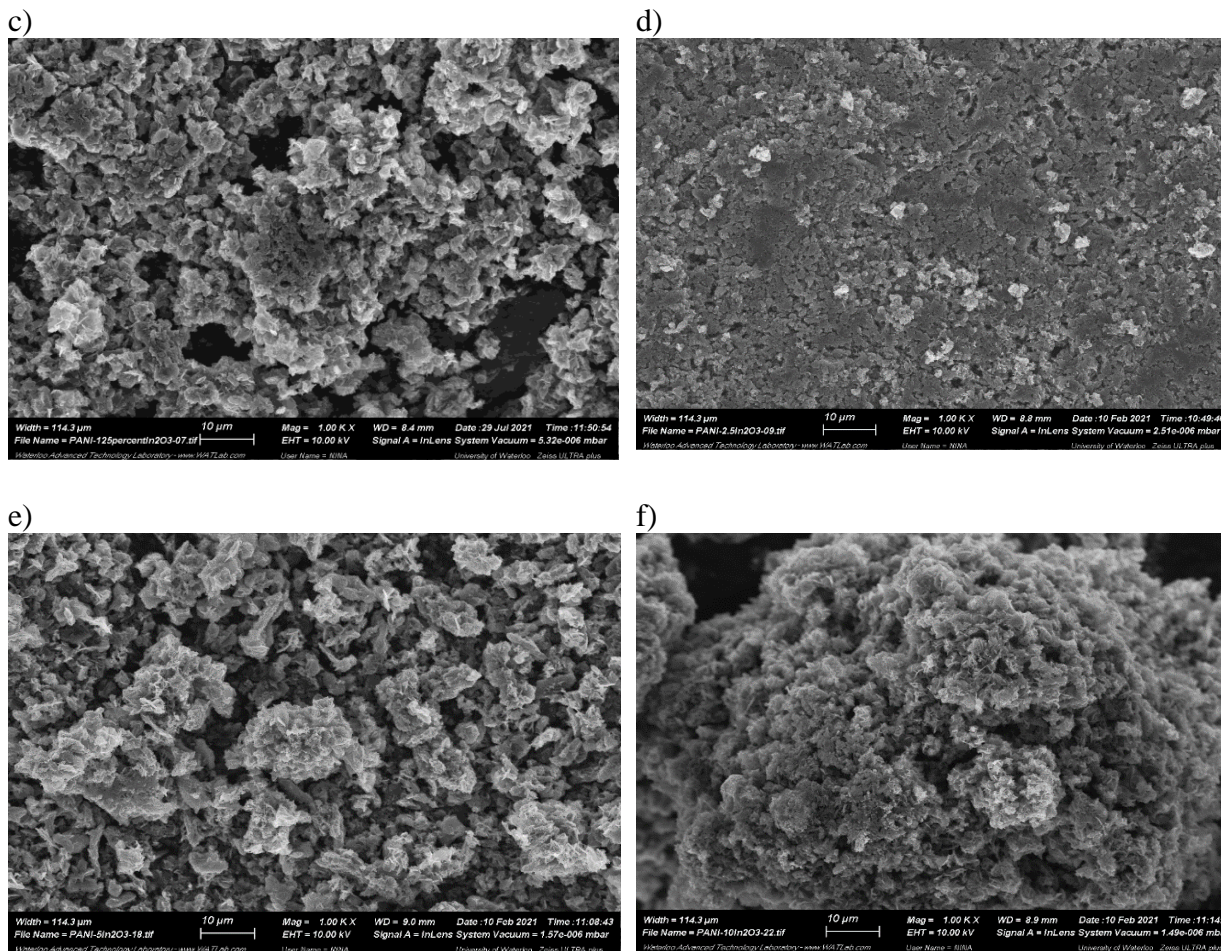
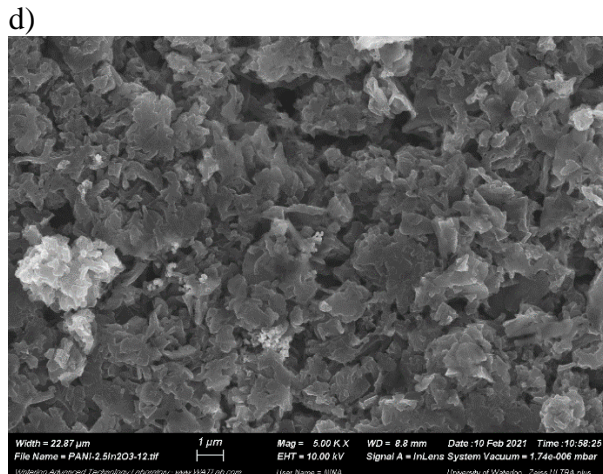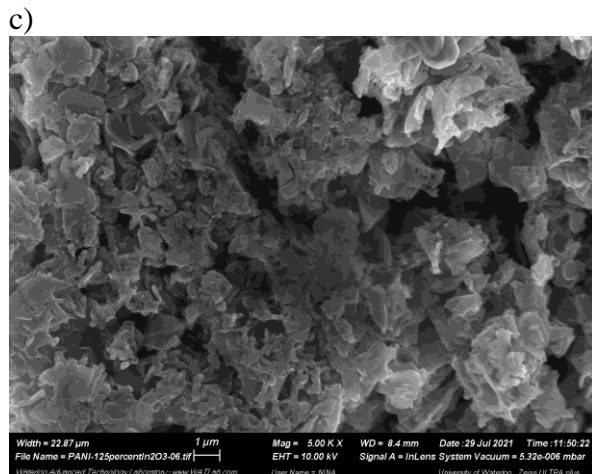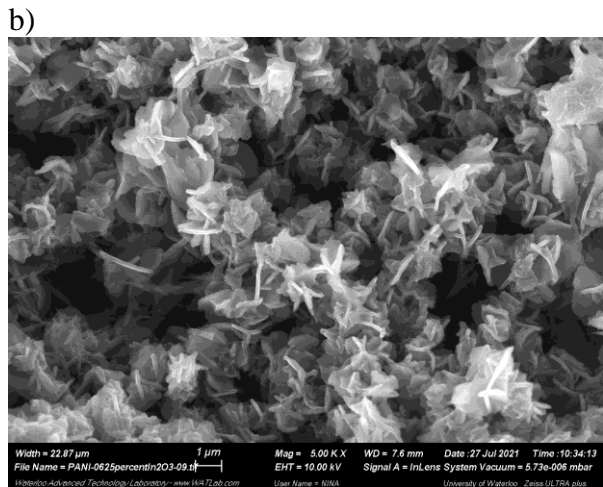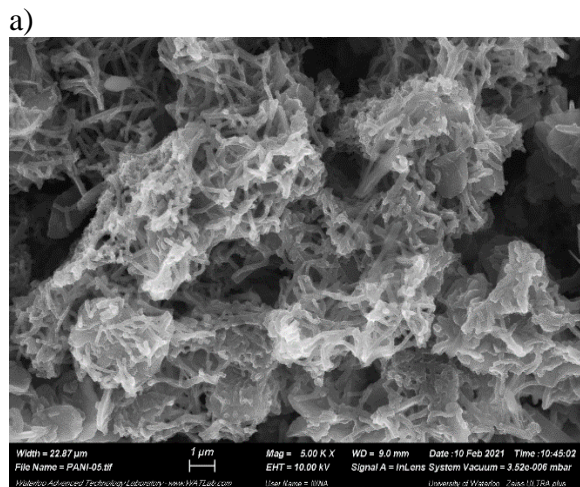a)   b)
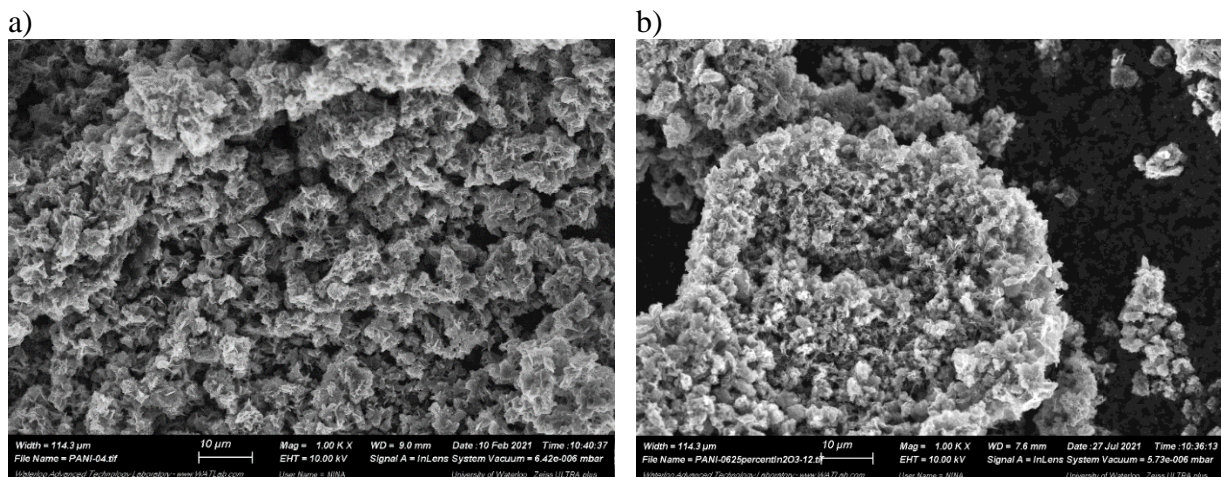
Figure 50: Surface morphology of a) PANI, b) PANI doped with 0.625% In$_2$O$_3$, c) PANI doped with 1.25% In$_2$O$_3$, d) PANI doped with 2.5% In$_2$O$_3$, e) PANI doped with 5% In$_2$O$_3$, f) PANI doped with 10% In$_2$O$_3$, all at 1000X magnification

In$_2$O$_3$ was used as a dopant to improve (hopefully) the sensing properties of (undoped) PANI as discussed in Chapters 4 and 5. In$_2$O$_3$ metal oxide has been observed to enhance sensing properties due to its unique hollow porous shell structure [67]. It is a good semiconductor with a bandgap of 3.55-3.75eV and has been used for the detection of formaldehyde [66]. It is evident in Figure 50b-f that indium oxide has affected the surface morphology of the PANI (scrutinize especially Figure 50c-d). The metal oxide nanoparticles tend to agglomerate and/or aggregate when dispersed in aqueous media during the synthesis of PANI, which limits its incorporation with the monomer and polymer, and this supports the results obtained using EDX in Table 26 (Section 7.1). In the case of PANI with In$_2$O$_3$ (Figure 50 and Figure 51), the incorporation of the metal oxide (and homogeneity of its distribution within the polymer matrix) is likely improving with a decrease in the wt.% of the metal oxide available during synthesis. The incorporation of metal oxide is directly related to the surface morphology of the final polymer. PANI on its own (Figure 50a/Figure 51a) seems to have an entangled fibrous chained structure with 'cavities'. PANI with 0.625 wt.% of In$_2$O$_3$ seems to have a mixture of sheet-like (although to a lesser extent) and fibrous structures

86

(Figure 50b/Figure 51b). PANI with 1.25 wt.% In_2O_3 and PANI with 2.5 wt.% In_2O_3 seem to have a morphology like a (layered) stack of "sliced cactus sheets" with rounded edges; the latter also have some fibrous ends (these details can be seen better in Figure 50c-d/Figure 51c-d). On the other hand, PANI with 5 wt.% In_2O_3 and PANI with 10 wt.% In_2O_3 (Figure 50e-f/Figure 51e-f) appear as a mixture of entangled fibrous structures (from the original PANI) but with relatively minor, i.e., less, sheet-like topology similar to that observed for PANI with 0.625 wt.% In_2O_3. The modification in the PANI structure from "basic fibrous" to "layered sheet-like" seems to be due to the addition of In_2O_3 dopant during synthesis.

More specifically, one can see from Figure 50c-e/Figure 51c-e that the fibrous PANI structure seems to evolve towards a more layered sheet-like morphology with a decrease in wt. % of In_2O_3 from 10 wt.% to 1.25 wt.%. It seems that on decreasing wt.% of In_2O_3 in PANI further than 1.25 wt.%, the morphology recedes back to fibrous morphology from sheet-like morphology.
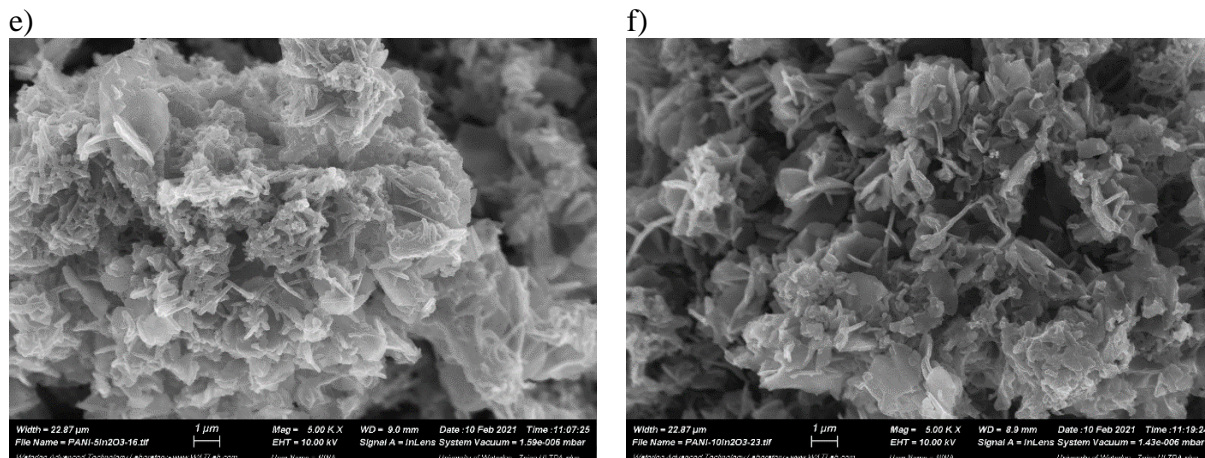
a)

b)

c)

d)

e)   f)

Figure 51: Surface morphology of a) PANI, b) PANI doped with 0.625% In_2O_3, c) PANI doped with 1.25% In_2O_3, d) PANI doped with 2.5% In_2O_3, e) PANI doped with 5% In_2O_3, f) PANI doped with 10% In_2O_3, all at 5000X magnification

To further confirm the morphology of PANI with 0.625 wt.% In_2O_3, PANI with 1.25 wt.% In_2O_3, and PANI with 2.5 wt.% In_2O_3, their morphology was observed at 10,000X magnification. On scrutinizing the accentuated images (Figure 52), it is again evident that PANI with 0.625 wt.% In_2O_3 has a combination of sheet-like and fibrous morphology and not a layered sheet-like morphology like PANI with 1.25 wt.% In_2O_3 (Figure 52b) and PANI with 2.5 wt.% In_2O_3 (Figure 52b).

It is known that the surface to volume ratio increases with the flattening of the surface for the same volume. The flat sheet-like morphology of PANI with 1.25 wt.% In_2O_3 and PANI with 2.5 wt.% In_2O_3 seems to possess a relatively higher surface area to volume ratio compared to the fibrous morphology, thus increasing the area available to promote more sorption of the target gas analyte. The stacking of the polymeric sheets seems to create a layered 2D structure (for Figure 50c/Figure 51c and Figure 50d/Figure 51d) that not only increases surface area but also mechanical integrity of the polymer structure compared to the roughly entangled polymeric chains (in Figure 50a, c-d/Figure 51a, c-d). Essentially, one can observe that the images of Figure 50c-d (and Figure 51c-d) tend to resemble more and more the images of Figure 50a (and Figure 51a). The (more beneficial and) more layered stacking can be observed clearly from Figure 52b of PANI with 1.25% In_2O_3 captured at 10,000X magnification. The morphology of PANI with 1.25% In_2O_3 (Figure 50c/Figure 51c/Figure 52b) seems to be optimal for promoting more sorption (more sensitivity), as per the results of Figure 49. This is probably due to striking a balance between the dispersion of the metal oxide and avoiding too much metal oxide that may cause some 'destruction'/fracturing of the polymer structure.
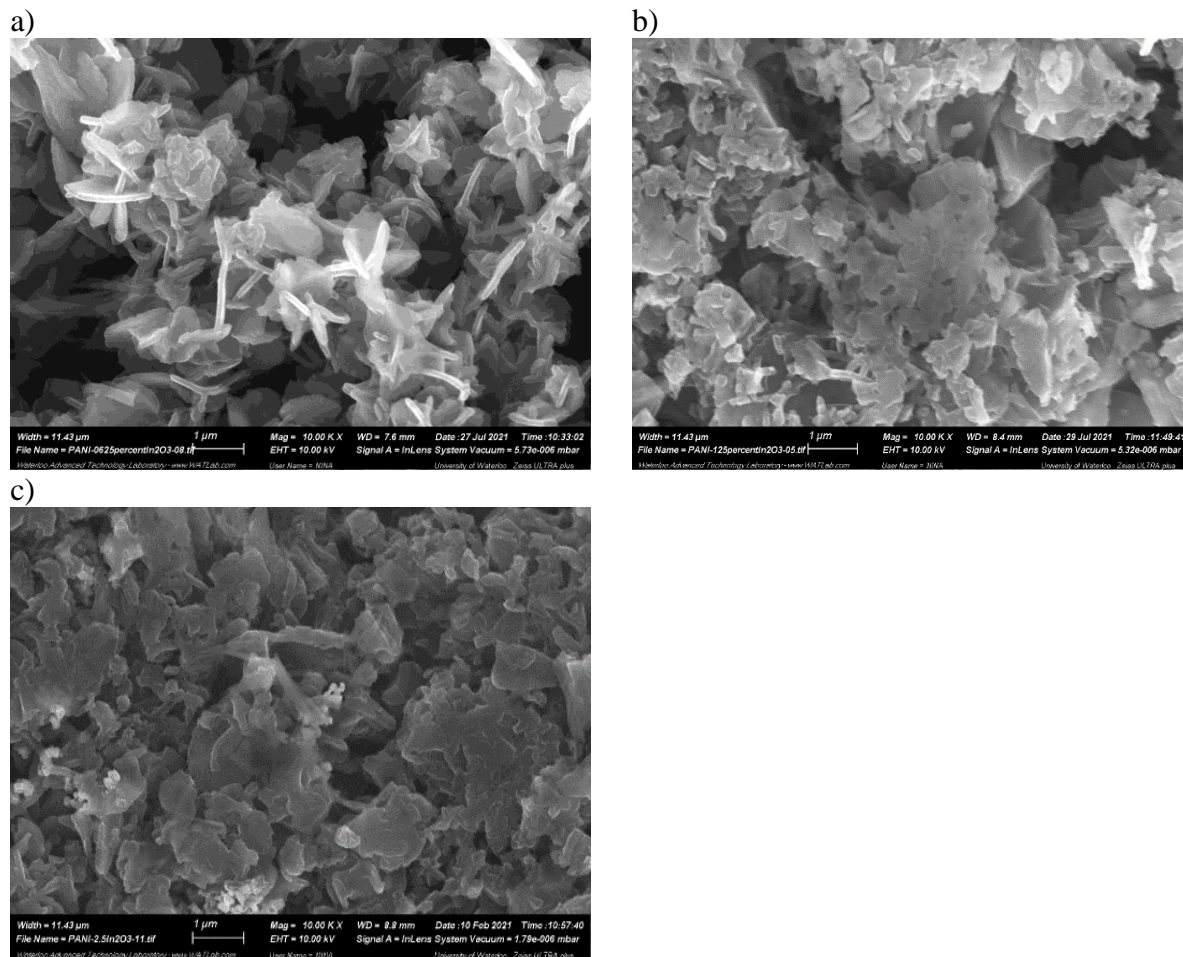
Figure 52: Surface morphology of a) PANI doped with 0.625% In$_2$O$_3$, b) PANI doped with 1.25% In$_2$O$_3$, c) PANI doped with 2.5% In$_2$O$_3$, at 10,000X magnification

Moreover, the evolving morphology of PANI with different loadings of In$_2$O$_3$ dopant not only affects the sensitivity trends but also the selectivity trends. From the selectivity trends discussed in Chapter 5, it was observed that the selectivity of PANI doped with different wt.% of In$_2$O$_3$ decreased with decreasing the wt.% of In$_2$O$_3$ dopant from 5 wt.% to 1.25 wt.% (but not from 10% to 5 wt.% (see Figure 53 as a reminder of the selectivity trends of Figure 35 in Chapter 5). The decrease in selectivity can be attributed to the evolving morphology of PANI from a mixture of sheet-like entities and entangled chains to a layered sheet-like morphology with the decrease in wt.% of In2O3 dopant from 5 wt.% to 1.25 wt.% in PANI.

The sheet-like morphology might have a higher surface to volume ratio and more "sites" for the analytes to diffuse and attach to the polymer compared to the mixture of sheet-like and entangled chain structure. But the additional sorption sites in the former morphology might not be specific to any particular gas analyte like formaldehyde; other larger molecules like benzene might also diffuse more readily. This led to a decrease in the specificity of PANI towards formaldehyde with a decrease in wt.% of In$_2$O$_3$ from 5 wt.% to 1.25 wt.% (Figure 53). It must also be noted that an increase in selectivity was observed upon a decrease in wt.% of In$_2$O$_3$ from 10 wt.% to 5 wt.%.

Therefore, it would be reasonable to say that PANI with 5 wt. % of In_2O_3 seems to be an "optimal" material based on selectivity grounds (of F over B), since it exhibits a good balance of sheet-like and entangled chain morphology. Selected PANI materials were also characterized using an optical microscope for extra corroboration. The imaging results from the optical microscope are presented in Appendix L.
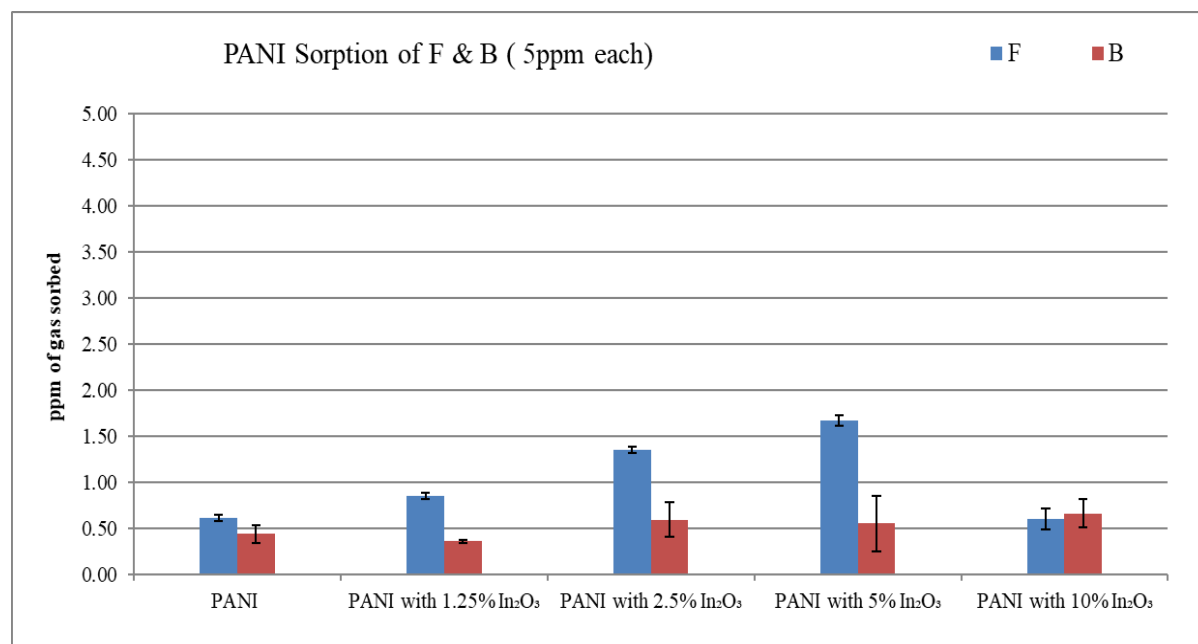

Figure 53: F & B sorption (in ppm) for PANI and doped PANI with different wt. % of In_2O_3; (Source: F/B, 5/5 ppm)

P25DMA- P25DMA, P25DMA with 20% TiO_2 and P25DMA with 10% NiO were also analyzed for their morphology and metal oxide incorporation. Figure 54 and 55 represent SEM images from the same P25DMA and doped P25DMA samples but with different magnifications (1000X in Figure 54 vs 5000X in Figure 55). Table 26 shows a good degree of incorporation of TiO_2 at expected levels (see the related discussion in Section 7.1).

With a degree of TiO_2 incorporation of about 14.5% (see Table 26), TiO_2 affected the morphology of P25DMA even more significantly (see Figure 54), relative to the indium oxide incorporation effect on the PANI structure (Figure 50, Figure 51, and Figure 52). P25DMA on its own (Figure 54a, Figure 55a) seems to have a mix of stacked flat plate-type and cauliflower-type entities. On the other hand, P25DMA doped with 20% TiO_2 (Figure 54b, Figure 55b) seems to have more of a particulate- (particle cluster) type surface. P25DMA with 10% NiO seems to have a cluster of rough circular-globules arranged in an irregular layered fashion (Figure 54c and Figure 55c).

Both NiO and TiO_2 did change the morphology of P25DMA from flat plate-like sheets to a more particulate, disorderly globular, surface morphology. This change in morphology could be due to

the Ni-N and Ti-N bonds, respectively, causing 'kinks' along the polymer chains where the ring of P25DMA changes the conformation, to reduce the strain caused by the metal oxide binding. More 'kinks' result in a more 'porous-like' structure as the P25DMA no longer has the earlier physical integrity [69]. It was also observed that P25DMA with 20% TiO_2 and P25DMA with 10% NiO appeared as more 'porous-like' in nature, as it was difficult to scatter the beam and obtain a clear image while performing SEM/EDX. The overall effect of these morphological changes was an increase in available surface area and sorption.
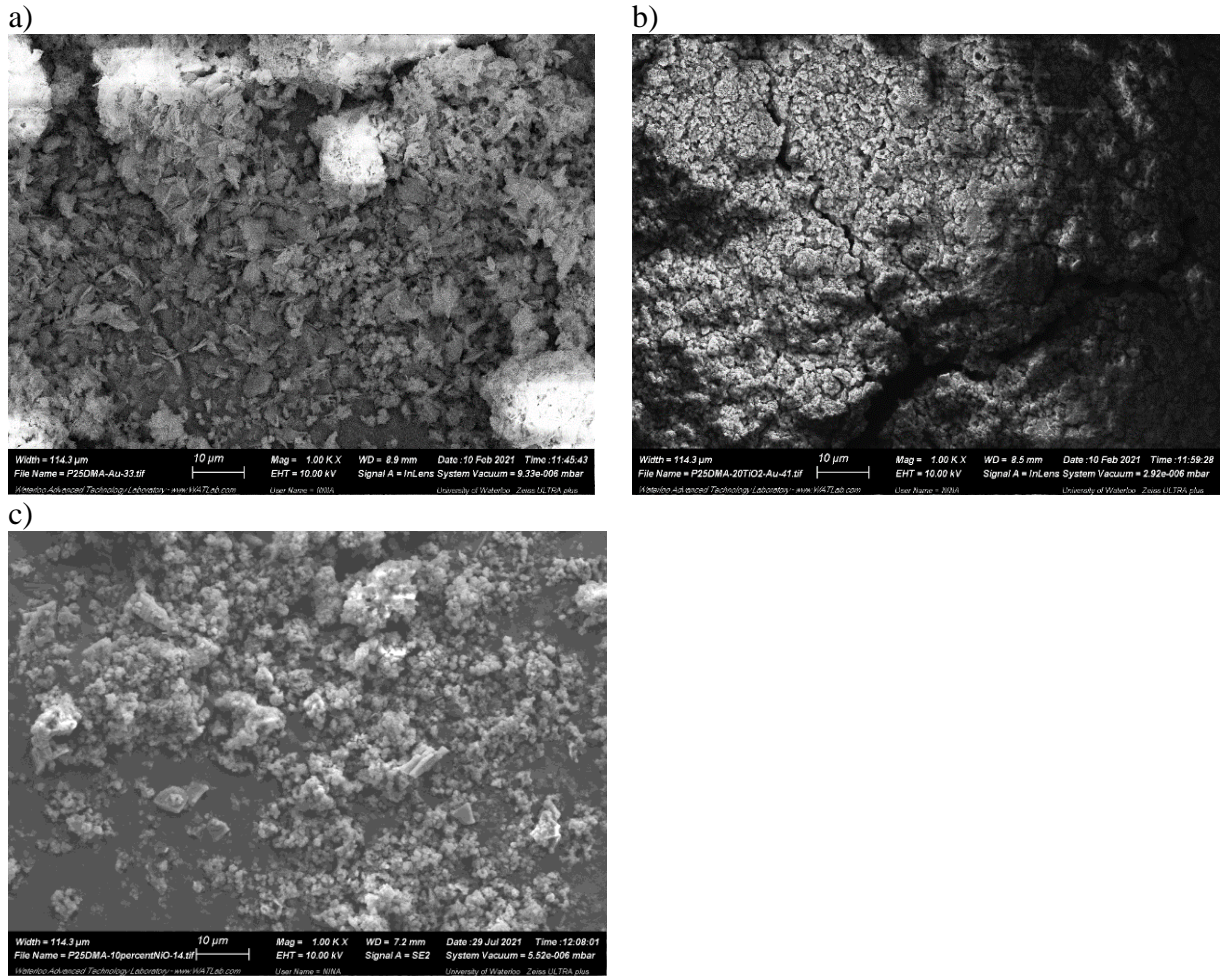
a)

b)

c)

Figure 54 Surface morphology of a) P25DMA, b) P25DMA with 20% TiO_2, c) P25DMA with 10% NiO at 1000X magnification
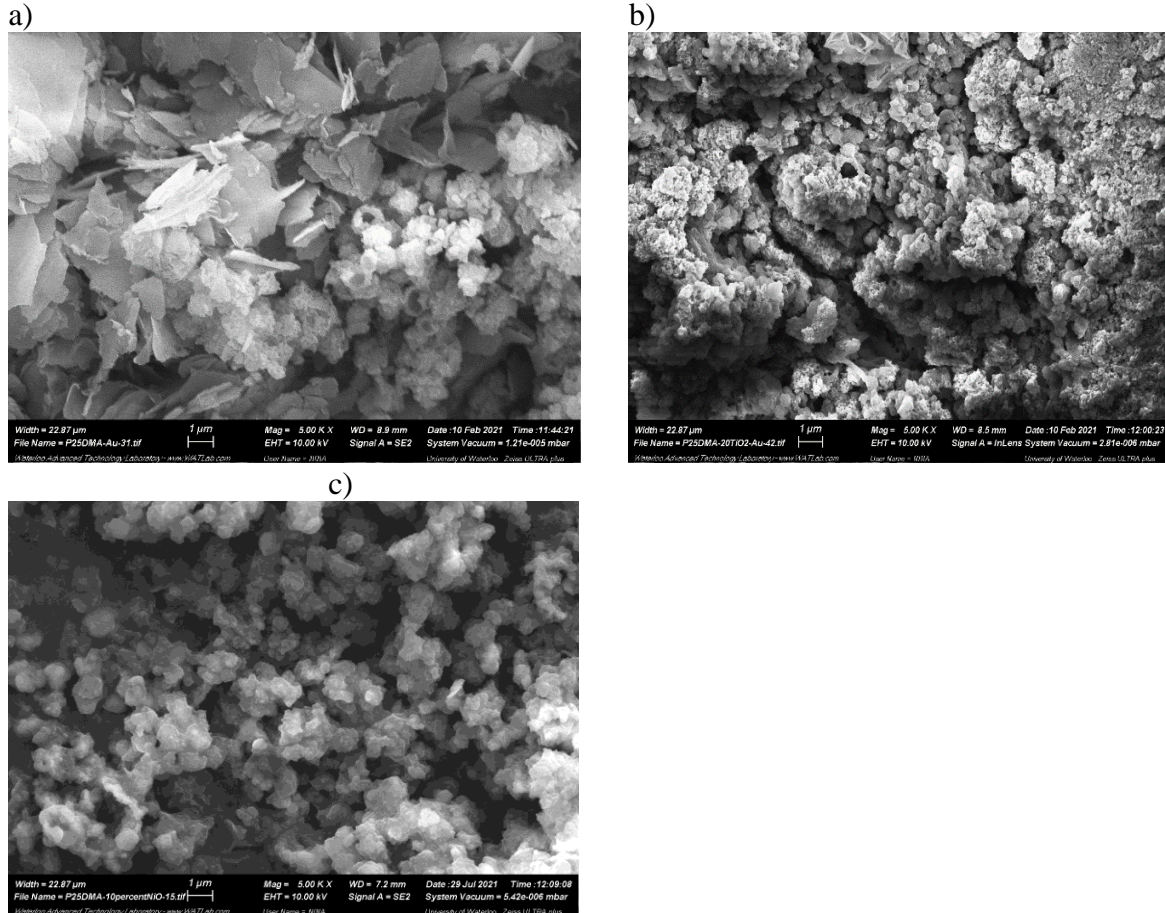
Figure 55: a) P25DMA, b) P25DMA with 20% TiO$_2$, and c) P25DMA with 10% NiO at 5000X magnification

Let's now try to corroborate the observations above with a quick visit to prior literature in analogous situations. One can see our statements above reflected on the SEM images of sensing materials obtained in previous but similar studies, thus putting the newly acquired results of Figure 50 to Figure 55 in better perspective. Figure 56 shows representative images from earlier studies. Figure 56a shows PMMA (poly(methyl methacrylate)), which immediately suggests (experimentally confirmed later) limited sorption capability due to its flat plate-like ('monolithic') smooth surface with no 'pores' or 'cavities' [74]. This was also observed when PMMA was tested for its sensitivity towards F and B.

Figure 56b-c represents the effect of doping P25DMA with two different metal oxides. In Figure 56b, doping with 20% ZnO disrupted (and 'destroyed') a good polymeric gas sensing material, which had otherwise exhibited a reasonable structure (as shown in Figure 54a and Figure 55a) for sorbing VOCs. On the other hand, doping P25DMA with 20% NiO (shown in Figure 56c) seemed to improve surface topography by promoting more roughness and 'cavity-like' entities compared to P25DMA on its own (see Figure 55c) and therefore, better sorption capabilities [71] [69].
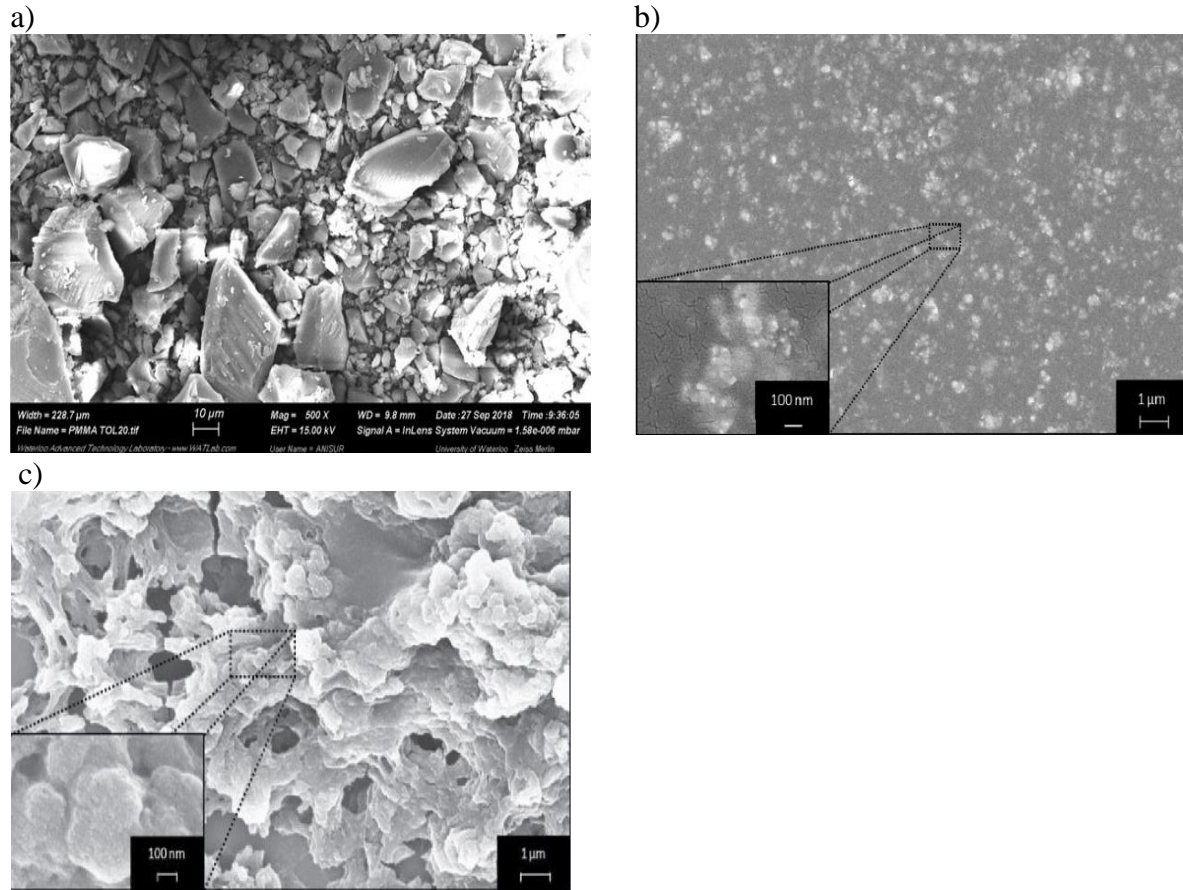
Figure 56: Surface morphology of a) PMMA at 500X magnification [74] (by permission); b) P25DMA with 20% ZnO at 5000X magnification [71] (by permission); c) P25DMA with 20% NiO at 5000X magnification [71] (by permission)

7.3 Crystallinity

Another property that comes into play is crystallinity. X-Ray Diffraction (XRD) was used to study the crystallinity of the synthesized polymers for selected samples.

Crystallinity was estimated using the 'intensity method', as per equation 7.1 and Figure 57 [75] :
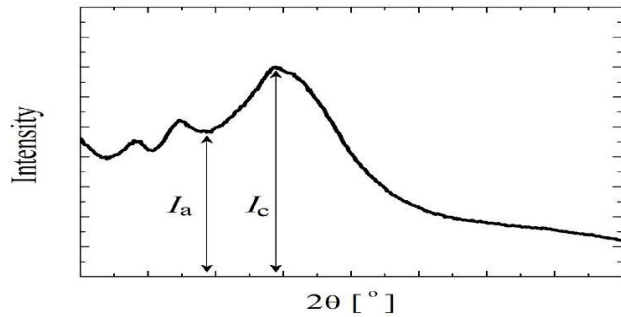
Crystallinity = $(I_c - I_a)/I_c \times 100\%$ (7.1)

Figure 57 Estimating % crystallinity by 'intensity method' using Ia and Ic [75]

Ic and Ia in Figure 57 (which depicts a generic intensity response) represent crystalline and amorphous intensities. The % (degree of) crystallinity for all the polymeric materials estimated (approximately) using equation 7.1 was 40% on average, in agreement with the visual speculation (see below) based on the type of diffractograms obtained.

The responses in Figure 58a-e represent intensity vs 2θ XRD plots for selected samples (as per Table 9). All polymer samples seem to have a similar degree of crystallinity as all XRD scans seem to fall within the same, rather narrow, 'corridor' (see Figure 58e). The absence of sharp peaks and the rather wide diffractograms in Figure 58 are typical of semi-crystalline polymers (with a larger component of an amorphous phase). One might argue about some distinct crystalline peaks (sharp peaks) in Figure 58c (even if slightly), which suggest the presence of more crystallinity in PANI with 10% In_2O_3.
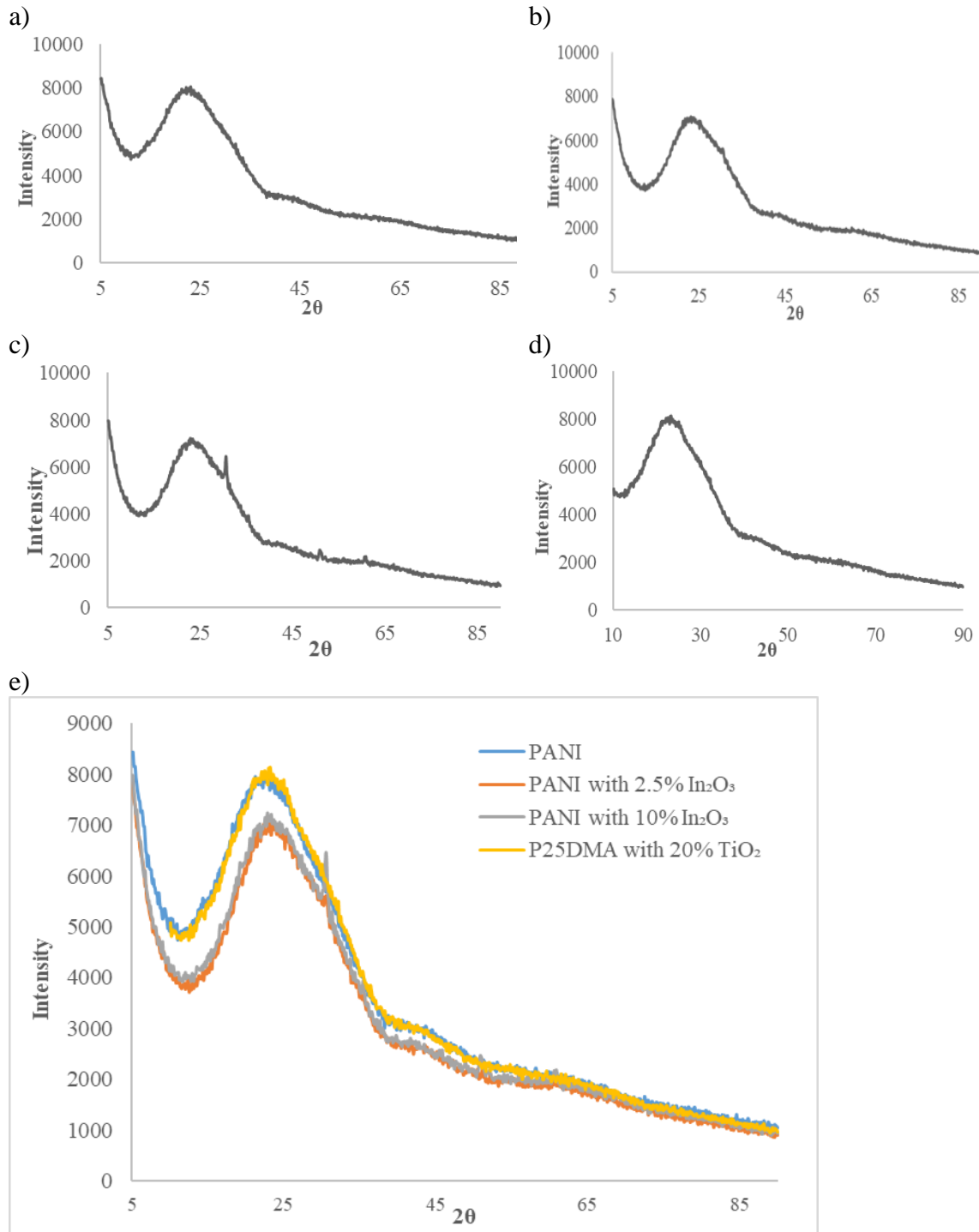
Figure 58: XRD scans for a) PANI, b) PANI with 2.5% In_2O_3, c) PANI with 10% In_2O_3, d) P25DMA with 20% TiO_2, and e) combined XRD responses for a-d

7.4 Note on Sensing Mechanisms

Sensing properties of a polymeric material are influenced by the underlying interactions between the analyte and the sensing material. These interactions are mainly due to repulsive or attractive electrostatic forces. Stewart et al. [30] proposed several primary and secondary mechanisms involved in sensing VOCs with polymeric materials.

Primary sensing mechanisms are based on electrostatic forces, whereas secondary mechanisms are the aftermath once the analyte comes in contact with the sensing material. The dominant sensing mechanism is influenced by the chemistry and functional group(s) of the target analyte. Multiple mechanisms might be in play while sensing formaldehyde by polymeric sensing materials.

1) **Hydrogen bonding-** Volatile organic compounds have covalent bonds and some VOCs are polar due to the presence of atoms with different electronegativity in the molecule. For instance, formaldehyde contains a H–C=O functional group. The electronegativity difference between the carbon atom and oxygen atom allows oxygen (since an oxygen atom is more electronegative compared to a carbon atom) to draw the shared pair of electrons (due to the covalent bond) towards itself and thus induce a dipole moment. This dipole moment within the molecule creates polarity in formaldehyde. The higher the dipole moment, the more polar is the molecule and this creates a stronger hydrogen bond.

   Similarly, in PANI, the difference in electronegativity between the nitrogen and hydrogen atoms of the amine functional group present on the benzene ring, makes the behaviour polar and capable of hydrogen bonding. Therefore, formaldehyde is attracted to PANI and P25DMA, and forms a hydrogen bond with the nitrogen or hydrogen atom of PANI and P25DMA.

2) **Lewis acid and Lewis base interaction-** A Lewis acid is an electron deficient molecule and a Lewis base possesses at least one or more lone pairs of electrons. Formaldehyde is a strong Lewis base due to the presence of the lone electron on the oxygen atom of the aldehydic functional group. On the other hand, PANI and P25DMA are Lewis acids (even though rather weak). Hence, Lewis acid-base interactions are likely to take place when formaldehyde comes in contact with PANI and P25DMA.

3) **Metal coordination-** Metal coordination comes into play only when a metal or metal oxide is present in a (doped) sensing material. Metals and metal oxides are commonly used as catalysts for facilitating the oxidation of organic compounds. In this study, PANI and P25DMA have been doped with metal oxides to enhance sensitivity. Metal coordination in polymers can enhance sorption in many ways. It must be noted that very small amounts of metal oxides are usually incorporated in the polymer matrix.

   Metal oxides offer mechanical integrity and strength. They may also increase the surface to volume ratio for sorption. More importantly, when a polymer comes in contact with a metal

oxide during synthesis, the polymer chains try to coordinate/form bonds with the metal oxide. This might create 'kinks' due to the strain caused by the metal oxide on the polymeric backbone bonds. The coordination between the metal oxide and polymeric chain reduces the number of the available spots for the analyte to bind with the metal and leads to the formation of "cavities" within the polymeric backbone. This is a common phenomenon while incorporating metal oxides like NiO and TiO_2 in PANI, as shown in Figure 59. On incorporation of NiO in PANI, a "boat-like" structure is created due to the bending of the PANI polymeric chain in order to coordinate with NiO. This coordination leads to more cavities (more available space) for the analyte to sorb on the sensing material.
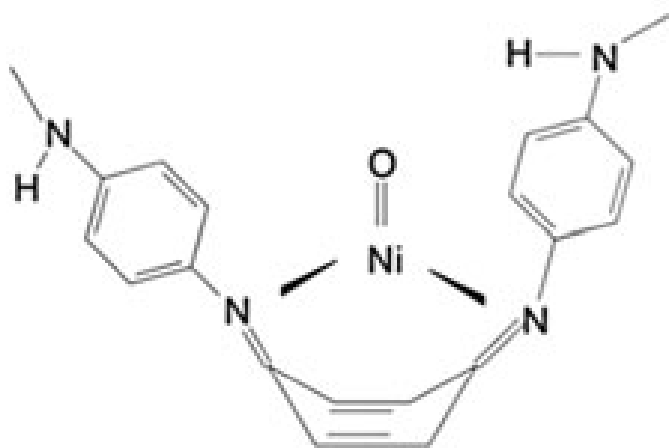

Figure 59: NiO coordination in PANI [30] (by permission)

4) **Steric hindrance-** Steric hindrance practically generates a repulsive force that repels the analyte away from the sensing material. The repulsive force is due to the presence of the electron cloud around the molecule. The repulsive force can be a result of the larger (bulkier) size of an analyte molecule like benzene or can be due to the presence of bulkier groups on the sensing materials.

Sensing materials like PANI and P25DMA might repel benzene and not interact with it as readily as with formaldehyde (due to the size of benzene). Sensing materials like P25DMA contain two additional methyl groups on the benzene ring compared to PANI. Due to the presence of these extra methyl groups on P25DMA, its backbone seems to repel and sorb less analyte molecules compared to PANI, in general.

Chapter 8: Concluding Remarks and Future Recommendations

8.1 Concluding Remarks

8.1.1 Sensitivity

Table 27 gives a summary of the sensitivity results for sorption of formaldehyde from F 10 ppm source.

Table 27: Summary of sensitivity results for polymeric sensing materials

Sensing material	Average sorption (in ppm)
PANI	1.32 ± 0.04
PANI with 1.25% In_2O_3	2.49 ± 0.02
PANI with 2.5% In_2O_3	1.99 ± 0.01
PANI with 5% In_2O_3	1.64 ± 0.01
PANI with 10% In_2O_3	1.08 ± 0.01
P25DMA	1.16 ± 0.03
P25DMA with 20% TiO_2	1.71 ± 0.04
P25DMA with 10% NiO	2.95 ± 0.03

Notes: $\pm$ values above indicate the estimate of one standard error (se) for the average sorption value; PANI or PANI (L) refers to PANI synthesized in the lab, whereas PANI (S) refers to commercially available PANI from Sigma.

From the sensitivity results it is evident that P25DMA with 10% NiO and PANI with 1.25% In_2O_3 seem to sorb the most formaldehyde from a 10 ppm source. The good sorption capability of PANI with 1.25% In_2O_3 can be attributed to it unique surface sheet-like layered morphology, while for P25DMA with 10% NiO it can be attributed to its polymer backbone and the 'kinks' formed between Ni-N upon incorporation of NiO in P25DMA.

8.1.2 Selectivity

Table 28 and Table 29 consist of summaries of selectivity results for sorption of formaldehyde over benzene (from F /B 5/5 ppm each source) and for sorption of formaldehyde over acetaldehyde (from F/Ac, 2.5/2.5 ppm each source), respectively.

Table 28: Summary of selectivity results for F over B from F/B, 5/5 ppm source

Sensing material	Average sorption (in ppm)		Average selectivity
	F	B	F/B
PANI	0.62 ± 0.01	0.44 ± 0.04	1.46
PANI with 1.25% In$_2$O$_3$	0.86 ± 0.02	0.36 ± 0.01	2.37
PANI with 2.5% In$_2$O$_3$	1.35 ± 0.02	0.60 ± 0.09	2.46
PANI with 5% In$_2$O$_3$	1.67 ± 0.03	0.55 ± 0.15	3.91
PANI with 10% In$_2$O$_3$	0.61 ± 0.05	0.67 ± 0.08	0.92
P25DMA	0.82 ± 0.05	0.39 ± 0.06	2.20
P25DMA with 20% TiO$_2$	0.66 ± 0.04	0.32 ± 0.06	2.23

Note: $\pm$ values above indicate the estimate of one standard error (se) for the average sorption value

Table 29: Summary of selectivity results for F over Ac from F/Ac, 2.5/2.5 ppm source

Sensing material	Average sorption (in ppm)		Average selectivity
	F	Ac	F/Ac
PANI	0.96 ± 0.01	0.95 ± 0.03	1
PANI with 1.25% In$_2$O$_3$	0.52 ± 0.01	0.38 ± 0.01	1.37
PANI with 2.5% In$_2$O$_3$	0.61 ± 0.05	0.50 ± 0.006	1.22
PANI with 5% In$_2$O$_3$	0.56 ± 0.02	0.49 ± 0	1.18
PANI with 10% In$_2$O$_3$	0.34 ± 0.06	0.22 ± 0.003	1.55
P25DMA	0.71 ± 0.13	0.64 ± 0.15	1.09
P25DMA with 20% TiO$_2$	0.51 ± 0.02	0.52 ± 0.003	0.98
P25DMA with 10% NiO	0.72 ± 0	0.55 ± 0.005	1.32

Note: $\pm$ values above indicate the estimate of one standard error (se) for the average sorption value

From Table 28, it is evident that PANI with 5% In$_2$O$_3$ and PANI with 2.5% In$_2$O$_3$ seem to be potentially better selective materials for sensing formaldehyde based on selectivity results of F over B. Although selectivity of the polymeric materials for F over Ac tested in this thesis is quite lower compared to their selectivity of F over B, from Table 29, it is evident that PANI with 10% In$_2$O$_3$ and PANI with 1.25% In$_2$O$_3$ seem to be the most selective materials based on F over Ac.

In addition to the individual sensitivity and selectivity trends, a few more comments are also in order:

All sensing materials showed good stability over a decade of use.

Sensitivity and selectivity trends are reverse of each other- For instance, the sensitivity of PANI doped with different wt.% of In$_2$O$_3$ towards formaldehyde increased on decreasing wt.% In$_2$O$_3$ dopant from 10% to 1.25% in PANI. On the other hand, selectivity of PANI increased on

increasing wt.% of In_2O_3 dopant in PANI from 1.25 wt.% to 5 wt.%. These reverse sensitivity and selectivity trends were also observed in reference [76].

It is a trade-off between sensitivity and selectivity for an "optimal" material to be selected for a specific application- Since selectivity and sensitivity trends are reverse of each other, "optimal" materials can be selected based on the specific application of the sensor. For instance, in the case of sensing formaldehyde for indoor air quality, the sensor needs to be very sensitive since the goal is to detect trace concentrations of formaldehyde. In other cases, it might be more important for a sensing material to be selective with reasonable sensitivity towards formaldehyde to avoid false-positive response signals.

Based on the above remarks on sensitivity and selectivity, an "optimal" sensor can be based on a dual-sensor that consists of two sensing materials- PANI with 5% In_2O_3 and PANI. PANI with 5% In_2O_3 has a high selectivity towards formaldehyde over benzene, whereas PANI has equal selectivity to formaldehyde and acetaldehyde. Therefore, PANI doped with 5% In_2O_3 can be used to detect formaldehyde and the signal from pristine PANI can be divided into half to determine the signal from acetaldehyde, which eventually can be subtracted for the PANI with 5% In_2O_3 signal. Having multiple sensors on an electronic circuit board is not only feasible but probably the way to go for practical sensor applications. In our recently manufactured electronic sensor boards (Systems Design and Electrical Engineering), we can accommodate multiple sensing materials on one board.

8.2 Future Recommendations

8.2.1 Short Term Recommendations

8.2.1.1 PANI with 0.625% In_2O_3

Although from the SEM images presented in Chapter 7 (Section 7.2) it is suspected that PANI with 0.625 % of In_2O_3 might be less sensitive to formaldehyde compared to PANI with 1.25% In_2O_3, the sensitivity of PANI with 0.625% In_2O_3 towards F should be confirmed.

8.2.1.2 P25DMA with 10% NiO

P25DMA with 10% NiO exhibited a good affinity towards both formaldehyde and acetaldehyde. In general, it is known that polymeric sensing materials that display good sensitivity might not be very selective. Hence, P25DMA with 10% NiO is sensitive and might not be selective towards formaldehyde over acetaldehyde; it might also not be selective towards formaldehyde over benzene. But formaldehyde and benzene are very different molecules with respect to functional

group and size, therefore it is worth testing P25DMA for its selectivity of formaldehyde over benzene.

8.2.1.3 P25DMA doped with NiO and TiO$_2$ selectivity studies

Doping P25DMA with NiO and TiO$_2$ seemed to improve sensitivity and selectivity towards formaldehyde. Hence, considering the changes in formaldehyde sorption that were observed when PANI was doped with different levels of In$_2$O$_3$, it may be worthwhile to investigate doping P25DMA with different levels of TiO$_2$ and NiO

Hence, P25DMA should be doped with different wt.% of NiO and TiO$_2$ to determine optimal wt.% for achieving enhanced sensitivity and selectivity towards F.

8.2.1.4 Surface Area Analysis

In Chapters 4 and 7, it was observed that on decreasing In$_2$O$_3$ loading from 5 wt.% to 0.625 wt.% in PANI, sensitivity towards F seemed to improve and this was attributed to changing morphology from an entangled chain structure to a sheet-like layered structure. It was speculated that the sheet-like layered morphology seemed to have a higher surface to volume ratio compared to the entangled chain structure. Hence, the surface area should be determined by performing surface area analysis for different materials of interest via the BET technique.

8.2.2 Long Term Recommendations

8.2.2.1 Combination of Metal Oxides

Metal oxides interact with polymeric chains differently. From SEM image analysis of PANI doped with In$_2$O$_3$ in Chapter 7, it seemed that In$_2$O$_3$ enhanced sorption in PANI by modifying its morphology from an entangled chain structure to a sheet-like morphology. It is speculated that NiO creates 'kinks' and forms a "boat-like" structure when incorporated in P25DMA, which enhances sorption of P25DMA. Therefore, it would be worth doping PANI and/or P25DMA with NiO and In$_2$O$_3$ together to study the combined effect on sorption capabilities of these polymeric materials.

8.2.2.2 Other Dopants

There are several metal oxides that are used as catalysts. On comparing and scrutinising sorption results and SEM images in earlier chapters, it was deduced that sorption of polymeric materials increased on increasing the surface to volume ratio. Hence, it would be worth doping polymeric sensing materials like PANI and P25DMA with different metal oxides, like MoO_3 and Al_2O_3, in order to investigate sorption properties further.

8.2.2.3 Other Polymeric Materials

It would be worth evaluating other undoped and doped (with metal oxides) polymeric materials like polypyrrole, and other PANI derivatives like poly(N-methylaniline) (PNMA) and poly(o-anisidine), (PoANI), for their potential.

8.2.2.4 Selectivity of Sensing Materials with multiple gases

It would be beneficial to evaluate selectivity of sensing materials by exposing them to a multiple gas mixture, like formaldehyde, acetaldehyde and benzene together, in order to study the performance of sensing materials even in more detail. This has not been attempted in the literature, except in [71] with ethanol as the target.

References

[1] H. FOLLOWS, "Convention on the prohibition of the development, production, stockpiling and use of chemical weapons and on their destruction," in *Organisation for the Prohibition of Chemical Weapons*, The Hague, The Netherlands, 2005.

[2] "Chemical Weapons Convention, Act, No.58 of 2007," Organisation of Prohibition of Chemical Weapons (OPCW), 2007. [Online]. Available: https://www.opcw.org/sites/default/files/documents/LAO/article_VII/legislation_database/LK_srilanka.pdf. [Accessed 14 July 2021].

[3] L. Szinicz, "History of chemical and biological warfare agents," *Toxicology*, vol. 214, no. 3, pp. 167-181, 2005.

[4] P. Aas, "The threat of mid-spectrum chemical warfare agents," *Prehospital and Disaster Medicine,* vol. 18, no. 4, pp. 306-312, 2003.

[5] K. Ganesan, S. K. Raza and R. Vijayaraghavan, "Chemical warfare agents," *Journal of Pharmacy and Bioallied Sciences,* vol. 2, no. 3, pp. 166-178, 2010.

[6] H. Sohn, S. Létant, M. J. Sailor and W. C. Trogler, "Detection of fluorophosphonate chemical warfare agents by catalytic hydrolysis with a porous silicon interferometer," *Journal of the American Chemical Society*, vol. 122, no. 22, pp. 5399-5400, 2000.

[7] A. K. Vaish, S. Consul, A. Agrawal, S. C. Chaudhary, M. Gutch, N. Jain and M. M. Singh, "Accidental phosgene gas exposure: A review with background study of 10 cases," *Journal of Emergencies, Trauma, and Shock,* vol. 6, no. 4, p. 271, 4 (2013): 271..

[8] M. Schwenk, "Chemical warfare agents. Classes and targets," *Toxicology Letters,* vol. 298, pp. 253-263, 2018.

[9] F. R. Sidell and J. Borak, "Chemical warfare agents: II. Nerve agents," *Annals of Emergency Medicine,* vol. 21, no. 7, pp. 865-871, 1992.

[10] S. L. Bartelt-Hunt, D. R. Knappe and M. A. Barlaz, "A review of chemical warfare agent simulants for the study of environmental behavior," *Critical Reviews in Environmental Science and Technology,* vol. 38, no. 2, pp. 112-136, 2008.

[11] M. A. Hayoun, M. E. Smith, C. Ausman, S. N. S. Yarrarapu and H. D. Swoboda, Toxicology, V-Series Nerve Agents, Treasure Island (FL): StatPearls Publishing, 2020.

[12] K. Kim, O. G. Tsay, D. A. Atwood and D. G. Churchill, "Destruction and detection of chemical warfare agents," *Chemical Reviews,* vol. 111, no. 9, pp. 5345-5403, 2011.

[13] E. J. Pacsial-Ong and Z. P. Aguilar, "Chemical warfare agent detection: a review of current trends and future perspective," *Front. Biosci., Scholar Ed 5,* pp. 516-543, 2013.

[14] R. A. Young and C. B. Bast, Blister agents, Academic Press, 2020, pp. 149-169.

[15] T. P. Panel, "American Chemistry conucil," 1972. [Online]. Available: https://www.americanchemistry.com/ProductsTechnology/Phosgene/. [Accessed 24 July 2021].

[16] S. Jo, J. Kim, J. Noh, D. Kim, G. Jang, N. Lee, E. Lee and T. S. Lee, "Conjugated polymer dots-on-electrospun fibers as a fluorescent nanofibrous sensor for nerve gas stimulant," *ACS Applied Materials & Interfaces 6,* no. 24, pp. 22884-22893., 2014.

[17] S. Zimmermann, S. Barth, W. K. Baether and J. Ringer, "Miniaturized low-cost ion mobility spectrometer for fast detection of chemical warfare agents," *Analytical Chemistry,* vol. 80, no. 17, pp. 6671-6676, 2008.

[18] Y. Sun and K. Y. Ong, Detection technologies for chemical warfare agents and toxic vapors, CRC press, 2004.

[19] M. S. J. Khan, Y.-W. Wang, M. O. Senge and Y. Peng, "Sensitive fluorescence on-off probes for the fast detection of a chemical warfare agent mimic," *Journal of Hazardous Materials 342,* pp. 10-19, 2018.

[20] S.-W. Zhang and T. M. Swager, "Fluorescent detection of chemical warfare agents: functional group specific ratiometric chemosensors," *Journal of the American Chemical Society 125, no. 12,* pp. 3420-3421, 2003.

[21] E. Editors: Garcia-Brejio, B. G.-L. Perez and P. Cossddu, "Section 1.1.1 Key components of sensor," in *Organic Sensors- Materials and Applications*, Institution of Engineering Technology, 2016, p. 310.

[22] D. Matatagui, M. J. Fernandez, J. Fontecha, J. P. Santos, I. Gràcia, C. Cané and M. C. Horrillo, "Love-wave sensor array to detect, discriminate and classify chemical warfare agent simulants," *Sensors and Actuators B: Chemical ,* vol. 175, pp. 173-178, 2012.

[23] G. Wu, R. H. Datar, K. M. Hansen, T. Thundat, R. J. Cote and A. Majumdar, "Bioassay of prostate-specific antigen (PSA) using microcantilevers," *Nature Biotechnology,* vol. 19, no. 9, pp. 856-860, 2001.

[24] D. C. Meier, C. J. Taylor, R. E. Cavicchi, M. W. Ellzy, K. B. Sumpter and S. Semancik, "Chemical warfare agent detection using MEMS-compatible microsensor arrays," *IEEE Sensors Journal ,* vol. 5, no. 4, pp. 712-725, 2005.

[25] S. Virji, R. Kojima, J. D. Fowler, J. G. Villanueva, R. B. Kaner and B. H. Weiller, "Polyaniline nanofiber composites with amines: Novel materials for phosgene detection," *Nano Research ,* vol. 2, no. 2, pp. 135-142, 2009.

[26] J. Lavoie, S. Srinivasan and R. Nagarajan, "Using cheminformatics to find simulants for chemical warfare agents," *Journal of Hazardous Materials 194,* pp. 85-91, 2011.

[27] H. Zhang and D. M. Rudkevich, "A FRET approach to phosgene detection," *Chemical Communications 12,* pp. 1238-1239, 2007.

[28] Y. Hu, L. Chen, H. Jung, Y. Zeng, S. Lee, K. M. K. Swamy, X. Zhou, M. H. Kim and J. Yoon, "Effective strategy for colorimetric and fluorescence sensing of phosgene based on small organic dyes and nanofiber platforms.," *ACS Applied Materials & Interfaces,* vol. 8, no. 34, pp. 22246-22252, 2016.

[29] H.-C. Xia, X.-H. Xu and Q.-H. Song, "BODIPY-based fluorescent sensor for the recognization of phosgene in solutions and in gas phase," *Analytical Chemistry,* vol. 89, no. 7, pp. 4192-4197, 2.17.

[30] K. M. Stewart and A. Penlidis, "Designing polymeric sensing materials: what are we doing wrong?," *Polymers for Advanced Technologies,* vol. 28, no. 3, pp. 319-344, 2017.

[31] P. Ariyageadsakul, V. Vchirawongkwin and C. Kritayakornupong, "Determination of toxic carbonyl species including acetone, formaldehyde, and phosgene by polyaniline emeraldine gas sensor using DFT calculation," *Sensors and Actuators B: Chemical ,* vol. 232, pp. 165-174, 2016.

[32] S. Pandey, "Highly sensitive and selective chemiresistor gas/vapor sensors based on polyaniline nanocomposite: A comprehensive review," *Journal of Science: Advanced Materials and Devices,* vol. 1, no. 4, pp. 431-453., 2016.

[33] D. Kukkar, K. Vellingiri, R. Kaur, S. K. Bhardwaj, A. Deep and K.-H. Kim, "Nanomaterials for sensing of formaldehyde in air: Principles, applications, and performance evaluation," *Nano Research,* vol. 12, no. 2, pp. 225-246, 2019.

[34] J. Albuquerque, L. Mattoso, D. Balogh, R. Faria, J. Masters and A. MacDiarmid, "A simple method to estimate the oxidation state of the polyanilines," *Synthetic Metals,* vol. 113, pp. 19-22, 2000.

[35] C. Dhand, N. Dwivedi, S. Mishra, P. R. Solanki, V. Mayandi, R. W. Beuerman, S. Ramakrishna, R. Lakshminarayanan and B. D. Malhotra, "Polyaniline-based biosensors," *Nanobiosensors in Disease Diagnosis,* vol. 4, pp. 25-46, 2015.

[36] C. Dhand, M. Das, M. Datta and B. D. Malhotra, "Recent advances in polyaniline based biosensors," *Biosensors and Bioelectronics,* vol. 26, no. 6, pp. 2811-2821, 2011.

[37] E. Song and J.-W. Choi, "Conducting polyaniline nanowire and its applications in chemiresistive sensing.," *Nanomaterials,* vol. 3, no. 3, pp. 498-523, 2013.

[38] J. Stejskal and R. G. Gilbert, "Polyaniline. Preparation of a conducting polymer (IUPAC technical report).," *Pure and Applied Chemistry,* vol. 74, no. 5, pp. 857-868, 2002.

[39] M. Joulazadeh, A. H. Navarchian and M. Niroomand, "A comparative study on humidity sensing performances of polyaniline and polypyrrole nanostructures," *Advances in Polymer Technology,* vol. 33, no. S1, 2014.

[40] N. A. Deshpande, M. A. Kulkarni and S. D. Chakane, "Study of conducting polyaniline as formaldehdye sensor," *The Pharma Innovation,* vol. 7, no. 1, pp. 139-141, 2018.

[41] S. Srinives, T. Sarkar and A. Mulchandani, "Primary amine-functionalized polyaniline nanothin film sensor for detecting formaldehyde," *Sensors and Actuators B: Chemical,* vol. 194, pp. 255-259, 2014.

[42] J. Zhu, J. Chen, P. Zhuang, Y. Zhang, Y. Wang, H. Tan, J. Feng and W. Yan, "Efficient adsorption of trace formaldehyde by polyaniline/TiO2 composite at room temperature and mechanism investigation," *Atmospheric Pollution Research ,* vol. 12, no. 2, pp. 1-11, 2021.

[43] T. Itoh, I. Matsubara, W. Shin, N. Izu and M. Nishibori, "Preparation of layered organic–inorganic nanohybrid thin films of molybdenum trioxide with polyaniline derivatives for aldehyde gases sensors of several tens ppb level," *Sensors and Actuators B: Chemical,* vol. 128, no. 2, pp. 512-520, 2008.

[44] X. Tang, J.-P. Raskin, D. Lahem, A. Krumpmann, A. Decroly and M. Debliquy, "A formaldehyde sensor based on molecularly-imprinted polymer on a TiO2 nanotube array," *Sensors 17, no. 4,* p. 675, 2017.

[45] I. Matsubara, K. Hosono, N. Murayama, W. Shin and N. Izu, "Synthesis and gas sensing properties of polypyrrole/MoO3-layered nanohybrids," *Bulletin of the Chemical Society of Japan,* vol. 77, no. 6, pp. 1231-1237, 2004.

[46] J. Wang, I. Matsubara, N. Murayama, S. Woosuck and N. Izu, "The preparation of polyaniline intercalated MoO3 thin film and its sensitivity to volatile organic compounds," *Thin Solid Films,* vol. 514, no. 1-2, pp. 329-333, 2006.

[47] T. Itoh, I. Matsubara, W. Shin and N. Izu, "Preparation and characterization of a layered molybdenum trioxide with poly (o-anisidine) hybrid thin film and its aldehydic gases sensing properties," *Bulletin of the Chemical Society of Japan,* vol. 80, no. 5, pp. 1011-1016, 2007a.

[48] T. Itoh, I. Matsubara, W. Shin and N. Izu, "Layered hybrid thin film of molybdenum trioxide with poly (2, 5-dimethylaniline) for gas sensor sensitive to VOC gases in ppm level," *Chemistry Letters 36,* vol. 36, no. 1, pp. 100-101, 2007.

[49] T. Itoh, I. Matsubara, W. Shin and N. I. ", "Synthesis and characterization of layered organic/inorganic hybrid thin films based on molybdenum trioxide with poly (N-methylaniline) for VOC sensor," *Materials Letters,* vol. 61, no. 19-20, pp. 4031-4034, 2007c.

[50] G. Yun, K. M. Koo and Y. Kim, "Chemiresistor type formaldehyde sensor using polystyrene/polyaniline core-shell microparticles," *Polymer 215,* p. 123389, 2021.

[51] F. Yılmaz and Z. Küçükyavuz, "Solution properties of polyaniline," *Polymer International,* pp. 59(4), 552-556., 2010.

[52] M. Angelopoulos, G. E. Asturias, S. P. Ermer, A. S. E. M. Ray, A. G. MacDiarmid and A. J. Epstein, "Polyaniline: solutions, films and oxidation state," *Molecular Crystals and Liquid Crystals,* pp. 160(1), 151-163, 1988.

[53] J. Q. Dong and Q. Shen, "Enhancement in solubility and conductivity of polyaniline with lignosulfonate modified carbon nanotube," *Journal of Polymer Science Part B: Polymer Physics,* pp. 47(20), 2036-2046, 2009.

[54] R. Jain and R. V. Gregory, "Solubility and rheological characterization of polyaniline base in N-methyl-2-pyrrolidinone and N, N′-dimethylpropylene urea," *Synthetic Metals,* pp. 74(3), 263-266, 1995.

[55] S. Shreepathi and R. Holze, "Spectroelectrochemical investigations of soluble polyaniline synthesized via new inverse emulsion pathway," *Chemistry of Materials,* pp. 17(16), 4078-4085, 2005.

[56] Angelopoulos, Marie, A. Ray, A. G. Macdiarmid and E. A. J., "Polyaniline: processability from aqueous solutions and effect of water vapor on conductivity 21," *Synthetic Metals,* pp. 21-30, 1987.

[57] S. A. Othman, S. Radiman and K. K. Siong, "Methanol as a Suitable Solvent for Polyaniline Emeraldine Base (PANI-EB)," in *In AIP Conference Proceedings*, 2010.

[58] Z. Qiang, G. Liang, A. Gu and L. Yuan, "Hyperbranched polyaniline: a new conductive polyaniline with simultaneously good solubility and super high thermal stability," *Materials Letters,* pp. 115, 159-161., 2014.

[59] C.-C. Han, L. W. Shacklette, Elsenbaumer and Ronald.U.S Patent 5,278,213, 1994.

[60] L. W. Shacklette and C. C. Han, "Solubility and dispersion characteristics of polyaniline," in *MRS Online Proceedings Library Archive*, 1993.

[61] J. Burke, "Solubility parameters: theory and application.Burke, J.," *The Book and Paper Group Annual, vol. The American Institute for Conservation, Washington, DC.,* (1984).

[62] K. M. Stewart and A. Penlidis, "Design of sensitive and selective sensing materials for ethanol detection," *Trends in Chemical Engineering,* vol. 6, 2017.

[63] N. Majdabadifarahani, *Evaluating Polymeric Materials for Sensing of Gaseous Analytes,* Waterloo ON: Master's thesis, University of Waterloo, 2019.

[64] K. M. E. Stewart and A. Penlidis, "Novel Test System for Gas Sensing Materials and Sensors," *Macromolecular Symposia (Special Issue: Polymer Reaction Engineering),* vol. 324, pp. 11-18, 2013.

[65] "A microplotter Desktop User Manual," SonoPlot Inc, Middleton, WI, ", [Online]. Available: https://static1.squarespace.com/static/56ab6e84859fd0d3e69acbed/t/572cc19ca3360c58b5 64c52b/1462550953598/MicroplotterDesktopManual.pdf. [Accessed 18 August 2021].

[66] T. Chen, Q. J. Liu, Z. L. Zhou and Y. D. Wang., "The fabrication and gas-sensing characteristics of the formaldehyde gas sensors with high sensitivity," *Sensors and Actuators ,* pp. 301-305, 2008.

[67] R. Dong, L. Zhang, Z. Zhu, J. Yang, X. Gao and S. Wang, "Fabrication and formaldehyde sensing performance of Fe-doped In 2 O 3 hollow microspheres via a one-pot method," *CrystEngComm,* pp. 562-569, 2017.

[68] J. A. Dirksen, K. Duval and T. A. Ring, "NiO thin-film formaldehyde gas sensor," *Sensors and Actuators B: Chemical,* vol. 80, no. 2, pp. 106-115, 2001.

[69] K. M. Stewart and A. Penlidis, "Evaluation of polymeric nanocomposites for the detection of toxic gas analytes," *Journal of Macromolecular Science, Part A,* pp. 610-618, 2016a.

[70] A. J. Scott, *Design of Polymeric Materials: Novel Functionalized Polymers for Enhanced Oil Recovery & Gas Sorption Applications,* Waterloo ON: Dept. of Chemical Eng., University of Waterloo, 2019.

[71] K. M. Stewart, W. T. Chen, R. R. Mansour and A. Penlidis, "Doped poly (2, 5-dimethyl aniline) for the detection of ethanol," *Journal of Applied Polymer Science,* vol. 132, no. 28, 2015.

[72] A. Dey, "Semiconductor metal oxide gas sensors: A review," *Materials Science and Engineering,* pp. 206-217, 2018.

[73] K. M. Stewart and A. Penlidis, "Designing polymeric sensing materials for analyte detection and related mechanisms," *In Macromolecular Symposia,* pp. 123-132, 2016b.

[74] A. J. Scott, N. Majdabadifarahani, K. M. Stewart, T. A. Duever and A. Penlidis, "Straightforward Synthesis and Evaluation of Polymeric Sensing Materials for Acetone Detection," *Macromolecular Reaction Engineering,* p. 2000004, 2020.

[75] J. Khouri, "Chitosan Edible Films Crosslinked by Citric Acid," PhD thesis, Dept. of Chemical Eng., University of Waterloo, Waterloo, ON, 2019.

[76] Z.-K. Chen, S.-C. Ng, S. F. Li, L. Zhong, L. Xu and H. S. Chan, "The fabrication and evaluation of a vapour sensor based on quartz crystal microbalance coated with poly (o-anisidine) langmuir—blodgett layers," *Synthetic Metals,* vol. 87, no. 3, pp. 201-204, 1997.

[77] K. Tzou and R. V. Gregory, "Improved Solution Stability and Spinnability of Concentrated Polyaniline Solutions Using N,N'-Dimethyl Propylene Urea as the Spin Bath Solvent," *Synthetic Metals,* vol. 69, pp. 109-112, 1995.

[78] H. Zeghioud, S. Lamouri, Z. Safidine and M. Belbachir, "Chemical synthesis and characterization of highly soluble conducting polyaniline in mixtures of common solvents," *Journal of the Serbian Chemical Society,* vol. 80, no. 7, pp. 917-931, 2015.

[79] "Olympus Global Homepage," March 2021. [Online]. Available: https://www.olympus-global.com/news/2016/nr160126bx53me.html.

Appendices

Appendix A: Summary of Sensing Materials for Gas Analytes

Appendix A is related to Chapter 2.

A.1 Polymers for Hydrogen Cyanide

Polyaniline
Poly(4-vinylphenol); average Mw ~25,000 (Sigma Aldrich 436224-5G)

A.2 Polymers for Phosgene

Polyaniline
Polyvinyl alcohol
Poly acrylic acid

A.3 Polymers for Organophosphonates

Poly(acrylamide-co-acrylic acid) partial sodium salt Mw 520,000, Mn 150,000 (Typical), acrylamide ~80 wt. % (Sigma Aldrich 511471-250G)
Polymerize (2-hydroxyethyl)urea with formaldehyde
        (2-hydroxyethyl)urea; Sigma Aldrich 554693-25G
Poly-L-threonine (Sigma-Aldrich P8077-250MG)
        Note: Given that this is a polymer of an amino acid, it is probably not the most stable.

A.4 Polymers for Acetaldehyde

Polyaniline
Poly(2,5-dimethyl aniline)
Polymer doped with (indium oxide) In_2O_3

A.5 Polymers for Formaldehyde

Polyaniline doped with 5% NiO and 15% Al_2O_3
Poly(2,5-dimethyl aniline) (P25DMA) with 10% NiO
Polymer doped with In_2O_3
Polyethyleneimine

A.6 Polymers for Benzene

SXFA: Seacoast Science
Polyaniline doped with 20% NiO
Polyaniline doped with TiO_2

Appendix B: Solubility Tests

Appendix B is related to Chapter 3.

The solubility of PANI (S) (commercially available PANI from Sigma) was evaluated first. Initial concentrations were as suggested by literature [77]; solutions containing 1 wt%, 2 wt% and 5 wt% polymer in each solvent were prepared. However, the solutions prepared using both solvents (at all concentrations tested) gelled and did not seem suitable for deposition (see Figure B1). Some of these solutions were eventually cast into films, but gelation made casting difficult.

In an attempt to avoid crosslinking (gelation), solutions were prepared at lower concentrations: 0.25 wt% and 0.5 wt% (again, using both NMP and DMF as solvents). These concentrations were also selected based on recommendations from the literature [52]. While both solvents caused some gelation, it was not as considerable as for the higher concentration solutions. It was observed that the polymer particles agglomerated, forming large lumps within the solutions. It is anticipated that this will still cause problems with future deposition steps. Representative photos are available in Figure B1.

a)   b)

c)   d)
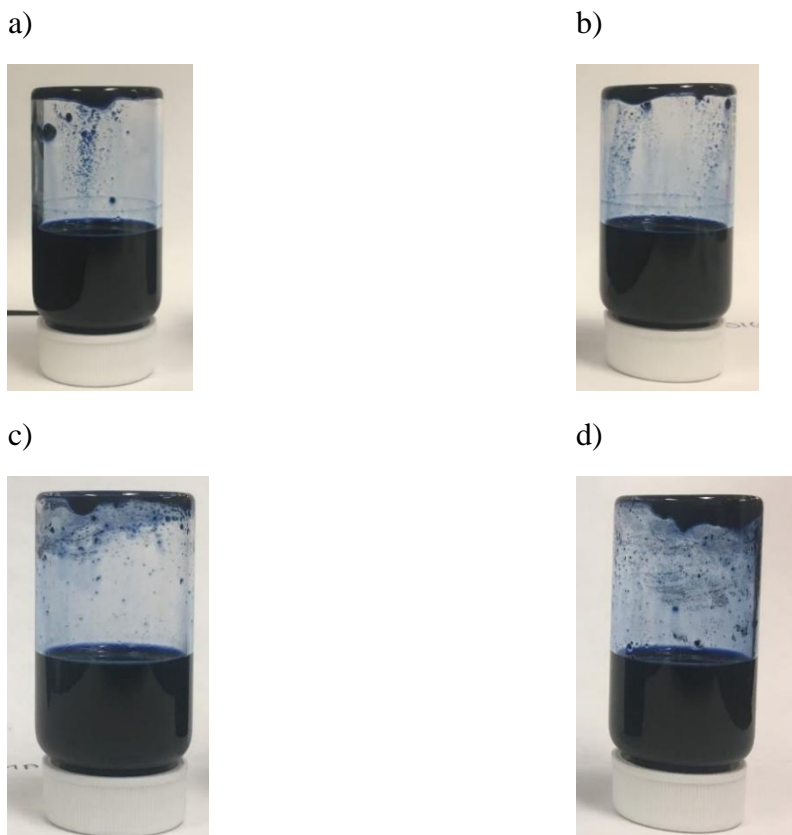
Figure B1: Gelation of commercial polyaniline (PANI (S)) in four solutions a) 0.25 wt% PANI in NMP; b) 0.5 wt% PANI in NMP; c) 0.25 wt% PANI in DMF; d) 0.5 wt% PANI in DMF

Next, the solubility of polyaniline prepared in-house (lab polyaniline; PANI (L)) was evaluated. In this case, combining the polymer and the solvents created suspensions; while these solutions did not gel, the polymer did not dissolve completely either. When the solution was left stationary, the polymer particles seemed to settle and/or stick to the vial walls (as shown in Figure B2). However, when the solutions were stirred/agitated, the particles were dispersed back into the solution.

(a) (b)
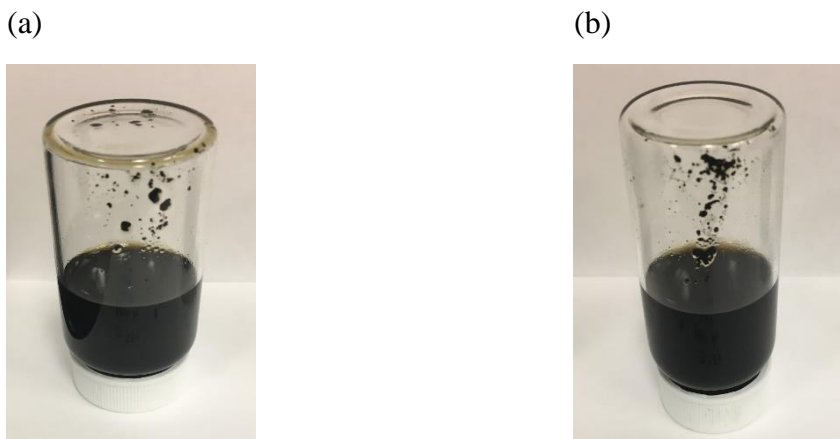
Figure B2: Settling of PANI (L) (synthesized in lab) in four mixtures a) 0.25 wt% PANI in NMP; b) 0.25 wt% PANI in DMF

These results indicate solubility differences between the PANI (S) and PANI (L) materials and demonstrate the solubility limitations of polyaniline. Since these 'solutions' were not able to dissolve the PANI, other solvents like dimethyl sulfoxide (DMSO) and tetrahydrofuran (THF) were considered.

Concentrations of 0.5 wt.% and 1 wt.% PANI (S) in DMSO and THF were prepared. When DMSO was used as the solvent, the 0.5 wt.% and 1 wt.% PANI (S) solutions were dark (navy) blue and some gel formation was observed. The gel that formed seemed to stick to the bottom of the vials. Therefore, 0.5 wt.% and 1 wt.% DMSO solutions did not look promising for solvent deposition and were not considered further. When THF was used as the solvent, the PANI did not dissolve per se, but PANI (S) in THF formed a 'better suspension' than with the other solvents (as shown in Figure B3). Within the vials, it was observed that the particles formed a 'better dispersion' at the bottom of the vial and "mixed" back into the 'solution' when agitated. No lumps or gel were visible as in previous solvents; nonetheless, the dissolution was not perfect.
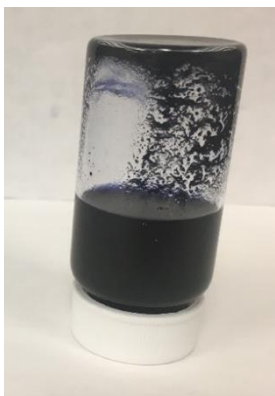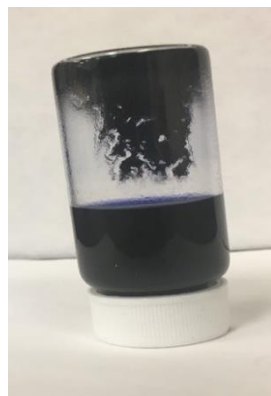
Figure B3: a) 0.5 wt.% PANI (S) in THF; b) 1 wt.% PANI (S) in THF

Given the promising results obtained for 0.5wt.% and 1 wt.%. PANI (S) in THF, mixtures of PANI (S) and PANI (L) in THF were investigated further. As a next step, 0.25 wt.% and 0.1 wt.% PANI (S) and PANI (L) in THF were prepared to observe and understand whether solubility characteristics changed with different concentrations in THF. 0.25 wt.% and 0.1 wt.% PANI (S) and PANI (L) in THF were dark (navy) blue and orange-red, respectively. Neither concentration (0.25 wt.% and 0.1 wt.%) gelled, but the polymers did not dissolve 100% . The dispersions that formed were better than the 0.5 wt.% and 1 wt.% mixtures. A very small amount of PANI particles settled at the bottom of the vial and "mixed" back into the solution on shaking. Representative photos of 0.25 wt.% and 0.1 wt.% PANI (S) in THF are shown in Figure B4.
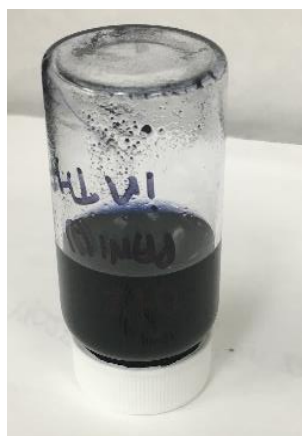
Figure B4: (a) 0.25 wt.% PANI (S) in THF; (b) 0.1 wt.% PANI (S) in THF

To further improve the dissolution of PANI in THF, PANI solutions were prepared using mixtures of water (W) and THF and mixtures of ethylene glycol (EG) and THF as solvents. This was based on a recent study by Zeghioud et al. in which the solubility of polyaniline salts doped with poly (itaconic acid) was achieved by optimizing the ratio of THF/water [78]

Given the success at low PANI concentrations, 0.25 wt.% solutions of PANI (S) were prepared in W/THF and EG/THF mixtures. The volume ratio of the mixture of water and THF (V_w/V_{THF}) was 0.33 (25% W and 75% THF). The same volume ratio was used for the mixture of EG and THF (25% EG and 75% THF). It was observed that the mixture containing 0.25 wt.% PANI in W/THF was dark navy blue. It seemed to be a good dispersion with little or no suspension of particles at the bottom of the vial (see Figure B5a). The uniformity of the 'solution' might make it suitable for deposition via spin coating.

The mixture containing 0.25 wt.% PANI in EG/THF was also dark navy blue (see Figure B5 b). Like the W/THF mixture, the EG/THF mixture also seemed to create a good dispersion. A very small amount of PANI particles that were suspended at the bottom of the vial would "mix" back into the 'solution' once shaken. This 'solution' might be suitable for deposition via drop coating, as it could help with evaporation as well as with drop formation.

a)   b)
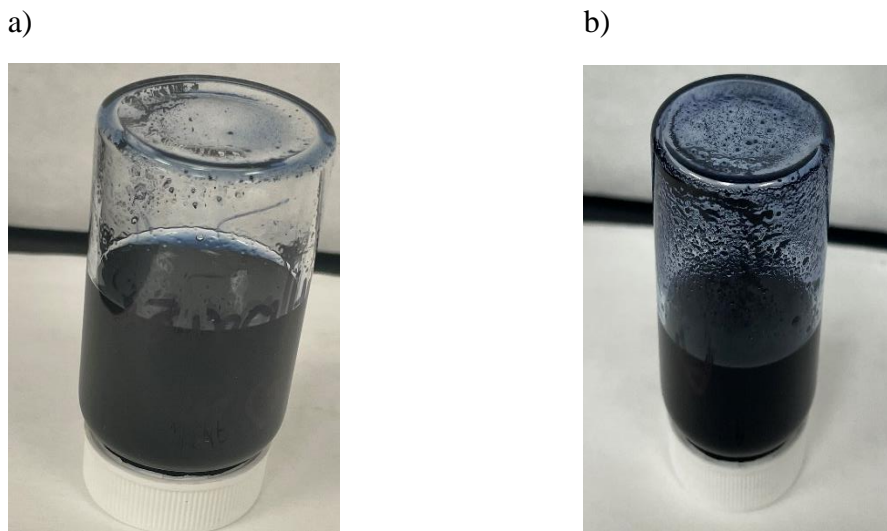
Figure B5: a) 0.25 wt.% PANI (S) in W/THF; b) 0.25 wt.% PANI (S) in EG/THF

It is worth noting that a 0.40 wt.% mixture of PANI(S) in EG/THF was also prepared; it was expected that a higher concentration of PANI might reduce the deposition time when the Microplotter (See Figure 13) was being used for drop coating. For this 0.40 wt% PANI mixture, the volume ratio of EG/THF was maintained at 0.33 (25% EG and 75% THF).

The 0.40 wt.% PANI in EG/THF (25/75) did not yield a good dispersion compared to the previously prepared 0.25 wt.% PANI (S) in EG/THF (25/75). At a higher PANI concentration

(0.40 wt.%), the PANI particles settled more quickly and in greater proportion than what was observed for the lower PANI concentration (0.25 wt.%). Thus, 0.25 wt.% PANI (S) in EG/THF seemed to be the optimum concentration of PANI (S) solution for drop coating deposition using the Microplotter.

To fine-tune the formulation and make the deposition process repeatable, the next step was to vary the volume ratio of the EG/THF mixture. While fixing the PANI concentration (0.25 wt.% PANI (S)), mixtures of EG and THF with EG/THF volume ratios of 40/60, 50/50 and 25/75 were evaluated as the "solvent".

As shown in Figure B6 (a) and (b), the 0.25 wt% PANI (S) solutions with EG/THF volume ratios of 40/60 and 50/50 were dark navy-blue in colour. The 40/60 EG/THF solution mixture seemed to create a good dispersion. The particles seemed to settle when the vial was left stationary and "mix" back into 'solution' once shaken. The 50/50 EG/THF mixture also seemed to create a good dispersion and a limited number of particles settled down when the vial was left stationary. The 0.25 wt.% PANI (S) solution in EG/THF (25/75), Figure B6 (c), is black. While a good dispersion was still achieved, it seemed more viscous compared to the other EG/THF solutions.
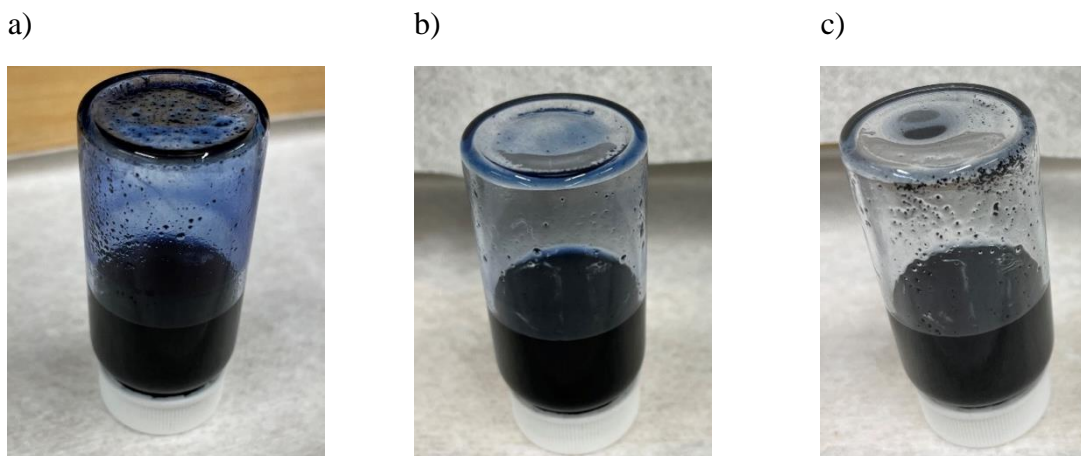
Figure B6: a) 0.25 wt.% PANI (S) in (EG/THF) (40/60); b) 0.25 wt.% PANI (S) in EG/THF (50/50); c) 0.25 wt.% PANI(S) in EG/THF (75/25)

While these qualitative observations present some new opportunities for solution preparation and PANI deposition, it was important to examine the behaviour of each solution during deposition. This was pursued further in collaboration with the Microplotter deposition set-up in Systems Design Engineering.

Appendix C: Film Casting

Appendix C is related to Chapter 3 and also to Appendix B.

- High concentration solutions (≥ 1 wt.% PANI) prepared with NMP and DMF were cast into Petri dishes
  - o Given the gelation that occurred during solution preparation, the solutions were 'lumpy' when deposited. This made it very difficult even to pipette the solution into the Petri dishes. Therefore, the volume of the solution deposited could not be controlled.
  - o Once cast, NMP did not evaporate; the film remained 'wet' after more than a week (see Figure C1).

(a)

(b)

(c)
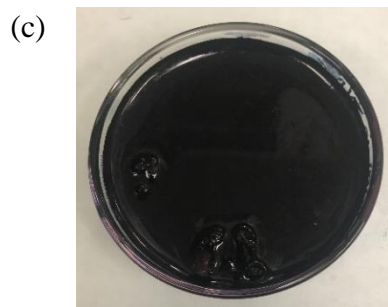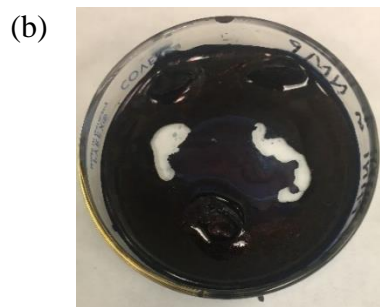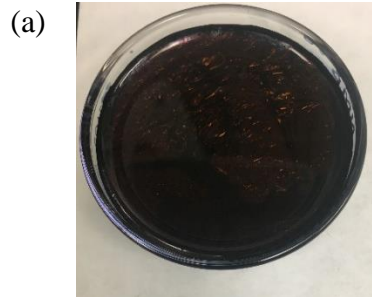
Figure C 1: Solution casting of commercial PANI (S) from solutions of (a) 1 wt.%, (b) 2 wt.% and (c) 5 wt.% PANI in NMP

o   For films cast from DMF solution, the solvent evaporated. However, films were not uniform and would not retain their shape if removed from the dish (see Figure C2)

(a)

(b)

(c)
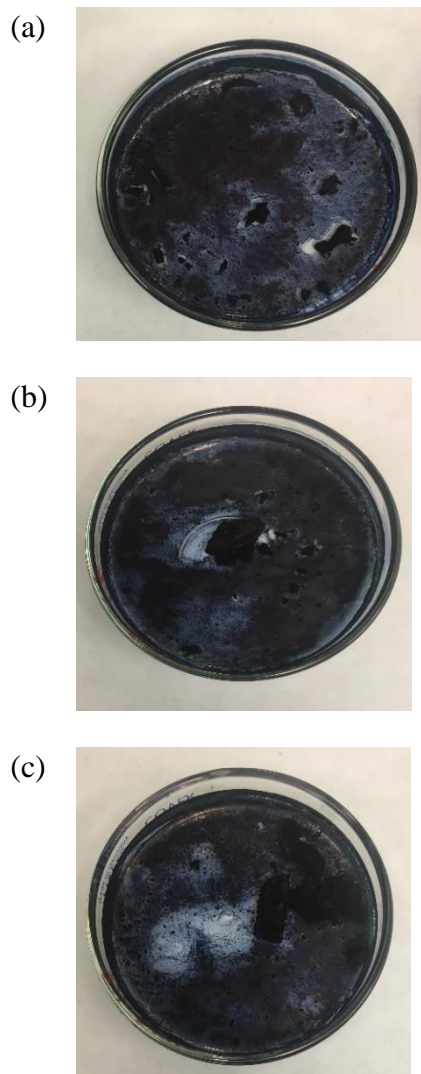
Figure C 2: Solution casting of commercial PANI (S) from solutions of (a) 1 wt.%, (b) 2 wt.% and (c) 5 wt.% PANI in DMF

- Since the 1%, 2% and 5% solutions in neither NMP nor DMF seemed suitable for casting, lower concentration solutions were made using PANI (L). The solutions were let to stand in vials for 5 days and observations were noted down.

o   PANI (L) solution in DMF and NMP were poured into a petri dish and left to evaporate in a fume hood. It was observed that 0.1 wt.% PANI (L) in DMF evaporated and formed

119

a film of PANI (L) in a petri dish after approximately 7 days. 0.1 % PANI (L) in NMP took more than 30 days to evaporate. See Figure C3.

o PANI (L) from the 0.1 wt% PANI (L) in DMF was collected (after DMF evaporated completely) and deposited in a round bottom flask (see Figure C3).

a)   b)
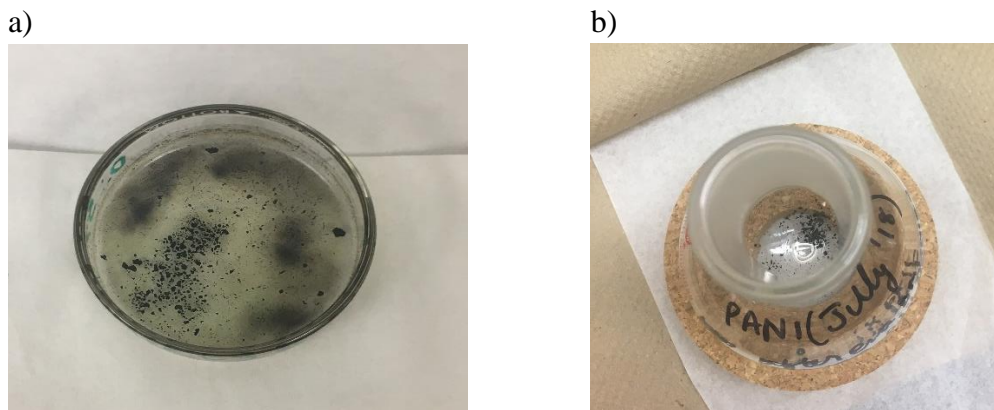
Figure C 3: F3 a) 0.1 wt% PANI (L) in NMP deposited in petri dish b) PANI (L) collected and deposited for sorption test after evaporating DMF from 0.1 wt% PANI (L) in DMF

- 0.5 wt% and 1 wt% PANI (S) in THF solutions prepared as mentioned in Section 3.4.1 were poured in a petri dish and were left on a flat surface for the solvent to evaporate, as shown in Figure C4.
- THF evaporated quickly (in less than 60 min) and left behind a film of PANI (S) on the petri dish, as shown in Figure C4.

a)   b)
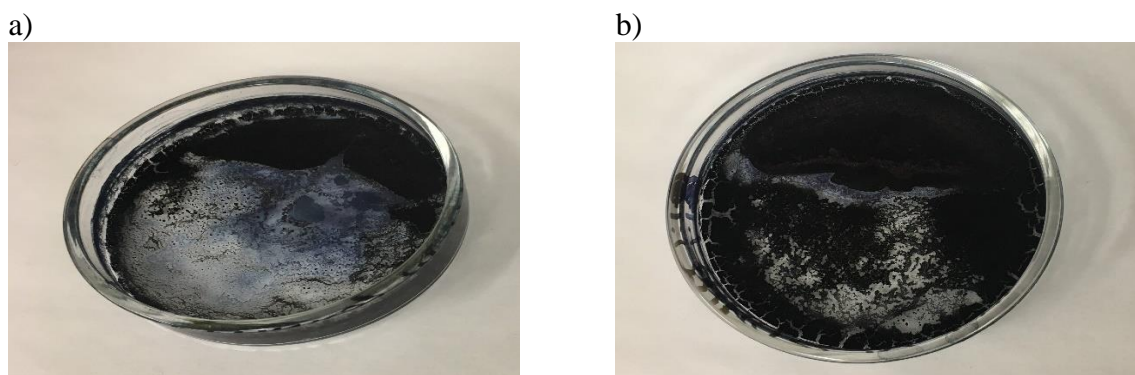
Figure C4: (a) PANI (S) film after evaporating THF from 0.5 wt.% PANI (S) in THF; (b) PANI (S) film after evaporating THF from 1 wt% PANI (S) in THF

- Overall, while PANI in NMP solutions, when deposited in a petri dish, could be considered in the case of forming films, NMP solutions gelled and it took much longer for the solvent (roughly 30 days) to evaporate; however, a strong and thick film can be obtained if one scrapes the material from the petri dish.

Appendix D: EKC 265

Appendix D is related, once more, to the effort to study dissolution of PANI in aid of deposition or other solvent treatments of electronic circuits.

D.1 Treatment of PANI with EKC 265 and IPA

- EKC 265 is a typical solvent used during etching. 0.1g of PANI (S) and PANI (L) were weighed and deposited in the petri dish using ethanol as a solvent. Ethanol was left to evaporate and PANI to settle in the petri dish for 2 days as shown in Figure D1. The dimensions of the petri dish used for the process is 60 x 15 mm (diameter x height).

a) b)
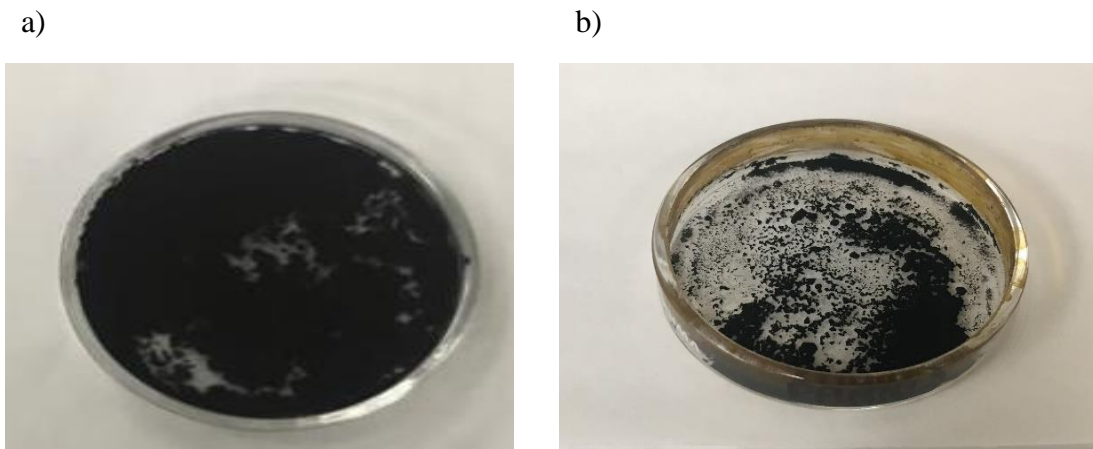
Figure D1: Film of a) PANI (S) deposited in a petri dish, b) PANI (L) deposited in a petri dish

- The Petri dish of PANI (L) and PANI (S) was filled with EKC 265 (about half of the height of the petri dish). After pouring the EKC 265, Petri dishes were placed on the heating plate. Petri dishes were heated for 12 min at 60 degrees Celsius. See Fig D2 for the pictures of the petri dish on the heater taken while heating them.
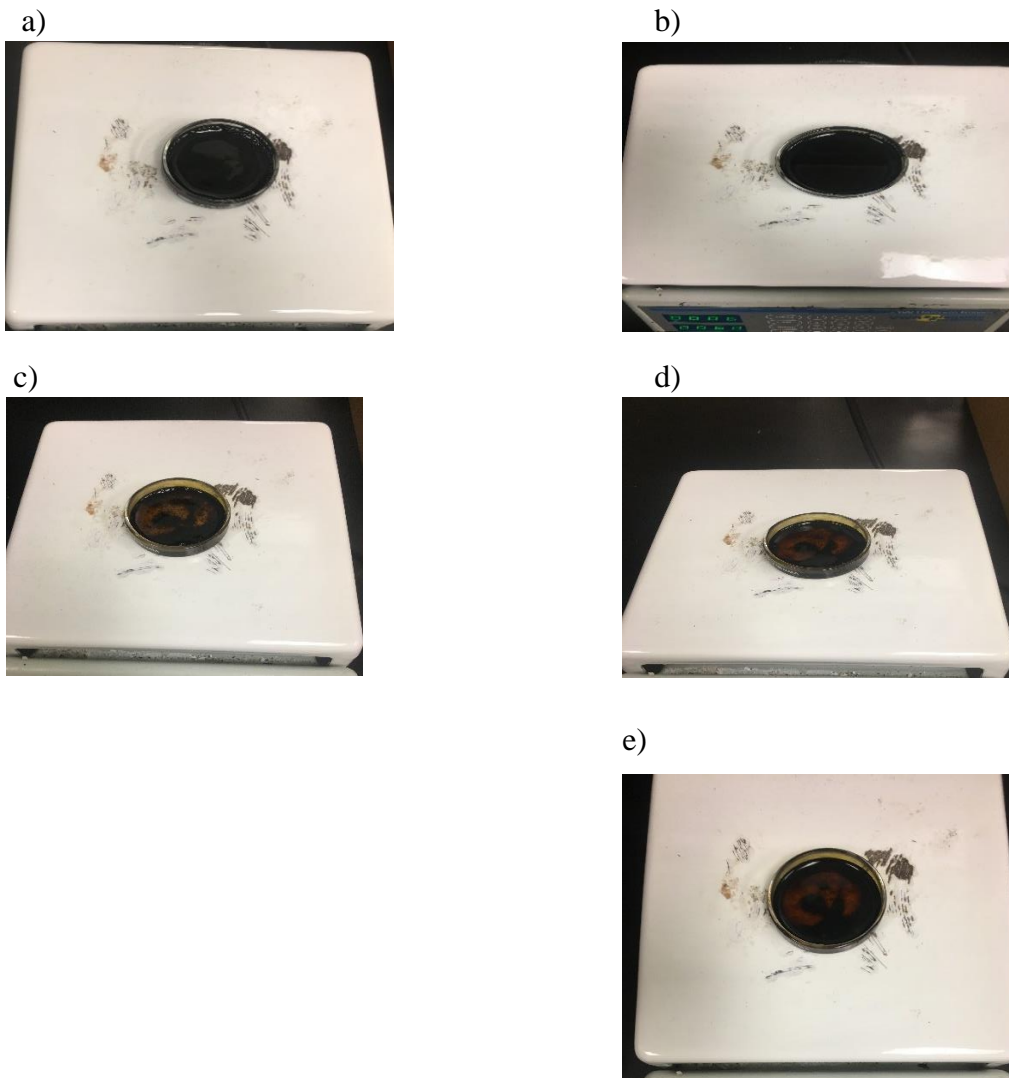
Figure D2: Heating PANI (S) and PANI (L); (a) PANI (S) at 0 min, (b) PANI (S) at 6min, (c) PANI (L) at 0 min, (d) PANI (L) at 6 min, (e) PANI (L) at 12 min

- Weights of the clear filter paper were noted before filtration
- PANI (S) and PANI (L) with EKC 265 were poured down the filter paper. Isopropanol (IPA) was added to the petri dish and poured down the same filter paper with the remaining PANI and EKC 265 from the first pour.
- The filter paper with the whole set-up (funnel and flask) (see Figure D3) was left in the fume hood for 7 days for the solvents to evaporate.

a)
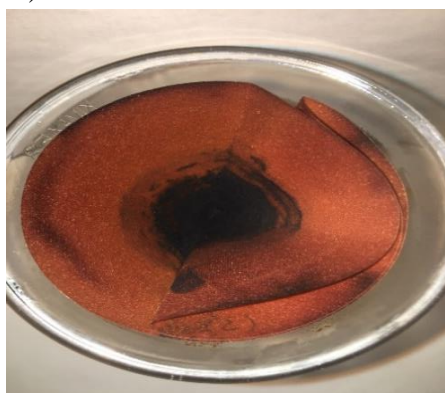
b)   c)
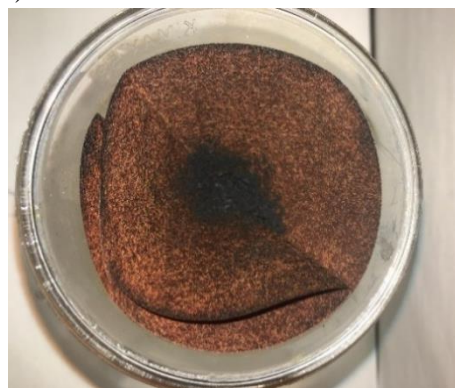
Figure D3: a) PANI (S) and PANI (L) left to evaporate the solvents, b) PANI (S) after 6 days of the treatment, c) PANI (L) after 6 days of the experiment

- Filter paper for PANI (S) and PANI (L) were weighed after 6 days of the treatment process. See Tables D1 and D2.
- The solvent did not evaporate, and a significant amount of the solvent was present in the filter paper even after it was left for 8 days to evaporate in the fume hood.
- On the 8th day, filter papers with solvent and PANI (S) and PANI (L) were heated for 3 hours on the heating plate (in a petri dish) at 60 degrees Celsius. See Fig D4.

Figure D4: PANI (S) and PANI (L) filter paper in a petri dish on the heater plate for heating at 60 degrees Celsius for 3 hrs

- See Tables D1 and D2 for solvents present and evaporated at every stage.

Table D1: Data collected for PANI (S) at different stages of the drying process

Date	Process	Weight of the filter paper (in g)	Solvent present on the filter paper (in g)	Amount of the solvent evaporated (in g)	
Aug 19, 2020	Clear filter paper was weighed	1.2529	0	0	**Wt. of PANI + clear Filter paper (in g) = 1.3529**
Aug 26, 2020	6 days after the treatment with EKC and IPA	3.3405	1.9876	0	
Aug 28, 2020	8 days after the treatment with EKC and IPA	3.2731	1.9202	0.0674	**The total amount of the solvent**

Aug 28, 2020	After heating for 3 hrs on the heating plate at 60 degrees C	2.931	1.5781	0.3421	**needed to be evaporated (in g) = 1.2831**
Aug 31, 2020	2 days after heating (3 hrs at 60 degrees C)	3.0414	1.6885	Gained 0.1104	
Aug 31, 2020	After heating for 6 hrs on a heating plate at 70 degrees C	2.6642	1.3113	0.3772	
Sept 1, 2020	1 day after heating (6 hrs at 70 degrees C)	2.8854	1.5325	Gained 0.2212	
Sept 1, 2020	After heating for 6 hrs on the heating plate at 80 degrees C	2.5388	1.1859	0.3466	
Sept 2, 2020	1 day after heating (6 hrs at 80 degrees C)	2.7135	1.3606	Gained 0.1747	
Sept 2, 2020	After heating for 6 hrs on the heating plate at 90 degrees C	2.4402	1.0873	0.2733	
Sept 3, 2020	1 day after heating (6 hrs at 90 degrees C)	2.6036	1.2831	Gained 0.1958	
Sept 8, 2020	**PANI (S) was scraped from the filter paper and collected in an empty petri dish (weight of an empty petri dish- 16.8204g)**				
Sept 8, 2020	After collecting PANI (S) in a petri dish and before placing it in the oven at 60 degrees C	17.1179	0.1975		**Total mass collected on a petri dish after scraping the filter paper**

Date	Process	Weight of the filter paper (in g)	Solvent present on the filter paper (in g)	Amount of the solvent evaporated (in g)	
Sept 9, 2020	Still in the oven and temperature was increased to 80 C				**is 0.2975g; 0.1g is PANI (S) approximately**
Sept 10, 2020	Still in the oven and temperature was maintained at 80 C				
Sept 11, 2020	After heating at 60 degrees Celsius for 1 day and at 80 C for 2 days	17.0437	0.1233	0.0742	
Sept 11, 2020	Placed back in the oven at 50 C for 3 days				
Sept 14, 2020	After heating for 3 days at 50 C	17.0453	0.1249	0.0016 (gained)	
Sept 14, 2020	Approximately 0.1g of PANI (S) was collected from the petri dish after the above process and deposited in a round bottom flask				

Table D2: Data collected for PANI (L) at different stages of the drying process

Date	Process	Weight of the filter paper (in g)	Solvent present on the filter paper (in g)	Amount of the solvent evaporated (in g)	
Aug 19, 2020	Clear filter paper was weighed	1.2169	0	0	**Wt. of PANI + clear Filter paper (in g) = 1.3169**
Aug 26, 2020	6 days after the treatment with EKC and IPA	2.9424	1.6255	0	
Aug 28, 2020	8 days after the treatment with EKC and IPA	2.8727	1.5558	0.0697	**The total amount of the solvent needed to be**
Aug 28, 2020	After heating for 3 hrs on the	2.6078	1.2909	0.2649	

	heating plate at 60 degrees C				evaporated (in g) = 1.1071
Aug 31, 2020	2 days after heating (3hrs at 60 degrees C)	2.6560	1.3391	Gained 0.0482	
Aug 31, 2020	After heating for 6 hrs on a heating plate at 70 degrees C	2.3719	1.055	0.2841	
Sept 1, 2020	1 day after heating (6 hrs at 70 degrees C)	2.5636	1.2467	Gained 0.1917	
Sept 1, 2020	After heating for 6 hrs on the heating plate at 80 C	2.3109	0.994	0.2527	
Sept 2, 2020	1 day after heating (6 hrs at 80 C)	2.4637	1.1468	Gained 0.1528	
Sept 2, 2020	After heating for 6 hrs on the heating plate at 90 C	2.2409	0.924	0.2228	
Sept 3, 2020	1 day after heating (6 hrs at 90 C)	2.3879	1.1071	Gained 0.1470	
Sept 8, 2020	**PANI (L) was scraped from the filter paper and collected in an empty petri dish (weight of an empty petri dish- 14.2843g)**				
Sept 8, 2020	After collecting PANI (L) in a petri dish and before placing it in the oven at 60 degrees C	14.4700	0.1975		**The total mass collected on a petri dish after scraping the filter paper is 0.1857g; 0.1g is PANI (S) approximately**
Sept 9, 2020	Still in the oven and temperature				

127

	was increased to 80 C				
Sept 10, 2020	Still in the oven and temperature was maintained at 80 C				
Sept 11, 2020	After heating at 60 degrees C for 1 day and at 80 C for 2 days	14.4209	0.0366	0.0491	
Sept 11, 2020	Placed back in the oven at 50 C for 3 days				
Sept 14, 2020	After heating for 3 days at 50 degrees C	14.4225	0.0382	0.0016(gained)	
Sept 14, 2020	Approximately 0.1 g of PANI (L) was collected from the petri dish and deposited in a round bottom flask.				

Appendix E: Standard Error Calculations

Standard error (SE) values for **all the sorption data** presented in this thesis were calculated as per below:

For instance, for PANI mentioned in Table 10 (Chapter 4, Section 4.1.1), the data are provided in Table E1.

Table E1:Data points for PANI

Sorption of PANI (ppm of F)	1.39	1.37	1.25	1.25

Average = $\overline{X}$ = 1.315 for Table E1 data points

Variance $(X) = S^2 = \frac{\sum_{i=1}^{n}(Xi-\overline{X})2}{n-1} = 0.0057$

Variance $(\overline{X})= S^2/n = 0.001425$

Standard error (SE) $= \sqrt{S^2/n} = 0.037749$

Therefore, **Average sorption ± SE = 1.315 ± 0.037749 ppm of F**

Confidence interval = $\overline{X}$ ± t $_{\alpha/2, \text{df}}$.(SE);

For 95% CI t $_{0.025, 3}$ = 3.182 (with α = 0.05, n = 4)

Therefore, **95% Confidence Interval for 0.1 of PANI (L) is 1.315 ± 0.120118 ppm of F**

Appendix F: Raw Data Trends

Sorption data were collected as described in Chapter 3 and discussed in Chapters 4 to 6. Since the GC takes a reading every 12 minutes, raw data points are available for analysis in 12-min intervals (or 20-min intervals when benzene was involved). Select raw data trends are presented in Figures F1 and F2. Trends from different cases (Case #3 and Case #50 of Table 8 in Chapter 3) demonstrate good reproducibility over different dates.
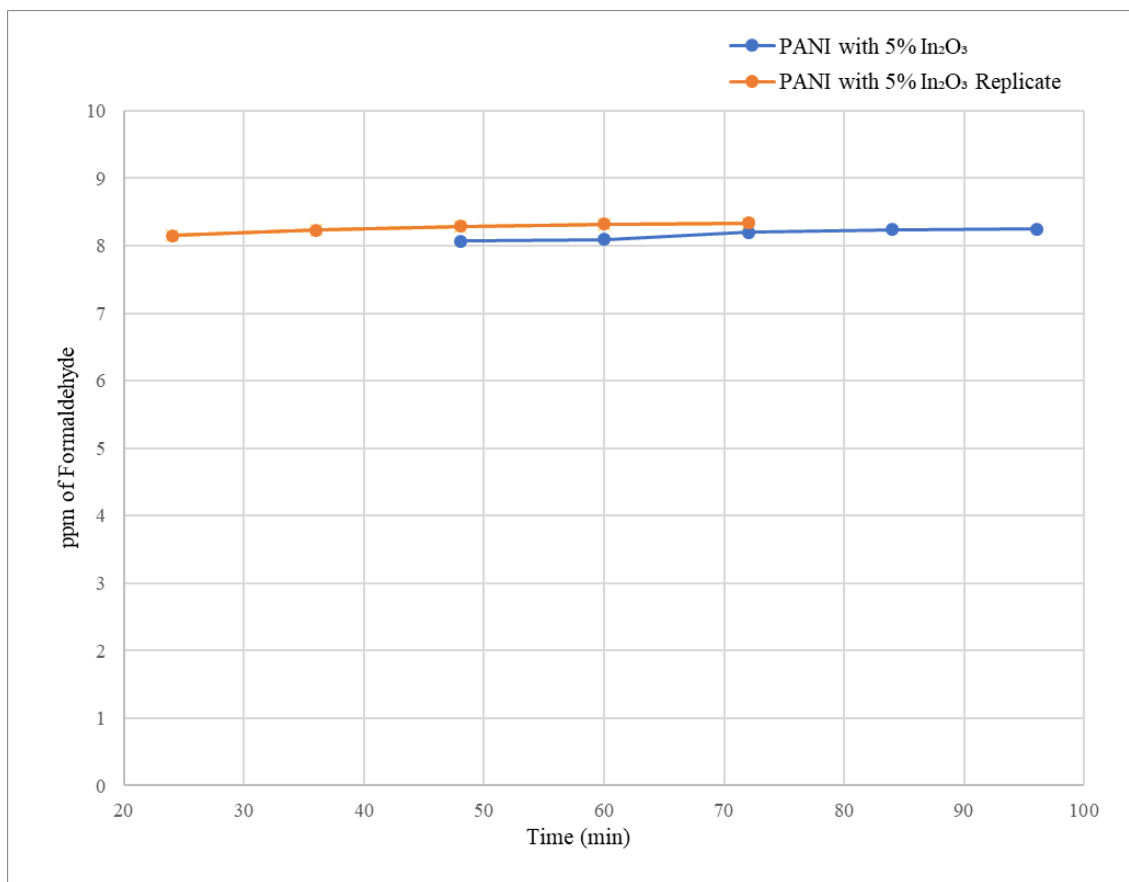
Figure F1: Raw data trends from sorption tests of PANI with 5% In_2O_3 (Case #3) and its replicate (Repl) (Case #3 Repl) for sorption of F; (Source: F 10 ppm)
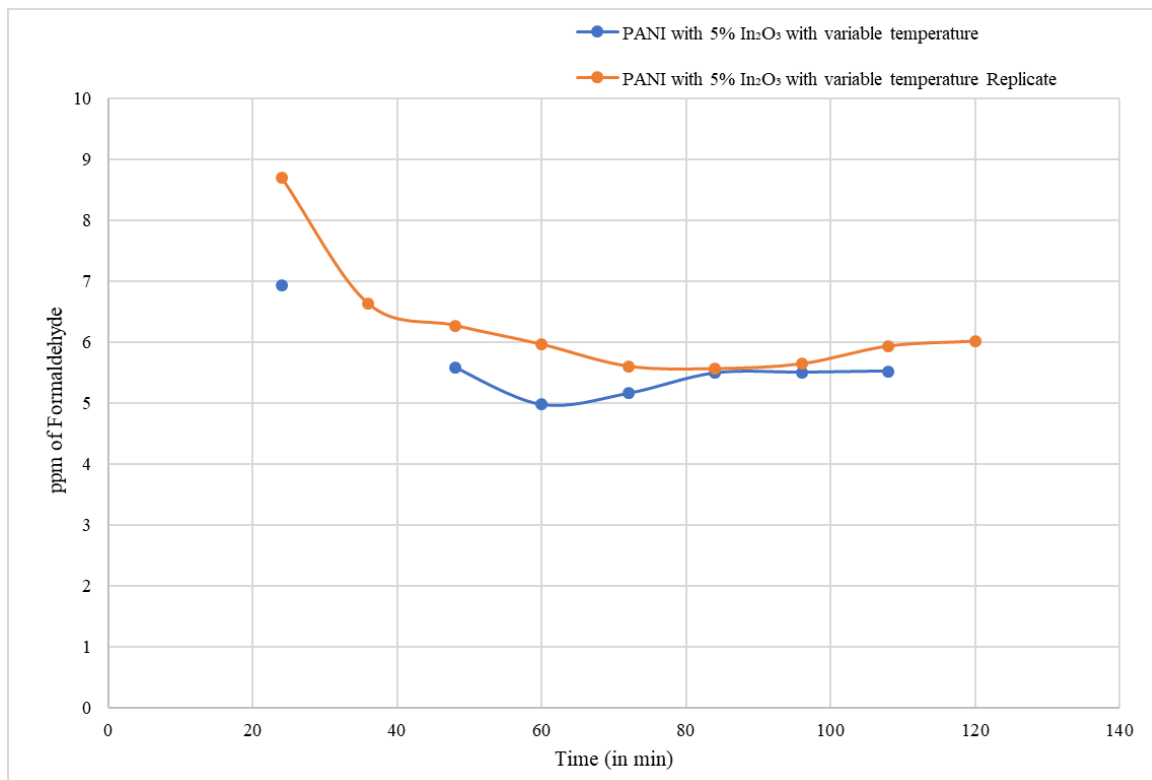
Figure F2: Raw data trends from sorption tests of PANI with 5% In_2O_3 with varying temperature (Case #50) and its replicate (Repl) (Case #50 Repl) for sorption of F; (Source: F 10 ppm)

Appendix G: Statistical Analysis of Sorption Data – F Sorption

Appendix G shows <u>representative</u> statistical analysis that was implemented <u>throughout</u> the thesis for typical comparisons between data sets. Table 8 in Chapter 3 cites all case #'s of the GC trials.

G.1 Data Analysis for Case #3 and Case #3 Replicate

Table G1: Raw data for Case #3 trials, as plotted in Figure F1.

Time (in min)	24	36	48	60	72	84	96
Raw data (ppm of F) for Case #3			8.07	8.09	8.2	8.24	8.25
Raw data (ppm of F) for Case #3 Repl	8.15	8.23	8.29	8.32	8.34		

Hypothesis testing –
$H_0 : \tau_t = 0$; (null hypothesis says that there is no significant difference between the two trials plotted in Figure F1)
$H_1: \tau_t \neq 0$ (alternative hypothesis says that there is a significant difference between the two trials)
$F_o < F_{1,10,0.05}$, therefore we accept the null hypothesis and can say that the two trials plotted in Figure F1 for Case #3 are essentially the same process; there are no significant differences between the two trials. See Table G2 for the ANOVA analysis of the data.

Table G2: ANOVA analysis for Figure F1 and Table G1

Source	SS (sum of squares)	dF (degrees of freedom)	MS	
Between the treatments	0.02304	1	0.02304	$F_o = 3.522936$
Within the treatments	0.05232	8	0.00654	$F_{1,10,0.05} = 5.32$
Total	0.07536	9		$F_o < F_{1,8,0.05}$

G.2 Data Analysis for Case #50 and Case #50 Replicate

Table G3: Raw data for Case #50 trials, as plotted in Figure F2

Time (in min)	24	36	48	60	72	84	96	108	120
Raw data (ppm of F) for Case #50	6.93		5.58	4.98	5.16	5.49	5.50	5.52	
Raw data (ppm of F) Case #50 Repl	8.7	6.63	6.27	5.96	5.60	5.56	5.64	5.93	6.01

Hypothesis testing –
$H_0 : \tau_t = 0$; (null hypothesis says that there is no significant difference between the two trials plotted in Figure F2)
$H_1 : \tau_t \neq 0$ (alternative hypothesis says that there is a significant difference between the two trials)
$F_o < F_{1,14,0.05}$, therefore we accept the null hypothesis and can say that the two trials plotted in Figure F2 for Case #50 are essentially the same process; there are no significant differences between the two trials. See Table G4 for the ANOVA analysis of the data.

Table G4: ANOVA analysis for Figure F2 and Table G3

Source	SS (sum of squares)	dF (degrees of freedom)	MS	
Between the treatments	1.721781	1	1.721781	$F_o = 2.401514$
Within the treatments	10.03739	14	0.716957	$F_{1,14,0.05} = 4.6$
Total	11.75918	15		$F_o < F_{1,14,0.05}$

Appendix H: Statistical Analysis of Sorption Data – 'Zero Sorption' of F and B

Appendix H shows representative statistical analysis that was implemented throughout the thesis for typical comparisons among data sets collected. The table citing all the GC trials case #'s is Table 8 in Chapter 3.

H.1 ANOVA Analysis for Blanks and Case #41

Table H1: Raw data readings for blanks and Case #41

Time (in min)	Blanks Readings (in ppm)	Case #41 (PAAc 450 K) (in ppm)
	B	B
20	8.81	9.9
40	9.75	9.81
60	9.93	10
80	9.99	9.97
100	9.98	9.94

Table H2: ANOVA analysis for data in Table H1

Source	SS (sum of squares)	dF (degrees of freedom)	MS	
Between the treatments	0.13456	1	0.13456	$F_o = 1.04371$
Within the treatments	1.0314	8	0.12892	$F_{1,10,0.05} = 5.32$
Total	1.16596	9		$F_o < F_{1,8,0.05}$

Hypothesis testing - H_0: $\tau_t = 0$; (null hypothesis says that there is no significant difference between the blanks and Case #41 results tabulated in Table H1) H_1: $\tau_t \neq 0$ (alternative hypothesis says that there is a significant difference between the blanks and Case #41)

Since $F_o < F_{1,8,0.05}$, we, therefore, accept the null hypothesis and can say that the blanks and the sorption results of Case #41 in Table H1 are essentially from the same process; there is no

significant difference between them. This indicates that no B was sorbed from a B 10 ppm source in Case #41.

H.2 ANOVA Analysis for Blanks and Case #44

Table H3: Raw data readings for blanks and Case #44

Time (in min)	Blanks Readings (in ppm)	Case #44 (PMMA 1 M) (in ppm)
	B	B
20	8.67	9.92
40	9.54	9.93
60	9.83	9.92
80	9.93	9.93
100	9.98	

Table H4: ANOVA analysis for data in Table H3

Source	SS (sum of squares)	dF (degrees of freedom)	MS	
Between the treatments	0.24939	1	0.24939	$F_o = 1.48661$
Within the treatments	1.1743	7	0.16776	$F_{1,7,0.05} = 5.59$
Total	1.42369	8		$F_o < F_{1,7,0.05}$

Hypothesis testing - H_0: $\tau_t = 0$; (null hypothesis says that there is no significant difference between the blank trial and Case #44 tabulated in Table H3) H_1: $\tau_t \neq 0$ (alternative hypothesis says that there is a significant difference between the blanks and Case #44)

Since $F_o < F_{1,7,0.05}$, we, therefore, accept the null hypothesis and can say that the blank trial and Case #44 tabulated above in Table H3 are essentially from the same process; there is no significant difference between them. This indicates that no B was sorbed from a B 10 ppm source in Case #44.

H.3 ANOVA Analysis for Blanks and Case #47

Table H5: Raw data readings for blanks and Case #47

Time (in min)	Blanks Readings (in ppm)	Case #47 (PAAc 450 K) (in ppm)
	F	F
12		7.4
24	7.46	7.44
36	7.53	7.54
48	7.54	7.53
60	7.56	
72	7.58	

Table H6: ANOVA analysis for data in Table H5

Source	SS (sum of squares)	dF (degrees of freedom)	MS	
Between the treatments	0.007	1	0.007	$F_o = 1.48661$
Within the treatments	0.0224	7	0.0032	$F_{1,7,0.05} = 5.59$
Total	0.02949	8		$F_o < F_{1,7,0.05}$

Hypothesis testing - H_0: $\tau_t = 0$; (null hypothesis says that there is no significant difference between the blank trial and Case #47 tabulated in Table H5) H_1: $\tau_t \neq 0$ (alternative hypothesis says that there is a significant difference between the blanks and Case #47)

Since $F_o < F_{1,7,0.05}$, we, therefore, accept the null hypothesis and can say that the blanks trial and Case 53 tabulated above in Table H5 are essentially from the same process; there is no significant difference between them. This indicates that no F was sorbed from a F 10 ppm source in Case #47.

H.4 ANOVA Analysis, Bonferroni and LSD Tests for Blanks, Case #41, and Case #44

Table H7: Raw data readings for blanks, Case #41 and Case #44

Time (in min)	Blanks Readings (in ppm) Feb 25, 2021	Blanks Readings (in ppm) Feb 26, 2021	Case #41 (PAAc 450 K)	Case #44 (PMMA 1 M)
	B	B	B	B
20	8.81	8.67	9.9	9.92
40	9.75	9.54	9.81	9.93
60	9.93	9.83	10	9.92
80	9.99	9.93	9.97	9.93
100	9.98	9.98	9.94	
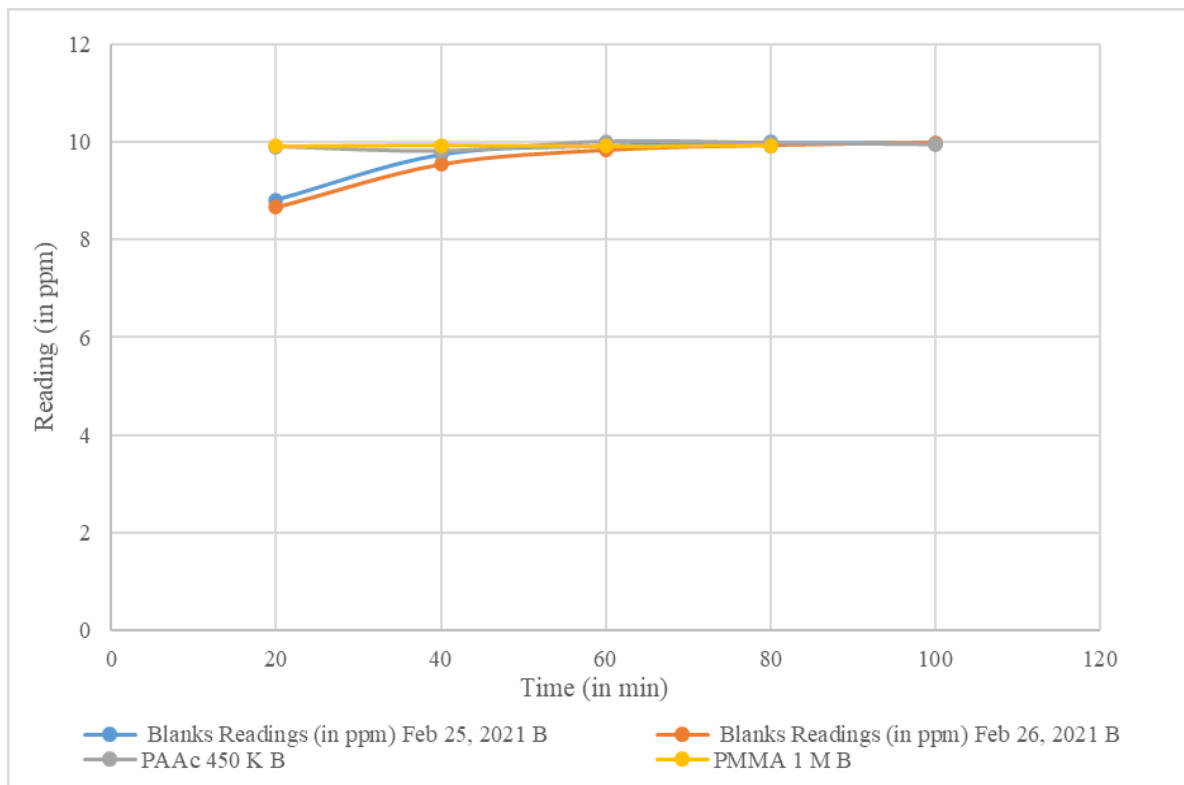
Figure H1: Raw data plot for Blanks and Cases # 41 and # 44

Table H8: ANOVA analysis for data in Table H7

Source	SS (sum of squares)	dF (degrees of freedom)	MS	
Between the treatments	0.406574	3	0.13552	$F_o = 0.92164$
Within the treatments	2.2057	15	0.14705	$F_{3,15,0.05} = 3.29$
Total	2.612274	18		$F_o < F_{3,15,0.05}$

Hypothesis testing - H_0: $\tau_t = 0$; (null hypothesis says that there is no significant difference between the two blank trials and Case #41 and Case #44 tabulated in Table H8) H_1: $\tau_t \neq 0$ (alternative hypothesis says that there is a significant difference between the two blank trials and Cases #41 and #44)

Since $F_o < F_{3,15,0.05}$, we, therefore, accept the null hypothesis and can say that the two blank trials and Case #41 and Case #44 tabulated above are essentially from the same process; there is no significant difference between them. This indicates that no B was sorbed from a B 10 ppm source in Case #41 and Case #44.

Bonferroni and LSD tests

Bonferroni and LSD tests were conducted to further evaluate and confirm the results obtained from the ANOVA analysis (regular multiple comparisons) tabulated in Table H8.

To calculate Fisher's LSD:

For b=0.25 (upper bound for overall α') and **c=6** (total number of a comparison test of interest) for **α=b/c,**

Therefore, α= 0.041. (Value of b was 0.25 using Bonferroni inequality α'≤1-(1-α)[c])

LSD = ($t_{α/2, n-k}$) x (s.e) = 0.54 [$t_{α/2, n-k}$ = $t_{0.0208,15}$ = 2.2281 from t-tables, s.e = $\sqrt{2S^2/\bar{n}}$ = 0.2425283 with S^2=0.14705, $\bar{n}$=5 from Table H8]

For b=0.05 (upper bound for overall α') and **c=6** (total number of a comparison test of interest) for **α=b/c,**

Therefore, α= 0.00833 (Value of b was 0.05 using Bonferroni inequality α'≤1-(1-α)[c])

LSD = ($t_{\alpha/2,\,n-k}$) x (s.e) = 0.736 [$t_{\alpha/2,\,n-k} = t_{0.004167,15} = 3.0362$ from t-tables, s.e $= \sqrt{2S^2/\bar{n}} = 0.2425283$ with $S^2=0.14705$, $\bar{n}=5$ from Table H8]

Table H9: Average values for data in Table H7

Sample	Blanks (Feb 25, 2021)	Blanks (Feb 26, 2021)	PAAc 450 K	PMMA 1 M
Mean (in ppm of B)	9.692	9.59	9.924	9.925

All four means in Table H9 are not significantly different at both the 4.1% and 0.08% level since the difference between 2 means for all 6 pairs is less than 0.54 and 0.736, respectively. This confirms the results obtained from the regular ANOVA analysis earlier, that there are no significant differences between blanks and Case #41/Case #44. Hence, we can say that Case #41 and Case #44 exhibit zero sorption.

Appendix I: Raw Data Trends for Sorption Data – F/B Sorption

Appendix I is representative of typical analysis of the GC sorption trials related to the selectivity studies discussed in Chapter 5. More specifically, Appendix I consists of data analysis of representative cases involving mixtures of formaldehyde and benzene (see Table 8 of Chapter 3 for specific case #'s).
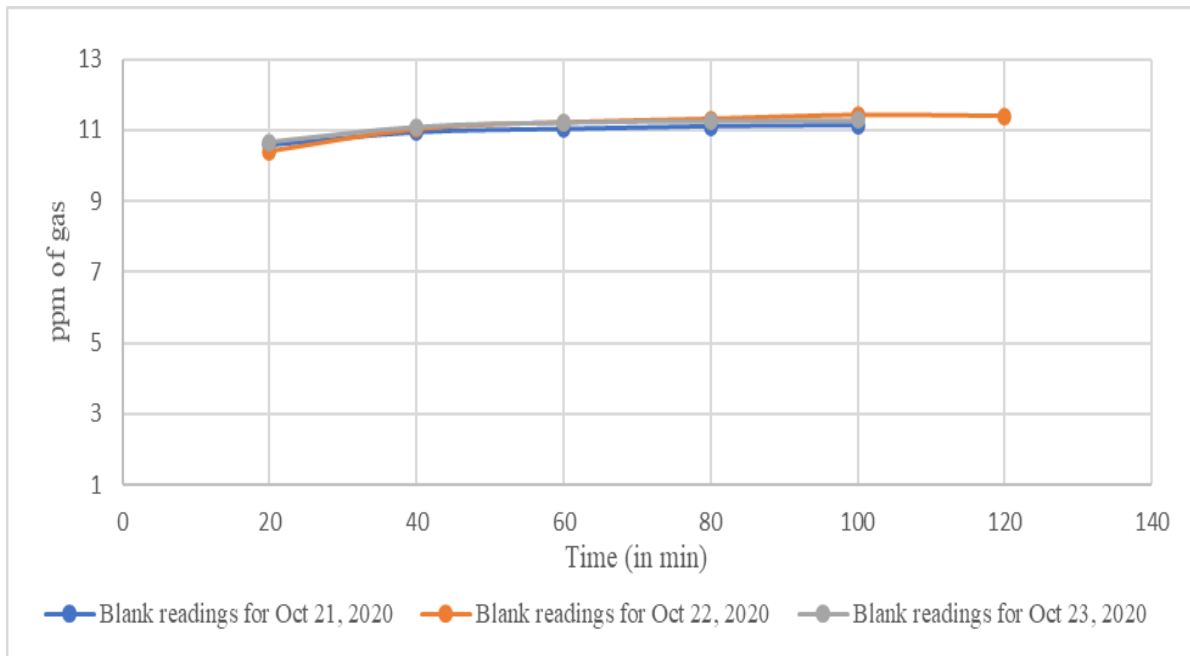
Figure I1: Raw data trends for blanks from sorption tests for F and B (Source: F/B, 5/5 ppm each)
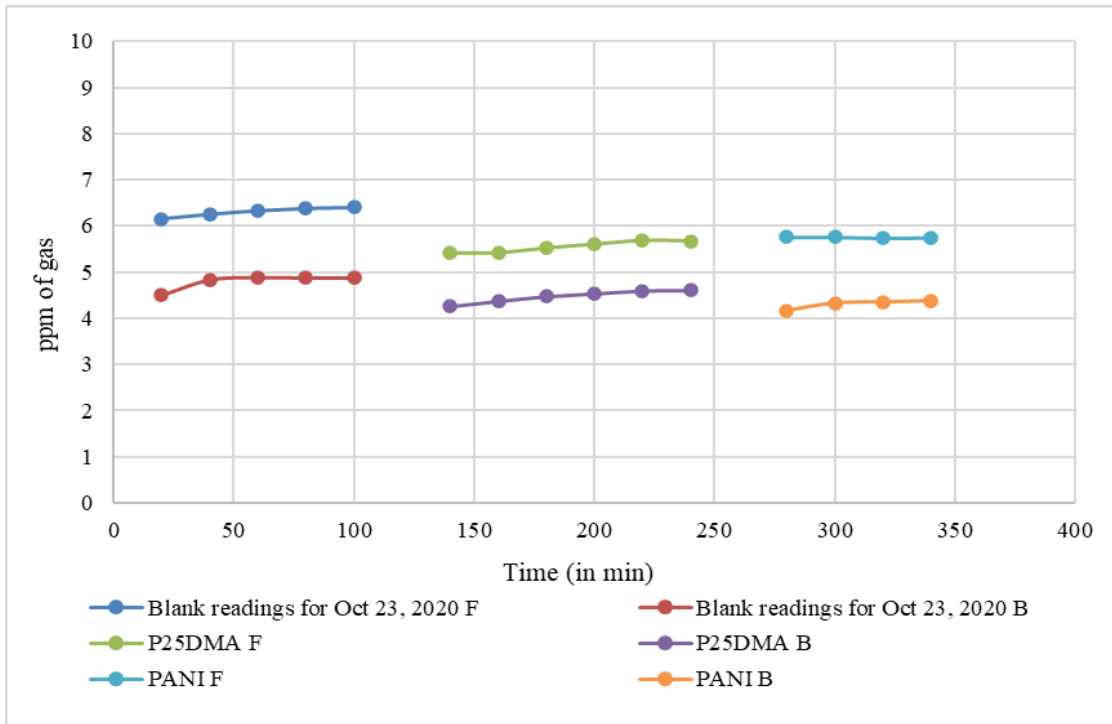
Figure I2: Raw data trends for blanks from sorption tests for F and B; (Source: F/B, 5/5 ppm)
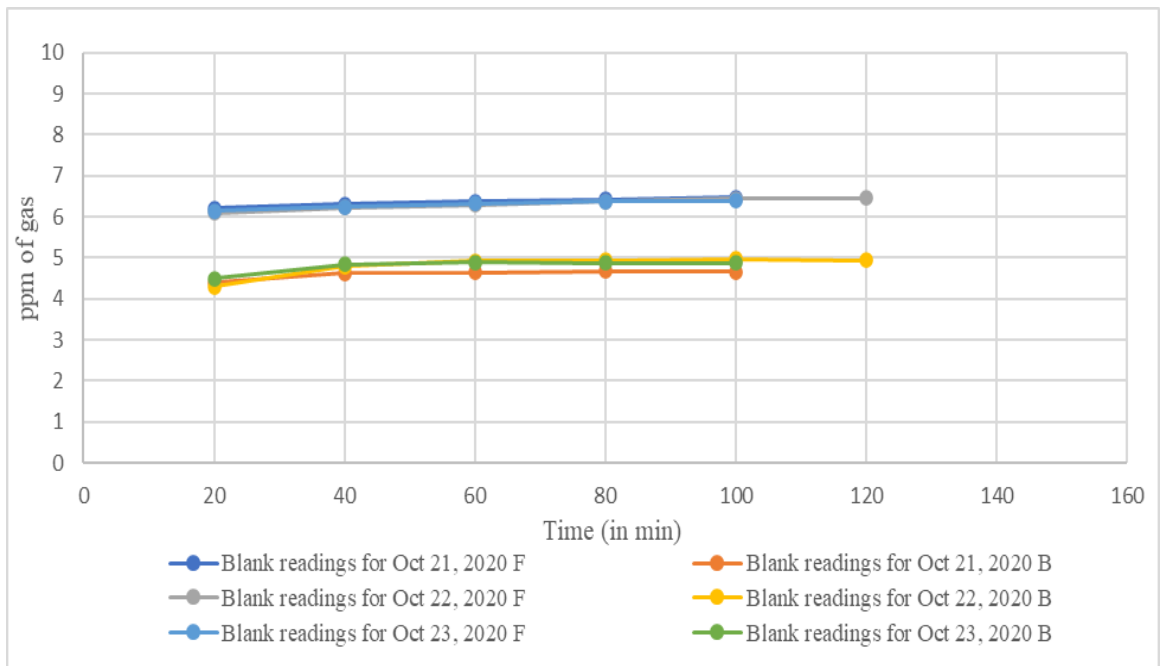
Figure I3: Raw data trends for blanks, P25DMA and PANI from sorption tests for F and B; (Source: F/B, 5/5 ppm)

141

Figure I3 confirms the results discussed in Chapter 5. P25DMA seems to sorb more F than PANI from F/B (5/5 ppm) mixture source (amount of gas sorbed can be obtained by subtracting polymer sample reading (in ppm) from blank reading (in ppm) for that day).
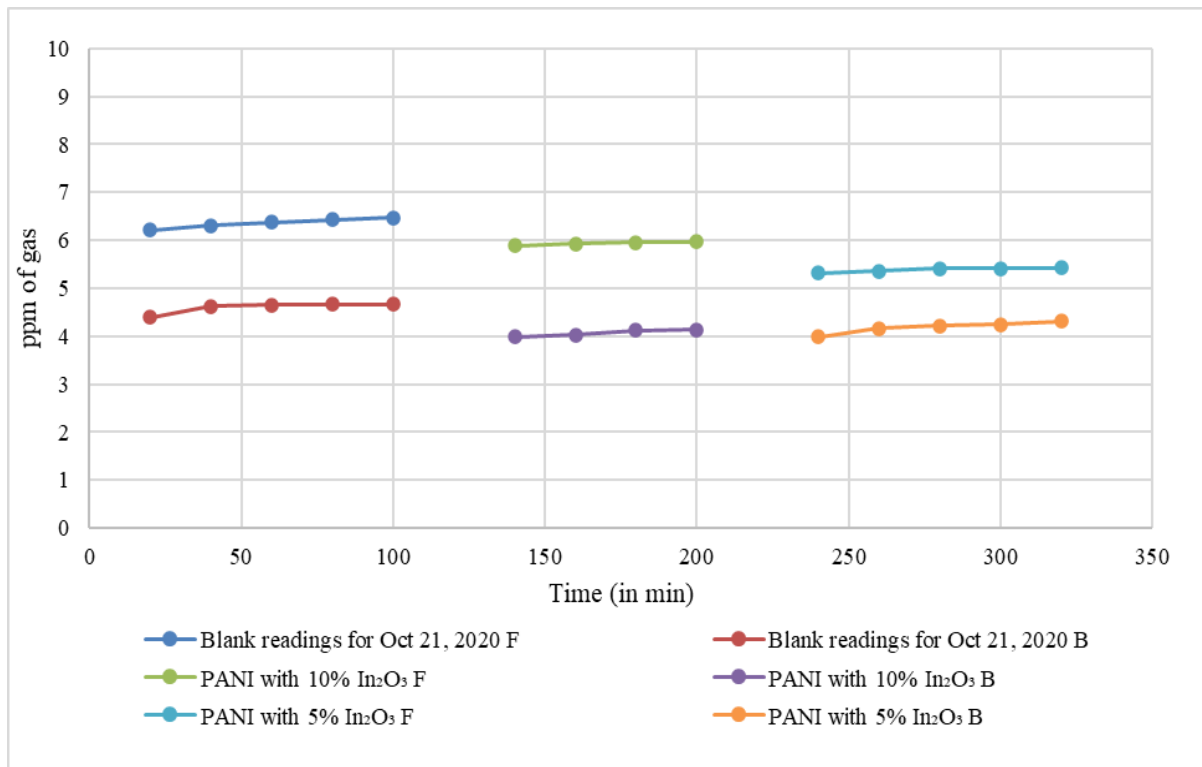
Figure I4: Raw data trends for blanks, PANI with 5% In_2O_3, and PANI with 10% In_2O_3 from sorption tests for F and B; (Source: F/B, 5/5 ppm)

Figure I4 confirms the results discussed in Chapter 5; PANI with metal oxide (In_2O_3) sorption from F/B (5/5ppm) mixture source decreases with an increase in the percentage of In_2O_3 dopant from 5% to 10 % wt. (amount of gas sorbed can be obtained by subtracting polymer sample reading (in ppm) from blank reading (in ppm) for that day).

Table I1: Reading for blanks, PANI with 2.5% In_2O_3 (Case #28 Repl) and PANI with 5% In_2O_3 (Case #26 Repl)

Time (in min)	Blanks Readings (in ppm)		Case #28 Repl (PANI with 2.5% In_2O_3) Readings (in ppm)		Case #26 Repl (PANI with 5% In_2O_3) Readings (in ppm)	
	F	B	F	B	F	B
20	6.08	3.9				

40	6.3	4.88				
60	6.37	5.05				
80	6.41	5.12				
100	6.44	5.12				
120			6.48	5.13		
140			4.87	3.99		
160			4.88	4.25		
180			4.93	4.43		
200			5.01	4.54		
220			5.02	4.61		
240			5.05	4.66		
260			5.07	4.71		
280					5.1	4.77
300					4.59	3.82
320					4.64	4.21
340					4.62	4.38
360					4.66	4.53
380					4.71	4.63
400					4.71	4.68
420					4.72	4.75
440					4.72	4.82
460					4.74	4.86
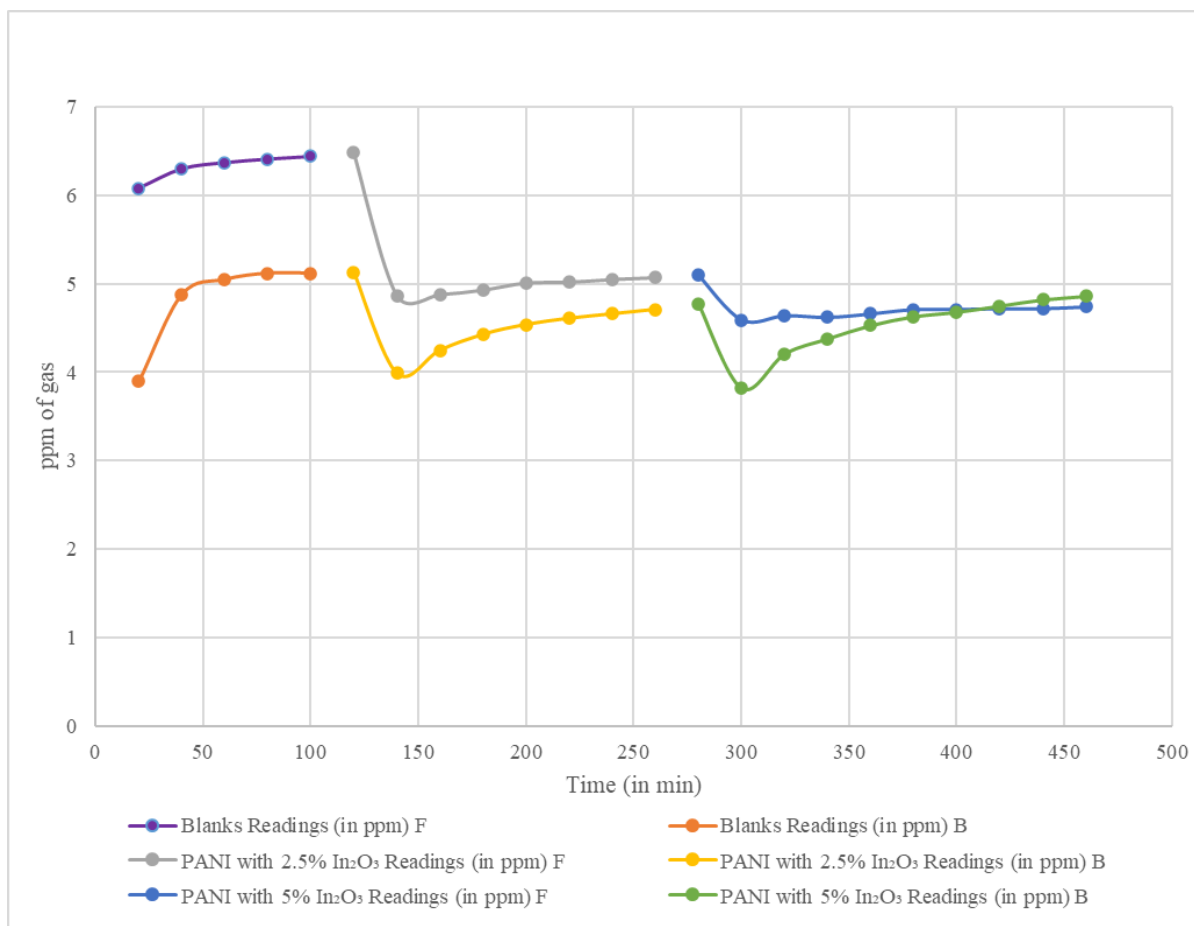
Figure I5: Raw data trends for Case #28 Repl and Case #26 Repl

The amount of gas sorbed for the data in Table I1 and Figure I5 can be obtained by subtracting polymer sample readings (in ppm) from blank readings (in ppm) for that day. Case # 26 was deliberately run for 200 min, as opposed to 160 min for Case # 28. Figure I5 shows that curve B for PANI with 5% In_2O_3 ('green') was asymptotically moving towards curve B for blank readings ('orange'), while F ('blue') stabilized after 100 min and did not change significantly. This supports the trend of PANI with 5% In_2O_3 being more selective towards F over B (as discussed in Section 5.1.1).

Appendix J: Raw Data Trends and Statistical Analysis of Sorption Data – Ac and F/Ac Sorption

Appendix J is representative of typical statistical analysis of the GC sorption trials related to the sensitivity and selectivity studies discussed in Chapters 4 and 5. More specifically, Appendix J consists of data analysis of representative sensitivity and selectivity studies involving mixtures of acetaldehyde gas (see again Table 8 of Chapter 3 for case #'s).

J.1 Raw Data Trends for Ac Blanks on Different Experimental Days
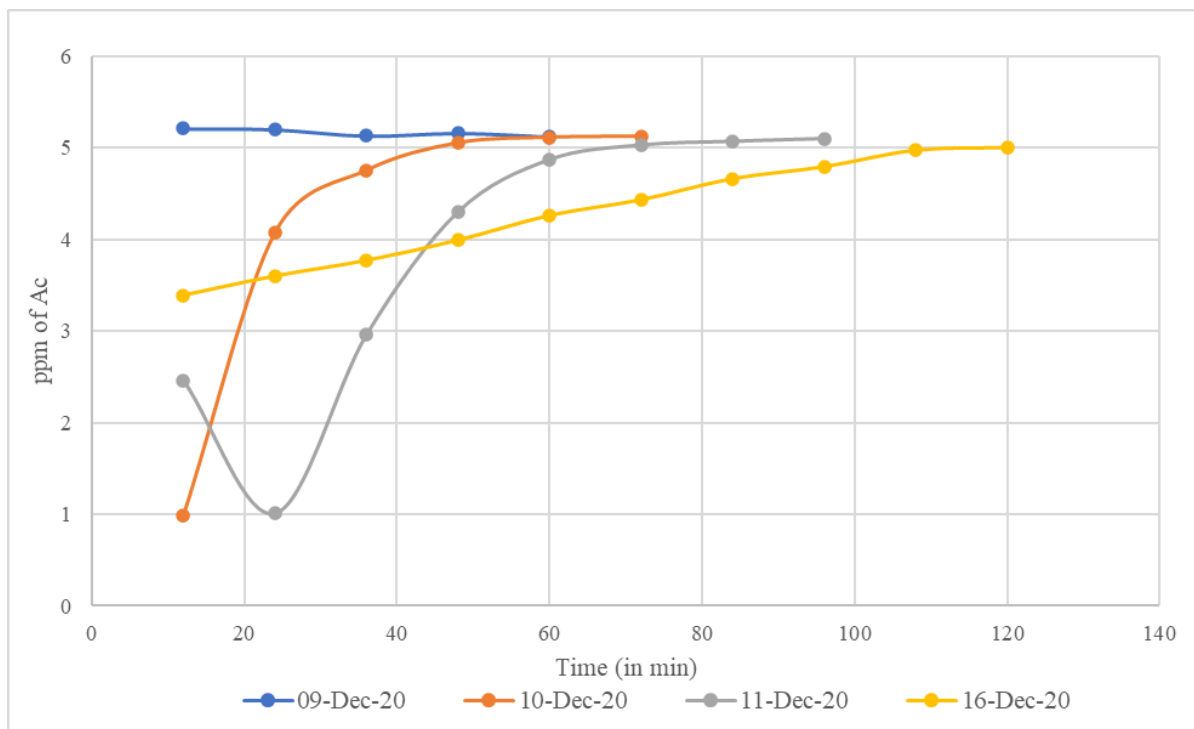
Figure J1: Raw data trends for PANI with 10% In_2O_3 (Case #18) and its replicate (Case #18 Repl); (Source: Ac 5 ppm)
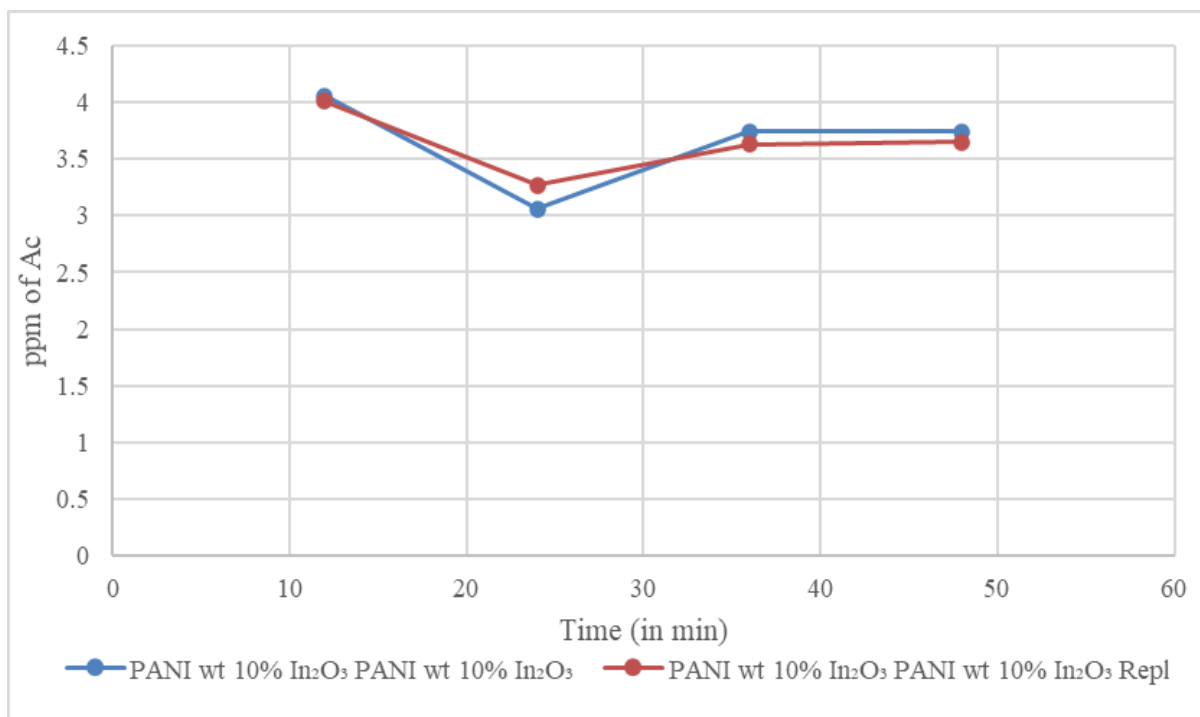
Figure J2: Raw data trends for PANI with 10% In_2O_3 (Case #18) and its replicate (Case #18 Repl); (Source: Ac 5 ppm)

J.2 Statistical Analysis for F/Ac Blanks on Feb 3, 2021

Table J1: Data for F/Ac blanks on Feb 3, 2021

Time (in min)	Morning Blanks Readings (in ppm)		Afternoon Blanks Readings (in ppm)	
	F	Ac	F	Ac
12	0.53	1.89	1.24	1.6
24	0.97	2.3	1.6	1.03
36	1.45	2.28	1.77	1.94
48	1.67	2.26	1.94	2.13
60	1.74	2.24	1.97	2.16
72	1.79	2.2	1.97	2.16

J.2.1 ANOVA Analysis for F+Ac

Table J2: ANOVA analysis for blanks

Source	SS (sum of squares)	dF (degrees of freedom)	MS	
Between the treatments	0.003	1	0.003	$F_o = 0.00712$
Within the treatments	4.22248	10	0.422248	$F_{1,10,0.05} = 4.96$
Total	4.22549	11		$F_o < F_{1,10,0.05}$

Hypothesis testing - H_0: $\tau_t = 0$; (null hypothesis says that there is no significant difference between the three blank trials tabulated in Table J1) H_1: $\tau_t \neq 0$ (alternative hypothesis says that there is a significant difference between the two blanks)

Since $F_o < F_{1,10,0.05}$, we, therefore, accept the null hypothesis and can say that the two blank trials tabulated above are essentially from the same process; there is no significant difference between them.

J.2.2 Comments on Comparisons
Only F reading
Both sets of blanks seem to be from the same process on performing the ANOVA analysis using only F readings tabulated inTable J1.

Only Ac readings
Both sets of blanks seem to be from the same process on performing the ANOVA analysis using only Ac readings tabulated in Table J1.

Data for ANOVA comparisons for only F and Ac readings are available but not shown here for the sake of brevity.

Appendix K: Typical Temperature Profiles

Appendix K consists of typical temperature profiles recorded while conducting the stability studies of PANI with 5% In_2O_3 discussed in Chapter 6. Different coloured symbols on figures K1 and K2 represent independently replicated trials over 2 different days.
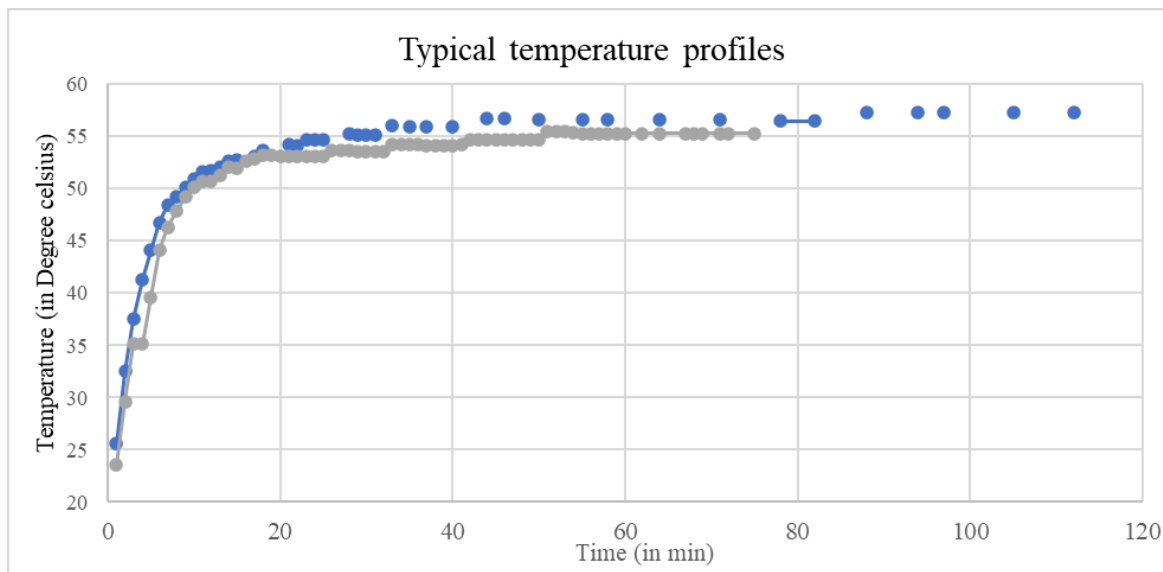
Figure K1: Temperature profile (heating plot) for PANI with 5% In_2O_3 variable temperature
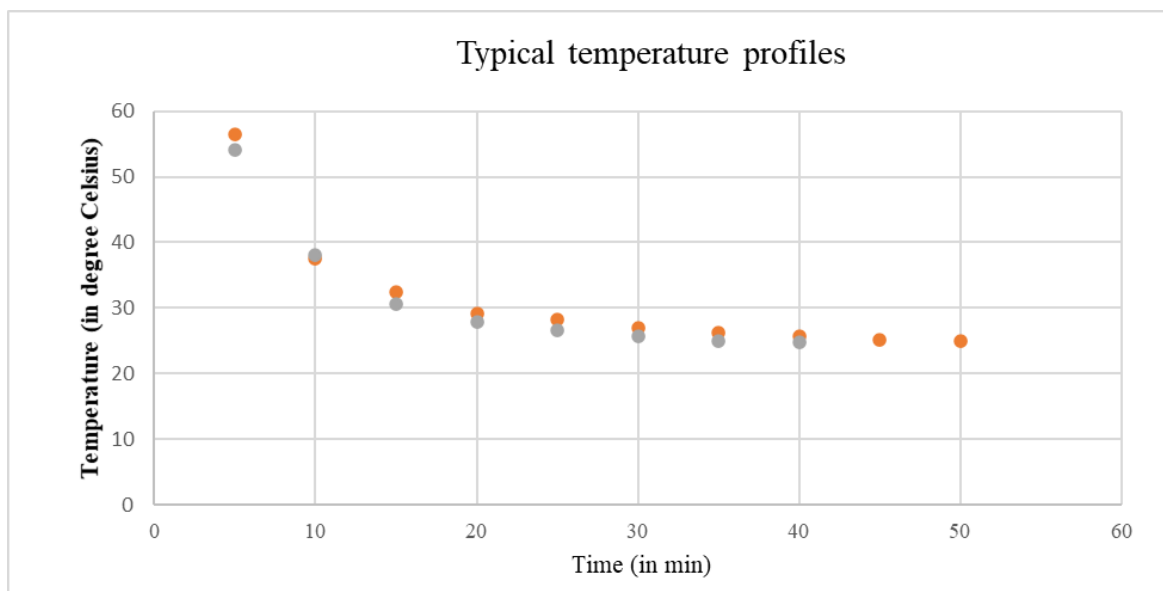
Figure K2: Temperature profile (cooling plot) for PANI with 5% In_2O_3 variable temperature

Appendix L: Optical Microscope

L.1 Introduction

An Optical Microscope (OM) is typically used to view specimens and often study the surface properties of a substrate, which in our case is the polymeric material (with or without metal oxide dopant). OM is also known as a light microscope, as it uses a beam of light (and the appropriate set of lenses) to magnify the image of the material under observation. The basic functionality of OM is to magnify and illuminate the sample under observation. It works on a similar principle as that of the compound microscope. A magnified image of the sample is created by the combination of the objective lens that produces an inverted virtual image and an eyepiece that makes an erect virtual image. The magnified image is captured using a camera and subsequently on a TV screen (see Figure L1: Optical microscope BX53M for a typical optical microscope set-up).

The resolution and magnification of the optical microscope are limited and therefore it is not capable to give as detailed information about the structure and morphology of the polymeric material as a scanning electron microscope (SEM), for instance. The information obtained from OM imaging is thus complementary to the surface morphology studies using more advanced and higher resolution techniques like SEM. The equipment used for imaging was an Olympus BX53M Optical Microscope available in Prof. Mekonnen's lab (E6-5107).

Figure L1: Optical microscope BX53M [79]

L.2 List of Samples Characterized Using OM

Table L1: List of samples observed under OM

Sample name	Condition of the polymeric sample
PANI (L) (synthesised in lab)	As is, ground
PANI with 2.5% In_2O_3	As is
PANI with 5% In_2O_3	As is, ground
PANI S (Sigma; purchased)	As is

Note- In Table L1 'As is' condition of polymeric materials means the sample particles were exactly of same size as they were collected and stored after synthesis (particle cluster sizes could be quite non-uniform). 'Ground' condition means the material was further ground into a smaller particle size, hence the samples had overall a more uniform particle size compared to 'As is'.

L.3 Sample Preparation

The images of the four samples in Table L1 were taken via OM. The samples were prepared by depositing the polymer suspended in Ethanol on an indentured glass slide; the sample was subsequently left at room temperature for ethanol to evaporate. The glass slides were then placed under the microscope to capture the images.

L.4 Results and Discussion

The surface properties of undoped and doped PANI were studied under OM (as is); selective samples were ground further, just to observe any differences. The 'as is' samples were observed under 10X magnification, ground samples were observed under 25X magnification and PANI (S) was observed under 50X magnification because of its nanoscale particle size. Figure L2 contains different image scans on the samples obtained using OM.

a)
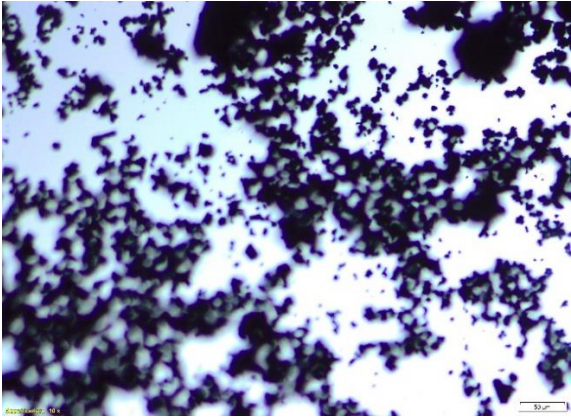
b)
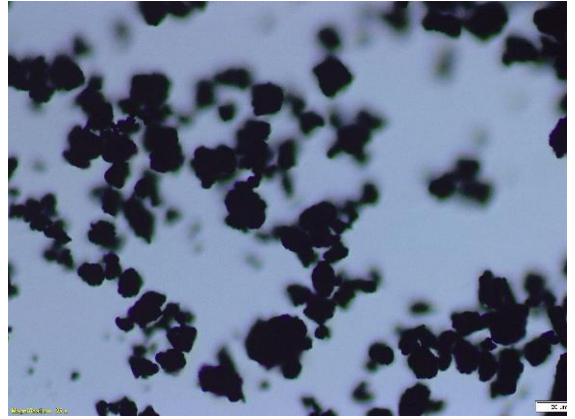
c)
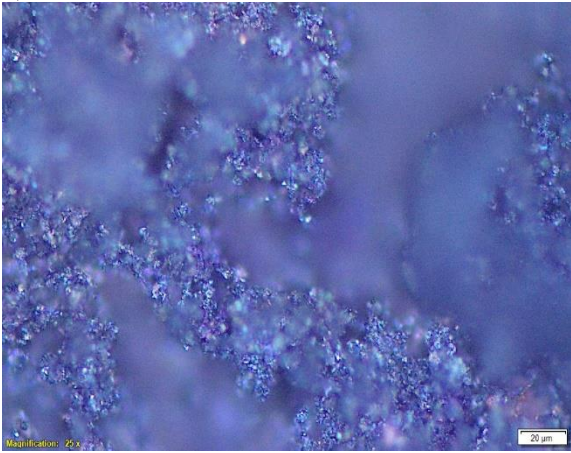
d)
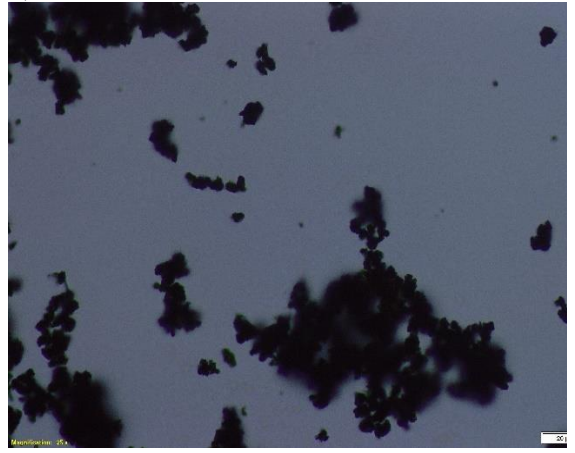
e)
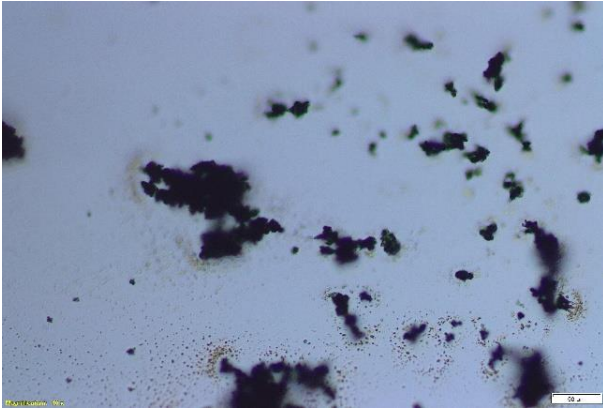
f)
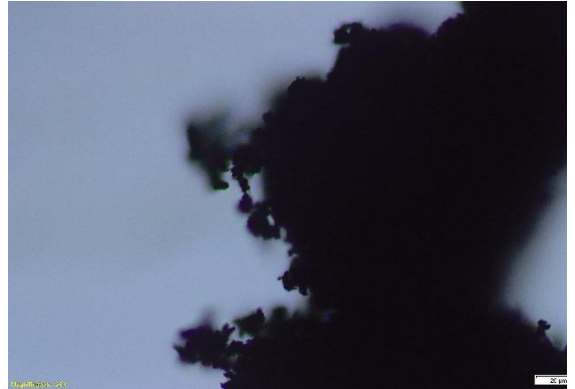
g)
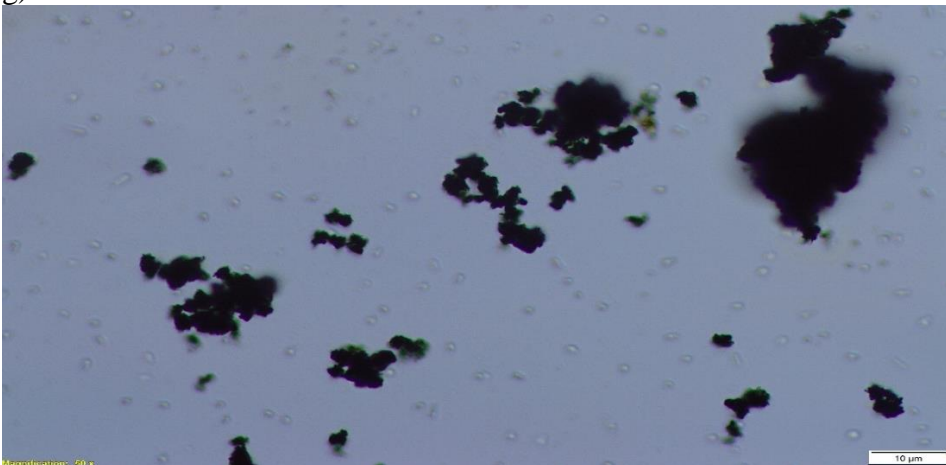
Figure L2: Optical microscope images of a) PANI (L) with 10X, b) PANI (L) with 25X, c) PANI with 2.5% In_2O_3 25X, d) PANI with 2.5% In_2O_3 25X (replicate), e) PANI with 5% In_2O_3 with 10X, f) PANI with 5% In_2O_3 with 25X, g) PANI (S) with 50X

Undoped PANI ((L) & (S)) and doped PANI with 5% In_2O_3 at all magnifications looked similar under the optical microscope, as shown in Figure L2 (a-b, e-g). In Figure L2 (a-b, d-g), the black dots and/or clusters are PANI polymer particles, whereas the whiter (empty) parts are the transparent glass side on which samples were deposited (as per Section L3). The 'as is' samples had a larger non-uniform particle size and therefore were more difficult to observe under the microscope because of magnification limitations. Therefore, selected samples were ground (see Table L1) into smaller/finer particle size clusters and observed under OM; however, nothing further or nothing finer or nothing more than small particles of the black powder was observed (as shown in Figure L2 (b and e)). However, for PANI with 2.5% In_2O_3 (Figure L2 c), the 'as is' particle size was relatively smaller. In addition, upon focusing the beam of light, the black powder seemed to scatter light and produce a navy blue colour image with some tiny dark blue clusters (suspected to be indium oxide). One can also see some blurry patches in the image captured under the microscope for PANI with 2.5% In_2O_3, which could be explained by the 2D layered structure of the material.

A final comment: It seemed difficult to reproduce reasonably similar images of the same sample under the microscope even after following the exact same sample preparation and instrument settings. This is evident when comparing images Figure L2 c-d for PANI with 2.5% In_2O_3.

Appendix M: Certificates for Copyrighted Material

Appendix M consists of licence agreements for Figure 2, Figure 5, Figure 6, Figure 7, Figure 8a, Figure 8b, Figure 9, Figure 56a, Figure 56b, Figure 56c and Figure 59, respectively.

License agreements for Figure 2

Will you be translating?	no
Circulation/distribution	50000 or greater
Author of this Springer Nature content	no
Title	Polymeric Materials for Detection of Chemical Warfare Agents
Institution name	University of Waterloo
Expected presentation date	Dec 2021
Order reference number	1
Portions	Figure 1
Requestor Location	Bhoomi Mavani University of Waterloo Engineering 6, 200 University Ave. W Waterloo, ON Waterloo, ON N2L 3G1 Canada Attn: University of Waterloo
Total	0.00 USD

Terms and Conditions

Springer Nature Customer Service Centre GmbH
Terms and Conditions

This agreement sets out the terms and conditions of the licence (the **Licence**) between you and **Springer Nature Customer Service Centre GmbH** (the **Licensor**). By clicking 'accept' and completing the transaction for the material (**Licensed Material**), you also confirm your acceptance of these terms and conditions.

1. Grant of License

1. 1. The Licensor grants you a personal, non-exclusive, non-transferable, world-wide licence to reproduce the Licensed Material for the purpose specified in your order only. Licences are granted for the specific use requested in the order and for no other

155

License agreements for Figure 5

Will you be translating?	no
Circulation/distribution	50000 or greater
Author of this Springer Nature content	no
Title	Polymeric Materials for Detection of Chemical Warfare Agents
Institution name	University of Waterloo
Expected presentation date	Dec 2021
Order reference number	2
Portions	Figure 1
Requestor Location	Bhoomi Mavani University of Waterloo Engineering 6, 200 University Ave. W Waterloo, ON Waterloo, ON N2L3G1 Canada Attn: University of Waterloo
Total	0.00 USD

Terms and Conditions

Springer Nature Customer Service Centre GmbH
Terms and Conditions

This agreement sets out the terms and conditions of the licence (the **Licence**) between you and **Springer Nature Customer Service Centre GmbH** (the **Licensor**). By clicking 'accept' and completing the transaction for the material (**Licensed Material**), you also confirm your acceptance of these terms and conditions.

1. Grant of License

1. 1. The Licensor grants you a personal, non-exclusive, non-transferable, world-wide licence to reproduce the Licensed Material for the purpose specified in your order

License agreements for Figure 6

License agreements for Figure 7

159

Type of Use	reuse in a thesis/dissertation
Portion	figures/tables/illustrations
Number of figures/tables/illustrations	1
Format	both print and electronic
Are you the author of this Elsevier article?	No
Will you be translating?	No
Title	Polymeric Materials for Detection of Chemical Warfare Agents
Institution name	University of Waterloo
Expected presentation date	Dec 2021
Order reference number	3
Portions	Figure 3
Requestor Location	Chemical Engineering University of Waterloo Engineering 6, 200 University Ave W Waterloo, ON Waterloo, ON N2L3G1 Canada Attn: University of Waterloo
Publisher Tax ID	GB 494 6272 12
Total	0.00 USD

Terms and Conditions

License agreements for Figure 8a

Type of Use	reuse in a thesis/dissertation
Portion	figures/tables/illustrations
Number of figures/tables/illustrations	1
Format	both print and electronic
Are you the author of this Elsevier article?	No
Will you be translating?	No
Title	Polymeric Materials for Detection of Chemical Warfare Agents
Institution name	University of Waterloo
Expected presentation date	Dec 2021
Order reference number	4
Portions	Figure 6
Requestor Location	Chemical Engineering University of Waterloo Engineering 6, 200 University Ave W Waterloo, ON Waterloo, ON N2L3G1 Canada Attn: University of Waterloo
Publisher Tax ID	GB 494 6272 12
Total	0.00 USD

Terms and Conditions

License agreements for Figure 8b

COPYRIGHT PERMISSION REQUEST FORM

Date: ___Oct 25, 2021_____

To: The Chemical Society of Japan
    1-5,Kanda-Surugadai,Chiyoda-ku,
    Tokyo 101-8307, Japan

    Fax: +81-3-3292-6318
    E-mail: info@chemistry.or.jp

From: Bhoomi Mavani
    Engineering 6, 200 University Ave W,
    University of Waterloo, Waterloo
    N2L 3G1, Ontario
    Phone: 416-839-4190
    Fax:
    E-mail: bmavani@uwaterloo.ca

I am preparing a thesis entitled:

Polymeric Materials for Detection of Chemical Warfare Agents

to appear
in my Master of Applied Science Thesis

which is published by

    University of Waterloo

Expected publication date: ___December 2021_____

I request your permission to include the following material in this and in all subsequent editions of this work to be published by _____ University of Waterloo or its licensees for distribution throughout the world, in all media including electronic/online and microfilm.

Title of Publication: Synthesis and gas sensing properties of polypyrrole/MoO3-layered nanohybrids
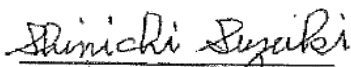
Author(s)/Editor(s): I. Matsubara, K. Hosono, N. Murayama, W. Shin and N. Izu

Title of Selection: ___Fig. 10. The magnitude of the sensitivity (Rg/Ra) of (PPy)xMoO3 at a room temperature upon exposure of VOCs with the concentration of 1000 ppm___

Year: ___2004___   Vol.: __77___   No.: ___6___

Figure(s)/Table(s): _Figure 10_ ~~+~~   Page(s): ___~~1231-1237~~ 1236___

We hereby grant permission for the use of the material requested above.

Shin-ichi Suzuki
Shin-ichi Suzuki
Secretary-general
The Chemical Society of Japan

Date: 26 October, 2021

Our Ref. No. CY-RT 21-214

License agreements for Figure 9

164

Type of Use	reuse in a thesis/dissertation
Portion	figures/tables/illustrations
Number of figures/tables/illustrations	1
Format	both print and electronic
Are you the author of this Elsevier article?	No
Will you be translating?	No
Title	Polymeric Materials for Detection of Chemical Warfare Agents
Institution name	University of Waterloo
Expected presentation date	Dec 2021
Order reference number	5
Portions	Figure 5
Requestor Location	Chemical Engineering
University of Waterloo
Engineering 6, 200 University Ave W
Waterloo, ON
Waterloo, ON N2L3G1
Canada
Attn: University of Waterloo
Publisher Tax ID	GB 494 6272 12
Total	0.00 USD

Terms and Conditions

License agreements for Figure 56a

Type of use	Dissertation/Thesis
Requestor type	University/Academic
Format	Print and electronic
Portion	Figure/table
Number of figures/tables	1
Will you be translating?	No
Title	Polymeric Materials for Detection of Chemical Warfare Agents
Institution name	University of Waterloo
Expected presentation date	Dec 2021
Order reference number	6
Portions	Figure 3c
Requestor Location	Chemical Engineering University of waterloo Engineering 6, 200 University Ave W Waterloo, ON Waterloo, ON N2L3G1 Canada Attn: University of Waterloo
Publisher Tax ID	EU826007151
Total	0.00 USD

Terms and Conditions

License agreements for Figure 56b and 56c

Portion	Figure/table
Number of figures/tables	2
Will you be translating?	No
Title	Polymeric Materials for Detection of Chemical Warfare Agents
Institution name	University of Waterloo
Expected presentation date	Dec 2021
Order reference number	7
Portions	Figure 4b and Figure 4c
Requestor Location	Chemical Engineering University of Waterloo Engineering 6, 200 University Ave W Waterloo, ON Waterloo, ON N2L3G1 Canada Attn: University of Waterloo
Publisher Tax ID	EU826007151
Total	0.00 USD
Terms and Conditions	

TERMS AND CONDITIONS

169

License agreements for Figure 59

Format	Print and electronic
Portion	Figure/table
Number of figures/tables	1
Will you be translating?	No
Title	Polymeric Materials for Detection of Chemical Warfare Agents
Institution name	University of Waterloo
Expected presentation date	Dec 2021
Order reference number	8
Portions	Figure 2
Requestor Location	Chomical Engineering University of Waterloo Engineering 6, 200 University Ave W Waterloo, ON Waterloo, ON N2L3G1 Canada Attn: University of Waterloo
Publisher Tax ID	EU826007151
Total	0.00 USD

Terms and Conditions

TERMS AND CONDITIONS